THESIS

GIS-BASED SOIL EROSION MODELING AND SEDIMENT YIELD OF THE N'DJILI RIVER BASIN, DEMOCRATIC REPUBLIC OF CONGO

Submitted by

Patrick Ndolo Goy

Department of Civil and Environmental Engineering

In partial fulfillment of the requirements

For the Degree of Master of Science

Colorado State University

Fort Collins, Colorado

Summer 2015

Master's Committee:

Advisor: Pierre Y. Julien

Darrell G. Fontane
Lee H. MacDonald

ABSTRACT

GIS-BASED SOIL EROSION MODELING AND SEDIMENT YIELD

OF THE N'DJILI RIVER BASIN, DEMOCRATIC REPUBLIC OF CONGO

In the Democratic Republic of Congo, the N'djili River and its tributaries are the most important potable source of water to the capital, Kinshasa, satisfying almost 70% of its demand. Due to increasing watershed degradation from agricultural practices, informal settlements and vegetation clearance, the suspended sediment load in the N'djili River has largely increased in the last three decades. With an area of 2,097 km^2, the N'djili River basin delivers high suspended sediment concentration, and turbidity levels that cause considerable economic losses, particularly by disrupting the operation in the N'djili and Lukaya water treatment plants, and increasing dramatically the cost of chemical water treatment.

The objectives of this study are to: (1) determine the change in the land cover/use of the N'djili River basin for 1995, 2005 and 2013; (2) predict and map the annual average soil losses at the basin scale and determine the effects of land cover/use change on the soil erosion; (3) estimate the sediment yield and the sediment delivery ratio at the water intake of the N'djili water treatment plant; and (4) quantify the effects of ash concentration on water turbidity in order to understand the high turbidity observed at the beginning of the rainy season.

The Revised Universal Soil Loss Equation (RUSLE) model was implemented in a Geographic Information System (GIS) to estimate the spatially distributed soil loss rates in the N'djili basin under different land uses. RUSLE model parameters were derived from digital

elevation model (DEM), average annual precipitation, soil type map and land cover maps (1995, 2005, 2013) obtained from Landsat images.

The land cover/use change analysis shows that bare land/burned grass/agricultural land cover represented almost 22% of the N'djili basin area in 2013 whereas it was covering only 6% of the basin area in 1995. Settlements, which covered about 8% of the basin area in 1995, represented about 18% of the N'djili Basin area in 2013. The expansion of settlements, bare land, burned areas and agricultural lands was realized at the expense of the forest, grass, and shrubs cover. The annual average soil loss rate of the N'djili River Basin is estimated to be 7 tons/acre/year for 1995, 8.7 tons/acre/year for 2005 and 16 tons/acre/year for 2013. In 2013, bare land, burned areas and rainfed crops produced about 60% of the soil loss. The analysis of the relationship between probability of soil erosion and annual average soil loss rates indicated that up to 82, 79, and 73% of the basin area are in the range of tolerable soil erosion (0 – 5 tons/acre /year) in 1995, 2005 and 2013 respectively. Based on the gross erosion and sediment yield observed in 2005 and 2013, the sediment delivery ratio of 4.6% and 4.1% were predicted in 2005 and 2013, suggesting that most of the soil eroded from upland areas of the basin is trapped on flood plains covered by grass, shrubs and trees. Regarding the effects of ash concentration on turbidity, this study found that turbidity increased as a power function of ash concentration.

ACKNOWLEDMENTS

First, I would like to express my deepest gratitude to my advisor, Dr. Pierre Julien for his support and encouragement throughout my time at CSU. I really feel honored to have had the opportunity to work on my thesis under his guidance. I would like to extend my gratitude to my Master's degree committee members Dr Darrell Fontane and Lee MacDonald for their comments and suggestions that helped me to improve this thesis.

I would like to extend my appreciation to those who shared their knowledge and time during the thesis process: Ahmad Shukran Sahaar and Dr. David Gwenzi. I also would like to thank those who helped me with the data: Steve Lemba Dieto,, Michael Strobel and Linda Scheffe from USDA-NRCS. A special thanks go to the general manager of REGIDESO and his staff members for granting me access to turbidity data.

I would also like to extend a special thanks to my friend Dieudo Mulamba, the Abyssinian Christian Church members, Reverend David Williams and Debbie Minor Williams for their precious support. I acknowledge all stars of Dr Julien's Dream Team, including Hwayoung Kim, Ken Lai, Haider Haddab and Dr Jaeon Lee for their friendship. I am deeply grateful to other CSU members including Laurie Alburn, Linda Hinshaw and Dr. Jorge Ramirez.

I would like to express my gratitude to Dr. Tozin of the Civil Engineering Department of the University of Kinshasa and the Fulbright Program of the U.S. Department of State's Bureau of Educational and Cultural Affairs for their financial support.

Finally, I would like to extend my deepest gratitude to my family. To my lovely wife, Clément Pfingu and my little boy, Jean-Pierre. Without their love and encouragement, I could not have finished this thesis.

TABLE OF CONTENTS

LIST OF TABLES

LIST OF FIGURES

LIST OF SYMBOLS

A	Average annual soil loss (ton * $acre^{-1}$ * yr)
A_S	Specific catchment area (m^2 * m^{-1})
A_T	Gross erosion per unit area (tons * $acre^{-1}$ * yr^{-1})
C	Cover management factor (dimensionless)
$C_{mg/l}$	Sediment concentration (mg/l)
E	Storm energy (ft. * tons * $acre^{-1}$)
I_{30}	Maximum 30-min intensity (in*h^{-1})
K	Soil erodibility factor (ton acre h [hundreds of acre-ft tons in-1]
L	Slope length factor (dimensionless)
M	Ranked position
m	a variable slope length exponent
n	a variable slope steepness exponent
OM	Organic matter (%)
P	Support practice factor (dimensionless)
P	Annual precipitation (mm * $year^{-1}$)
p	Exceedance probability (% of time)
Q	Water discharge (m^3)
Q_s	Sediment discharge (ton*day^{-1})
R	Average annual erosivity factor (hundreds of ft * tons * $acre^{-1}$ * yr^{-1})
S	Slope steepness factor (dimensionless)
SD	Specific degradation (tons * km^{-2} * yr^{-1})
SDR	Sediment delivery ratio
SLR	Soil loss ratio (dimensionless)
T	Time since burning (years)
TSS	Total Suspended Solid (mg/l)
X_h	Horizontal slope length (ft)

Y	Sediment yield (tons yr-1)

Greek Symbols

ε	Rill erosion coefficient (dimensionless)
σ	Slope gradient (percentage)
θ	Slope angle (degree)

LIST OF ACRONYMS

ANSWERS	Areal Nonpoint Source Watershed Environmental Resources Simulation
ASTER	Advanced Spaceborne Thermal Emission and Reflection Radiometer
BCEOM	Bureau Central d'Études pour les Équipements d'Outre-Mer
CASC2D-SED	CASCade 2 Dimensional SEDimentation
CIA	Central Intelligence Agency
CREAMS	Chemicals, Runoff, and Erosion from Agricultural Management System
CSU	Colorado State University
DEM	Digital Elevation Model
DOC	Dissolved Organic Carbon
DRC	Democratic Republic of Congo
ESRI	Environmental System Research Institute
GAMES	Guelph Model for evaluating the effects of Agriculture Management Systems on Erosion and Sedimentation
GDEM	Global Digital Elevation Model
GIS	Geographic Information System
IDW	Inverse Distance Weighting
ISRIC	International Soil Reference and Information Centre
METTELSAT	Agence Nationale de Météorologie et de Télédétection par satellite
METI	Ministry of Economy, Trade and Industry
MUSLE	Modified Universal Soil Loss Equation
NASA	National Aeronautics and Space Administration
NRCS	Natural Resources Conservation Service
NTU	Nephelometric Turbidity Unit
REGIDESO	Régie de Distribution des Eaux
RUSLE	Revised Universal Soil Loss Equation
SAFRICAS	Société Africaine de Constructions
SD	Specific Degradation

SDR	Sediment Delivery Ratio
SHE	Système Hydrologique Européen
SLC	Scan Line Corrector
SLR	Soil Loss Ratio
SOGREAH	Société Grenobloise d'Études et d'Applications Hydrauliques
SOTERCAF	Soil and TERrain of Central AFrica
SRTM	Shuttle Radar Topography Mission
TREX	Two dimensional, Runoff, Erosion, and Export
UNEP	United Nations Environmental Program
UN-FAO	Food and Agriculture Organization of the United Nations
U.S.	United State of America
USDA	U.S. Department of Agriculture
USGS	U.S. Geological Survey
USLE	Universal Soil Loss Equation
USPED	Unit Stream Power based Erosion Deposition
WASP/IPX	Water Quality Analysis Simulation Program/ In-Place Pollutant Export
WEPP	Water Erosion Prediction Project

CHAPTER 1 : INTRODUCTION

Overview

The Democratic Republic of Congo (known as Zaïre between 1971 and 1997) is located in Central Africa. It borders the Republic of the Congo, the Central African Republic, and South Sudan to the north, Uganda, Rwanda, Burundi and Tanzania to the east, Zambia and Angola to the south and the Atlantic Ocean to the west (Figure 1.1).

Figure 1.1 – Location of the Democratic Republic of Congo

The Democratic Republic of Congo (DRC) is the second largest country in Africa by area and the eleventh largest in the world. With a population of over 75 million (CIA 2014), the DRC is the most populous officially Francophone country, the fourth most populous nation in Africa, and the nineteenth most populous country in the world.

The DRC is extremely rich in natural resources, especially in fresh water resources. With an estimated 52 % of Africa's surface water reserves (rivers, lakes and wetlands), the D.R.C. occupies almost 62% of the Congo River Basin. The Congo River boasts the largest discharge volume in Africa (1,260 km^3), equivalent to 15 times the mean annual runoff the Nile River and second in the world after the Amazon River (UNEP 2011). With high precipitation, the highest frequency of thunderstorms in the world and the annual rainfall varying between 800 mm/year and 2000 mm/year, DRC sustains the Congo Rainforest, the second largest rain forest in the world (after Amazon), which is surrounded by plateaus merging into savannas in the south and southwest, by mountainous terraces in the west, and dense grasslands extending beyond the Congo River to the north (UNEP 2011).

More than 60% of the DRC population live in rural areas whereas the rest lives in the numerous cities across the country. Kinshasa, the capital city, is the largest city of Congo. Its population is continually increasing since the independence of country in 1960. As with other major African cities, the growing population between 1960 and 1996 was due to rural-urban migration. With about 200,000 people in 1960, the population of Kinshasa city was about 2 million people in 1996. Between 1996 and 2013, the population of Kinshasa city increased from about 2 million to over 9 million people, essentially because of the civil wars which happened in the country between 1996 and 2003. Indeed, people from the inland country were fleeing to Kinshasa city and its neighborhood, which was the only safe place during this troubled period.

Kinshasa area (Figure 1.2) relies on 3 main watersheds for potable water: N'djili basin, Lukunga basin and N'sele basin. The N'djili River and its tributaries (Lukaya River) are the most important potable water resource of Kinshasa city, satisfying almost 70% of its demand (about 365,000 m^3/day of potable water) (BCEOM 2006).

Figure 1.2 – Map of Kinshasa area

With the increasing of the population during the last decades, the national water utility (REGIDESO) is continuously required to update the water supply in order to satisfy the population needs, despite several political, economic, technical and environmental constraints. Over the last three decades, a critical environmental issue erupted, making the water abstraction operations from the alluvial rivers of the Kinshasa area erratic during and/or after heavy rainfalls. Indeed, increasingly high turbidity levels are observed since the beginning of the 1980s in the three rivers that provided potable water to the Kinshasa city: N'djili, Lukaya and Lukunga Rivers (UNEP 2011). Specifically for the N'djili River, which drains water from an area of 2,097 km^2, the average daily turbidity level was less than 30 NTU in 1970's at the intake of the N'djili water treatment plant. Nowadays, it typically varies between 100 and 400 NTU with peak values as high as 1000 and 6000 NTU during rainstorms (UNEP 2011). Those high turbidity levels and suspended sediment concentrations are also observed in the Lukaya River, which is the main tributary of the N'djili River. Figure 1.3 shows turbid water discharge in the Lukaya River after a rainstorm in 2011.

Figure 1.3 – Discharge of highly turbid water in the Lukaya River during a rainstorm.

According to the guidelines of the raw water pumping operations in the N'djili and Lukaya water treatments plants (Figure 1.4), pumping operations are stopped when turbidity values reach or exceed 500 NTU. Figure 1.5 is based on data from REGIDESO. It provides the number of disruptions of pumping operations due to high turbidity events.

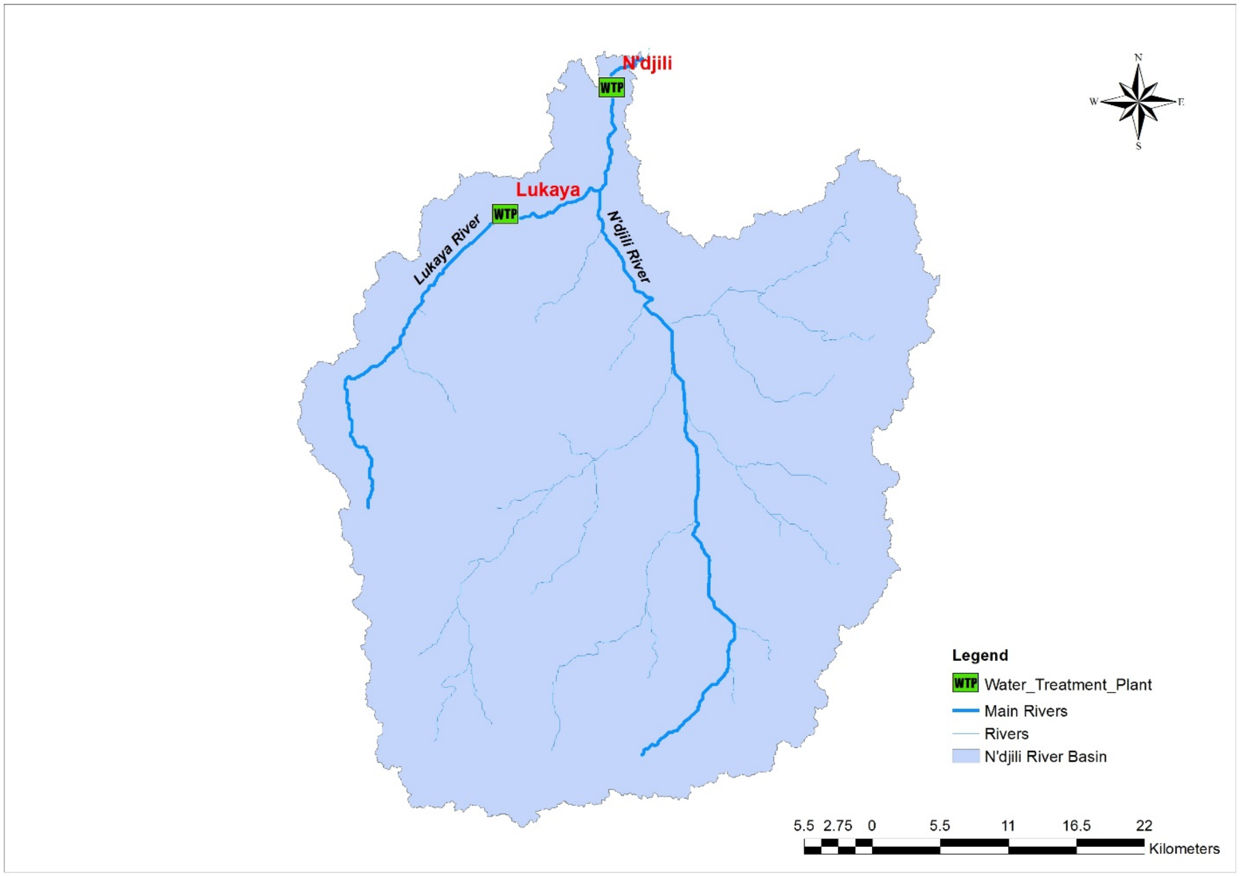

Figure 1.4 – Water treatment plants in the N'djili River Basin

Furthermore, using turbidity measurements from 2000 to 2013, two turbidity exceedance probability curves were constructed for the periods 2000 – 2005 and 2006 – 2013 respectively (Figure 1.6). Looking at these turbidity exceedance probability curves, it can be noticed that the value of 500 NTU had 2.7 % of chance to be equaled or exceeded between 2000 and 2005; between 2006 and 2013, the chance to equal or exceed this turbidity value had practically doubled to 5.14 %.

Those high levels of turbidity contribute a lot to the disruption of pumping operations and increase dramatically the cost of chemical water treatment for the water treatment plants located in the N'djili River Basin. To illustrate the economic losses caused by excessive turbidity levels, Table 1.1 presents summary of those losses at the Lukaya water treatment plant due to the disruption of water pumping operations. Figure 1.7 shows the cleaning of the diversion canal of water coming from the Lukaya River to the water plant.

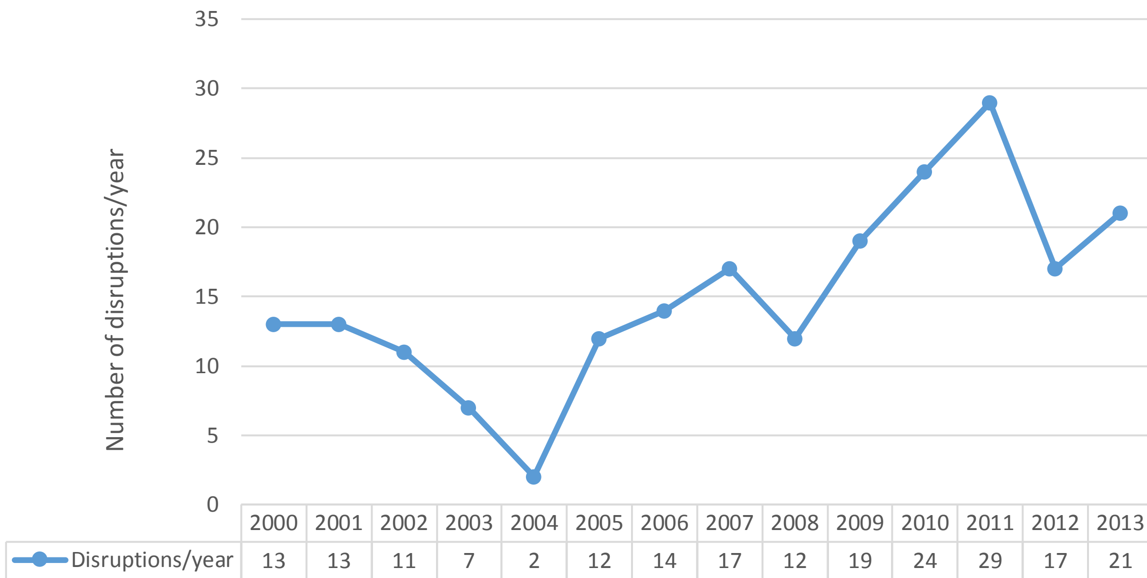

Figure 1.5 – Number of water pumping disruptions per year at the N'djili water treatment plant due to high turbidity

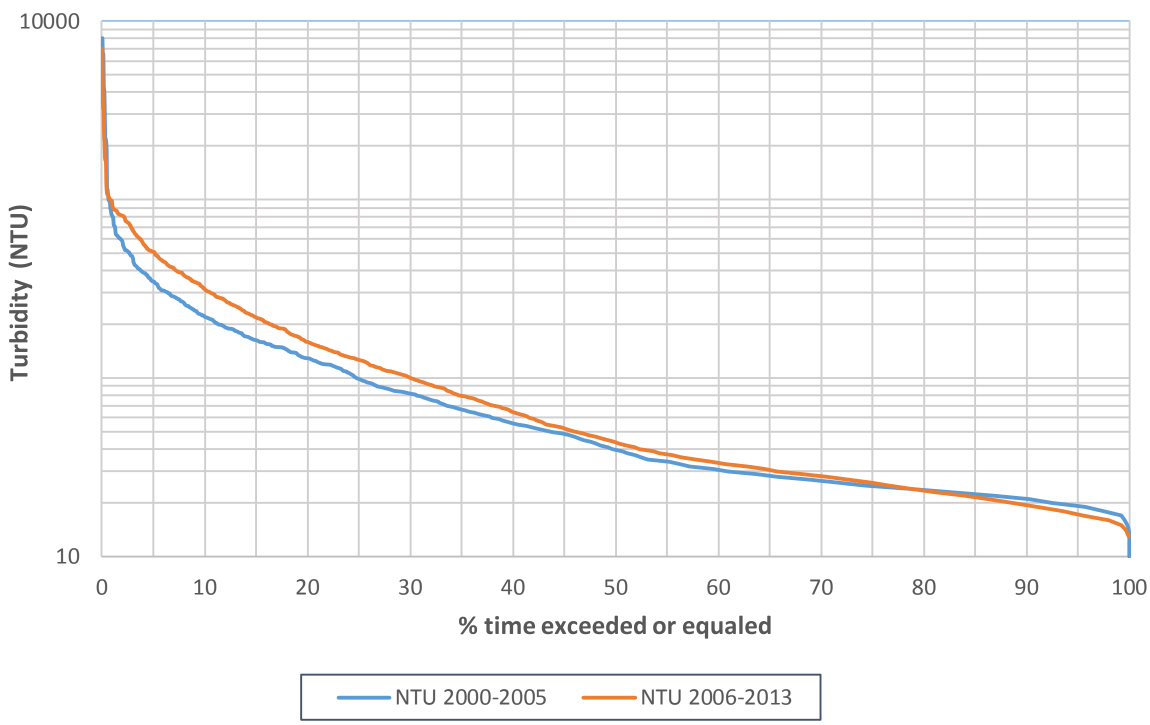

Figure 1.6 – Exceedance probability curves of turbidity at the intake of the N'djili water plant for the periods 2000-2005 and 2006-2013

Table 1.1 - Total losses caused by pumping disruption due to high turbidity in 2013 (Lukaya Treatment Plant)

Month	Jan	Feb	Mar	Apr	May	Jun
Disruption hours	32	17	46	44	11	7
Month	**Jul**	**Aug**	**Sep**	**Oct**	**Nov**	**Dec**
Disruption hours	0	0	6	34.5	32	47
Total hours of disruption	**276.5**					
Hourly Capacity (m3/h)	**1,700**					
Total Losses (m3)	**470,050**					

In its Post-Conflict Environmental Assessment report on DRC (2011), the United Nations Environmental Program (UNEP) monitored the environmental degradations throughout the country and especially in the N'djili River Basin. According to this report, watershed degradations due to the rapid population growth, deforestation, unplanned and anarchic urban development, and agricultural practices like burning are consistently cited as the main causes of elevated sediment concentration in the main rivers of the N'djili basin (UNEP 2011). Although this high suspended sediment concentration and turbidity issue is a threat for a safe drinking water supply for Kinshasa City, there is no study that relates the effects of watershed degradation on the turbidity in the N'djili River during the last decades.

Figure 1.7 – Cleaning operations of diversion canal of the Lukaya water plant (Picture: Regideso, 2013)

Objectives

The overall objective of this thesis is to quantify the effects of watershed changes on gross soil erosion, which ultimately affects the turbidity in the N'djili River. The soil erosion rates for different land use and land cover scenarios in the N'djili River Basin will be predicted and the sediment yield at the intake of the N'djili water treatment plant estimated. The soil erosion rate prediction will be based on the Revised Universal Soil Loss Equation (RUSLE) model in a GIS-based environment. The specific objectives are:

1. Determine the change in land cover/use of the N'djili basin for 1995, 2005 and 2013.
2. Predict and map the annual average soil loss rate at the basin scale and determine the effects of land cover/use change on soil erosion.
3. Estimate the sediment yield and the sediment delivery ratio at the water intake of the N'djili water treatment plant.

4. Quantify the effects of ash concentration on the turbidity in order to understand the high turbidity values observed at the beginning of the rainy season.

Chapter 2 reviews soil erosion processes, soil erosion models, post-fire recovery, wildfire impact on turbidity, Geographic Information Systems (GIS) and sediment delivery ratio. A short description of the N'djili River Basin along with the data set needed for the soil erosion prediction and the sediment yield computation is given in Chapter 3. Chapter 4 describes the procedure to estimate the annual average soil loss rate using the RUSLE model parameters. In Chapter 5, soil erosion rates at different dates due to different land cover/use scenarios will be presented and discussed. Chapter 6 presents the conclusions.

CHAPTER 2 : LITERATURE REVIEW

Introduction

This chapter gives a brief overview of erosion in section 2.1, soil erosion process in section 2.2 and erosion models in section 2.3. In section 2.3, sediment delivery ratio is discussed while remote sensing and image interpretation are presented in section 2.4. The last section (section 2.5) presents an overview on the Geographic Information System (GIS) in which the Revised Universal Soil Loss Equation (RUSLE) model will be implemented for soil erosion prediction.

2.1 Overview of erosion

In the past century, a distinction between natural (geological) erosion and human-induced (or accelerated) erosion was widely admitted, regarding the latter as a mainly local phenomenon (Vanoni 1975). Nowadays, this view is outdated. Analyzing the estimated annual global volumes of erosion due to various agents, Hooke (1994) came to the conclusion that humans can be considered as the "most important geomorphic agent currently shaping the surface of the Earth." However, other authors like Valdiya (1998) demonstrated that geological erosion in mountains, such as the one that taking place in the Himalayas, continues to produce enormous sediment volumes.

The distinction between natural erosion process and those due to human influences is often difficult. Although some erosional processes like gullying and landslides appear natural, they may have been triggered or aggravated by overgrazing, infiltration of irrigation water, or deforestation (MacArthur et al. 2008).

Natural or Geologic Erosion

The main causes of the natural erosion are tectonic uplift, weathering, chemical decomposition and the long-term action of water, wind, gravity, and ice (MacArthur et al. 2008). Based on the average rates of natural erosion estimated for major world drainage basins by Summerfield and Hutton (1994), rates of geologic erosion vary widely over regions and time, and tend to be slow in terms of human lifetime. For some projects, the control of this natural erosion can be necessary, though it is often difficult or impractical because of large distributed areas involved in such erosion type and divided among multiple owners. Prior natural erosion rates can be dramatically accelerated by poorly designed and implemented land or water use projects.

Human-Induced or Accelerated Erosion

Human activities are the major cause of the accelerated erosion. The impacts of human activities start slowly but can lead to dramatic rapid changes in morphology, sediment production, and deposition (MacArthur et al. 2008). Whereas humans possessed a relatively limited impact on geologic landscape prior to the nineteenth century, the degradation of the global landscape and the environment was accelerated by the human activities in the nineteenth and twentieth centuries (Hatheway 2005). Some of these activities often lead to environmental degradation and damage habitat, while causing sedimentation problems and impacting constructed facilities. There are multiple causes of accelerated erosion including agricultural activities, forest activities, urbanization, roads, railways, bridges, and levees, mining activities, dams and river regulation, warfare and population migrations (MacArthur et al. 2008).

2.2 Soil Erosion Process

As shown in Figure 2.1, several erosion processes can be identified. The first one, the splash erosion, starts when raindrop impact on the ground surface detaches particles (Julien 2002). After been detached, particles are transported to the rills by a thin overland flow. Rill erosion is an erosion process that occurs when water from the sheet erosion combines to form small concentrated channels (Fortuin 2006). This is the most common type of surface erosion and is small enough to be removed by normal tillage operation. When water in rills concentrates to form larger channels, it results in gully erosion (Fortuin 2006). Stream channel erosion takes place when concentrated water which forms from rills and gullies, and contains sediment removed from streambed and stream bank (Fortuin 2006). When the amount of detached soil overcomes the transport capacity, only the sediment corresponding to the transport capacity will be carried downslope and the rest will be deposited in the channel.

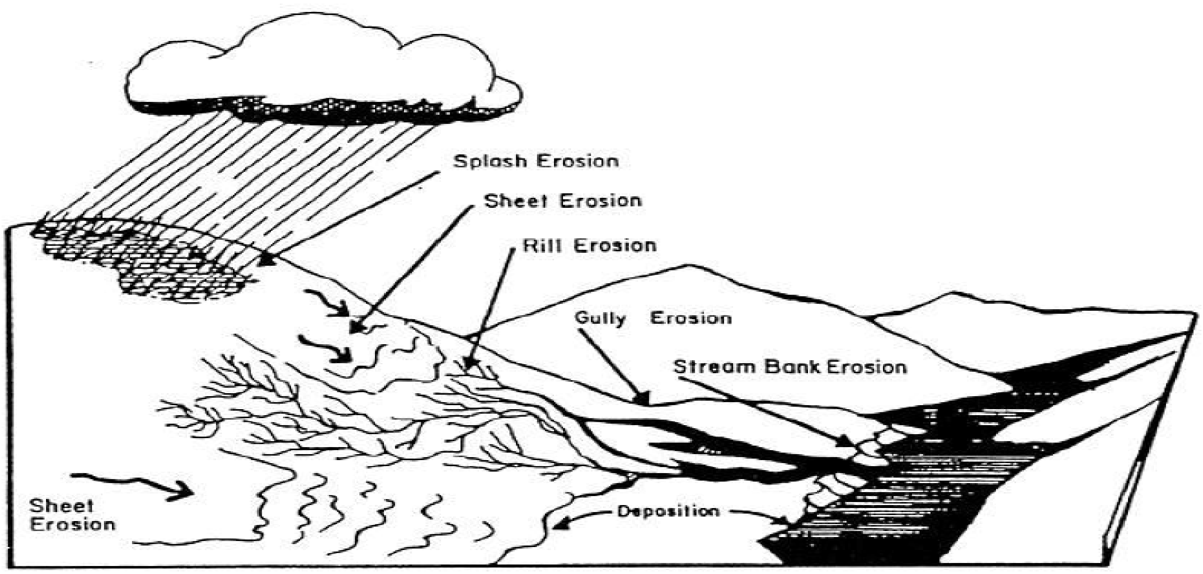

Figure 2.1 – The mechanisms of soil erosion (USACE 1985)

2.3 Soil Erosion Models

In order to understand and to predict upland soil and stream erosion, as well as the transport and deposition of sediment, several erosion models have been developed. Most of the soil erosion prediction methods were first developed in the US, based on different equations. Over the years, these equations were improved by adding new variables and factors.

One of the first rational soil erosion equation was developed by Smith and Whitt and its goal was to estimate soil losses from fields of claypan soils (Smith and Whitt 1947). The factors in this equation are the specific rotation, slope length, slope steepness, row direction, soil erodibility and support practice.

One of the major innovation in soil and water conservation during the past century was the development of the Universal Soil Loss Equation (USLE), which is an empirical model used around the world to estimate soil erosion by raindrop impact and surface runoff. In 1965, Wischmeier and Smith developed the USLE model, based on the data collected from more than 10,000 test plot-years across the US in 20 years (Wischmeier and Smith 1965). These test plots were designed to accurately estimate soil erosion under different conditions. Each experimental plot was 6 feet wide by 72.6 feet long, representing 1% of an acre. In this research, a variety of factor affecting soil erosion including precipitation, slope steepness, slope length, soil type, type of crops, and conservation practices were studied. An updated of this model was published in 1978 in Agriculture Handbook 537.

Successive efforts have been made by researchers in the last 3 decades to upgrade and improve the USLE model. Many erosion models represent great improvements of the original model, among of them the Modified Universal Soil Loss Equation (MUSLE) developed by Williams in 1975, the Areal Nonpoint Source Watershed Environmental Resources Simulation

(ANSWERS) (Beasley et al. 1980), the Guelph Model for evaluating the effects of Agriculture Management Systems on Erosion and Sedimentation (GAMES) (Rudra et al. 1986), the Unit Stream Power – based Erosion Deposition (USPED) (Mitasova et al. 1996), and the Revised Universal Soil Loss Equation (RUSLE) (Renard et al. 1997).

The Revised Universal Soil Loss Equation (RUSLE) is a computerized version of the USLE. It incorporates improvements in many of the factor estimates including a new procedure to calculate cover factor, new algorithms to reflect rill to interill erosion in slope length and steepness factors. Also, the climatic factors based on extended database of rainfall-runoff in Western US was added in the RUSLE model. Further-enhanced Windows version of the software, known as RUSLE2, was recently released for guiding conservation planning, inventory erosion rates and estimate sediment delivery.

In 1985, the USDA initiated the Water Erosion Prediction Project (WEPP) model for soil erosion prediction. This model is used in soil and water conservation planning and assessment (Foster and Lane 1987). The WEPP model is a process-based, distributed parameters, capable of doing both single-event and continuous simulation erosion prediction. This model relies on the fundamentals of stochastic weather generation, infiltration theory, hydrology, soil physics, plant science, hydraulics and erosion mechanics (Flanagan et al. 1995). Although this model does not implement the USLE for parameter estimation, it can predict soil erosion, sediment transport, and deposition across the landscape by using a steady-state sediment continuity equation for predicting rill and interill erosion processes. WEPP model can be used for small watersheds or hillslopes.

CASC2D or CASCade of planes in 2-Dimensions, was initially developed at Colorado State University in Fort Collins, Colorado (Julien and Saghafian 1991; Julien et al. 1995).

Further, it was modified at the University of Connecticut (Ogden 1998; Ogden and Julien 2002). CASC2D is a physical based model that simulates water and sediment in two-dimensional overland grids and one-dimensional channels and has both single-event and long-term continuous simulation capabilities.

Based on SHE, the European Hydrological System (Abbott et al. 1986a; 1986b), MIKE SHE (Refsgaard and Storm 1995) is a comprehensive, distributed, and physically based model that simulates water, sediment, and water-quality parameters in two-dimensional overland grids, one-dimensional channels, and one-dimensional unsaturated and three saturated flow layers. As the CASC2D model, MIKE SHE can perform both single-event and long-term continuous events. The model was developed by a consortium of the U.K. Institute of Hydrology, the French consulting firm SOGREAH, and the Danish Hydraulic Institute (Borah et al. 2007).

Two-dimensional Runoff Erosion and Export (TREX) model is a watershed models developed at Colorado State University in Fort Collins, Colorado. It combines surface hydrology and sediment transport features from CASC2D watershed model with chemical transport feature from the WASP/IPX series of water quality models to simulate chemical transport and fate process at the watershed scale (Velleux et al. 2008; England et.al. 2007; Ambrose et al. 1993; Velleux et al. 2001).

2.4 Post-fire Recovery and Restoration

According to MacDonald (2012), high-severity wildfires increase runoff and sediment production rates by several orders of magnitude. Accordingly, sediment production rates from high-severity sites are nearly an order of magnitude higher than sites burned at moderate or low severity. Also, MacDonald (2012) found that percent ground cover is the most important control on post-fire erosion rates (Figure 2.2), and seeding and scarification do not increase ground cover or reduce erosion rates.

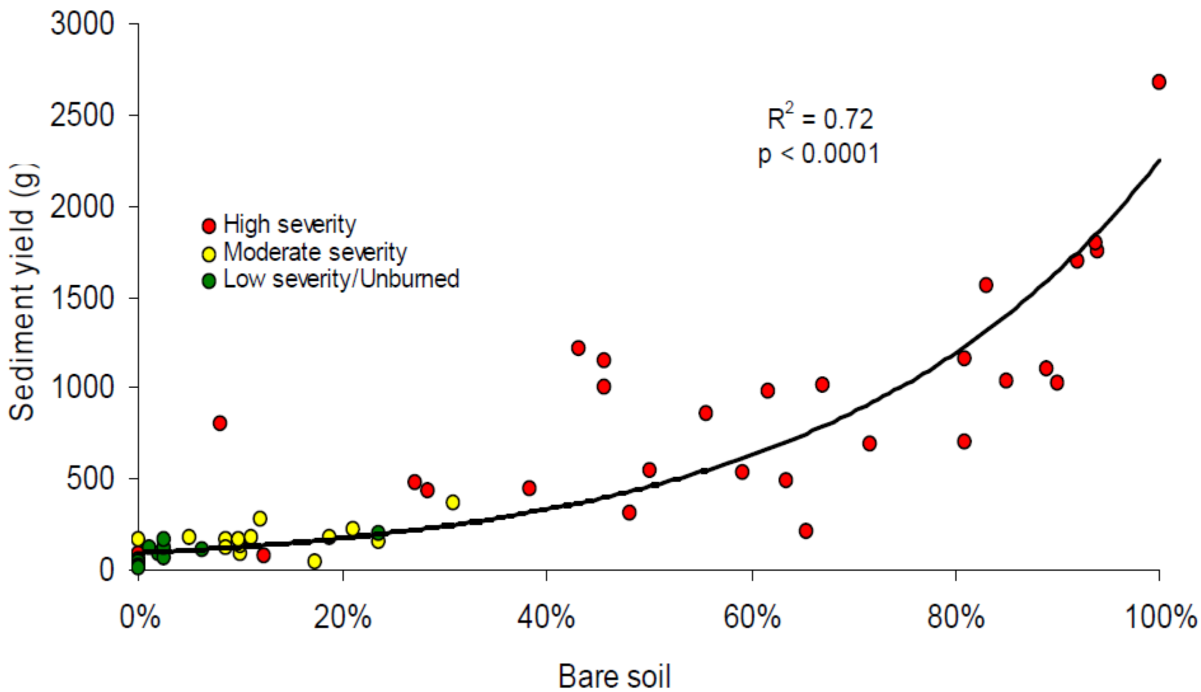

Figure 2.2 - Sediment yield vs percent bare soil for rainfall simulations, Bobcat Fire (MacDonald 2012)

Moreover, results from MacDonald (2012) demonstrates that the percentage of bare soil (and so the gross soil erosion) tends to decrease when the time since burning increases (Figure 2.3) and the percentage of bare soil varies tremendously with the time since burning.

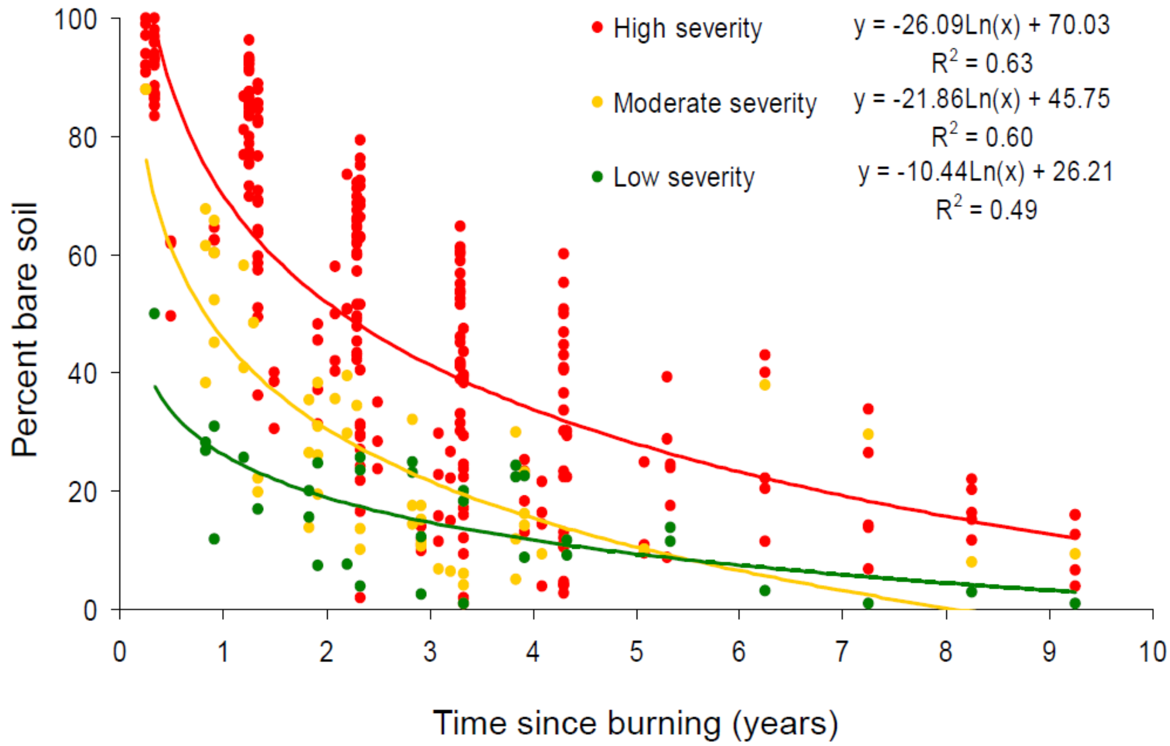

Figure 2.3 - Percent bare soil vs time since burning, Bobcat Fire (MacDonald 2012)

2.5 Turbidity – Wildfire Impact on Turbidity

Turbidity is the amount of cloudiness or relative clarity of a liquid. It is an optical property of fluid containing particles, expressed as the amount of light that is scattered by particles in the fluid. In case of water, high turbidity is observed in a river full of mud and silt where it would be impossible to see through the water while low turbidity is observed in spring water which appears to be completely clear. Turbidity is usually measured in Nephelometric Turbidity Units (NTU) or Jackson Turbidity Units (JTU), or even in Formazin Turbidity Unit (FTU). Turbidity can be caused by:

- Clay, silt, sand and mud;
- Bacteria and other germs;

- Algae, soluble colored organic compound, plankton and other microscopic organisms;
- Chemical precipitates.

Burned watersheds are subject to increased flooding and erosion, with consequences on water quality, drinking-water treatment processes and water-supply reservoirs. After 2010 Fourmile Canyon fire near Boulder, Colorado, US Geological Survey initiated a study to assess the impacts of this wildfire (Writer et al. 2012). Principal findings from the first year of research demonstrated that stream discharge and nitrate concentrations increased downstream of burned area. Also, during and after high-intensity thunderstorms, turbidity, dissolved organic carbon, nitrate and some metals increased by 1 to 4 orders of magnitude within and downstream of the burned area. These findings are illustrated in Figures 2.4 and 2.5. Figure 2.4 presents the discharge observed at the most downstream point of the Fourmile creek and caused by daily precipitation since the fire date (September 6th to 10th) the discharge. Figure 2.5 shows the water-quality response to post-fire precipitation events. In this figure, it can be noticed that the thunderstorms on July 7 and July 13, 2011 transported huge amount of sediment from hillslopes to Fourmile Creek leading to large increases in concentration of DOC (greater than 70 mg/L) and of nitrate (greater than 9 mg/L) and in turbidity (as much as 50,000 NTU) (Murphy et al. 2012; Writer et al. 2012)

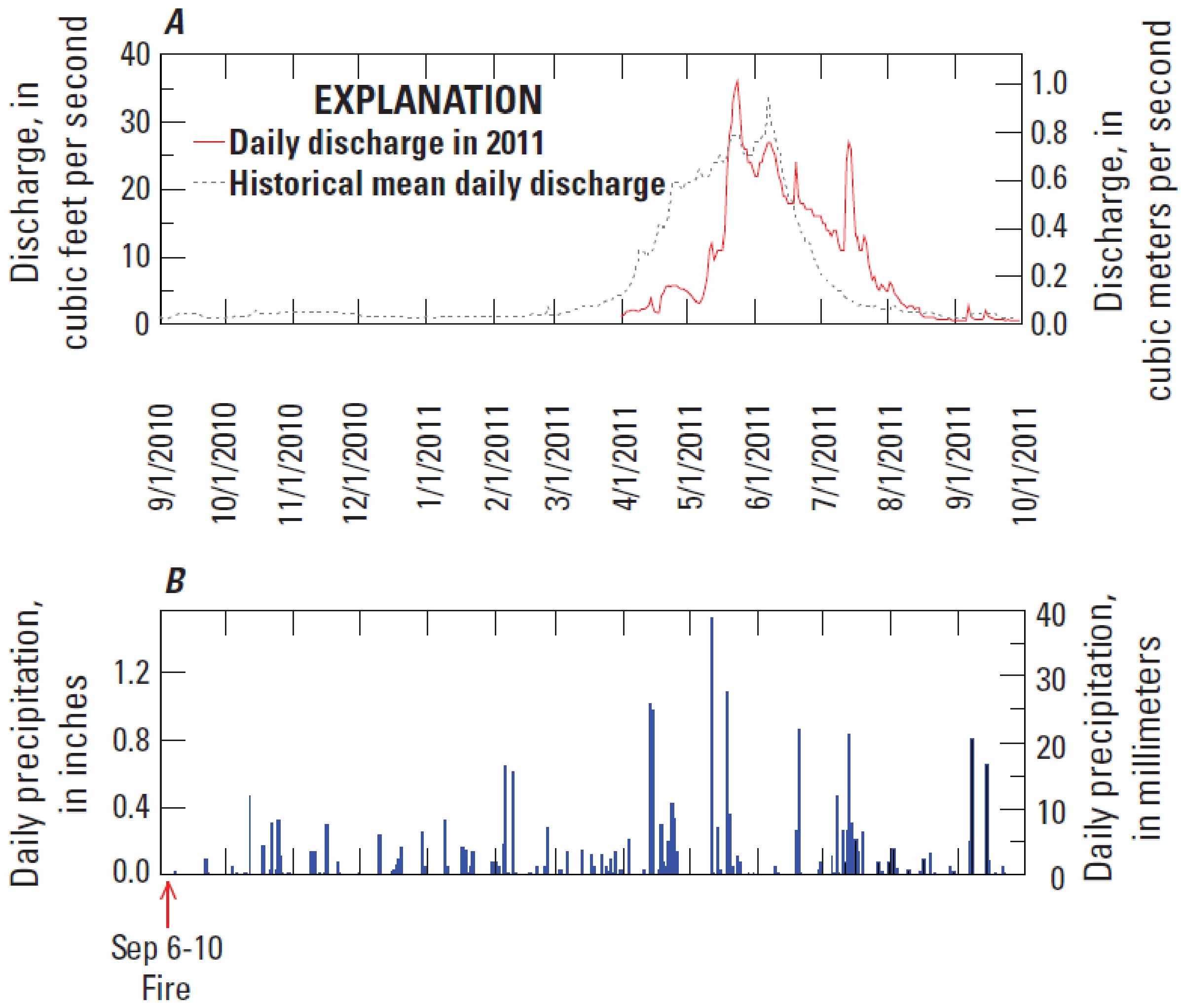

Figure 2.4 - A, Mean daily discharge in 2011 and historical mean daily discharge, Fourmile Creek. B, Daily precipitation. Data from Murphy et al., 2012.

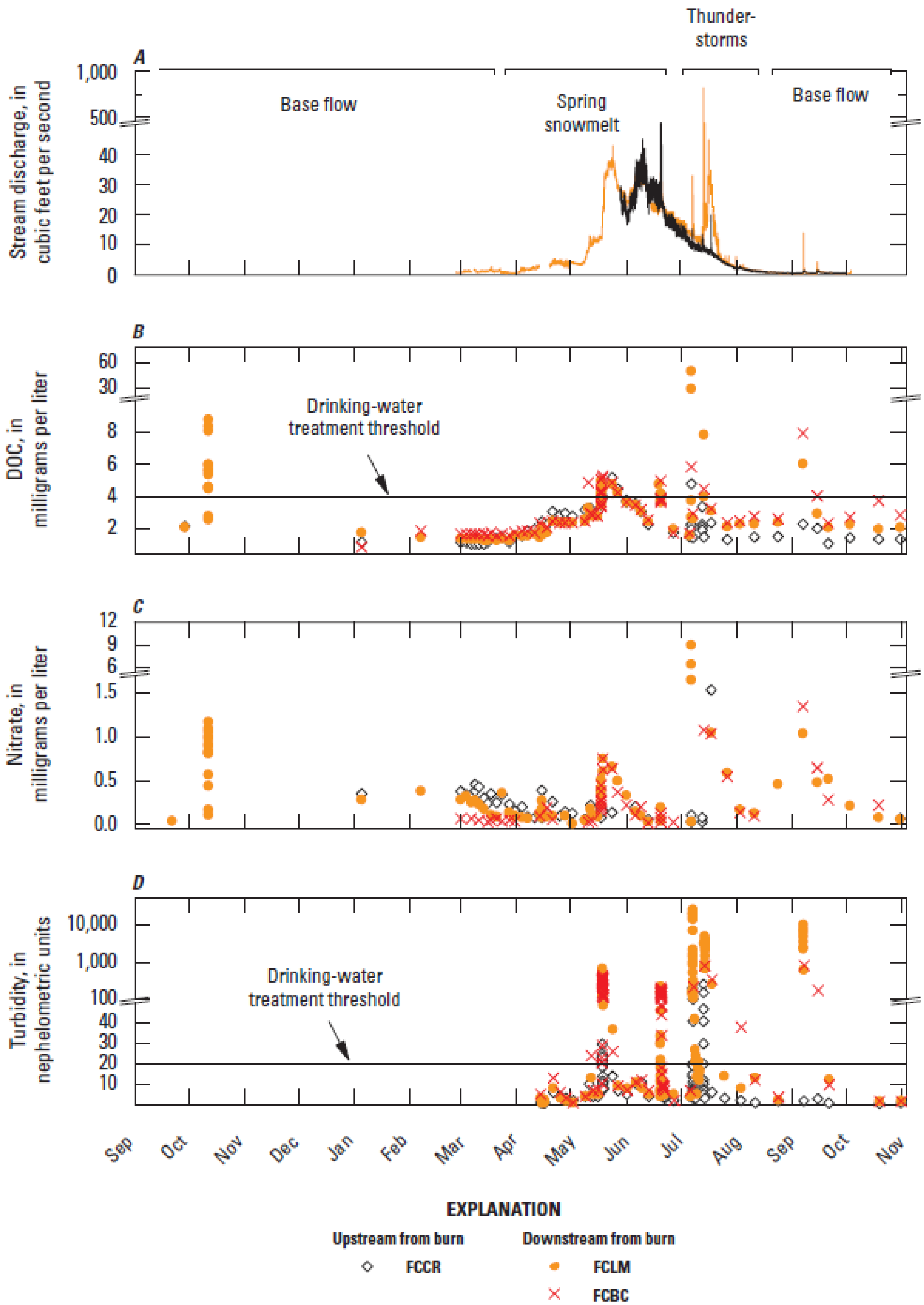

Figure 2.5 - Stream discharge at 5-minute intervals and selected water quality characteristics in 2010-2011 measured in Fourmile Creek, Colorado, at monitoring stations FCCR, FCLM, and FCBC (Writer et al., 2012).

2.6 Sediment yield – Sediment rating curve

Sediment yield by a stream or the stream sediment load is the total sediment delivered past a point of interest or the watershed outlet during any given time (Borah et al. 2007). The stream sediment load can be determined using either a short-term or a long-term analysis. The short-term analysis of sediment load is performed generally on a daily basis expressing often the magnitude and variability of sediment transport during rainstorm or snowmelt events (Julien 2010). On the other hand, the long-term sediment load analysis estimates the amount of sediment yielded by a stream. On an annual basis, it gives the mean annual sediment load of a stream (Julien 2010). The long-term sediment is utilized for reservoir sedimentation, sediment budget and degradation studies.

2.8.1. Daily sediment load or sediment rating curve

The sediment rating curve or daily total sediment discharge in tons per day is the product of the daily mean water discharge, the flux-averaged total sediment concentration, and a unit conversion factor, as expressed by Equation 2.1 (Julien 2010).

$$\mathrm{Q_s}(\text{metric tons/day}) = 0.864\, C_{mg/l}\mathrm{Q}(\text{in m}^3/\text{s}) \qquad \text{(Eq 2.1)}$$

Where:

$\mathrm{Q_s}$ = the total sediment discharge in tons per day;

$\mathrm{C_{mg/l}}$ = the flux averaged total sediment concentration in mg/l;

Q = the daily mean water discharge in m^3/s.

2.8.2. Annual sediment load

Two basic approaches can be used to determine the long-term average sediment load of a river: (1) the summation approach; and (2) the flow duration curve approach. The summation approach utilizes the mass curves method to determine the cumulative sediment load as function of time in years. The second approach combines a sediment-rating curve between total sediment discharge or flux-averaged concentration, and water discharge; and a flow-duration curve (Julien 2010)

2.7 Specific Degradation of the N'djili River Basin

As defined, sediment yield Y is the total sediment delivered past a point of interest or the basin outlet over a specified period of time and it is generally measured in tons per year. For a given watershed or basin, the specific degradation SD is obtained by dividing the yield Y by the drainage area A of the watershed. Therefore:

$$\mathrm{SD} = \frac{\mathrm{Y}}{\mathrm{A}} \qquad \text{(Eq 2.2)}$$

Where: SD = specific degradation in metric tons/km^2.year, A = drainage area in km^2.

2.8 Sediment Delivery Ratio

The sediment delivery ratio (S_{DR}) is the ratio of the sediment yield Y at a given stream cross-section to the gross erosion A_T from the watershed upstream of the measuring point (Julien 2010). The gross erosion A_T is the total soil eroded in a drainage area or watershed through interrill, rill, gully, and stream erosion processes. Therefore, the sediment delivery ratio is given by the expression:

$$\mathrm{S_{DR}} = \frac{\mathrm{Y}}{\mathrm{A_T}} \qquad \text{(Eq 2.3)}$$

Where: S_{DR} = sediment delivery ratio, A_T = gross erosion from the watershed upstream of the measuring point.

The sediment delivery ratio can be considered as the fraction of the gross erosion that is expected to be delivered to the point of the watershed under consideration. It is dependent upon drainage area size, watershed characteristics such as relief and stream length, sediment source and its proximity to the stream, transport system, and texture of the eroded material (Borah et al. 2007). Therefore, the sediment delivery ratio decreases with larger drainage areas which have more chance to trap sediment in lakes, reservoirs, and flood plains, reducing the amount of sediment reaching the streams. Also, for example, watershed with steep slope is more likely to have higher sediment delivery ratio than a watershed with mild to low slope. Moreover, watersheds with more bare soil are more likely to have a higher sediment delivery ratio compared to the same watershed with a forest cover. Taking into account the previous considerations, no generalized sediment delivery ratio relationship can be applied successfully to every situation. However, many studies established trends in the sediment delivery ratio for specific areas. The most common trend for sediment delivery ratio is the S_{DR} curve which establishes a relationship between the sediment delivery ratio and basin area. The following lines present different S_{DR} curves from The United States Soil Conservation Service (1971), Boyce (1975) and Renfro (1975).

2.8.1. Sediment delivery ratio based on United States Soil conservation Service (1971)

In 1971, the United States Soil Conservation Service developed a general sediment delivery ratio versus drainage area relationship from data of earlier studies, showing that the sediment delivery ratio varies approximately inversely as the 0.2 power of the drainage area in acres. Additional variables affect this relationship, since wide scatter of data has been used in this relationship. Table 2.1 shows some estimates of the delivery ratios.

Some considerations regarding other factors that may affect the values at a particular location lead to consider the sediment delivery ratios of Table 2.1 with caution. So, a higher delivery ratio should be used when the eroding soil is fine-textured (high in silt or clay content) and a lower one if the eroding soil is a coarse-textured (high in sand content).

Table 2.1 - General Sediment Delivery Ratios (Based on United States Soil Conservation Service (1971)).

Drainage Area (km^2)	Sediment delivery ratio
0.05	0.58
0.10	0.52
0.50	0.39
1	0.35
5	0.25
10	0.22
50	0.15
100	0.13
500	0.08
1000	0.06

2.8.2. Sediment delivery ratio after Renfro (1975)

In 1975, Renfro developed a relationship based on the Maner's (1962) equation, relating S_{DR} with drainage area. This relationship was derived from the sediment yield observation of 14 watersheds in the Blackland Prairie, Texas. The correlation between S_{DR} and drainage area (R^2 = 0.92) is expressed by:

$$\log(S_{DR}) = 1.7935 - 0.14191 \log(A) \qquad \text{(Eq 2.4)}$$

Where A is the drainage area in km^2, and S_{DR} is the sediment delivery ratio in percentage (%).

2.8.3. Sediment delivery ratio after Boyce (1975)

Boyce (1975) developed a relationship between sediment delivery ratio and drainage area by compiling and analyzing sediment yield observation from five areas in continental US. This relationship is:

$$S_{DR} = 0.41\, A_T^{-0.3} \qquad \text{(Eq 2.5)}$$

Where A_T is the drainage area in km^2, and S_{DR} is the sediment delivery ratio.

2.9 Geographic Information System and Soil Erosion Modeling

Geographic Information System (GIS) is a computerized system that can execute some spatial tasks including capturing, storing, integrating, analysis and visualization of data linked to coordinates or locations (ESRI 2005). GIS combines geostatistical analysis, database and cartography functions that allows the user to identify geographic information, relationships, patterns, and trends (Omar 2010).

GIS has been utilized the environmental management field since 1970s (Kim 2006). About twenty years later, GIS application began in hydrologic and hydraulic modeling as well as in flood mapping. According to Renschler and Harbor (2002), the Geographic Information System has emerged as a powerful decision-making tool allowing to handle spatial information and interaction with erosion models to help solve erosion problems.

The GIS software used in this study is ArcGIS 10.2. Because of satellite image treatment capabilities, the software Idrisi Selva 17.02 is coupled with ArcGIS 10.2 to implement the RUSLE factors and model the soil erosion rate in the N'djili River Basin. Figure 2.6 shows the procedures of the RUSLE implementation in ArcGIS and Idrisi.

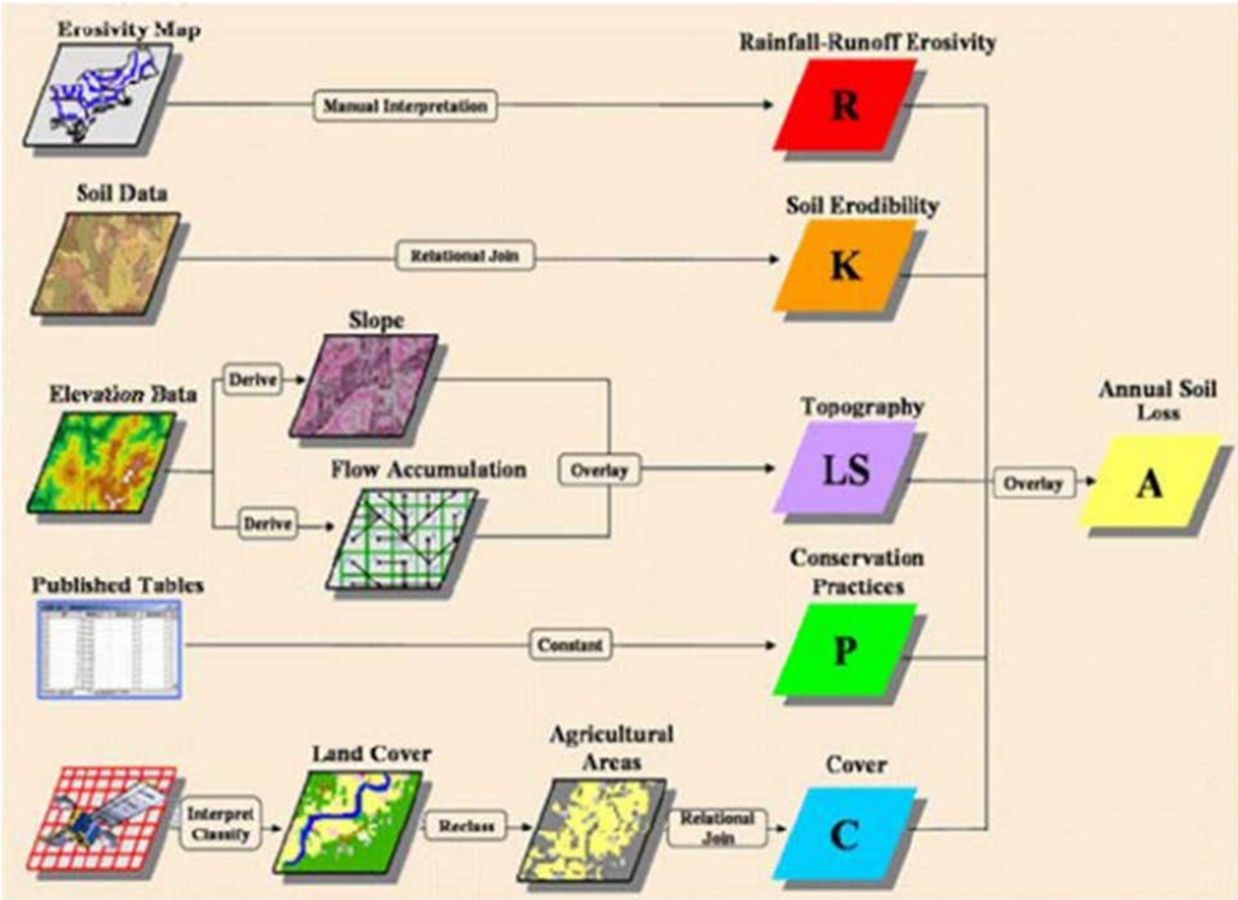

Figure 2.6 – Procedures of RUSLE implementation in ArcGIS (after Omar 2010)

CHAPTER 3 : SITE DESCRIPTION AND DATASET

Introduction

This chapter describes briefly the study area and the dataset used to perform the erosion and sedimentation study in the N'djili basin. Acquisition and pre-processing of topographic, precipitation, soil type and satellite image data are presented in detail.

3.1 Overview of the study area

The N'djili River Basin is located in the western part of the Democratic Republic of Congo, between - 4^{o} 21' to - 4^{o} 55' latitude and 15^{o} 07' to 15^{o} 36'longitude (Figure 3.1). Covering an area of about 2,097 km^2, the N'djili River basin lies between two districts of the Kinshasa City: Tshangu district (eastern part of Kinshasa City) and Mont Amba district (south western part of the Kinshasa city).

The N'djili River basin has several rivers, and the most important are the N'djili River and one of its tributaries, the Lukaya River. With two water supply plants built along the N'djili and the Lukaya Rivers and another one in project, the N'djili basin is the main potable water source of Kinshasa city (BCEOM 2006), providing almost 70% of its demand (about 365,000 m^3/day of potable water).

The average, maximum and minimum elevations of the N'djili basin are 428 m, 744 m(south eastern part of the basin) and 274 m respectively (at the basin outlet). In the meanwhile, the average, maximum and minimum slope are 16.2%, 148.4% and 0%, respectively. Maximum and minimum temperature ranges observed in the N'djili River are 28^{o} C – 38^{o}C and 16^{o} C – 21^{o}C, respectively.

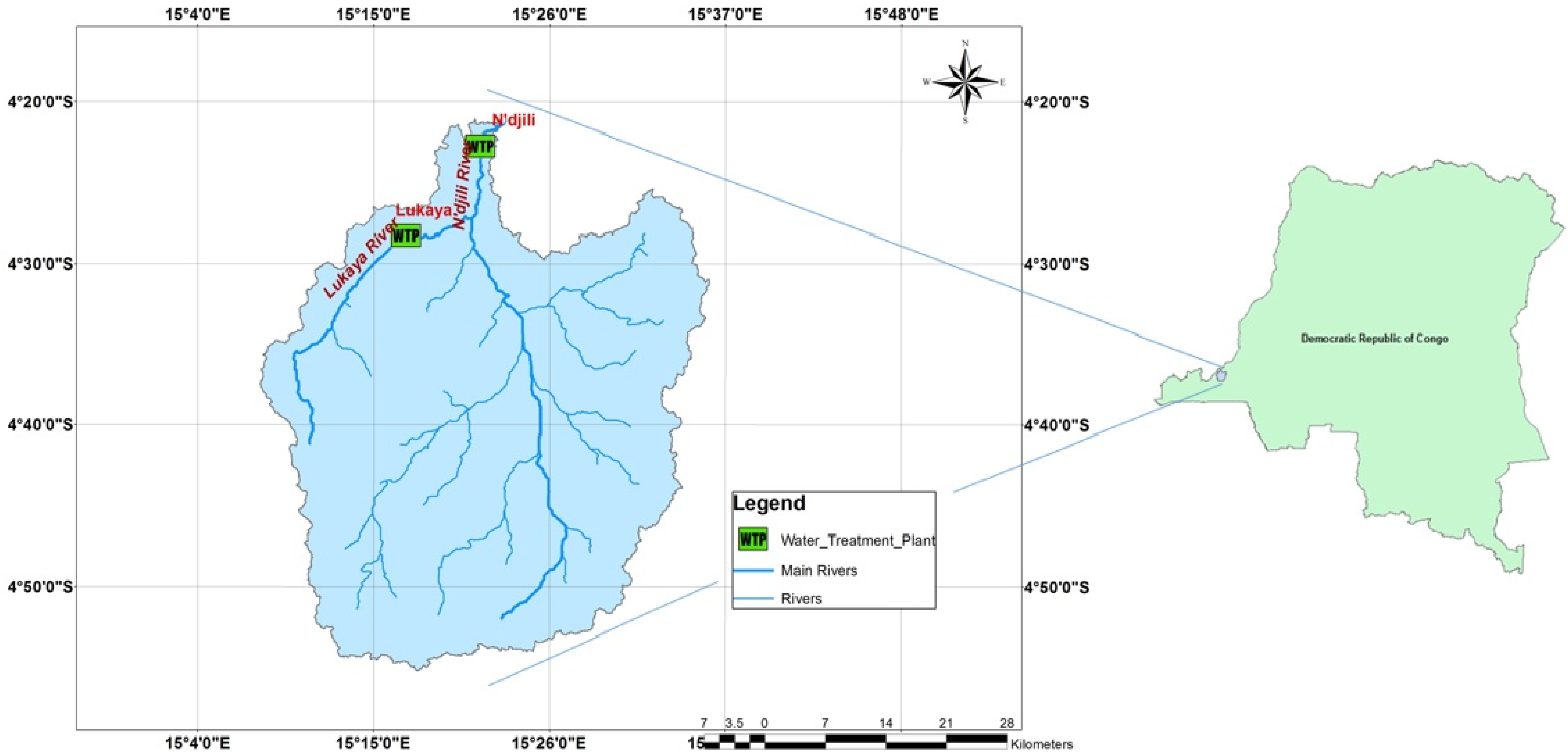

Figure 3.1 - Map of the N'djili River Basin

The precipitation rate in the N'djili basin is evenly distributed throughout the entire basin. The average annual precipitation is about 1470 mm. A tropical climate is observed over the basin, with 8 months of rain season and 4 months of dry season. More than 90% of the annual precipitation is during the rainy season (Figure 3.2).

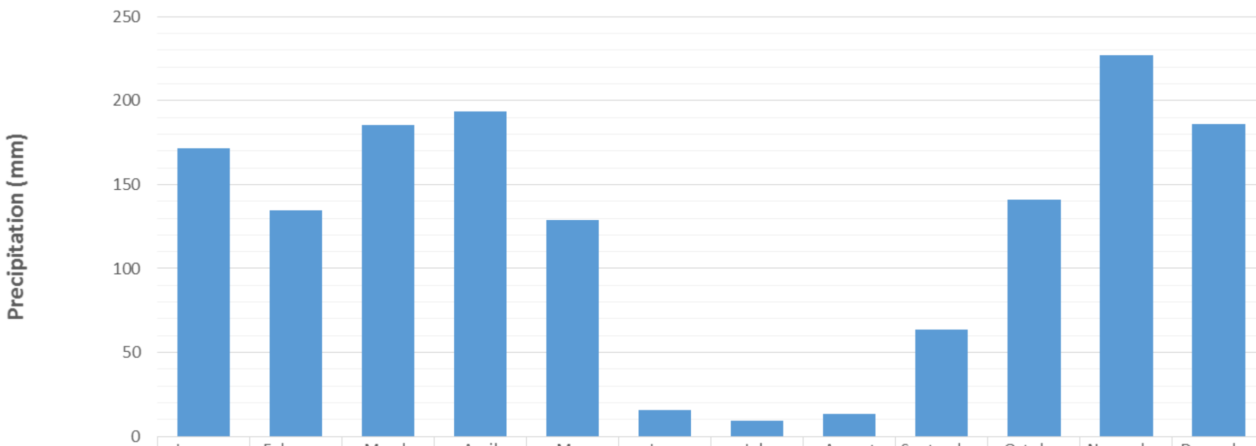

	January	February	March	April	May	June	July	August	September	October	November	December
Monthly Rainfall	171.5	134.6	185.2	193.6	128.7	15.7	9.2	13.4	63.8	141.1	227.2	186

Figure 3.2 - Monthly rainfall in the N'djili basin

The N'djili River is one of the most important tributaries of the Congo River in Kinshasa (Van Caillie 1983), flowing with an average discharge of 22 m^3/s through the eastern part of the Kinshasa city, from the south to the north where it enters the Congo River.

3.2 Data set of the N'djili basin

Several factors such as rainfall distribution and intensity, watershed topography, soil types, land cover and land use influence directly the soil erosion process. Because of institutional weaknesses and recurrent armed conflicts, data availability and quality for hydrologic and/or hydraulic study is a critical issue in the Democratic Republic of Congo. Since the N'djili River is one of the many ungauged rivers in Congo, this study relies on turbidity data measured at the intake of the N'djili water plant by National Water Utility (REGIDESO) and discharge data derived from measurements carried up by the Agriculture (Kabuya 2005) and Civil Engineering colleges of the University of Kinshasa, and by a private company, Opti-Plus. Moreover, some data such as land cover and land use maps for the DRC are available with coarse resolution (at least 1 km by 1 km) that does not fit most of watershed studies. Therefore, satellite images are used in this study to derive land cover and land use maps with the appropriate resolution (30 m by 30 m), rather than coarse land cover/use maps published by UN agencies.

To predict soil erosion and sediment delivery ratio in the N'djili River basin, the following dataset are required:

1) Digital elevation model (Data source: METI/NASA/USGS)
2) Average daily, monthly and annual precipitation Data (Source: METTELSAT)
3) Soil type map (Data source: SOTERCAF)
4) Satellite images (Source: NASA/USGS)
5) Turbidity and stream flow data (water surface level, sediment concentration, flow rating curve) (Data source: REGIDESO, Opti-Plus, COLLEGES of AGRICULTURE and NATURAL SCIENCES of the University of Kinshasa)

3.2.1. Digital Elevation Model

The DEM of the N'djili basin is presented in Figure 3.3. With a spatial resolution of 30 m x 30 m, this DEM is derived from the Advanced Spaceborne Thermal Emission and Reflection Radiometer (ASTER) Global Digital Elevation Model Version 2 (GDEM V2), released jointly on October 17, 2011 by the Ministry of Economy, Trade, and Industry (METI) of Japan and the United States National Aeronautics and Space Administration (NASA). This version 2 of ASTER GDEM has less voids than the previous one (ASTER GDEM V1) and gives better results than the SRTM DEM for flat areas (Guosong et al. 2010), like the major part of the

N'djili basin. Also, the spatial resolution of 30 m x 30 m is the determinant advantage for ASTER GDEM V2 over the SRTM DEM, which has a poor spatial resolution (90 m x 90 m).

According to Figure 3.3, the terrain elevation of the N'djili basin ranges from 274 m to 744 m, with an average of 428 m. Several basin and stream features can be determined from the DEM such as: elevation, slope steepness and slope length factors of the RUSLE model, drainage area, stream relief ratio, etc.

3.2.2. Precipitation Data

Daily average precipitation data were provided by the National Meteorological agency, (Agence Nationale de Météorologie et de Télédétection par satellite, METTELSAT), which is in charge of collecting precipitation data for the entire country since 1950s. For the N'djili basin, daily average precipitation data from 10 manual gauging stations located around (6 gauging stations) and inside of (5 gauging stations) the basin were obtained and processed to compute the rainfall runoff erosivity factor of the RUSLE method. The table 3.1 shows summarized information about these 10 stations: name, identification number, location, available recorded years and average annual precipitation.

According to Wischmeier and Smith (1978), at least 20 years of rainfall records should be used to compute the rainfall runoff erosivity factor of the RUSLE model in order to accommodate the variation of the climate. Also, the correct assessment of this rainfall runoff erosivity factor requires rain gauge recording at short time intervals (for example 1-10 min) no more than 30 minutes. So, since the data provided by METTELSAT are daily average and some gauging station for the N'djili basin show recording time less than 20 years, some limitation on calculating the rainfall runoff erosivity factor appears in this study. Figure 3.4 presents the location of the rain gauge stations around and inside of the N'djili River Basin.

Table 3.1 - Rainfall Gauge Stations of the N'djili basin

Station_Id	Rainfall station	Longitude	Latitude	Available recorded year	Average Precipitation (mm/year)
64210	N'djili	1.544	-4.39	1961-2006	1497
64220	Binza	1.524	-4.36	1961-2012	1468
64211	Ndolo	1.532	-4.32	1962-2004	1348
-	Rifflart	1.535	-4.42	1957-1983	1472
-	Kimwenza	1.529	-4.46	1957-1965	1491
-	Luzumu	1.536	-4.66	1956-1968	1486
-	Kasangulu	1.517	-4.59	1955-1990	1462
-	Luila	1.505	-4.54	1957-1984	1389
-	Kisembo	1.517	-4.66	1957-1977	1491
-	Kindamba	1.514	-4.75	1957-1981	1394

The Appendix A gathers detailed information about the annual average and monthly average rainfall by climatic stations.

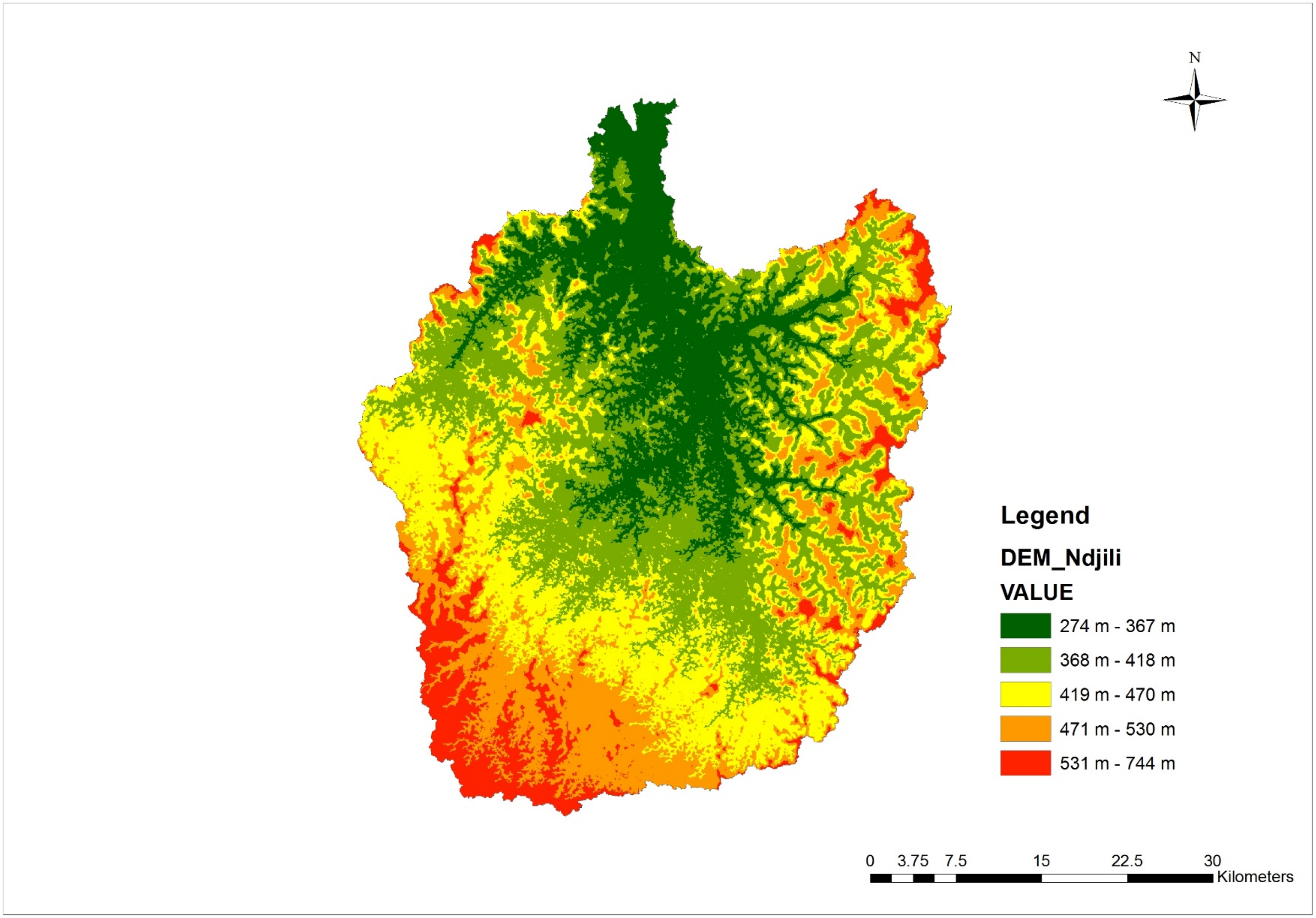

Figure 3.3 – Digital elevation model (DEM) of the N'djili River Basin

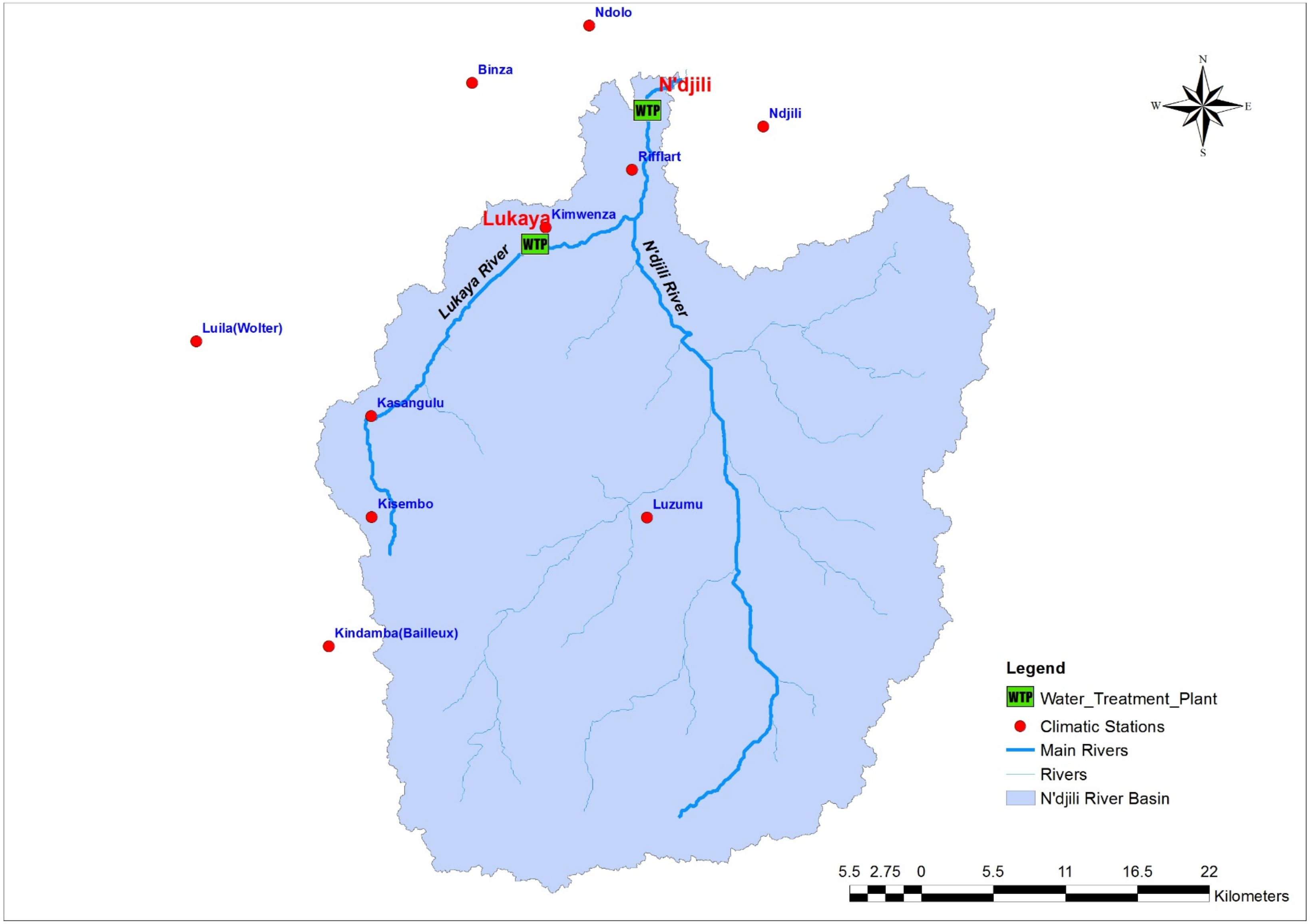

Figure 3.4 – Location of the climatic stations in and around the N'djili River Basin

3.2.3. Soil Classification Map

The soil classification map of the N'djili River Basin is based on the 1:2,000,000 map for the Democratic Republic of Congo compiled from the Soil and Terrain database of Central Africa (SOTERCAF, version 1.0) completed in November 2006. The SOTERCAF compilation has been jointly developed by the Soil Science Laboratory of the University of Ghent (Belgium) and the International Soil Reference and Information Centre (ISRIC) - World Soil Information, Wageningen under contract with the Food and Agriculture Organization of the United Nations (FAO), with the assistance of the Royal Museum for Central Africa (Tervuren, Belgium) and data holders in the DRC. The SOTERCAF derived physiographic units from SRTM grid data based on the Soil and Terrain (SOTER) landform definitions (FAO 2002).

ArcGIS layers were downloaded from the SOTERCAF and clipped over the N'djili River Basin. Using the Conversion tools of ArcToolbox, layers were converted to raster with a spatial resolution of 30 m x 30 m to meet the spatial resolution of other thematic maps used in the RUSLE model.

Based on the clipped soil classification map of the SOTERCAF presented in figure 3.5, three soil regions are encountered in the N'djili River Basin. The table 3.2 gives information about classification and soil texture of the N'djili Basin. The most prevalent texture in the basin is the sandy clay loam, covering about 88.7 % of the basin.

Table 3.2 - Soil classification of the N'djili River Basin

No	Soil classification	Soil texture	(%) of Sand	(%) of Silt	(%) of Clay	Covered Area (%)
1	Haplic Acrisols	Sandy clay loam	64	10	26	88.7
2	Ferralic Arenosols	Loamy sand	81	7	12	7.9
3	Ferralic Arenosols	Sand	95	4	1	3.4

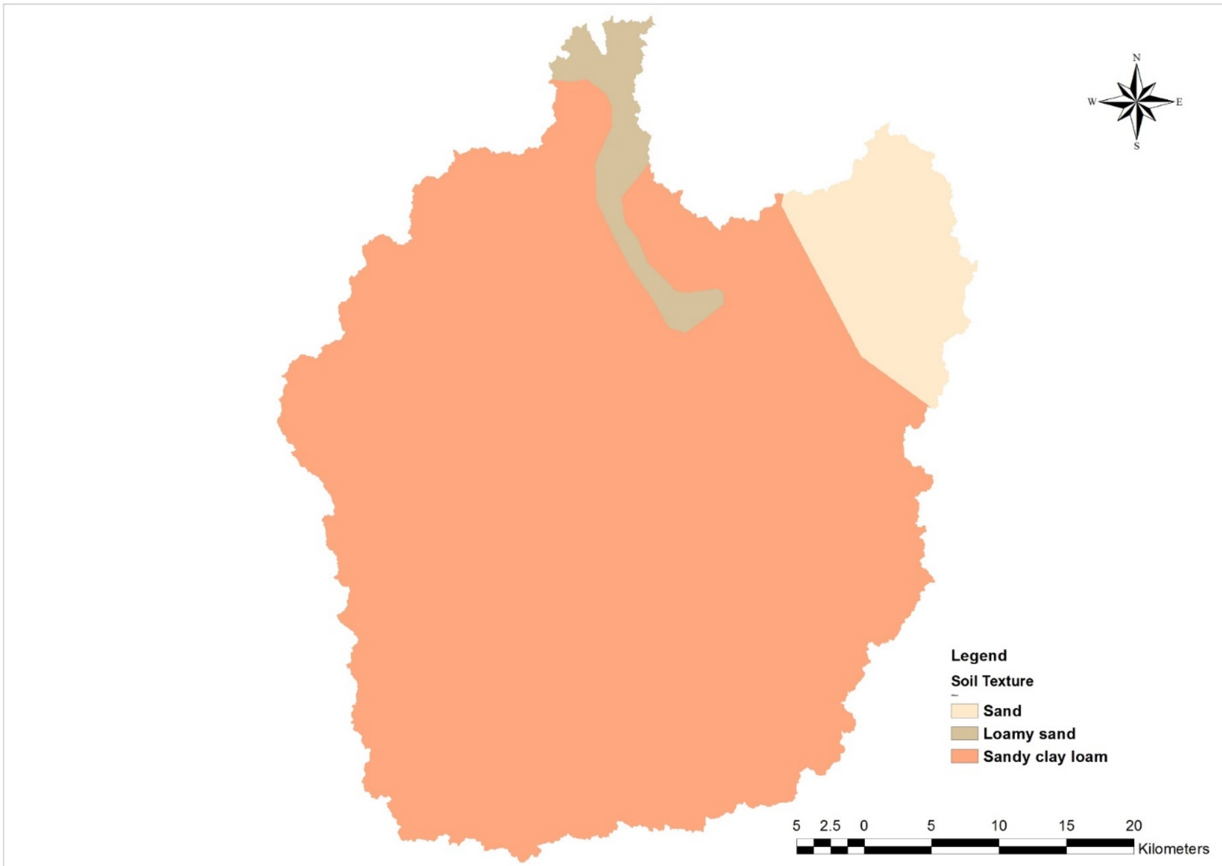

Figure 3.5 – Soil map of the N'djili River Basin

3.2.4. Satellite images

As briefly mentioned in the introduction of point 3.2, a land cover map covering the N'djili Basin is available from the FAO database, but with coarse resolution that doesn't fit the RUSLE modeling of a mid-size basin like the N'djili Basin. Therefore, the choice of creating N'djili Basin Land Cover Maps from the free satellite images became obvious.

To assess the impact of land cover variation over the N'djili basin, satellite images from the Landsat program – which is the longest enterprise for acquisition of satellite imagery of Earth - were selected.

With 8 Earth observation satellites launched since the beginning of the program in 1972, the instruments on the Landsat satellites have acquired millions of archived images which are a unique resource for global change research and applications in agriculture, cartography, geology, forestry, regional planning, surveillance and education (NASA 2000).

To closely study the effect of the temporal variation of land cover on the gross soil erosion in the N'djili basin, several Landsat scenes taken at different dates are required. Unfortunately, because of important percentage of cloud coverage over the N'djili basin and mainly the issue of the scan line corrector which affects the Landsat 7 mission since May 2003 (Chen et al. 2011), only few satellite images of acceptable quality are available over the basin. Since the scan line corrector failed on Landsat 7, images from this mission show gaps that can be corrected using the SLC-Off/SLC-Off Gap-filled Methodology (Chen et al. 2011), but this correction methodology may affect soil erosion prediction in an area like the N'djili Basin which experienced rapid land cover changes over a year.

Taking into account the constraints above mentioned, 3 Landsat scenes covering the N'djili basin (Path: 182, Row: 063) were downloaded from the USGS Earth Explorer. The table 3.3 presents the features of the downloaded images. It should be mentioned that the images were Level 1 products, preprocessed by the USGS before downloading. Figures 3.6, 3.7 and 3.8 show the false color composite images (Bands 3, 4, 5) of the downloaded scenes as assembled in ArcGIS. To perform a consistent analysis of the increase of soil erosion in the N'djili Basin, the 3 Landsat scenes should have been taken at the same date. Unfortunately, due to the issues previously developed, the last condition is not met.

3.2.5. Turbidity, Sediment and Stream Flow Data

As mentioned before, the N'djili River is an ungauged river. The only stream flow data and sediment data available were collected by some punctual projects or studies, such as the study carried out by the Agriculture College of the University of Kinshasa (Kabuya 2005), the rehabilitation project of the N'djili water treatment plant (SAFRICAS 2005), and the feasibility project for a new bridge across the N'djili River (Opti-Plus 2013). Turbidity data are collected by the National Water Utility (REGIDESO) on a daily basis.

Table 3.3 - Features of downloaded images

#	Date Acquired	Landsat Sensor	Landsat Scene identifier	Cloud cover (%)	Observations
1	2013/08/13	L8 OLI_TIRS	LC81820632013225LGN00	1.87	
2	2001/04/30	L7 ETM + SLC – on (1999-2003)	LE71820632001120EDC00	54.14	The cloud cover percentage over the N'djili basin is less than 10%.
3	1995/02/01	L4-5 TM	LT51820631995032XXX01	30	The cloud cover percentage over the N'djili basin is less than 10%.

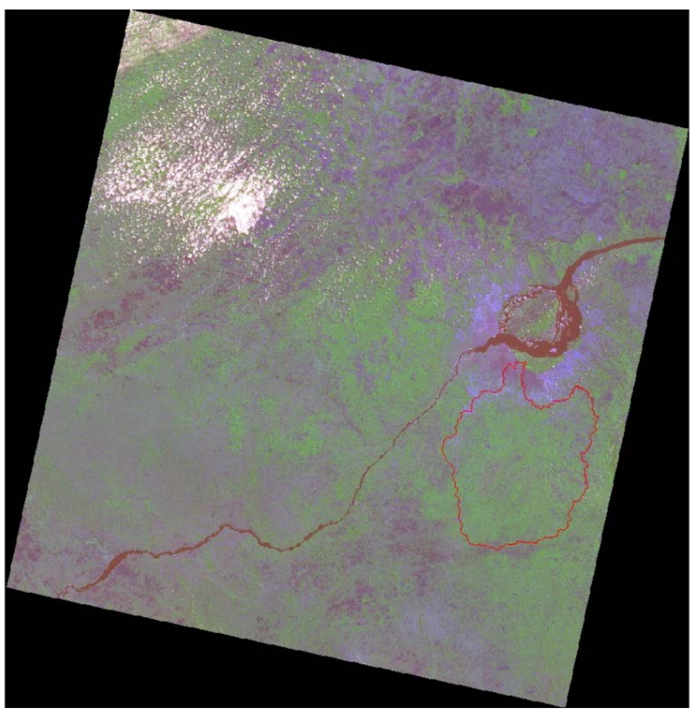

Figure 3.6 – False color composite image over the N'djili River Basin (outlined in red) on 2013/08/13

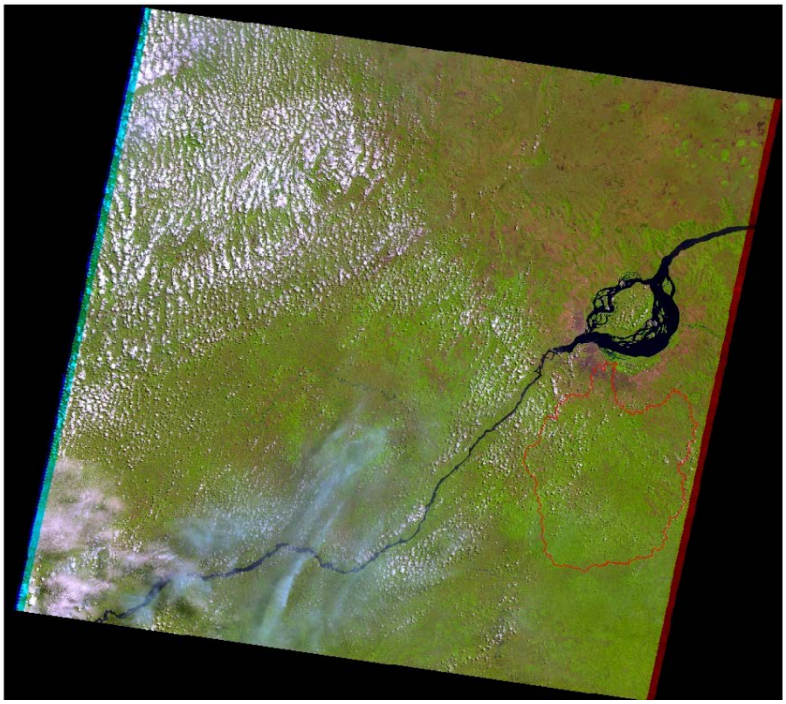

Figure 3.7 – False color composite image over the N'djili River Basin (outlined in red) on 2001/04/30

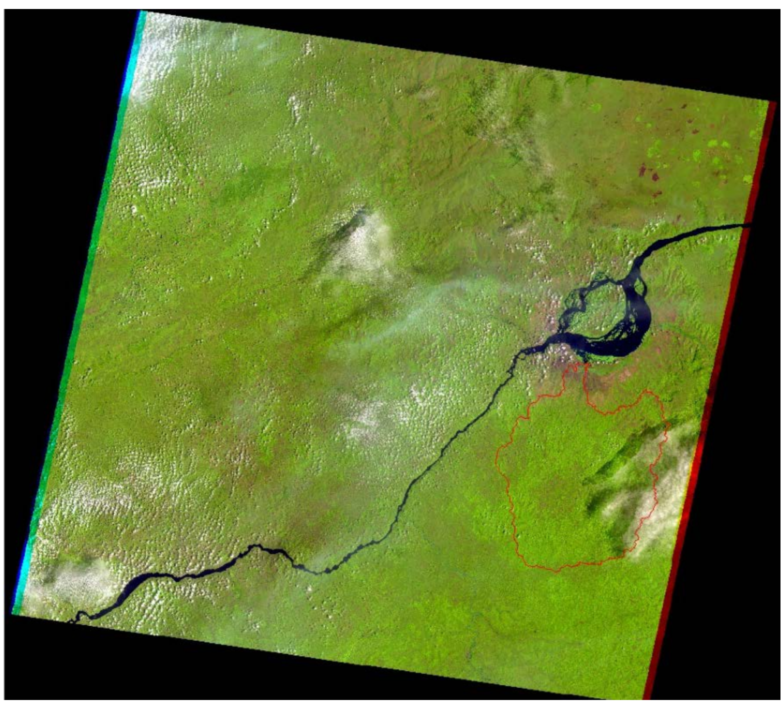

Figure 3.8 – False color composite image over the N'djili River Basin (outlined in red) on 1995/02/01

Turbidity and Sediment Data

Maximum, minimum and average daily turbidity data have been collected by the National Water Utility (REGIDESO) since the construction of the N'djili and Lukaya Water Treatment Plants respectively in 1970s and 2011. Unfortunately, sediment concentration vs turbidity curves are available only for the years 2005 and 2013. The 2005 - Sediment Concentration vs turbidity curve is derived from the Kabuya study for the Agriculture College (Kabuya 2005), while the 2013- relationship has been established by the College of Science of the Kinshasa University (Tshibangu 2014). Figures 3.9 and 3.10 present, respectively, the observed values of the turbidity in 2005 and 2013 and the turbidity exceedance probability curves for years 2000, 2005 and 2013. Figure 3.11 shows the sediment concentration vs turbidity curves for the same years. Two regression relationships between the turbidity and the TSS are derived from Figure 3.11 (Equations 3.1 and 3.2)

$$\text{Log TSS} = 0.9269 \log \text{NTU} + 0.613, \text{ for 2005} \quad \text{(Eq 3.1)}$$

$$\text{Log TSS} = 0.9327 \log \text{NTU} + 0.6306, \text{ for 2013} \quad \text{(Eq 3.2)}$$

Where:

TSS = total suspended solid expressed in mg/l;

NTU = the turbidity, expressed in Nephelometric Turbidity Unit

More details on observed values of turbidity are presented in Appendix A, including the turbidity exceedance probability curves for each year since 2000.

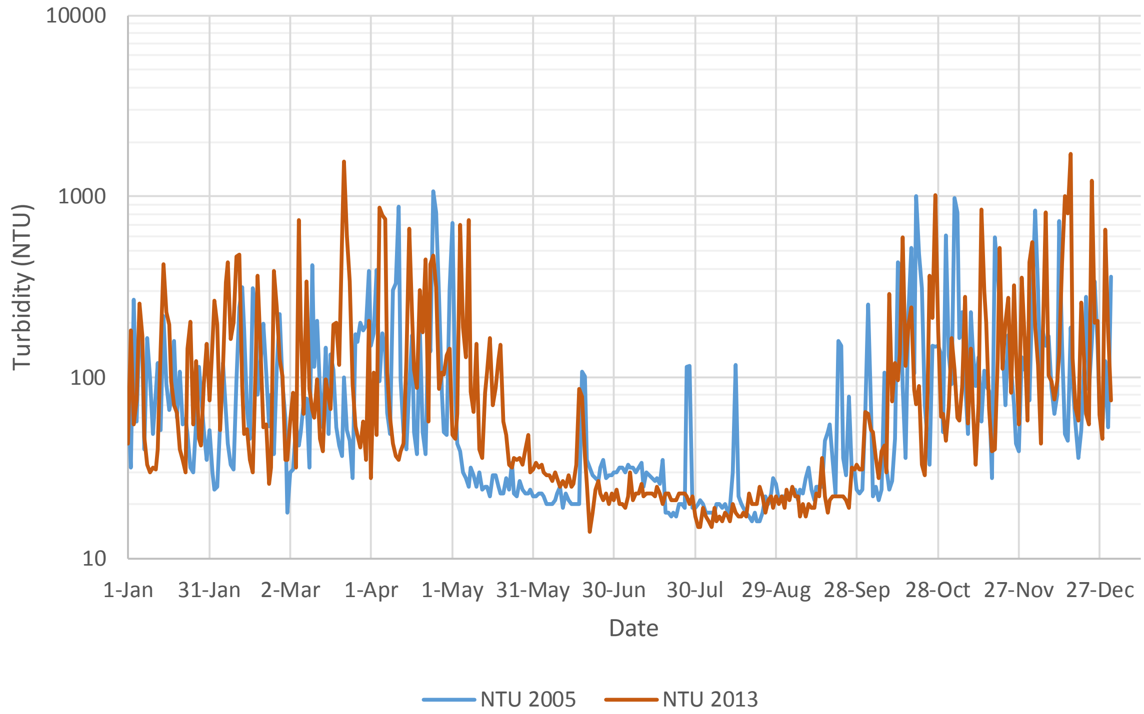

Figure 3.9 -: Observed values of turbidity in 2005 and 2013

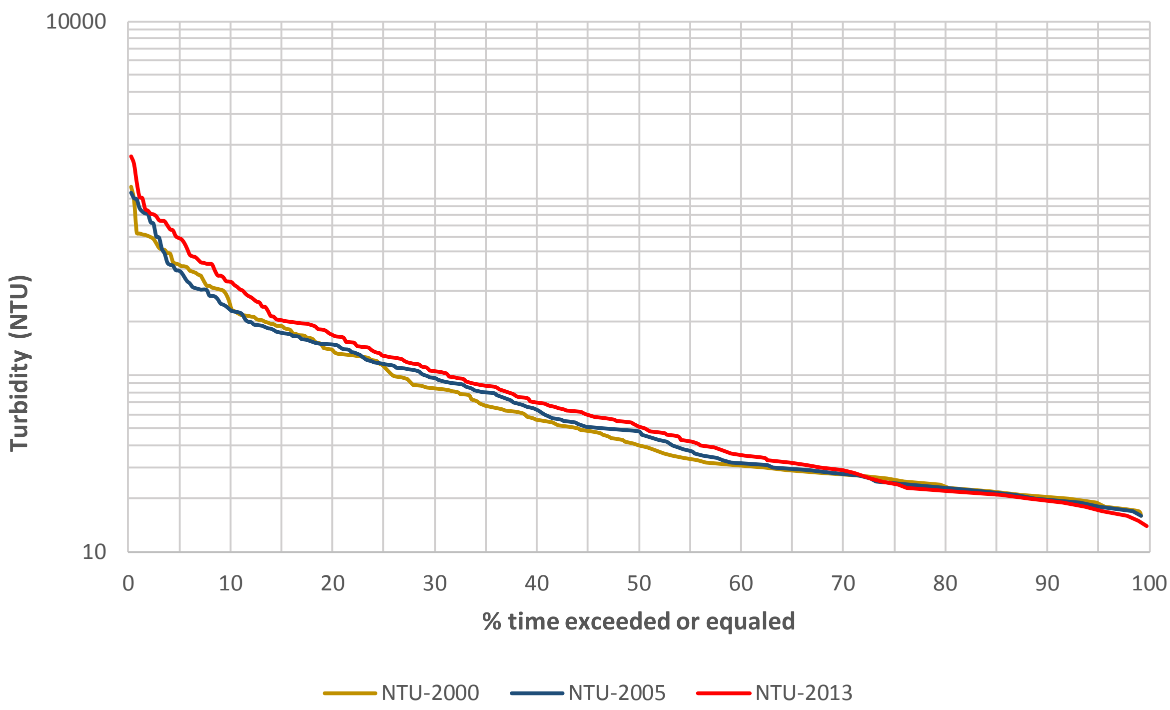

Figure 3.10 -: Turbidity exceedance probability curves for years 2000, 2005 and 2013

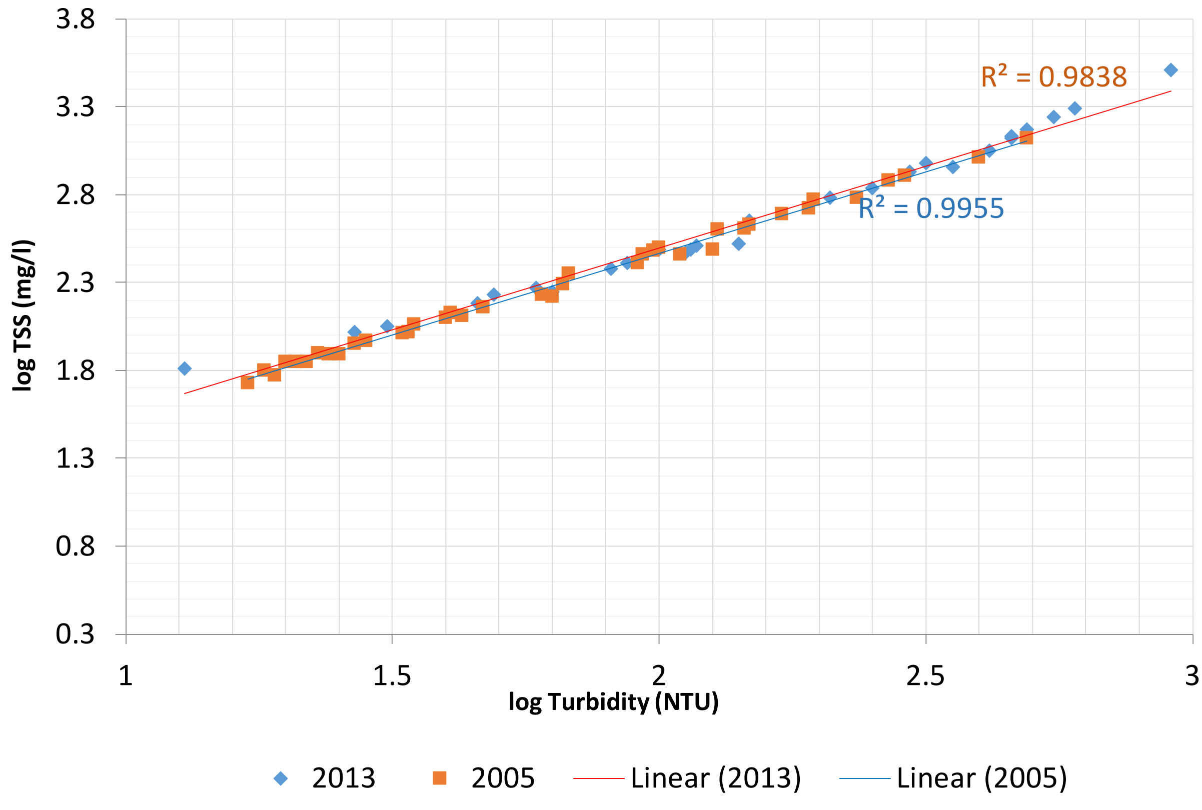

Figure 3.11 - Sediment concentration vs Turbidity in 2005 and 2013

Stream Flow Data

Water depth data have been collected by the Kabuya study (Kabuya 2005) and the Congolese Engineering firm SAFRICAS (SAFRICAS 2005) during the rehabilitation project of the water intake of the N'djili Water treatment plant in 2005. Using the flow rating curve of this section, discharge values related to these water depths have been computed. In 2013, a local private company, Opti-Plus, conducted 2 flow measurement campaigns at the N'djili Station 2 and upstream at the location selected for the new bridge across the N'djili River. Figure 3.12 shows the flow rating curve at the intake section (N'djili Station 2). Figure 3.13 presents the observed values at the N'djili Station 2 derived from the measured water depth using the flow rating curve at this section.

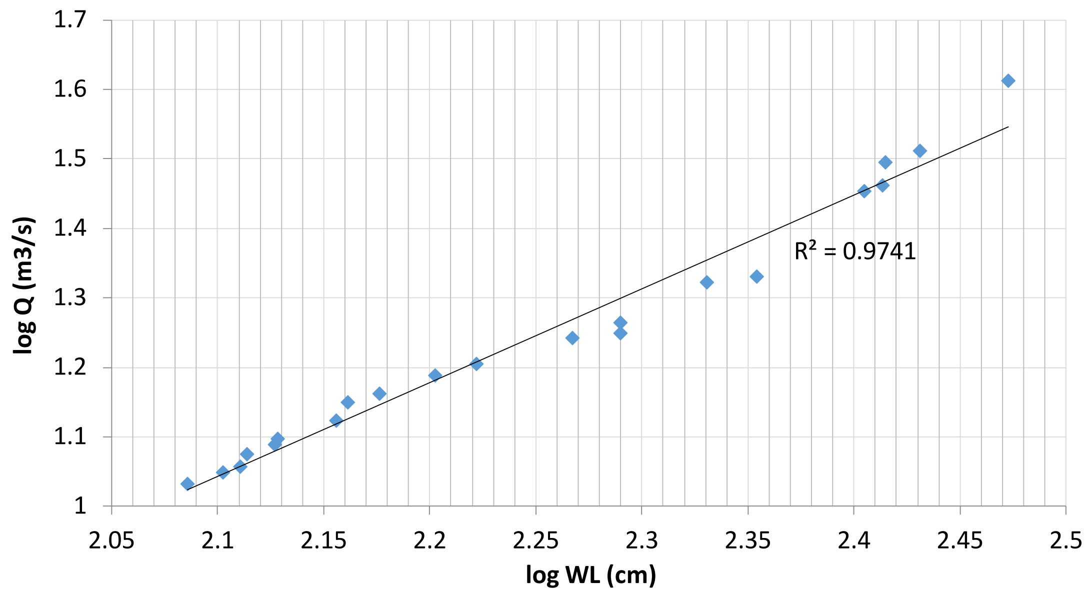

Figure 3.12 - Flow rating curve at the N'djili Station 2

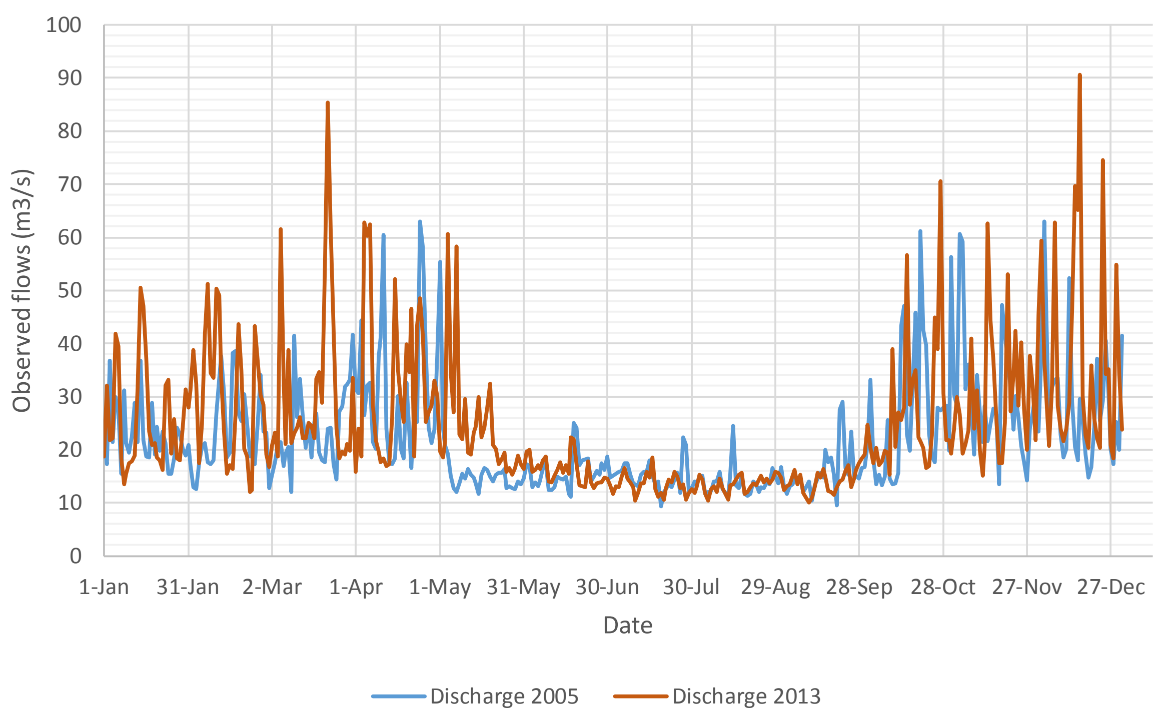

Figure 3.13 - Observed flow in 2005 and 2013 at N'djili Station 2

3.3 Summary

Chapter 3 describes the area of study and the datasets available for the study: topography, daily, monthly and average annual precipitation, soil types, satellite images, turbidity and stream flow data. These data are the input for the soil erosion modeling with the RUSLE equation. Chapter 4 will presents the use of DEM data to compute the slope length – slope steepness factor (LS) map, the development of the rainfall-runoff erosivity factor (R) map from the average annual precipitation, the derivation of the soil erodibility factor (K) map from the soil type map and the land cover classification map from Landsat images to predict the cover management factor (C). Chapter 4 will also present the methodology used to conduct a laboratory experiment whose the goal was to study the effect of ash concentration on the water turbidity.

CHAPTER 4 : METHODOLOGY, PARAMETER ESTIMATION AND MAPPING

Introduction

This chapter describes the concepts of the RUSLE model and the methods to estimate the annual average soil loss rate using the RUSLE equation in a GIS environment. Section 4.1 presents the methods for the RUSLE parameter estimation, the mapping procedures used to derive maps of the soil erosion parameters, and the methodology used to perform a laboratory experiment for measuring the effect of ash concentration on turbidity. In section 4.2, a summary and discussion on the results obtained in section 1 are presented.

4.1. RUSLE parameter estimation

The main factors affecting soil erosion are topography, climate, soil, vegetation, land use, and man-made developments (Shen and Julien 2013). Of these, climate is assumed to be beyond human control, and vegetation – and to a lesser extent soil and topography – may be controlled through management (Borah et al. 2008). Predictions of soil erosion and sediment yield are necessary for guiding the making of rational decisions in conservation planning. Therefore, soil erosion prediction equations are developed to enable planners to predict the average rate of soil erosion for alternative combinations of cropping systems, management techniques, and erosion-control practices on any particular site (Borah et al. 2008). These equations combine the factors representing these erosion-influencing characteristics. One of these equations is the Universal Soil Loss Equation (USLE) developed originally by Wischmeier and Smith (1965; 1978). The relationships in the USLE are based on thousands of plot-years of data from runoff plots and small watersheds. The USLE predicts soil loss from sheet or interrill erosion and rill erosion from roughly planar hillslope areas (Borah et al. 2008). Using this equation, land management planners can estimate average annual soil erosion rates from upland slopes for a wide range of rainfall, slope, soil, cover, and management conditions. This equation is a good asset for land management planners to select alternative cover and management combinations that would limit erosion rates to acceptable levels.

In 1997, a revised version of the USLE (RUSLE) was developed (Renard et al. 1997). This revised version is widely used in computer applications and allows more detailed consideration of farming practices and topography for soil erosion prediction. The RUSLE model also represents the impact of climate, soil, topography, and land use combination on rill and interril soil erosion caused by raindrop impact and surface runoff (Renard et al. 1997). In the RUSLE model, it is assumed that soil detachment and deposition are controlled by the sediment load in the flow. Also, it assumed that the erosion, which is not source limited, is only limited by the flow capacity. Under this condition, soil detachment can no longer occur once the sediment load exceeds the sediment flow capacity. The following equation is used by both USLE and RUSLE to compute average annual soil erosion expected on upland (field) slopes:

$$A = R \cdot K \cdot L \cdot S \cdot C \cdot P \qquad \text{(Eq 4.1)}$$

Where:

A = computed spatial and temporal average soil loss per unit area, expressed in the units selected for K and for the period selected for R. In practice, K and R are selected so that A is expressed in tons/acre/year or tons/ha/year.

R = rainfall-runoff erosivity factor – the rainfall erosion index plus a factor for any significant runoff from snowmelt.

K = soil erodibility factor – the soil-loss rate per erosion index unit for a specific soil as measured on a standard plot, which is defined as a 72.6-ft (22.1-m) length of uniform 9% slope in continuous clean-tilled fallow.

L = slope length factor – the ratio of soil loss from the field slope length to soil loss from a 72.6-ft length under identical conditions.

S = slope steepness factor – the ratio of soil loss from the field slope gradient to soil loss from a 9% slope under otherwise identical conditions.

C = cover-management factor – the ratio of soil loss from an area with specified cover and management to soil loss from an identical area in tilled continuous fallow.

P = support practice factor – the ratio of soil loss with a support practice such as contouring, strip cropping, or terracing to soil loss with straight-row farming up and down the slope.

L and S are the topographic-influencing factors of the soil erosion, while C and P are the cropping and management systems factors of influence of the soil erosion. L, S, C and P are dimensionless and normalized with respect to the unit plot conditions along with R and K factors, in accordance with the Agriculture Handbook 703.

4.1.1 Rainfall-Runoff Erosivity Factor (R)

The rainfall-runoff erosivity factor R quantifies the effects of raindrop impact and reflects the amount and rate of runoff likely to be associated with rain (Renard et al. 1997). By holding factors other than rainfall constant, field data indicate that soil losses from cultivated fields are directly proportional to the total storm energy (E) times the maximum 30-min intensity I_{30} (Borah et al 2008). Accordingly, the long-term average product of the total storm energy (E) and the maximum 30-min rainfall intensity (I_{30}) is, by definition, the R factor. The R factor used to estimate average annual soil loss A, must include the cumulative effects of the many moderate-sized storms as well as the effects of the occasional severe ones.

To compute the rainfall-runoff erosivity factor using the original method described by Wischmeier and Smith (1978) and by Renard et al. (1994), extended pluviographical records over a period of 20 years at least, with temporal resolution less than or equal to 30 minutes are strictly required to accommodate apparent cyclical rainfall patterns. However, in many parts of the world like in Central Africa, this kind of information is difficult to obtain and its processing is time-consuming and hardworking (Bertoni and Neto 1990).

For areas without data and/ or resources required to compute the R-factor values, a general approach has been used by several researches over the world to compute this factor using monthly or annual precipitation data, easier to obtain in most parts of the world. This general approach is based on the extrapolated relationship between R-values estimated from climatic stations having the required data and the associated precipitation data (monthly or annual precipitation data). Renard and Freimund (1994) summarized this general approach in the four following steps:

(1) R-factor values are computed by the original prescribed method (Wischmeier and Smith, 1978; Renard and Freimund 1994) for stations with recording rain gages;

(2) a relation between the computed R-values and more readily available types of precipitation data (monthly or annual totals) is established;

(3) the relation is extrapolated and R-values estimated for stations with the associated precipitation data;

(4) isolines are drawn between stations and R-values for sites between isoerodents are estimated by linear interpolation.

Several authors have used this approach to develop R-value selection guidelines or isoerodents maps for many parts of the world (Stocking and Elwell, 1976; Rose, 1977; Arnoldus, 1977; Bollinne et al., 1980; Smithen and Schulze, 1982; Lo et al., 1985, Bertoni and Lombardi Neto, 1990; Renard and Freimund, 1994; Yu and Rosewell, 1996; Mikhailova et al., 1997; Torri et al., 2006).

For the N'djili River basin case for which no rainfall intensity or rainfall-runoff erosivity data are available, this study focuses on relationships developed by Renard and Freimund (1994), and Rose (1977) to derive rainfall-runoff erosivity factor for estimating the annual average soil loss of the basin.

The Renard and Freimund's method (1994) for estimating the R-values for climatic stations without long-term rainfall intensity data was developed after analyzing available R-factor from isoerodent maps and the annual precipitation data from 155 gauge stations in continental USA. The method proposed the following equations for estimating the R-factor:

$$R = 0.04830\ P^{1.610}, \qquad P < 850\ \text{mm} \qquad \text{(Eq 4.2)}$$

$$R = 587.7 - 1.219P + 0.004105P^2, \qquad P \geq 850\ \text{mm} \qquad \text{(Eq 4.3)}$$

Where:

R = the annual rainfall erosivity, expressed in Mj · mm · ha^{-1} · h^{-1}· $year^{-1}$;
P = the annual precipitation (mm).

The results obtained using the Renard and Freimund relationship are presented in the table 4.1.

In 1977, Rose derived a simple relation between the average annual R and the average annual rainfall P for West Africa. This relationship is based on rain gage records over 5 – 10 years period from 20 meteorological stations in Ivory Coast, Burkina Faso, Senegal, Niger, Chad, Cameroon and Madagascar. The derived relationship is:

$$R = \alpha P \qquad \text{(Eq 4.4)}$$

With:

$$0.45 \leq \alpha \leq 0.55 \qquad \text{(Eq 4.5)}$$

Where:

R = the annual rainfall erosivity, expressed in ft · tons · inch · $acre^{-1}$ · h^{-1}· $year^{-1}$;
P = the annual precipitation (mm).

The Rose relationship is not valid for stations in mountainous regions, for stations directly on the coast, or for stations in the tropical zones between unimodal and bimodal annual rainfall distributions. Since the stations used to derive the rainfall-runoff erosivity factor of the N'djili basin meet the Rose's relationship conditions, the results found by applying his equations can be found in the table 4.1. The table 4.1 gives the results obtained to derive the rainfall-runoff erosivity factor using the Renard and Freimund's method both in SI and US customary units, and the Rose equation in US customary units.

R-values of the N'djili basin from the Renard and Freimund's equation along with those derived from the Rose's expression have been verified for reasonability before using them in the RUSLE model. Due to the similar annual average precipitation and climatic patterns to the N'djili basin, 475 values from the Database of USDA Natural Resources Conservation Service (NRCS) of the rainfall-runoff erosivity factor of counties in states of Alabama, Arkansas, Georgia, Louisiana, Mississippi, Puerto Rico, South Carolina and Tennessee were selected to perform this verification (Figure 4.1). By analyzing the results presented in Figure 4.1, it can be noted that the R values computed using the relationships developed by Renard and Freimund are similar to values of rainfall-runoff erosivity factor from the eight states, in contrast of R-values derived using the Rose's equation. It can also be noticed that the values computed with the Rose's equation are greater than those observed in the eight states for the same amount of annual precipitation.

Based on the reasonability verification performed using the results plotted in Figure 4.1, the R-factor values computed for the stations of the N'djili basin using the Renard and Freimund's equations will be used throughout this study. Results obtained by applying the Precipitation – Erosivity Factor relationships from Bols (1978), Yu and Rosewell (1996), Mikhailova et al. (1997), Torri et al. (2006) on the N'djili data have been added to Figure 4.1. The Appendix B presents detailed information on these relationships and on the data from the eight states used for the reasonability verification.

To use the R-factor values derived for the N'djili basin for the soil erosion prediction in the ArcGIS environment, an interpolated surface must be created from the R-values at each station. Two sets of interpolation methods can be used for this purpose: deterministic interpolation methods and geostatistical interpolation methods. Deterministic interpolation refers to non-statistical methods that use the measured values at each point to determine values at the remaining locations across the surface. On the other hand, geostatistical interpolation methods use statistics based on measured points to statistically predict the remaining locations' values across the surface. The main advantage of geostatistical methods is that they provide standard error values to indicate the accuracy of the predictions (Krivoruchko 2011). The geostatistical interpolation technique widely used is the Kriging method. Before applying this method for spatial interpolation, some assumptions related to the method must be verified. Unfortunately, normal distribution and stationarity assumptions for data are not verified for the N'djili R-values.

Since the Kriging method is not appropriate for the N'djili Basin data, deterministic interpolation methods have been selected to create an interpolated surface of R-values for the N'djili basin. Using cross validation criteria based on the mean and the root-mean-square, the Inverse Distance Weighting method (IDW) appears to be the best deterministic method. Inverse distance weighting is a commonly used deterministic interpolation method. It predicts cell values at unknown locations based on the distance between the unknown cell and the known points. In this method, a power option can be used to limit the influence of distant points.

Table 4.1 - Rainfall-runoff erosivity factor

Station_Id	Rainfall_ station	Longitude	Latitude	Average Precipitation (mm/year)	Reinard and Freimund (1994)		Rose (1977)	
					R-factor SI Units	R-factor US Units	Maximum R-factor US Units	Minimum R-factor US Units
64210	Ndjili	1.544	-4.39	1497	7962	468	823	674
64220	Binza	1.524	-4.36	1468	7645	449	807	661
64211	Ndolo	1.532	-4.32	1348	6404	376	741	607
-	Rifflart	1.535	-4.42	1472	7688	452	810	662
-	Kimwenza	1.529	-4.46	1491	7896	464	820	671
-	Luzumu	1.536	-4.66	1486	7841	461	817	669
-	Kasangulu	1.517	-4.59	1462	7580	445	804	658
-	Luila	1.505	-4.54	1389	6814	400	764	625
-	Kisembo	1.517	-4.66	1491	7896	464	820	671
-	Kindamba	1.514	-4.75	1394	6865	403	767	627

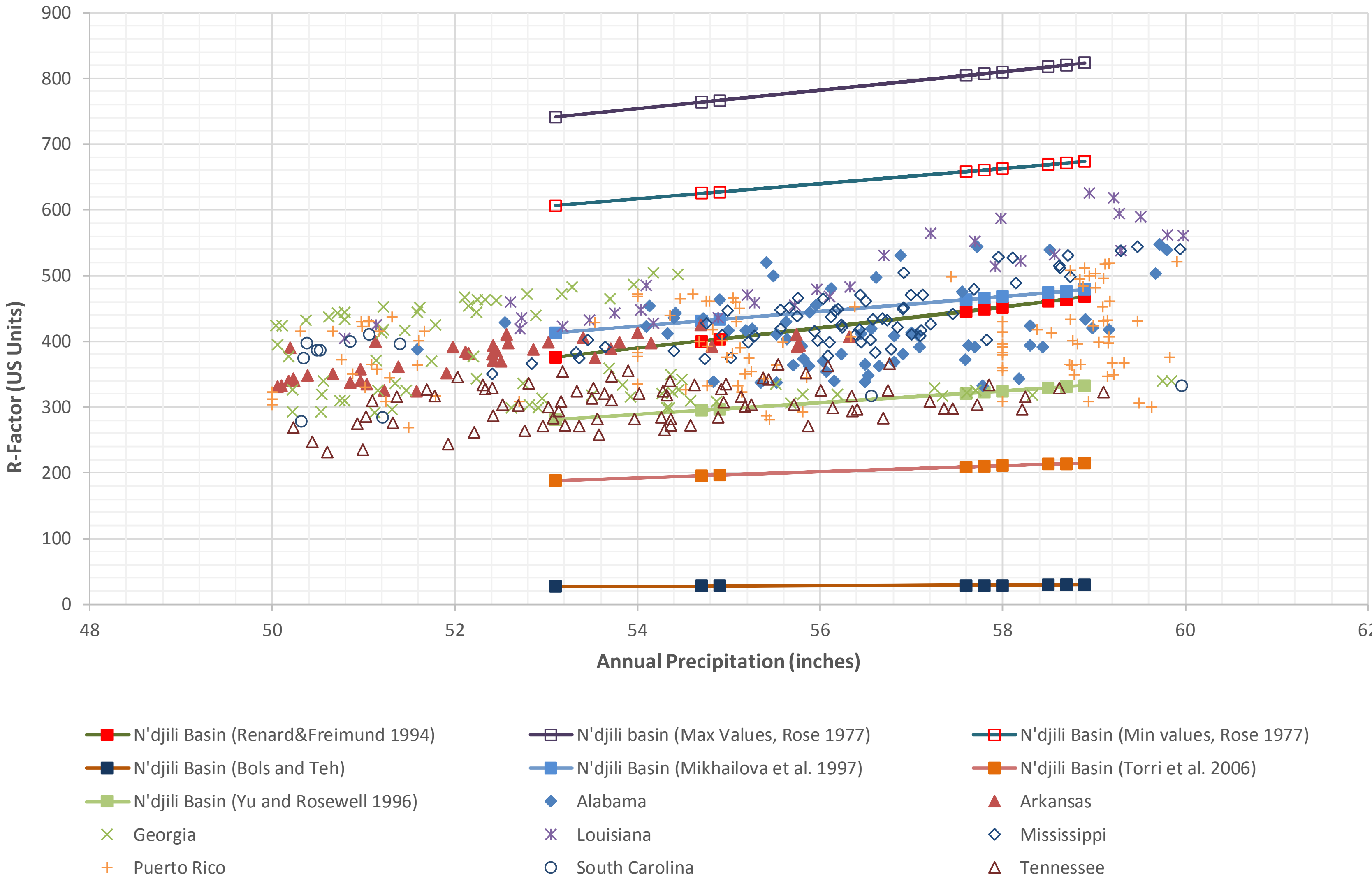

Figure 4.1 - Comparison of Erosivity Factor (R) between USA and N'djili Basin stations

Since this method doesn't make statistical assumptions about the data, it can replace more advanced interpolation methods where they are not appropriate (Krivoruchko 2011). In Appendix B, the assessment of different deterministic methods applied for the N'djili R–values is presented. The optimized surface derived from this process using IDW served to build the isohyetal and isoerodent map of the N'djili river basin. It should be noticed that the raster surfaces from which these maps are derived were built by setting up a cell size grid of 30 m to accommodate the spatial resolution of other thematic maps required to build the RUSLE model of the N'djili Basin.

Figure 4.2 and 4.3 present isohyetal and isoerodent maps of the N'djili river basin respectively. From the annual average precipitation distribution in the basin as shown in Figure 4.2, the maximum value of 1494 mm is observed in the northeastern part of the basin which is under the influence of the "Pool Malebo", while the minimum value of 1362 mm is observed in the northwestern part of the basin. From Figure 4.3, the rainfall-runoff erosivity factors (R) range from 385 to 466 throughout the basin.

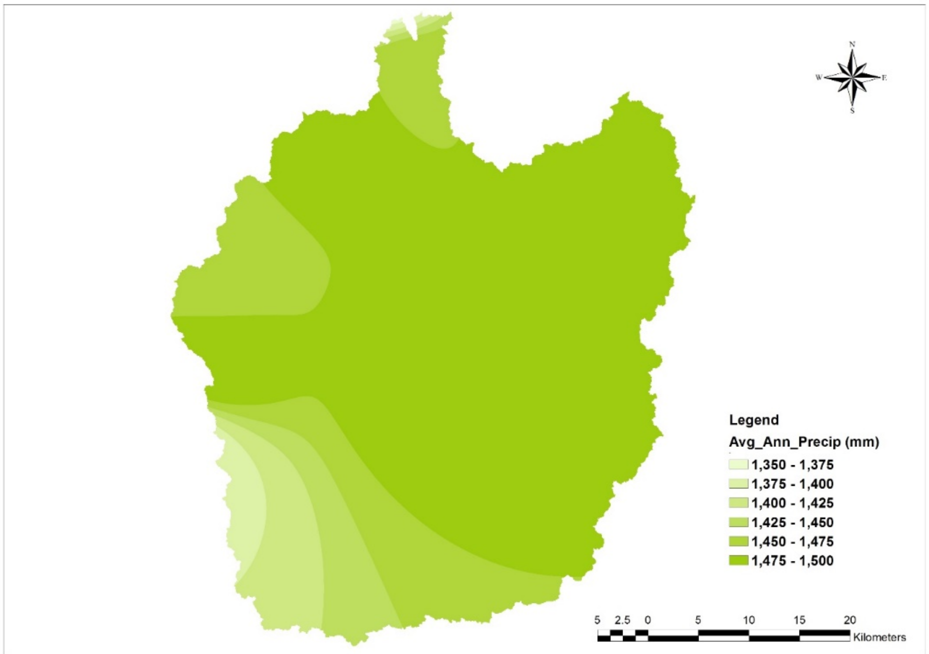

Figure 4.2 - Precipitation map of the N'djili River Basin (mm)

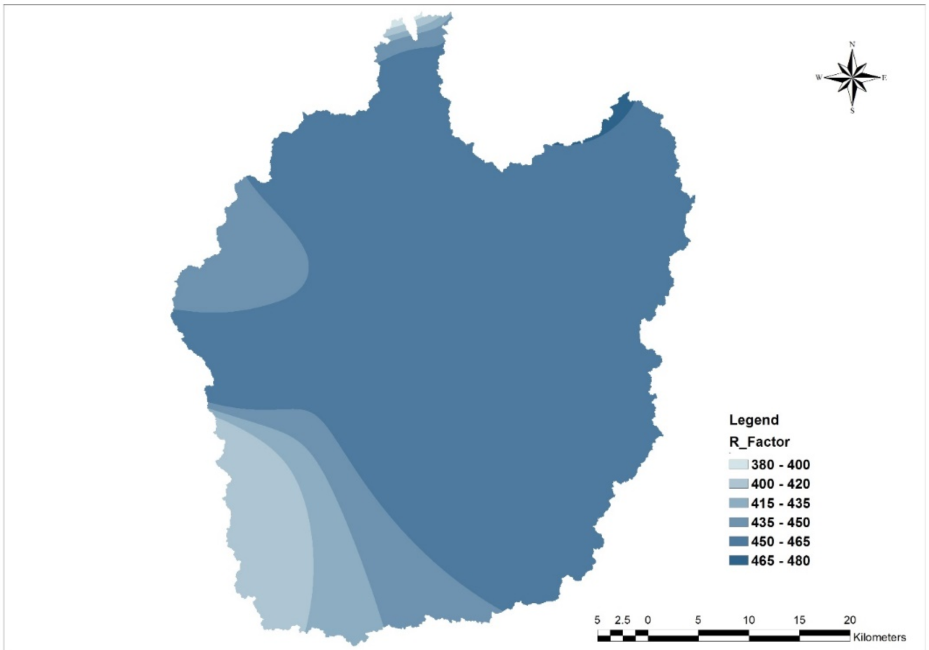

Figure 4.3 - Rainfall-Runoff erosivity factor map of the N'djili River Basin (hundreds ft.tons.in/acre.year)

4.1.2 Soil Erodibility Factor (K)

Soil erodibility is a measure of a soil's resistance to the erosive powers of rainfall energy and runoff. Practically, in the RUSLE, soil erodibility is an integration of the impacts of rainfall and runoff on soil loss for a given soil (Haan et al. 1994). Experimentally, the soil erodibility factor (K) is the rate of soil loss per rainfall erosion index unit for a specific soil as measured on a unit plot, which is defined as being 72.6 ft (22.1 m) long, with a width of 6 ft (1.83 m), 9% slope, and in a continuously clean-tilled fallow condition with tillage performed up and down slope (Wischmeier and Smith 1978). Under these conditions, L, S, C and P in the equation (4.1) are all equal to 1.0 and the soil erodibility factor K is equal to the ratio of the measured erosion (average annual erosion) to the rainfall-runoff erosivity factor R. Several researches concluded that the best erodibility factors are obtained from long-term direct soil loss measurement on natural plots. Although the minimum adequacy of the observation period for soil erodibility is taken as two years, better results due to covering broader range of climatic and soil condition changes are obtained for longer periods (Morgan 2011). Moreover, researchers have worked on estimating soil erodibility from soil properties such as particle size distribution, organic matter content, soil structure and permeability (Wischmeier et al. 1971). Figure 4.4 presents the nomograph developed by Wischmeier et al (1971). This nomograph is used to determine the K factor for a soil, based on its percentage of silts and percentage of very fine sand (0.002 – 0.1 mm), percentage of sand (0.1 – 2.0 mm), percentage of organic matter, soil structure and permeability.

From the nomograph of the Wischmeier and the results of Goldman, Jackson, and Bursztynsky (1986), the soil erodibility factor ranges in value from 0.02 to 0.69. Due to their resistance to detachment, soils with high clay content have low K values ranging from 0.05 to 0.15. Coarser texture soils, such as sandy soil, have low K values ranging from 0.05 to 0.2. Although these soils have easily detachable particles, the low surface runoff caused by excessive infiltration is responsible of the low values of K observed for this type of soil. For medium texture soils, such as the silt loam soils, K values typically range from 0.25 to 0.4. It can be assumed that these K values are due to moderate runoff and easier detachment of medium textured soils.

As mentioned previously, silt content is an important factor of soil erodibility. Since they are easily detached, silts tend to crust and produce high rates of runoff, soils with high silt content are the most erodible of all soils. Accordingly, their soil erodibility factors are greater than 0.4. Organic matter has a measurable effect on soil erosion. It reduces erodibility, decreases susceptibility to soil detachment, and increases infiltration rates. High infiltration rates reduce runoff and erosion.

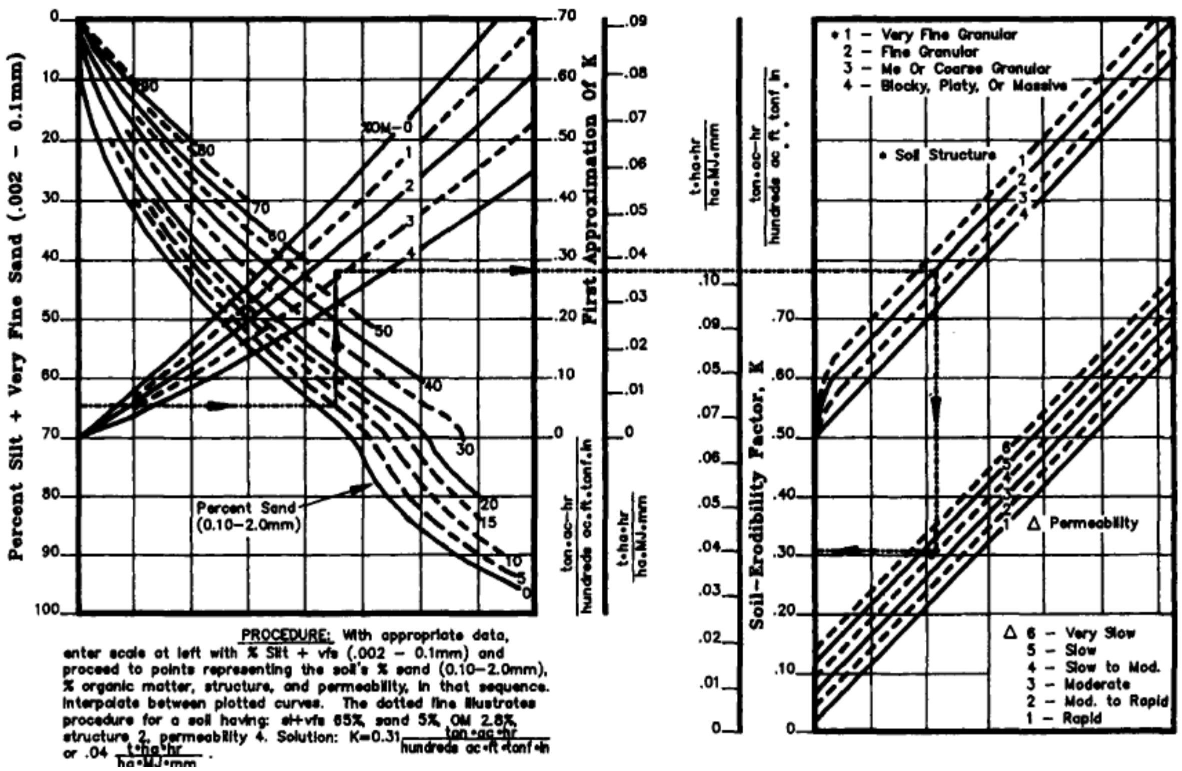

Figure 4.4 - Soil erodibility nomograph (after Wischmeier and Smith 1978)

Schwab et al. (1981) results summarized these observations in a soil erodibility factor (K) table (Table 4.2).

Table 4.2 - Soil Erodibility Factor (K) (Schwab et al. 1981)

Textural Class	Organic Matter Content (%) 0.5	2
Fine sand	0.16	0.14
Very fine sand	0.42	0.36
Loamy sand	0.12	0.10
Loamy very fine sand	0.44	0.38
Sandy loam	0.27	0.24
Very fine sandy loam	0.47	0.41
Silt loam	0.48	0.42
Clay loam	0.28	0.25
Silty clay loam	0.37	0.32
Silty clay	0.25	0.23

Based on table 4.2 and the soil erodibility nomograph of Figure 4.4, the soil erodibility factor (K) of the N'djili River basin is determined for each soil texture class. Assuming an organic matter content of 0.5%, corresponding K values have been assigned to the soil texture class in the N'djili basin. Table 4.3 presents the results of K values in the N'djili basin. These values range from 0.12 to 0.27. To derive the K-value of sandy clay loam from the soil erodibility nomograph (after Wischmeier and Smith 1978), it was assumed that this soil texture has 2% of organic matter, medium or coarse granular, and its permeability is moderate.

Table 4.3 - Soil erodibility factor (K) of the N'djili River Basin

No	Soil classification	Soil texture	(%) of Sand	(%) of Silt	(%) of Clay	Covered Area (%)	K Factors	Source
1	Haplic Acrisols	Sandy clay loam	64	10	26	88.7	0.10	Soil nomograph
2	Ferralic Arenosols	Loamy sand	81	7	12	7.9	0.12	*S*chwab et al., 1981
3	Ferralic Arenosols	Sand	95	4	1	3.4	0.15	*S*chwab et al., 1981

To create the soil erodibility map of the N'djili basin, the soil map shape file of the N'djili basin derived from the SOTERCAF database was added as a layer into ArcGIS and a lookup table was created to link the K values of Table 4.3 to the attribute table of soil map shape file by the joining attribute table functions of ArcGIS. Then, the shape file was converted to raster using the conversion tool "Feature to Raster" of the ArcToolbox, with a cell size of 30 m. Figure 4.5 shows the soil erodibility (K) map of the N'djili basin.

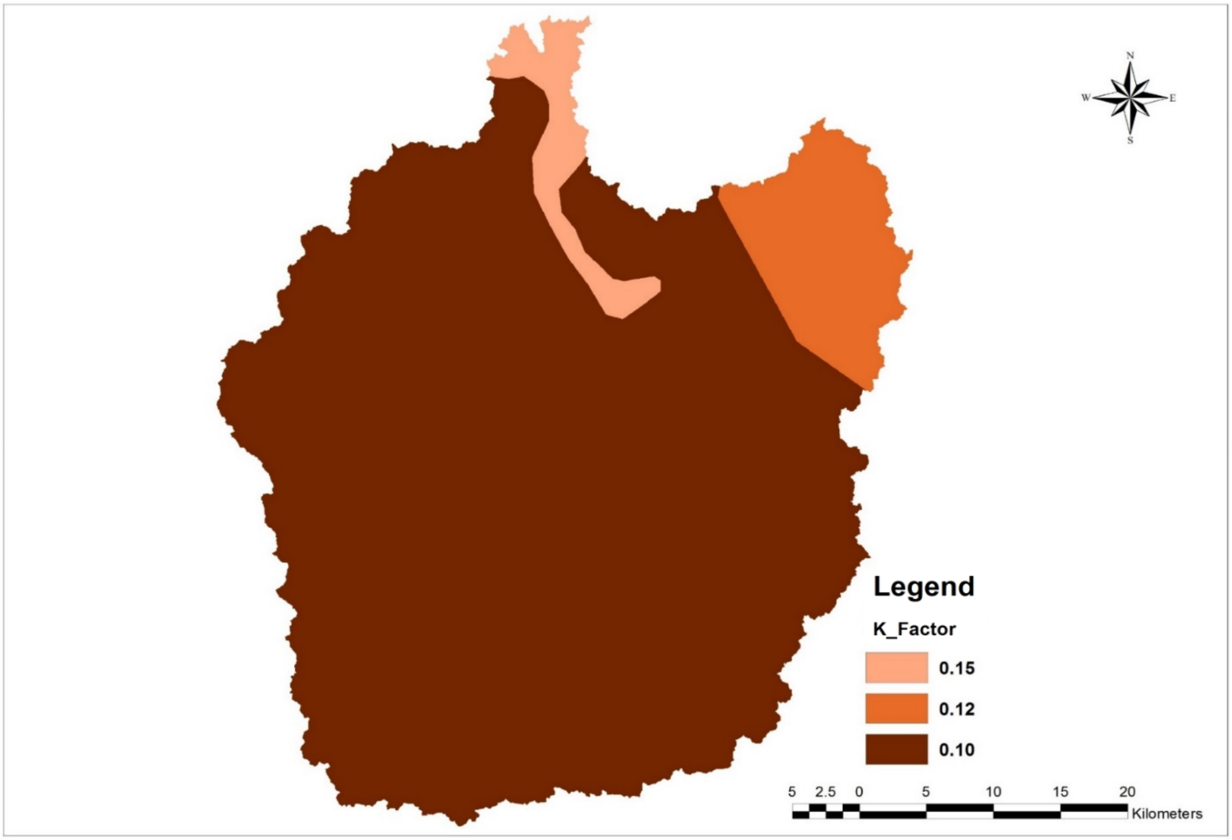

Figure 4.5 - Soil erodibility map of the N'djili River Basin (ton acre h $(100)^{-1}$ acre^{-1} ft^{-1} tonf^{-1}inch)

4.1.3 Slope Length and Slope Steepness Factor (LS)

The slope length factor (L) and the steepness factor (S) account for the effects of topography on soil erosion modeling in RUSLE. In general, as slope length (L) increases, erosion increases due to a progressive accumulation of runoff in the downslope direction. As slope steepness (S) increases, soil erosion also increases as a result of the increase in velocity.

Slope length (L) is defined as the horizontal distance from the origin of overland flow to the point where either the slope gradient (steepness) decreases enough so that deposition begins or runoff becomes concentrated in a defined channel (Wischmeier and Smith 1978). Slope length (L) is also defined as the ratio of soil loss from the field slope length to that from a 72.6 ft length under otherwise identical conditions. Figure 4.6 presents the schematic profile of the slope length. For cropping land, L is evaluated by the equations used in RUSLE (McCool et al., 1987; McCool et al., 1997; Renard et al., 1997):

$$L = \left(\frac{X_h}{72.6}\right)^m \qquad \text{(Eq 4.6)}$$

Where:

X_h = the horizontal slope length in ft

m = a variable slope length exponent

m is related to the ratio ε of rill erosion to interrill erosion by the following equation:

$$m = \frac{\varepsilon}{1+\varepsilon} \qquad \text{(Eq 4.7)}$$

ε is computed for conditions when the soil is moderately susceptible to both rill and interrill erosion using the following equation:

$$\varepsilon = \frac{\sin\theta}{0.0896\,[3.0(\sin\theta)^{0.8} + 0.56]} \qquad \text{(Eq 4.8)}$$

Where:

θ = the slope angle.

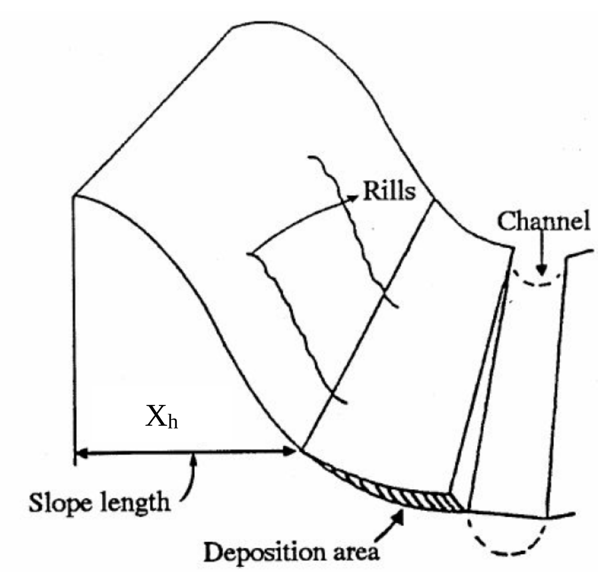

Figure 4.6 - Schematic slope profiles of RUSLE applications (Renard et al., 1997)

The slope steepness (S) is defined as the ratio of soil loss from the field slope to that from a 9% slope under identical conditions. The RUSLE slope steepness equations is given by (McCool et al., 1987; McCool et al., 1997; Renard et al., 1997):

$S = 10.8 \text{ x} \sin\theta + 0.03 \qquad \sigma \leq 9\%$ (Eq 4.9)

$S = 16.8 \text{ x} \sin\theta - 0.50 \qquad \sigma > 9\%$

Where:

θ = the slope angle;

σ = the slope gradient in percentage.

The slope length factor (L) is more difficult to compute than the slope steepness factor (S) (Ouyang and Bartholic 2001). Fortunately, the soil loss equation is much less sensitive to L than S. For typical slope conditions, a 10% error in slope length results in a 5% error in computed soil loss. In contrast, a 10% error in slope steepness will result in about 20% error in computed soil loss (Morgan 2011).

The L and S factors can be determined in ArcGIS from the Digital Elevation Model (DEM) using the approach developed by Moore and Burch (1985). They developed an equation similar to Equation 4.5 to compute length-slope factor:

$$LS = \left(\frac{A_S}{22.13}\right)^m \text{x} \left(\frac{\sin\theta}{0.0896}\right)^n \qquad \text{(Eq 4.10)}$$

Where:

m = 0.4 – 0.6 and n = 1.2 – 1.3.

LS = computed LS factor.

A_S = specific catchment area, i.e. the upslope contributing area per unit width of contour (or rill), in m^2/m. It is calculated in ArcGIS using the function called “flowaccumulation” multiply by the squared cell size and divided by the cell size. The “flowaccumulation” is a function of the Hydrology - Spatial Analyst Tool included in ArcToolbox.

A_S = (Calculated flow accumulation) x 30.76 x 30.76/30.76 (for cell size = 30.76 m, from the N'djili basin DEM)

θ = slope angle in degrees. It is calculated in ArcGIS using the function called "slope" with option "percent rise" which is 100 times Tanθ. Then θ is calculated using "Atan" function in ArcGIS. The function "slope" with the option "percent rise" is a function of the Surface - Spatial Analyst Tool included in ArcToolbox. "Atan" function can be used from the raster calculator of the Map Algebra Tool of ArcToolbox.

$$\tan \theta = \text{slope (in percent rise)}/100$$

$$\theta = \text{Atan}(\tan \theta)$$

The "flow accumulation" function in ArcGIS is a tool which computes accumulated flow as the accumulated weight of all cells flowing into each downslope cell in the output raster. With this function, the value of cells in the output raster is the number of cells that flow into each cell (O'Callaghan and Mark 1984). In Figure 4.7, the top left image shows the direction of travel from each cell while the top right shows the number of cells that flow into a cell. The bottom left indicates the possible direction of flow which can be in either one of the cardinal direction (i.e. N, S, E, W) or the diagonal directions (i.e. NE, SE, SW, NW) using a colored direction coding.

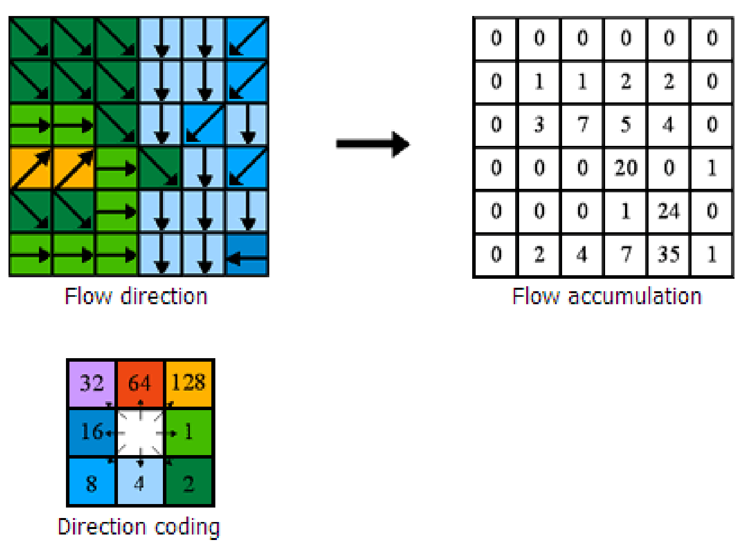

Figure 4.7 - Determining the accumulation of flow

Another important function used in the determination of the LS factor grid in ArcGIS is the function "slope" with the option "percentrise". Slope is the first derivative of a digital elevation model (DEM). It represents the rate of change of elevation for each DEM. The inclination of slope can be output as either a value in degrees or percent rise. Figure 4.8 shows the histogram of slope distribution in the N'djili River Basin.

Equation 4.9 has been plotted in Figures 4.9 and 4.10 to assess the sensitivity of the exponents m and n on the computation of the LS factor. From Figures 4.9 and 4.10, it can be noticed that the LS factor is highly sensitive to a variation of the exponent m and less sensitive to a variation of the exponent n. For example, when the exponent m varies from 0.4 to 0.6 while keeping constant the exponent n and the slope angle, the LS factor increases from about 8% to 85%, depending on the value of the specific catchment area. In contrast, when the exponent n varies from 1.2 to 1.3 while keeping the other parameters, except the specific catchment area, the LS factor is increased by 11%. To predict the soil erosion loss in this study, values of m = 0.5 and n = 1.25 have been selected.

Figures 4.11 and 4.12 present the slope map in percent rise and the LS factor map of the N'djili basin respectively. All of these maps are derived from a 30 meter resolution DEM and have the same resolution, accordingly. From the LS factor map, LS value ranges from 0 to 61.

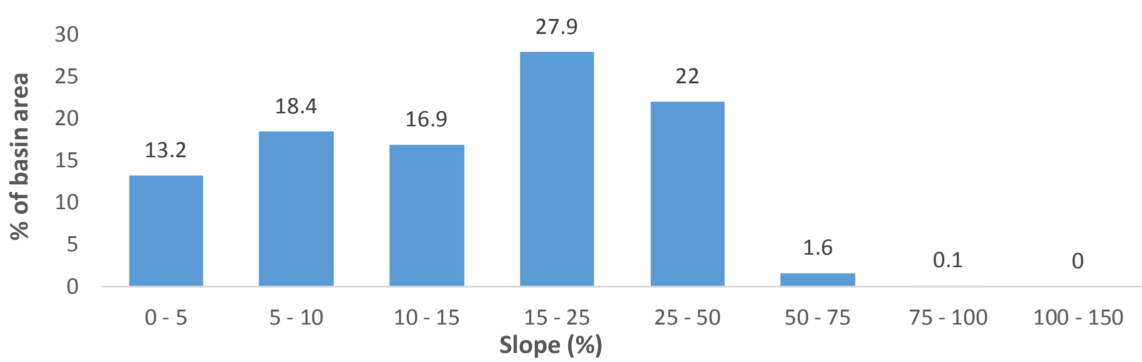

Figure 4.8 – Histogram of slope distribution in the N'djili River Basin

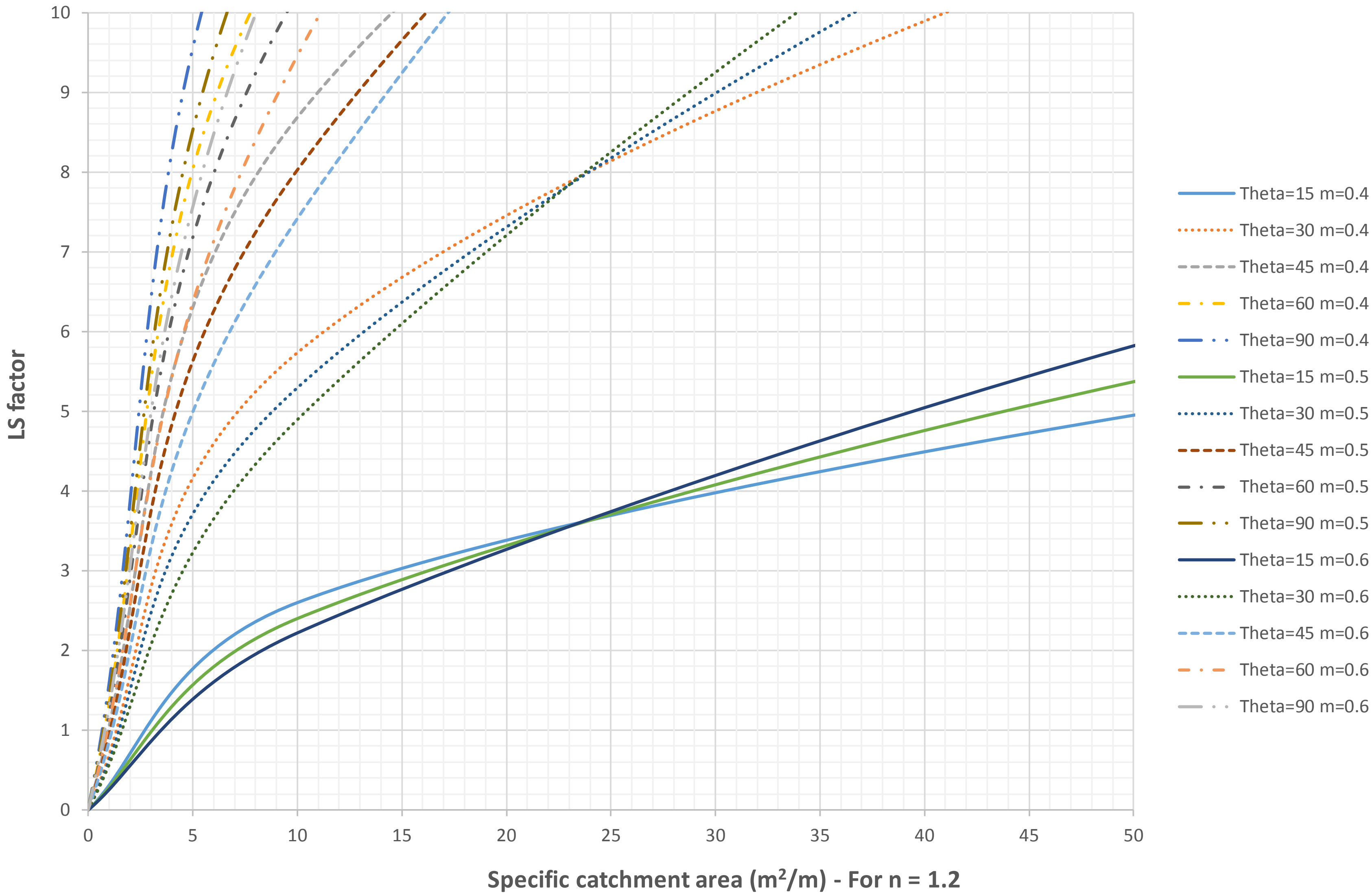

Figure 4.9 - LS factor derived from Moore and Burch Equation (1985) – Exponent n = 1.2

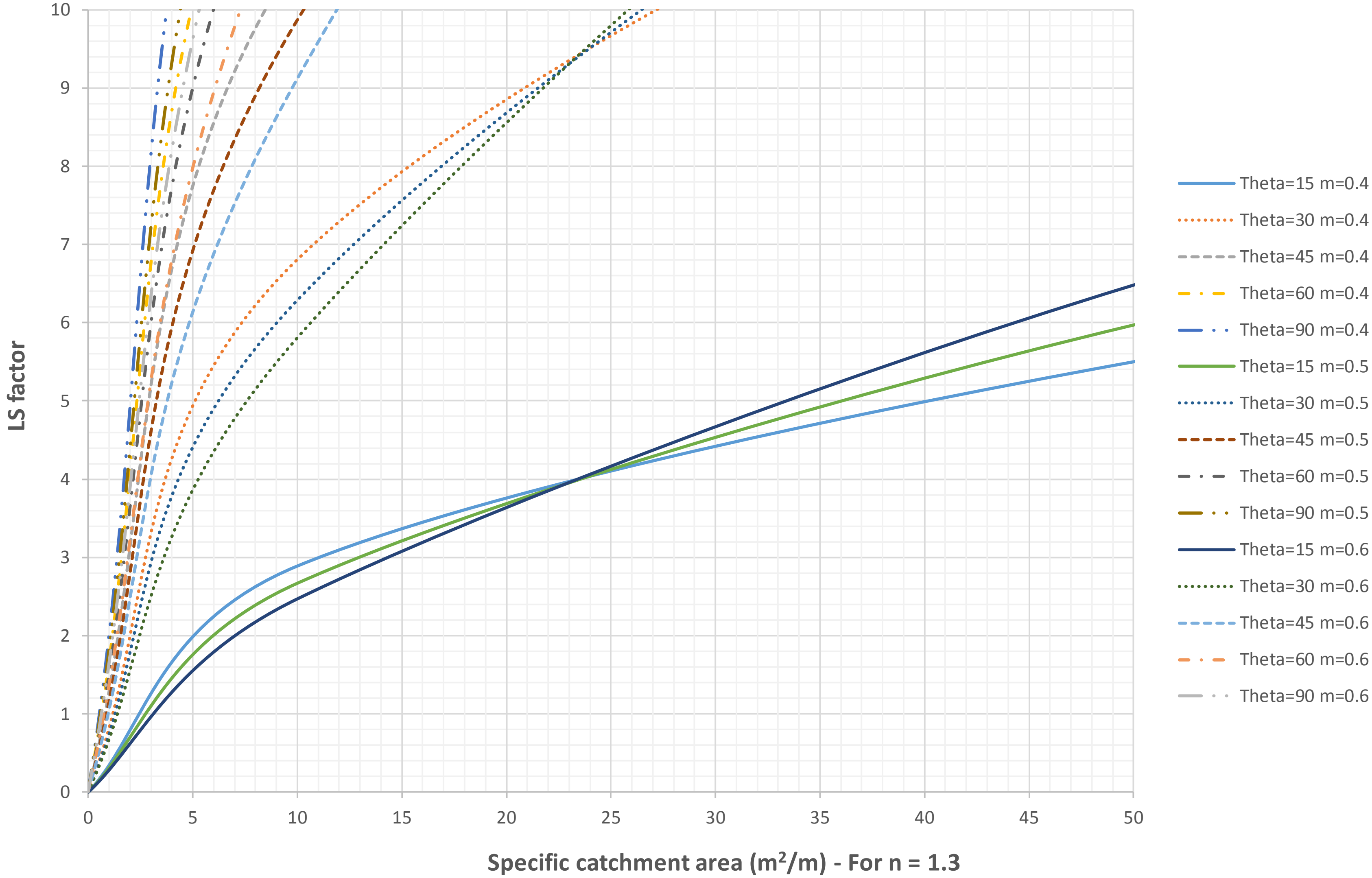

Figure 4.10 - LS factor derived from Moore and Burch Equation (1985) – Exponent n = 1.3

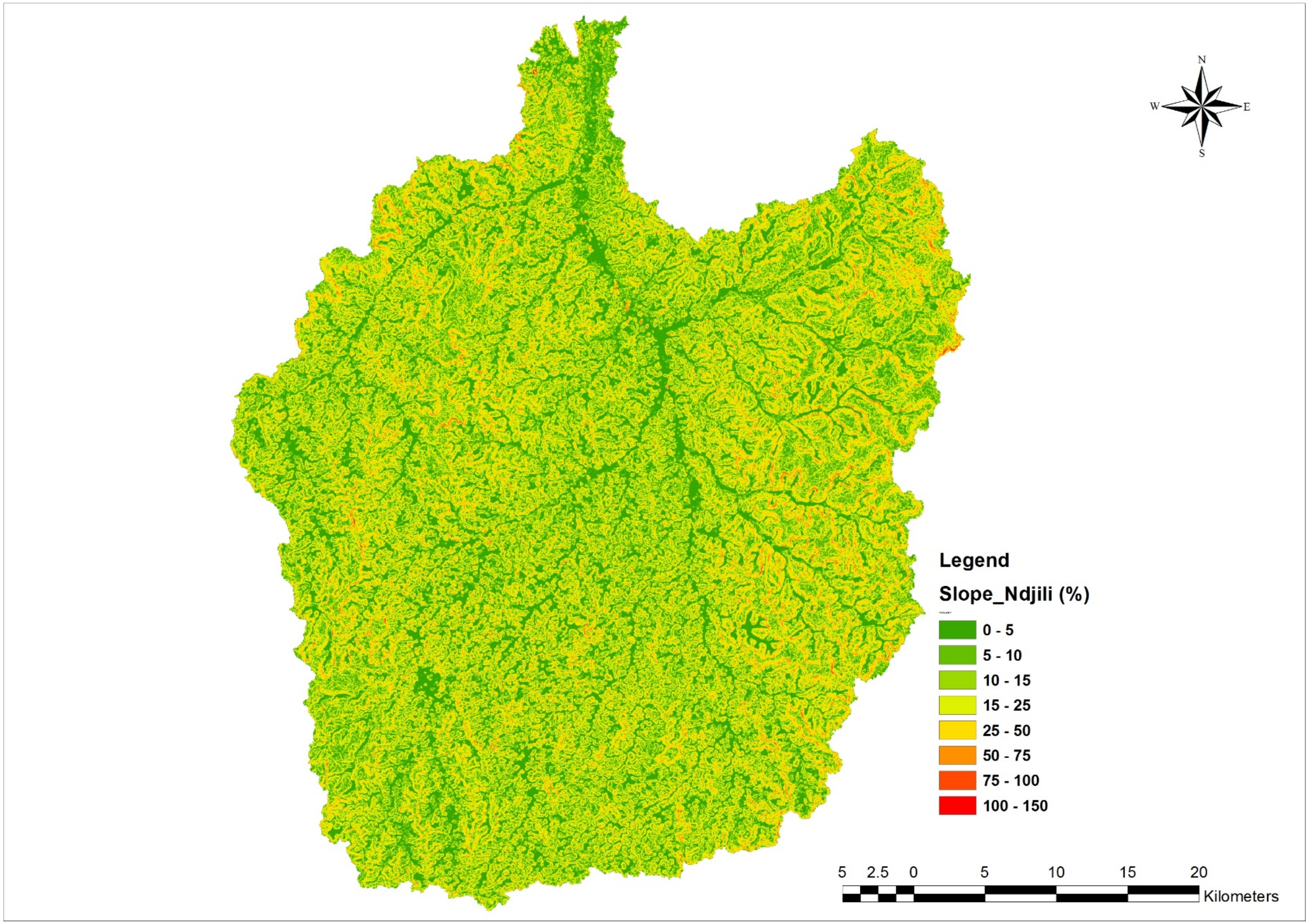

Figure 4.11 - Slope map of the N'djili Basin in percent rise

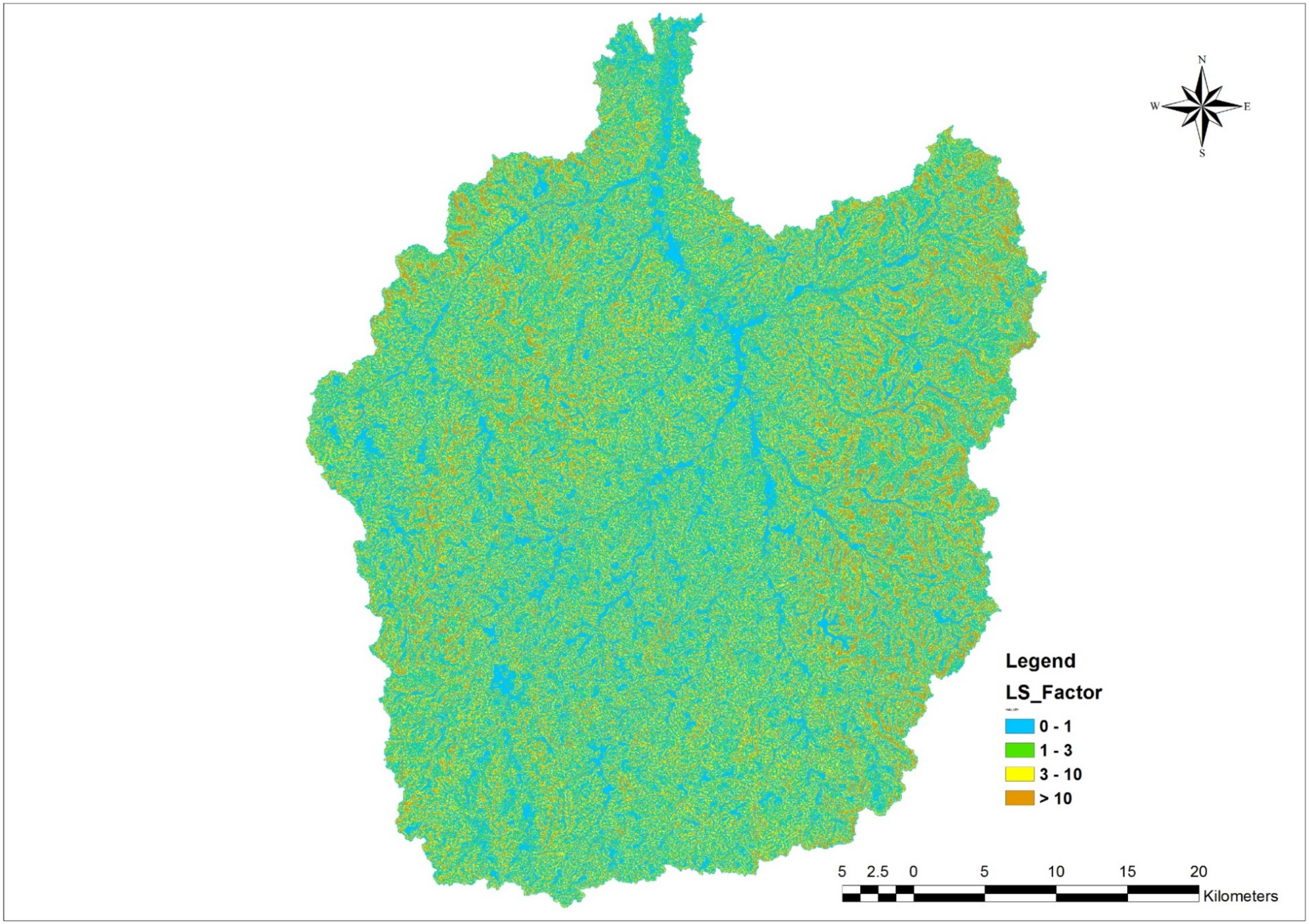

Figure 4.12 – LS factor map of the N'djili Basin in percent rise

4.1.4 Cover Management Factor (C)

The Cover Management Factor (C) represents the effect of vegetation, soil cover, below-ground biomass, cropping, soil-disturbing activities and management practices on soil erosion. The C factor is essentially a soil loss ratio (SLR) which is defined as the ratio of soil losses under actual conditions to losses experienced under the clean-tilled continuous fallow reference conditions. This soil loss ratio is the result of multiplying subfactor values that depend on previous cropping and management, vegetative canopy, surface cover and roughness, and, in some cases, soil moisture (Laflen et al. 1985).

The density of protective cover of crops or vegetation on the land surface affects directly the soil erosion rates. Therefore, the cover management factor (C) value will be 1 in the case of continuous bare fallow with no vegetation coverage (in standard plot condition) and lower in case of more vegetation or crop cover producing lower amount of soil erosion. In case of dense and mature forest with trees canopy and undergrowth vegetation covering between 75 to 100% of the land area, C value is close to 0.001. In this last case, erosion prevention actions are not required.

To estimate C factor in the RUSLE model, two options can be used: the time-variant and the time-invariant option (Kuenstler 1998). The time-variant option is used when plant and/or soil conditions change enough to significantly affect erosion during the year, during a rotation cycle, or over an extended period. This option is typically used for croplands and/or rangelands where cover changes significantly during the year such as from grazing, burning, or herbicide application. It is also applied for sites regenerating following soil-disturbing activities on forest lands and recovery following construction or earth moving activities (Jones et al. 1996). In the time-variant option, the SLR values area calculated frequently enough over the course of a year or a crop rotation to provide an adequate measure of how they change. In RUSLE1, these calculations were performed for half-month periods; in RUSLE2, they are performed for on a daily time-step (Borah et al 2008). The time-invariant option is used where constant conditions can be assumed mainly in the case of range and pasture land. In the time-invariant option, average annual values of soil erosion are predicted.

Luboya (2002) and Semeki (2003) give several indications about the vegetation and the cropping rotation scenario in the N'djili river basin. From the information given by Luboya (2002), the timeline of cropping rotation scenario has been established in Figure 4.13.

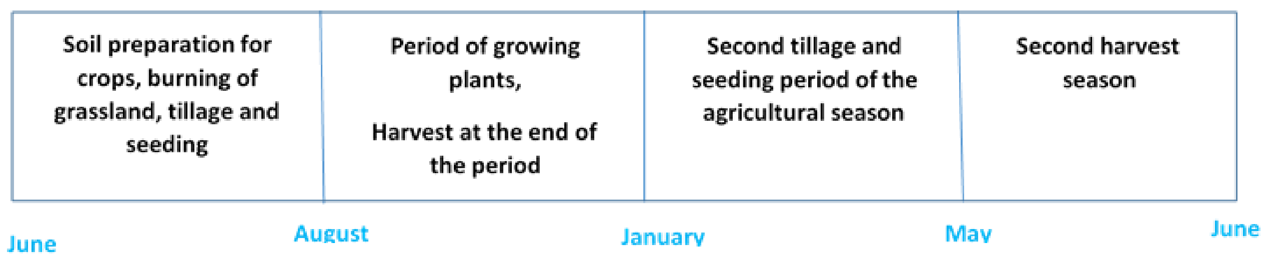

Figure 4.13 - Timeline of the cropping rotation scenario in the N'djili basin

From Figure 4.13, two distinct agricultural seasons can be determined over a year: the first season between August and January and the second one between January and June. During these two seasons, the vegetation cover changes slightly and can therefore be assumed to be time-invariant. Between June and August, the vegetation cover changes dramatically due to burning and tillage practices, although precipitation in this period represents a fraction of about 0.01 of the annual precipitation. With a low precipitation volume representing a fraction of about 0.01 of the annual precipitation, the period between June and August doesn't really contribute to the soil erosion rates. On the other side, all the vegetation cover degradation made during this period affect the erosion rate specifically during the first agricultural season (between August and January) because the burning areas not used for seeding recover slowly.

Land cover maps with adequate spatial resolution are needed to derive C values over a river basin. For the N'djili river basin, since the existing land cover maps are not available with the appropriate resolution, satellite images form the Landsat missions have been downloaded and classified in order to derive land cover maps of the basin.

4.1.4.1. Multispectral classification of the N'djili basin Landsat images

The objective of image classification procedures is to automatically categorize all pixels in an image into land cover classes or themes (Lillesand et al. 2008). This classification is normally performed with multispectral data. Multispectral classification usually requires some knowledge of the scene. The information about the scene may come from personal knowledge of the area, field trips and aerial photography. Since classification is also a grouping or generalization of the data, it is important to differentiate between spectral classes and informational classes. The spectral classes are the groups in the data; informational classes are the map classes, the groups the analyst would like to identify using classification procedures (Warner and Campagna 2013).

There are numerous classification methods. From the perspective of the image classification analyst, two main methods can be identified: the supervised and unsupervised classification. In the supervised classification, the image analyst "supervises" the pixel categorization process by specifying, to the computer algorithm, numerical descriptors of the various land cover types present in a scene. In this process, representative sample sites of known cover type, called "training areas", are used to compile a numerical "interpretation key" that describes the spectral attributes for each feature type of interest. The classification algorithm then classifies each pixel in the rest of the image based on comparisons with training data, or more commonly, summary properties of the training data. In the unsupervised classification, the image data are first classified by aggregating them into the natural spectral groupings, or “clusters”, present in the scene. Then the image analyst determines the land cover identity of these spectral groups by comparing the classified image data to ground reference data.

The Landsat Thematic Mapper data of the area including the N’djili basin have been classified using the software Idrisi by Clarks Labs (Clark University). The unsupervised classification technique was utilized to classify the Landsat scenes captured on 02-01-1995, 04-30-2001 and 08-13-2013 by employing the Isoclust method in Idrisi following the sequence of operations presented in Figure 4.14.

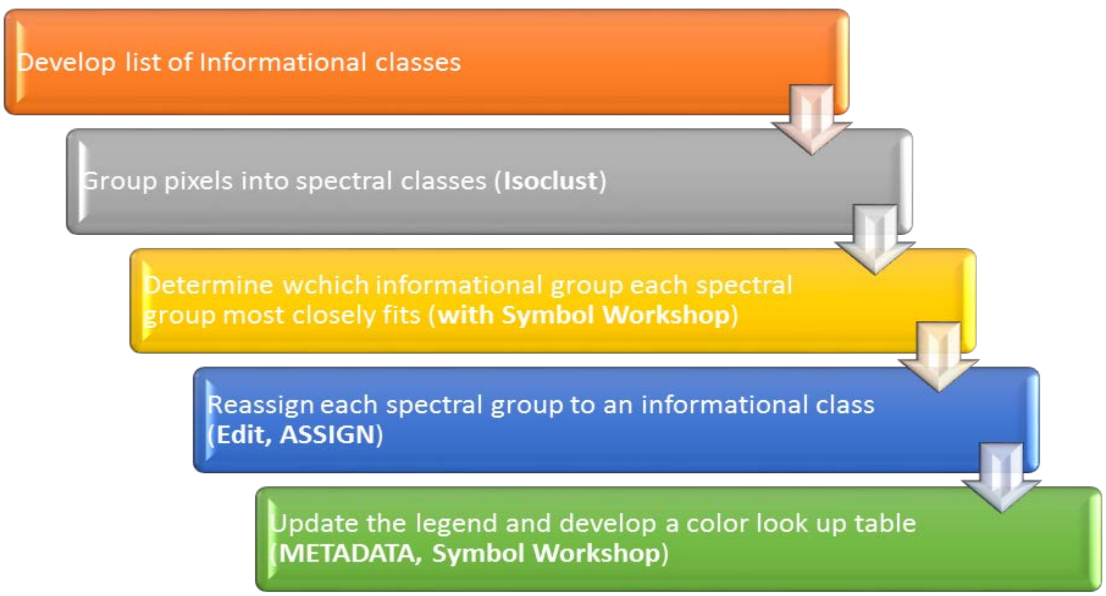

Figure 4.14 - Overview of unsupervised classification in IDRISI (derived from Warner and Campagna 2013)

Based on knowledge of the area, study results from Luboya (2002) and Semeki (2003) and an examination of the false color composite image, a list of informational classes (Table 4.4) was established in order to determine the likely classes that might be discriminated. Then the Isoclust method was performed in Idrisi to group pixels into spectral classes and the other operations listed in Figure 4.14 are executed.

Table 4.4 - Informational classes used for the image classification

Class Number	Name	Color in 345 false color composite
1	Water	Dark blue
2	Forest	Dark green
3	Grass and shrubs	Green
4	Bare land/burned grass/plowed land/ rainfed crops	Light yellow
5	Settlements	Pink

Since the vegetation cover changes dramatically between June and August, moving from bare or burning lands to plowed land or rainfed crops, these nad types were gathered for anlysis purpose. A unique informational class corresponding to these lands has been defined and named "Bare land/burned grass/plowed land/ rainfed crops".

After the classification process is done in Idrisi, the land cover raster were exported to ArcGIS, then converted from raster to shape files. Figures 4.15, 4.16 and 4.17 show the land cover map resulting from the classification performed in Idrisi and ArcGIS.

Table 4.5 presents the percentage of area covered by each land cover/use type. It shows that:

- The forest area decreased by about 32 % from 1995 to 2001 and by 50% from 2001 to 2013. In 2013, the area covered by the forest represented only 5 % of the N'djili river basin area whereas the forest was covering about 15% of the basin area in 1995. According to Luboya (2002), this forest mainly degraded into grass and shrubs cover during these periods.
- The area covered by grass and shrubs decreased by 1.4% from 1995 to 2001, and by about 14% between 2001 and 2013. The 322 km^2 area of grass and shrubs areas lost between 1995 and 2013 have been essentially turned into settlements and bare land/crop land.

- The bare land/burned grass/ plowed land/ rain-fed crop area increased dramatically between 1995 and 2013 by about 273%, gaining areas from grass, and shrub-covered areas.
- The settlement area increased by about 39% from 1995 to 2001, by 54% between 2001 and 2013. The total expansion of settlement area between 1995 and 2013 is estimated to be 113%.

Loss of forest, and grass and shrubs area for the benefit of settlement, and bare land/burned grass/ plowed land/ rain-fed crop area is likely due to the civil wars of 1996-1997 and 1998-2003 that brought millions of persons in the Kinshasa neighborhood from the eastern part of the Congo. It should be mentioned here that the derivation of the land cover using a satellite image of August 2013 introduces a bias in estimating the area of each land cover type. Indeed, the Landsat image of August 2013 was taken during the dry season in which burning practices, brush cutting and tillage mainly occur. So, a satellite image taken over the N'djili Basin during the dry season is more likely to generate more bare, burned and plowed land than the ones taken during the rainy season.

Table 4.5 - Area covered by each land cover/use type in the N'djili River Basin (1995 – 2013)

	1995		2001		2013	
Land cover/use type	A (km2)	% A	A (km2)	% A	A (km2)	% A
Water	21.95	1.0	21.93	1.0	21.92	1.0
Forest (open cover)	312.87	14.9	213.03	10.2	105.31	5.0
Grass and shrubs (cover > 60%)	1466.56	69.9	1436.94	68.5	1144.56	54.6
Bare land/burned grass/plowed land/ rain-fed crops	122.41	5.8	185.30	8.8	456.27	21.8
Settlements	173.03	8.3	239.81	11.4	368.71	17.6
Total	2096.8	100	2097	100	2096.8	100

Figure 4.18 illustrates the evolution of the area covered by different land cover/use types in the N'djili River basin from 1995 to 2013.

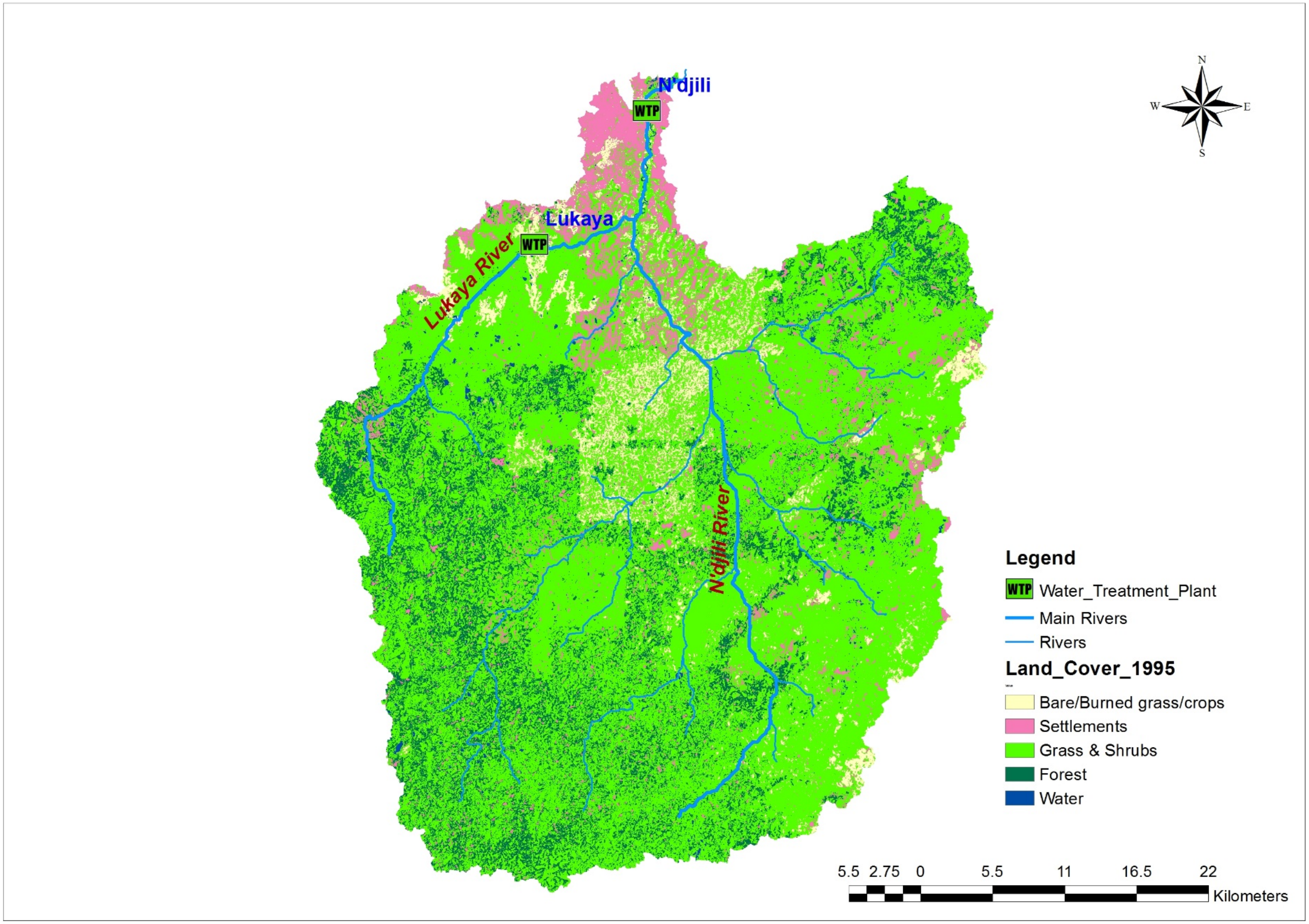

Figure 4.15 - Land cover map of the N'djili basin in 1995

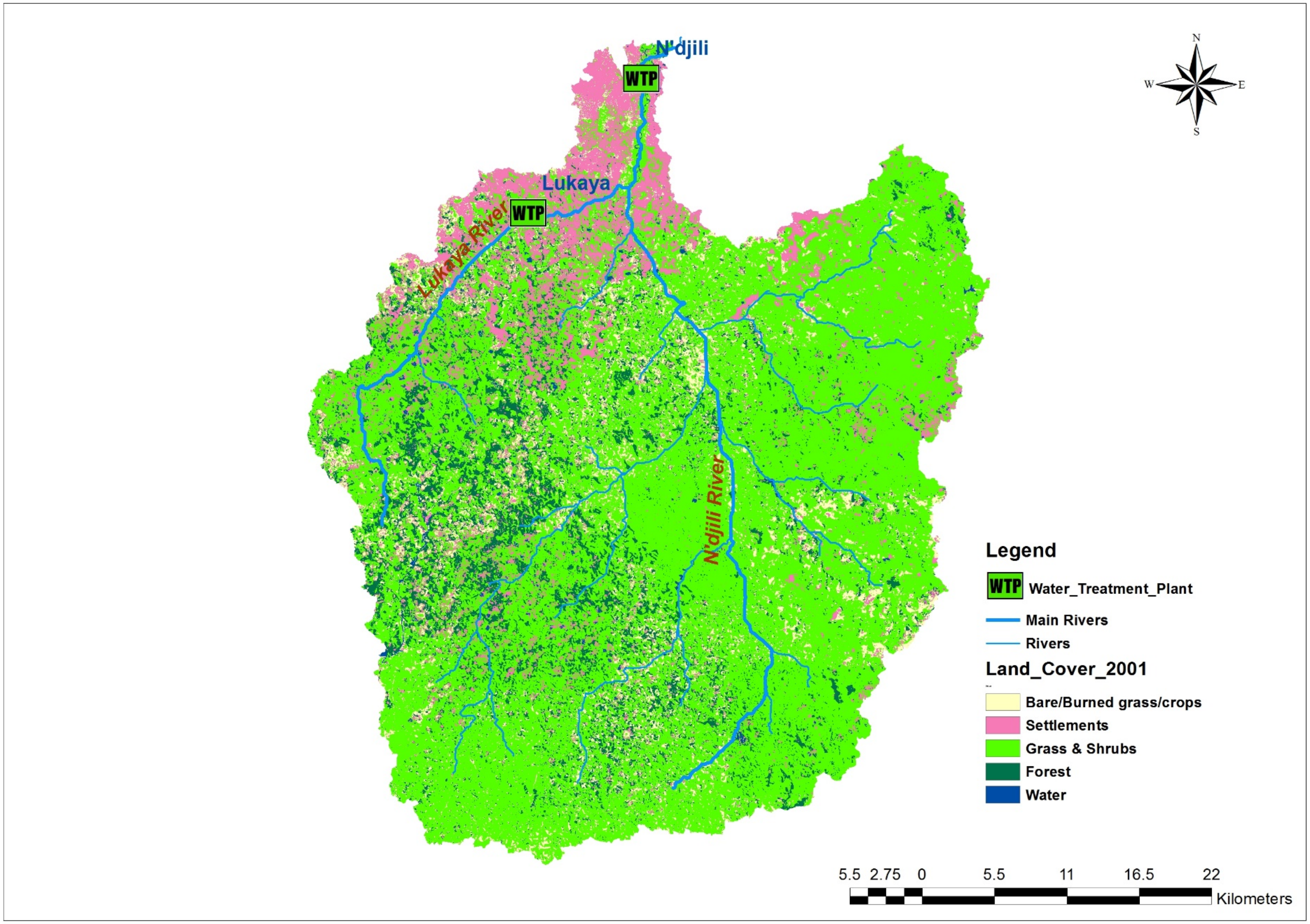

Figure 4.16 - Land cover map of the N'djili basin in 2001

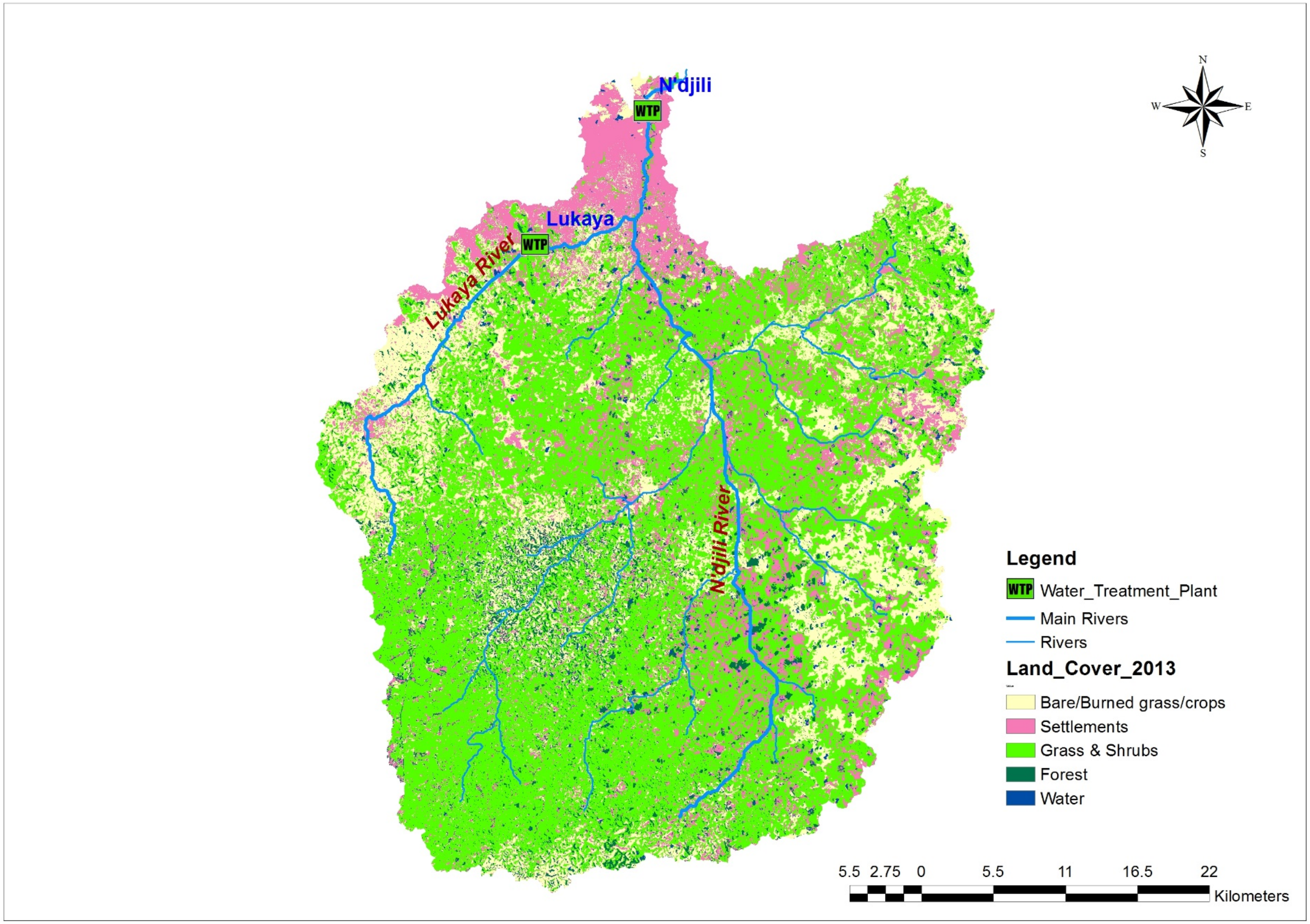

Figure 4.17 - Land cover map of the N'djili basin in 2013

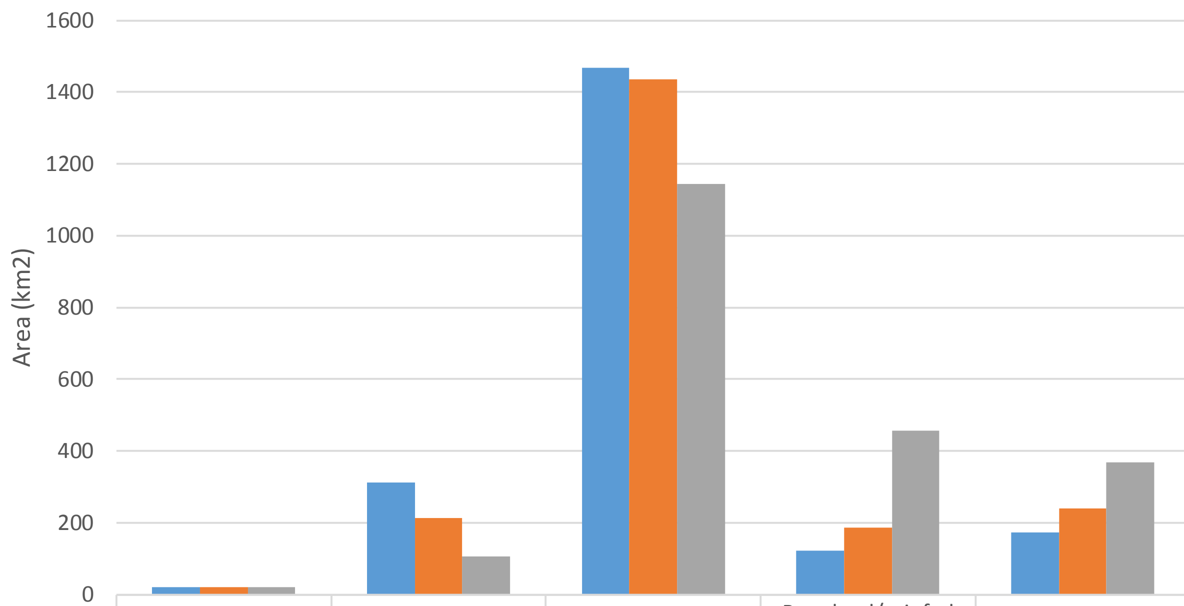

	Water	Forest	Grass and shrubs	Bare land/rainfed crops	Settlements
1995	22	313	1467	122	173
2001	22	213	1437	185	240
2013	22	105	1145	456	369

Figure 4.18 - Area covered by each land cover/use type in the N'djili River Basin (1995 – 2013)

4.1.4.2.Derivation of C factor

To derive the C factor of the N'djili River Basin for conditions in 1995, 2001 and 2013, an approach in three steps has been developed. Firstly, the time-invariant option was used to determine the C factor for the informational classes "water", "Forest", "grass and shrubs" and "settlements". Secondly, the C factor of the informational class "bare land/burned grass/ plowed land/ rain-fed crop" was estimated using the time-variant option.

4.1.4.2.1. C factor for the informational classes "Forest", "grass and shrubs" and "settlements"

The C values for the classes "Forest", "grass and shrubs" and "settlements" were estimated using the studies by Wischmeier and Smith (1978), Luboya (2002), Semeki (2003), Bakker et al. (2008), and Teh (2010).

a. C factor of the informational class “Forest”

According to Luboya (2002) and Semeki (2003), the forest encountered in the N’djili basin is an open cover natural forest (20% - 60%) with the main species: *Manilkara*, *Berlinia*, *Mitragyna*, *Milletia drastica* and *Hymenocardia acida*. The average canopy height of this open cover natural forest ranges between 20 and 25 m (Semeki 2003). Therefore, based on the Bakker et al. (2008) study, a C factor of 0.01 has been assigned to “Forest” land.

b. C factor of the informational class “grass and shrubs”

According to Luboya (2002), the shrub and grassland formations in the N’djili River Basin result from the degradation of the dense natural forest cover observed before the 1950s. The average canopy height of shrubs encountered in this basin range between 2.0 and 4.0 m (Luboya 2002) and the cover that contacts the soil surface is estimated to be greater than 80% of the ground surface. So, based on the Wischmeier and Smith (1978) findings on cropping-management factor for permanent pasture, range, and idle land, a factor of 0.012 has been selected for this informational class.

c. C factor of the informational class “settlements”

For the land cover “Settlements”, a weighted-average-C-factor has been computed based on the August 2013 land cover and C-values defined by Huey Teh (2010) for different urban cover types. The C-factor for the “settlement” land cover is calculated with the following expression:

$$C = \frac{\sum C_i A_i}{A} \qquad (Eq\ 4.11)$$

Where C = the cover management factor for the land cover “Settlements”;

C_i = the cover management factor for each type of Urban land cover (low density, medium density or high density);

A_i = area of each urban land cover type;

A = the total area of land cover “settlements”.

The C-factor estimate for the land cover "settlements" is presented in Table 4.6.

Table 4.6 - C-factor estimate for land cover "settlements"

	C (after Huey Teh 2010)	Area (km2)	Settlement C-factor
Urban (Low density)	0.25	123.2	0.13
Urban (Medium density)	0.15	141.4	
Urban (High density)	0.05	191.6	
Total		456.2	

4.1.4.2.2. C factor for the informational class "bare land/burned grass/ plowed land/ rain-fed crop"

The time-variant option was used to estimate the annual C value of the informational class "bare land/burned grass/ plowed land/ rain-fed crop" by employing a three-step methodology. During the first step, the percent of bare soil for the burned areas was estimated and the monthly C values for the same areas were evaluated. In the second step, the monthly C values were computed for the class "bare land/burned grass/ plowed land/ rain-fed crop". During the third step, the annual C-value of the informational class "bare land/burned grass/ plowed land/ rain-fed crop" was determined.

a. Step 1: Percent of bare soil for burned areas – Monthly C values of Burned area

To compute the percent of bare soil for burned areas in the N'djili River Basin, it was assumed a vegetation regrowth rate similar to the one observed after the Bobcat fire, as studied by MacDonald (2012). Since the wildfire severity observed in the N'djili basin can be classified from moderate to high (Ntale 2010), the percent of bare soil for burned areas can be estimated from Equation 4.11 for moderate severity fire and Equation 4.12 for high severity fire.

$$\text{Percent Bare Soil} = -21.86 \ln T + 45.75 \qquad \text{(Eq 4.12)}$$

$$\text{Percent Bare Soil} = -26.09 \ln T + 70.03 \qquad \text{(Eq 4.13)}$$

Where:

T = the time since burning (years)

Referring to the timeline of cropping rotation scenario in the N'djili Basin (Figure 4.13), Table 4.7 was established from Equations 4.12 and 4.13, assuming a regrowth rate similar to the one in Bobcat watershed. Hence, the percentage of bare soil for the burned areas increases since the end of May (45 – 70%) to reach the maximum value during the burning and tillage period (75 -95 % at the end of August). Since the end of August, the percentage of bare soil in burned locations decreases with the vegetation regrowth to reach its lower value (from 75 – 95 % to 45 – 70 %) at the end of the agricultural season.

Table 4.7 - Percent of bare soil for the burned areas based equations 4.12 and 4.13 in the case of time-variant option.

Land cover type	Period	Monthly variability in Percent of bare soil (%)
Burned areas	September	70 - 95
	October	65 – 93
	November	61 – 88
	December	57 – 84
	January	55 – 80
	February	52 – 78
	March	50 – 75
	April	48 – 72
	May	45 – 70
	June	75 – 95
	July	75 – 95
	August	75 – 95

Figure 4.19 presents the minimum and the maximum percent of bare soil, as estimated using the equations for the percent of bare soil after the Bobcat fire.

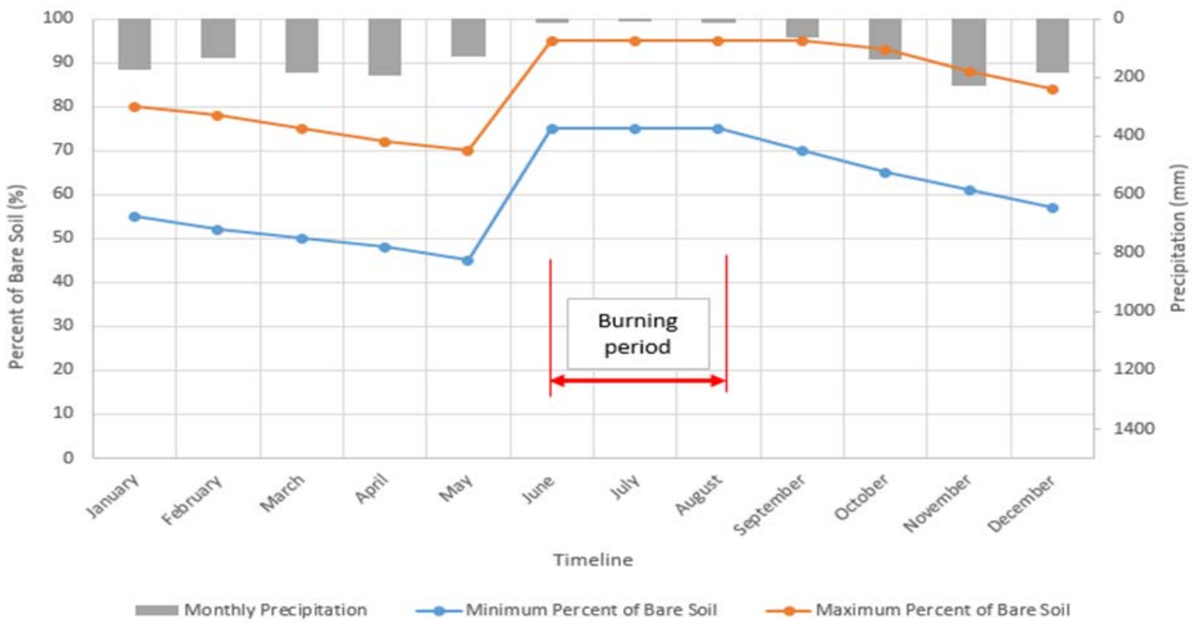

Figure 4.19 – Percent of bare land in burned areas

Since the precipitation rate over the N'djili River Basin is largely greater than the one over the Bobcat watershed, it can be inferred that the vegetation regrowth rate in the N'djili Basin is much faster than the regrowth rate in Bobcat watershed. Moreover, since grass doesn't burn at high severity, only the percent of bare soil derived using the moderate severity condition can be retained. Therefore, although it obvious that the percent of bare soil really observed in the N'djili Basin should be lower than the minimum of the one obtained after the Bobcat fire, the minimum of bare soil percentage, derived in Figure 4.19 using the Bobcat fire equations, is considered for estimating the percent of bare soil in the N'djili Basin.

The burned grass can be assimilated to a cover with no appreciable canopy. So, using the Wischmeier and Smith (1978) findings on cropping-management factor and the minimum percent of bare soil for burned areas previously determined, the monthly C values for these areas were estimated in Table 4.8. Figure 4.20 shows the plot of the monthly C values for the burned areas.

Table 4.8 – Monthly C values for the burned areas

Month	January	February	March	April	May	June
C values	0.14	0.13	0.12	0.11	0.1	0.24
Month	July	August	September	October	November	December
C values	0.45	0.45	0.2	0.17	0.16	0.15

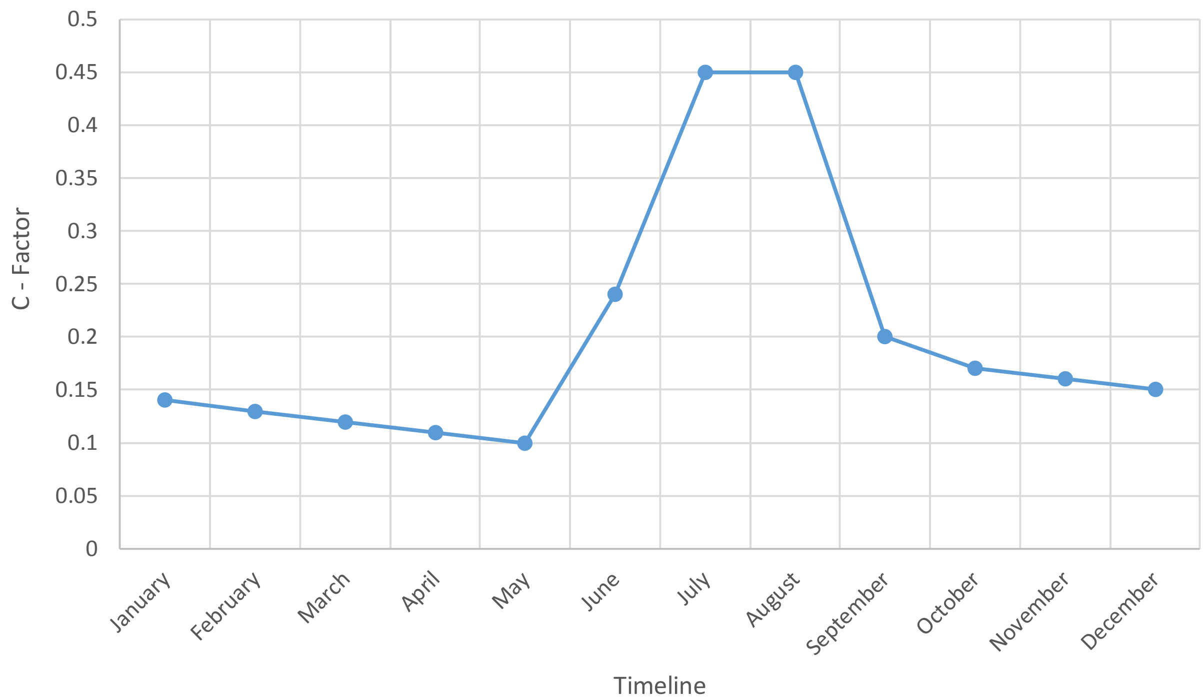

Figure 4.20 – Monthly C values for the burned areas

b. Step 2: Monthly C values of the class “bare land/burned grass/ plowed land/ rain-fed crop”

The calculation of the monthly C-values for the land cover “bare land/burned grass/ plowed land/ rain-fed crop” is based on the ratios of the bare land area, crop land area and burned grass area over the total area of the land cover “bare, burned and crop areas” as determined from the Landsat image of August 13th, 2013 over the N’djili Basin taken in dry season. Assuming that the rainfed crops and the bare land areas remain constant, and the bare land remains bare over the year, the C-factor assigned to the bare lands and the crop areas are invariant with time and selected according to the results from Wischmeier and Smith (1978). Table 4.9 presents these ratios and these time-invariant C values for the bare land, crop land and burned grass area.

Table 4.9 – Monthly C values for the burned areas

	Area (km2)	Ratio	Constant C-values
Bare land	45.6	0.1	0.5
Rainfed Crop Land	177.9	0.39	0.35
Burned areas	232.7	0.51	Variable C-value (Monthly)

The monthly C values for the land cover "Bare land/burned grass/plowed land/rainfed crops" are calculated using the expression:

$$C = \frac{\sum C_i A_i}{A} \qquad (Eq\ 4.14)$$

Where C = the monthly cover management factor for the land cover "Bare land/burned grass/plowed land/rainfed crops";

C_i = the cover management factor for each type of land cover (bare land, rainfed crop or burn areas);

A_i = area of each land cover type;

A = the total area of land cover "Bare land/burned grass/plowed land/rainfed crops".

Tables presenting the detailed calculations of the monthly C values for the land cover "Bare land/burned grass/plowed land/rainfed crops" can be found in Appendix C. Figure 4.21 is the plot of these monthly C values.

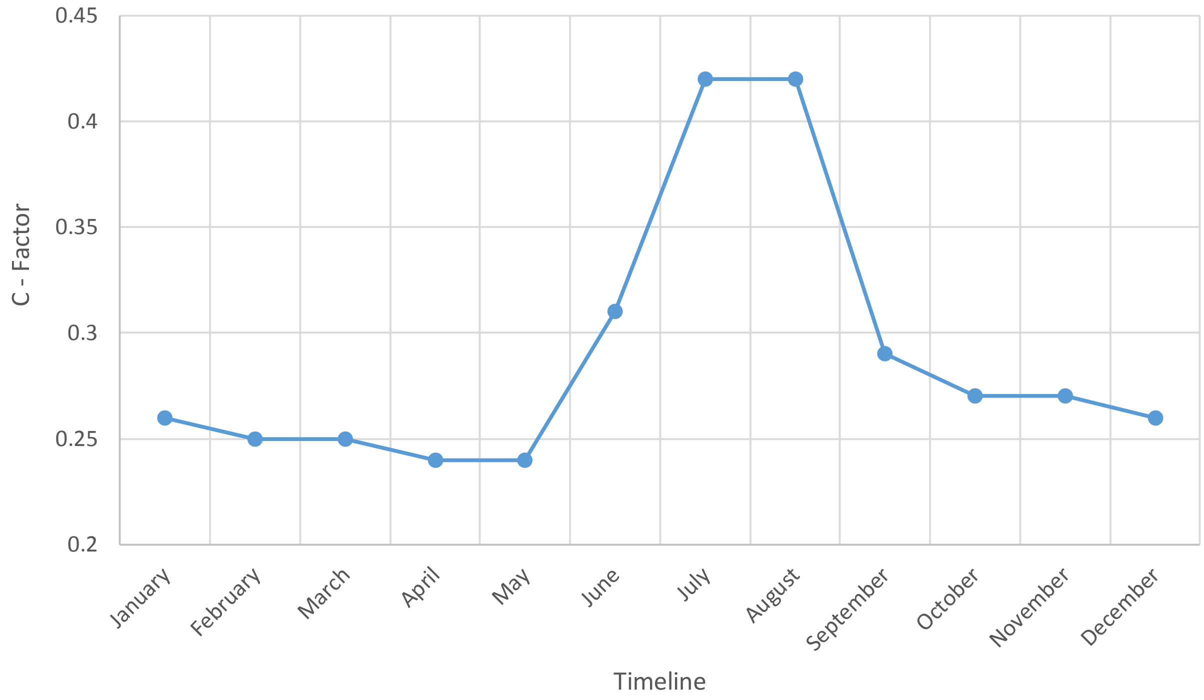

Figure 4.21 – Monthly C values for the cover “Bare land/burned grass/plowed land/rainfed crops”

c. Step 3: Mean Annual C Factor of the class “bare land/burned grass/ plowed land/ rain-fed crop”

Since the precipitation distribution over the year is the most determining factor affecting the regrowth rate in the N’djili Basin, the mean annual C-factor for the land cover “bare land/burned grass/ plowed land/ rain-fed crop” was normalized by percent of annual precipitation using the weighted –average expression:

$$C = \frac{\sum C_i P_i}{\sum P_i} \qquad (Eq\ 4.15)$$

Where C = the annual cover management factor for the land cover “Bare land/burned grass/plowed land/rainfed crops”;

C_i = the monthly cover management factor for each period (from Figure 4.20);

P_i = Average monthly precipitation.

The results of calculations in accordance with Equation 4.15 are presented in Table 4.10.

Table 4.10 – Annual cover management factor for the land cover "Bare land/burned grass/plowed land/rainfed crops"

Period	C	Monthly P (mm)	C_iP_i	C - long term
January	0.26	171.5	44.6	**0.26**
February	0.25	134.6	33.6	
March	0.25	185.2	46.3	
April	0.24	193.6	46.5	
May	0.24	128.7	30.9	
June	0.31	15.7	4.9	
July	0.42	9.2	3.9	
August	0.42	13.4	5.6	
September	0.29	63.8	18.5	
October	0.27	141.1	38.1	
November	0.27	227.2	61.3	
December	0.26	186	48.4	
Σ		1470	382.6	

Table 4.11 presents the cover management factors for all the informational classes.

Table 4.11 - Cover management factor for different land cover types

Land cover/use type	Cover Management Factor (C)	Source
Water	0	
Forest (open cover)	0.01	Bakker et al. (2008)
Grass and shrubs (cover > 80%)	0.012	Wischmeier and Smith (1978)
Bare land/burned grass/plowed land/ rainfed crops	0.26	Wischmeier and Smith (1978) + calculations
Settlements	0.13	Teh (2010) + calculations

To produce the C-factor map, a look up table containing two fields about the land cover types and the C-values corresponding had been created and joined to the attribute table of the land cover shape files derived from the Landsat image classification. Then, the land cover shape files had been converted to raster using the “To Raster” tool of the Conversion Tools included in ArcToolbox and the column of C-values. Figures 4.22, 4.23 and 4.24 show the C-factor maps of the N’djili River Basin derived in ArcGIS for the conditions in 1995, 2001 and 2013.

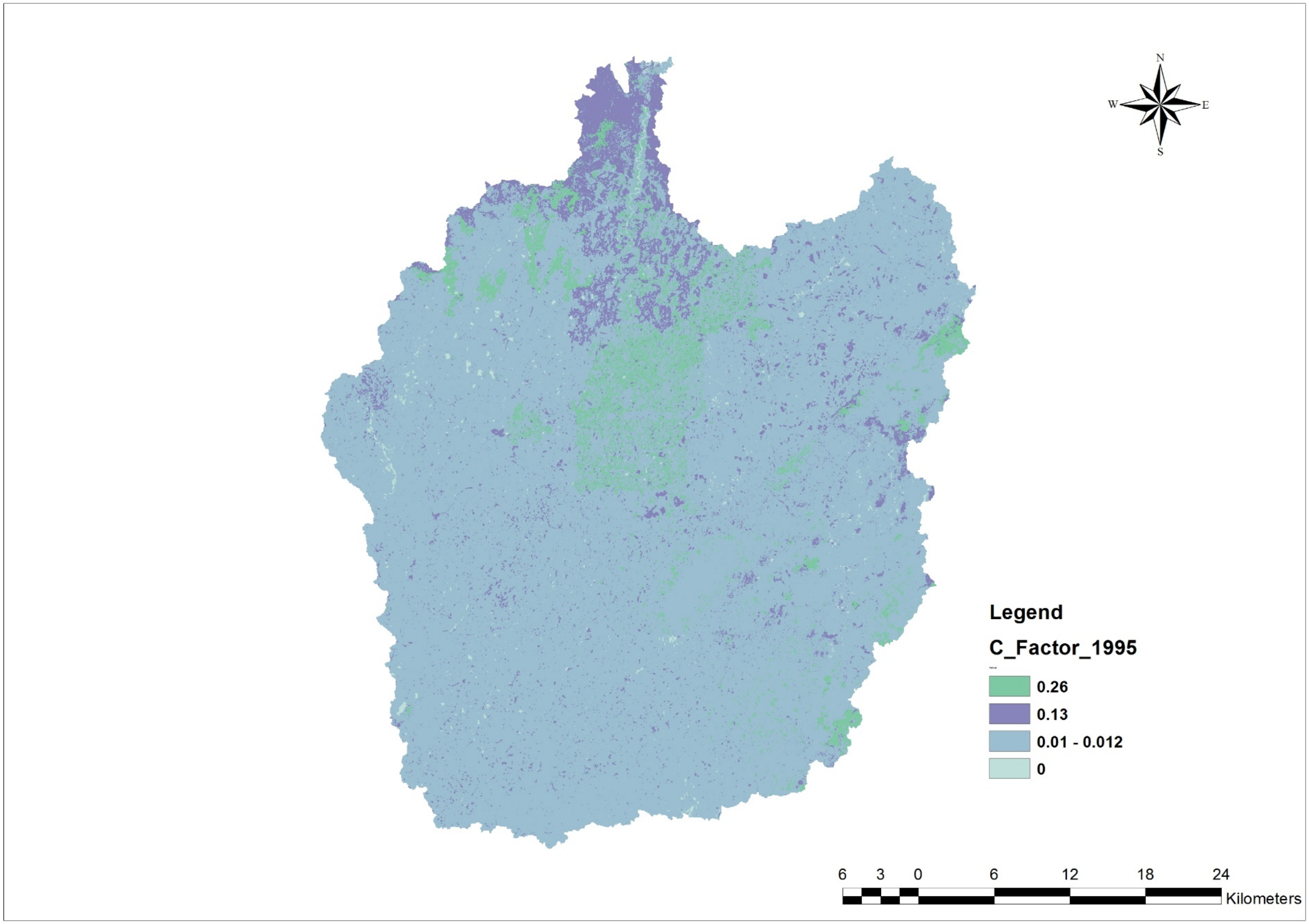

Figure 4.22 – C factor map of the N'djili basin in 1995

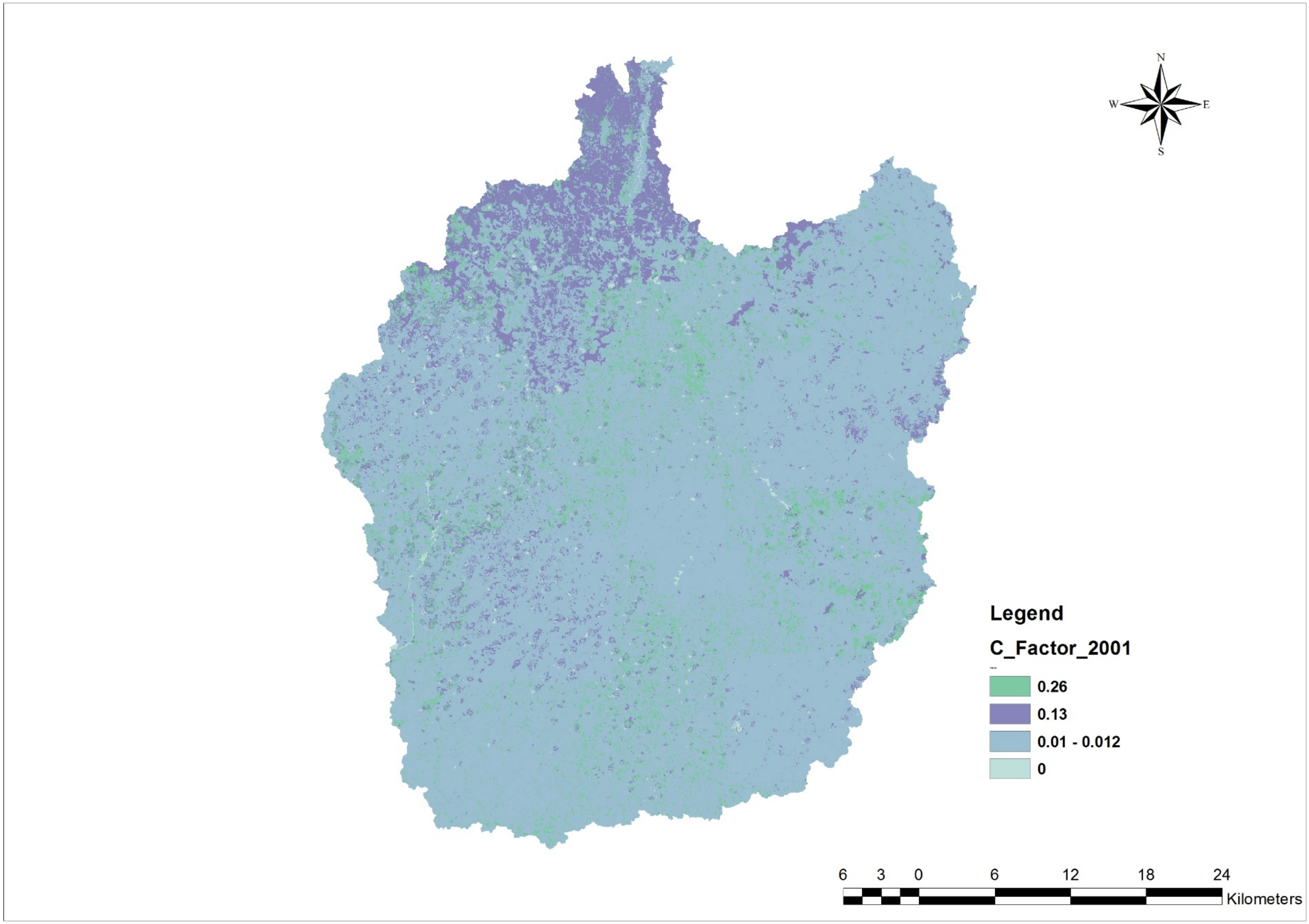

Figure 4.23 – C factor map of the N'djili basin in 2001

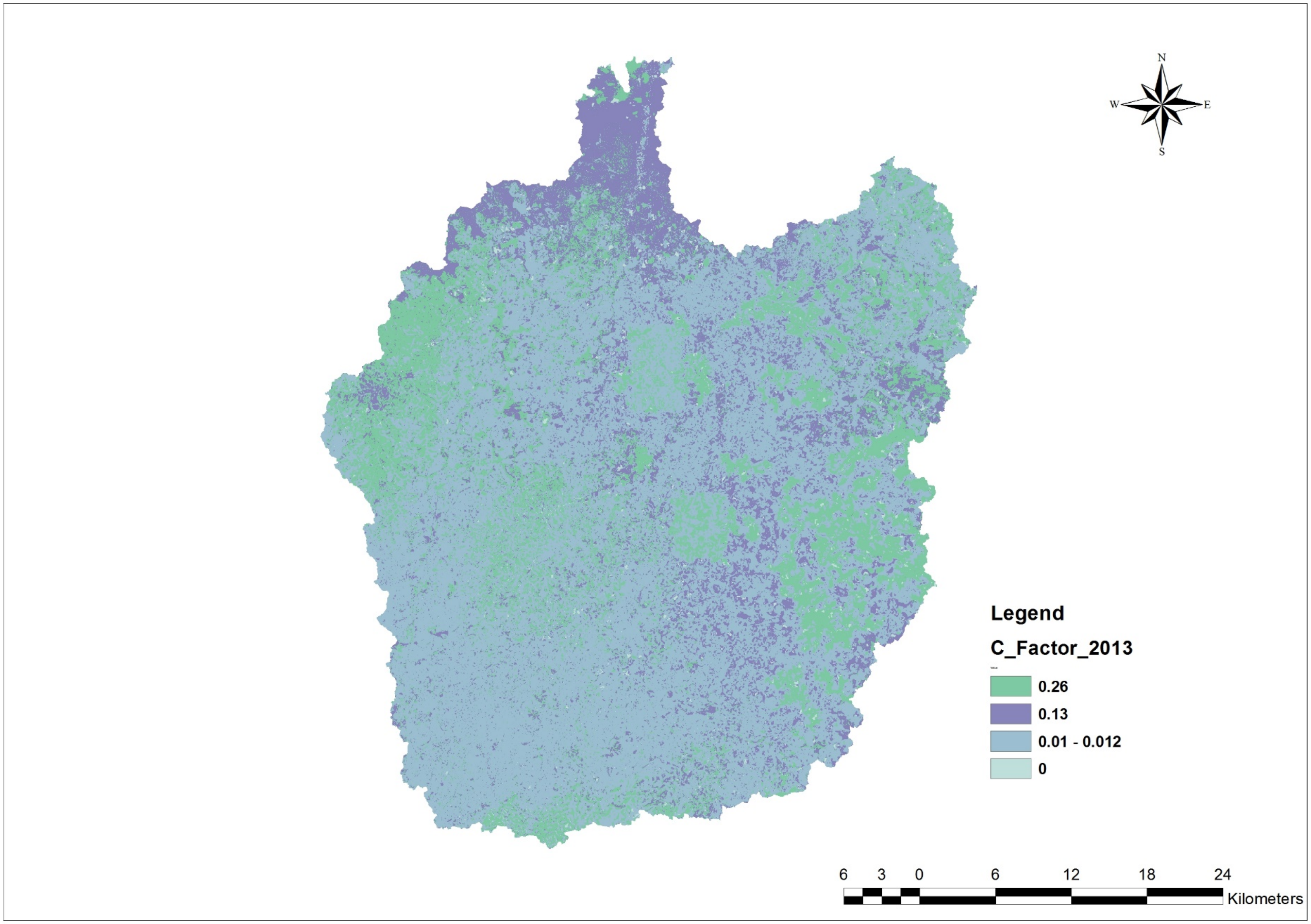

Figure 4.24 – C factor map of the N'djili basin in 2013

4.1.5 Support Practice Factor (P)

The P factor takes into account support practice effects on soil erosion. These practices generally affect the amount, flow pattern, rate or direction of surface runoff (Reynard and Foster 1983). Contouring (tillage and planting on, or near the contour), strip cropping, terracing, and subsurface drainage are used as support practices for cultivated land. Soil-disturbing practices oriented on or near the contour that result in storage of moisture and reduction of runoff are also considered as support practices for dryland or rangeland areas. For construction and mine reclamation areas, support practices include contour plowing and diversions.

The P-factor value results from the product of P subfactors that takes into account individual support practices, some of which are used in combination. P-factor values were obtained from experimental data by Renard et al. (1997). These results are supplemented by analytical experiments involving scientific observation of known cause-and-effect relationships in physically based models such as CREAMS (Knisel 1980). P-values range from 0 to 1. The P-factor value is equal to 1 for farming upslope and downslope, and less than 1 when the above mentioned support practices are implemented.

Although some terracing support practices are used for some rainfed crops in the N'djili River basin (Figure 4.25), it can be assumed that there are no support practices implemented in the basin, since the area concerned represents less than 1% of the basin area. Therefore, a value of 1 is assigned to the P factor in this study. To simulate or forecast different erosion prevention measures, the P-value could be adjusted accordingly.

Figure 4.25 - Terraced rainfed crops in the N’djili River Basin (photo by P. Ndolo Goy, 2013)

4.1.6 Effect of ash concentration on turbidity in the N’djili River

Watersheds in Central Africa are vulnerable to wildfires. With increasing human activities, wildfire size, fire severity, and length of burning season have increased since the beginning of the 1980s (Boko et al. 2007). Following the findings from Writer et al. (2012), it can be assumed that burning practices that occur between June and August in the N’djili River Basin can lead to increasing stream discharge, turbidity, and dissolved organic carbon, during and after high-intensity thunderstorms. Specifically, turbidity is caused by detached soil particles and ash during the first storms after burning that are washed away by water.

Turbidity is one of the most visible water quality effects of wildfires. After wildfire, surface water turbidity can increase due to the suspension of ash and silt-to-clay-sized particles.

To measure the impact of ashes in water turbidity, a simple experiment (Figure 4.26) was conducted in organic chemistry Laboratory of the Science Department of the University of Kinshasa in July 2014. Using water from N'djili River and ashes from a burned area in the N'djili basin, the experiment goal was to measure the impact of ash concentration on water turbidity.

Figure 4.26 - Turbidity measurement during the laboratory experiment.

Different concentrations of ashes had been added to water from N'djili River. Turbidity had been measured for those different concentrations immediately after mixing, 24 hours and 48 hours after mixing. The initial turbidity of water was 0.5 NTU. Table 4.12 presents the results from this experiment. Turbidity measurements performed 24 and 48 hours after mixing had been done on some selected concentrations. Figure 4.27 illustrates the results from this experiment on a logarithmic scale. Pictures from that experiment are provided in Appendix D.

Table 4.12 – Effect of ash on water turbidity

Ash Concentration (mg/l)	Turbidity (NTU) - 0h	Turbidity (NTU) - 24h	Turbidity (NTU) - 48h
0	3.5	2.8	1.9
5	4.35		
10	6.01	4.35	3.1
15	8		
20	8.98	5.5	4.27
30	11.74		
50	17.42		
75	21.5	15.4	9.23
100	25.93		
150	38.78		
200	42.82	28.1	17.61
500	82		
1000	228.55	105	52
2000	350		
3000	415	187	68
5000	465	205	84

Results from the experiment shows that water turbidity varies with the ash concentration following a power relationship which is given in Equation 4.15. This experiment reveals that relatively small quantity of ashes affect tremendously the water turbidity. For example, given ash concentration of only 5g per liter, the threshold limit of turbidity (500 NTU) – which is the turbidity value beyond which pumping operations are stopped – is almost reached. So, this experiment explains indirectly high turbidity values observed due to the combined effect of ashes and soil particles washed away after wildfires.

The power relationship between the ash concentration and the water turbidity is given in Equation 4.16.

$$\mathrm{NTU} = 1.0361\ \mathrm{C}^{0.7347} \qquad \text{(Eq 4.15)}$$

Where:

NTU = Turbidity, expressed in Nephelometric Turbidity Unit (NTU);

C = ash concentration, expressed in mg/L.

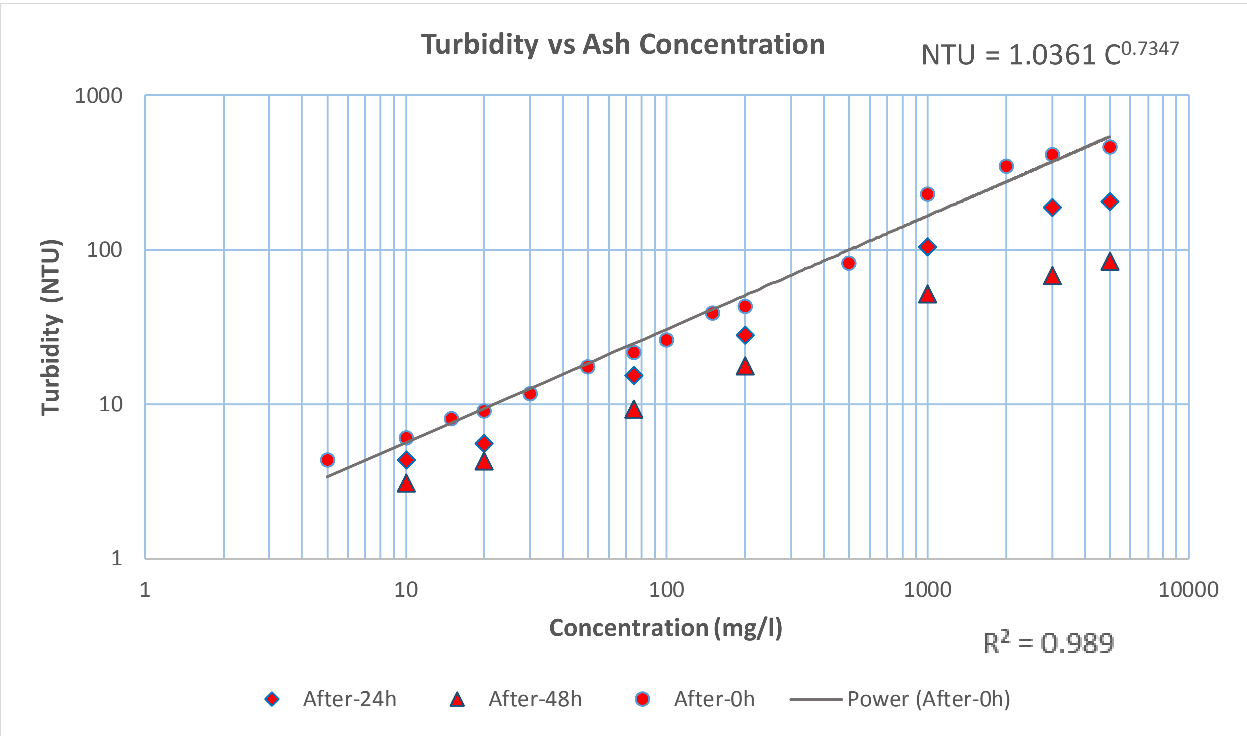

Figure 4.27 - Effect of ash concentration on water turbidity.

4.2. Summary

Chapter 4 presents the procedure and methodology employed to estimate the six parameters of the RUSLE: rainfall-runoff erosivity (R), soil erodibility (K), slope length and steepness or topographic factor (LS) or, cover management (C), and support practice factor (P).

In the N'djili River Basin, the annual R value ranges from 385 to 466 (100 ft tons inch acre^{-1} h^{-1} year^{-1}) based on the location of rainfall stations. The maximum rainfall-runoff erosivity factor is estimated in the northeastern region of the basin with a value of 466. Soil erodibility (K) is estimated based on the soil classification and varies from 0.10 to 0.15, with the maximum value (0.15) assigned in areas where the soil texture is sandy. The topographic factor LS is estimated using the DEM and the approach developed by Moore and Burch (1985) based on the concept of flow accumulation in ArcGIS. LS values range from 0 to 61. The cover management factor (C) is obtained from the land cover map derived from Landsat scenes of the N'djili Basin, based on results from MacDonald (2012) and Wischmeier and Smith (1978). C-factor range from 0 to 0.26. C-values of 0.26 is assigned to bare land, burned grass, and rain-fed crops areas. Based on these C-values, those areas are prone to severe erosion. Although some terracing support practices are observed in the N'djili River basin it is assumed that there are no support practices implemented in the basin, since the area concerned represents less than 1% of the basin area; therefore the support practice factor (P) is assigned a value of 1. The laboratory experiment on the effect of ash concentration over the water turbidity has come to the conclusion that water turbidity varies with the ash concentration following a power relationship.

CHAPTER 5 : APPLICATION AND RESULTS

Introduction

This chapter presents, in Section 5.1, discussion about the annual average soil loss rate distribution of the N'djili River Basin in 1995, 2001 and 2013 and the mid/long term effect of some watershed degradations like burning practices and deforestation on the predicted soil erosion rate. The Section 5.2 presents the calculations of sediment yield based on sediment rating curves for years 2005 and 2013 and makes some comparative analysis based on the results. Section 5.3 is related to specific degradation of the N'djili River Basin. In Section 5.4, the sediment delivery ratio is estimated using different methods.

5.1. The Annual Average Soil Loss Rate (A)

To estimate the annual average soil loss rate for the N'djili basin in 1995, 2001 and 2013, the raster grids representing the RUSLE parameters were multiplied in the raster calculator tool of ArcGIS, using the C-factor raster corresponding. Table 5.1 presents the annual average soil loss rate obtained for 1995, 2001 and 2013. The annual average soil loss is estimated to be 7 tons/acre/year (1,570 tons/km^2/year) in 1995, 8.7 tons/acre/year (1,950 tons/km^2/year) in 2001 and 16 tons/acre/year (3,650 tons/km^2/year) in 2013. Figures 5.1, 5.2, 5.3 and 5.4 present the annual average soil loss rate maps for years 2013, 2001 and 1995, respectively.

In agricultural context, the term "soil loss tolerance" denotes the maximum rate of soil erosion that can occur and still permit crop productivity to be sustained economically (Borah et al. 2007). For most of the soils, this maximum rate is set to 5 ton/acre/year and soil erosion rate ranging between 0 and 5 ton/acre/year is considering as tolerable. So, up to 82% of basin area are subjected to a tolerable erosion in 1995, 79% of basin area in 2001 and 72% in 1995. Figure 5.5 illustrates the evolution of soil loss tolerance in the N'djili Basin since 1995. From this figure, it can be noticed that, in general, the portion of basin area subjected to tolerable soil loss erosion tends to decrease whereas the portion with higher soil erosion rate increases.

Table 5.1 - Annual average soil loss rate for 1995, 2001 and 2013

Parameters	1995	2001	2013
Annual average soil loss rate (tons/acre/year)	7	8.7	16
Annual average soil loss rate (tons/km^2/year)	1,570	1,950	3,650

Tables 5.2, 5.3 and 5.4 provide the annual soil rate based on the land cover types of the basin for years 1995, 2001 and 2013 respectively. The total annual average soil loss of the N'djili river Basin is approximately 0.75 million tons/year in 1995, 0.875 million tons/year in 2001 and 1.8 million tons/year in 2013. Grass and shrub areas comprise between 62 and 77% of total annual average soil loss in 1995 and 2001, whereas the bare land/burning grass/rainfed crops area comprises about 60% of total annual average soil loss in 2013. Figure 5.6 illustrates the evolution of soil loss rate in the N'djili Basin per land cover since 1995.

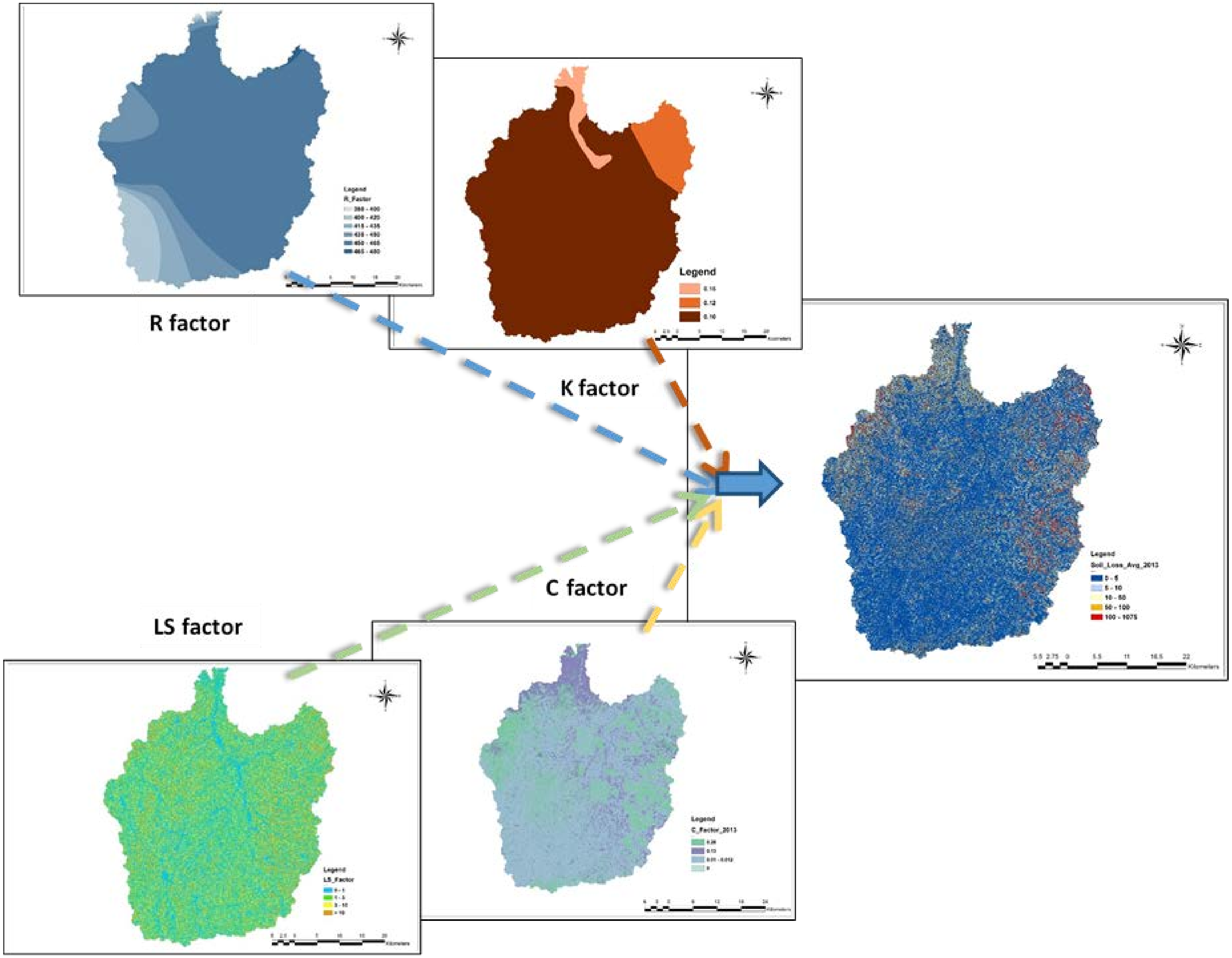

Figure 5.1 – Derivation of the average annual soil loss rate map of the N'djili River Basin.

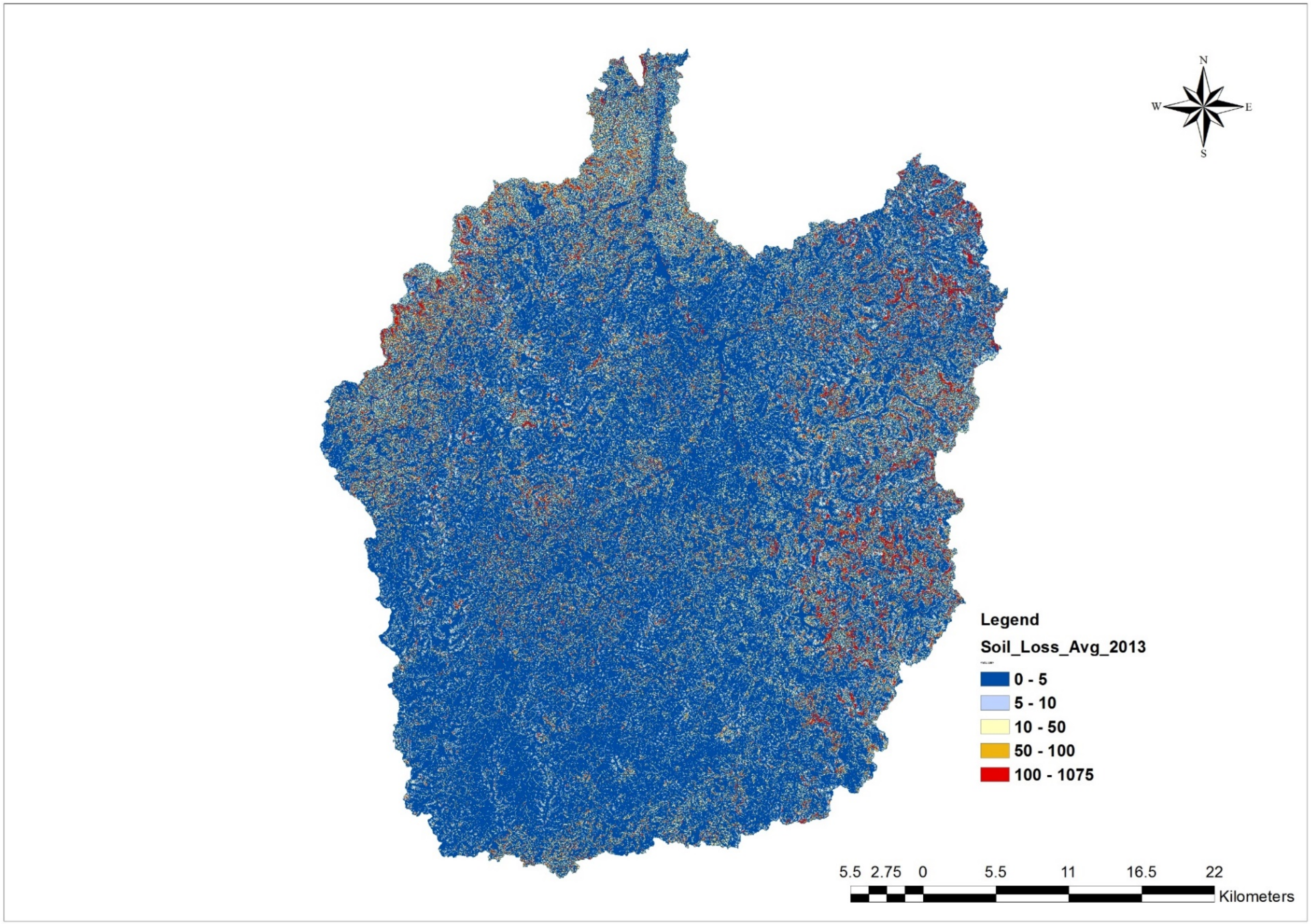

Figure 5.2 – Average annual soil loss rate map of the N'djili River Basin for conditions in 2013.

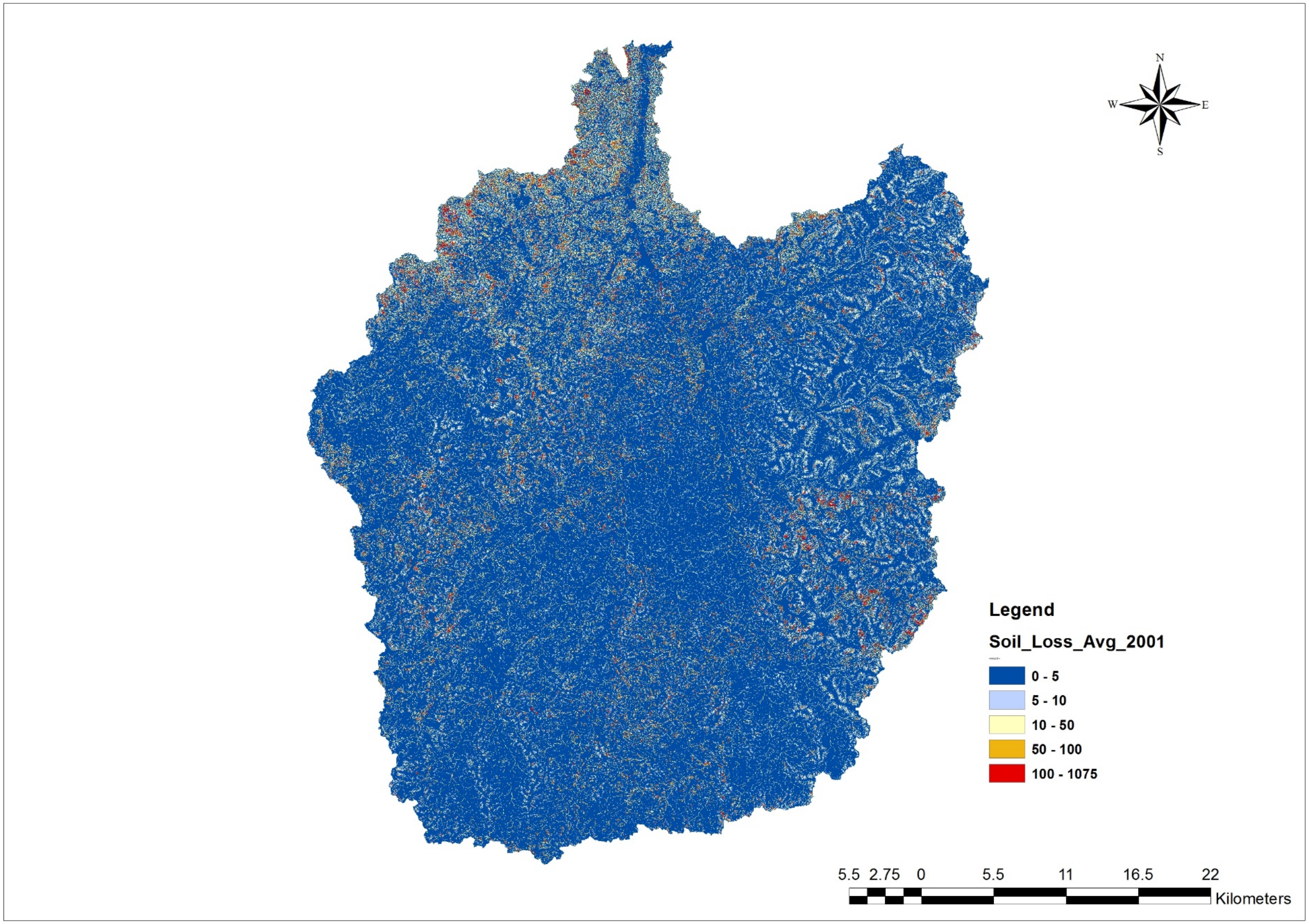

Figure 5.3 – Average annual soil loss rate map of the N'djili River Basin for conditions in 2001

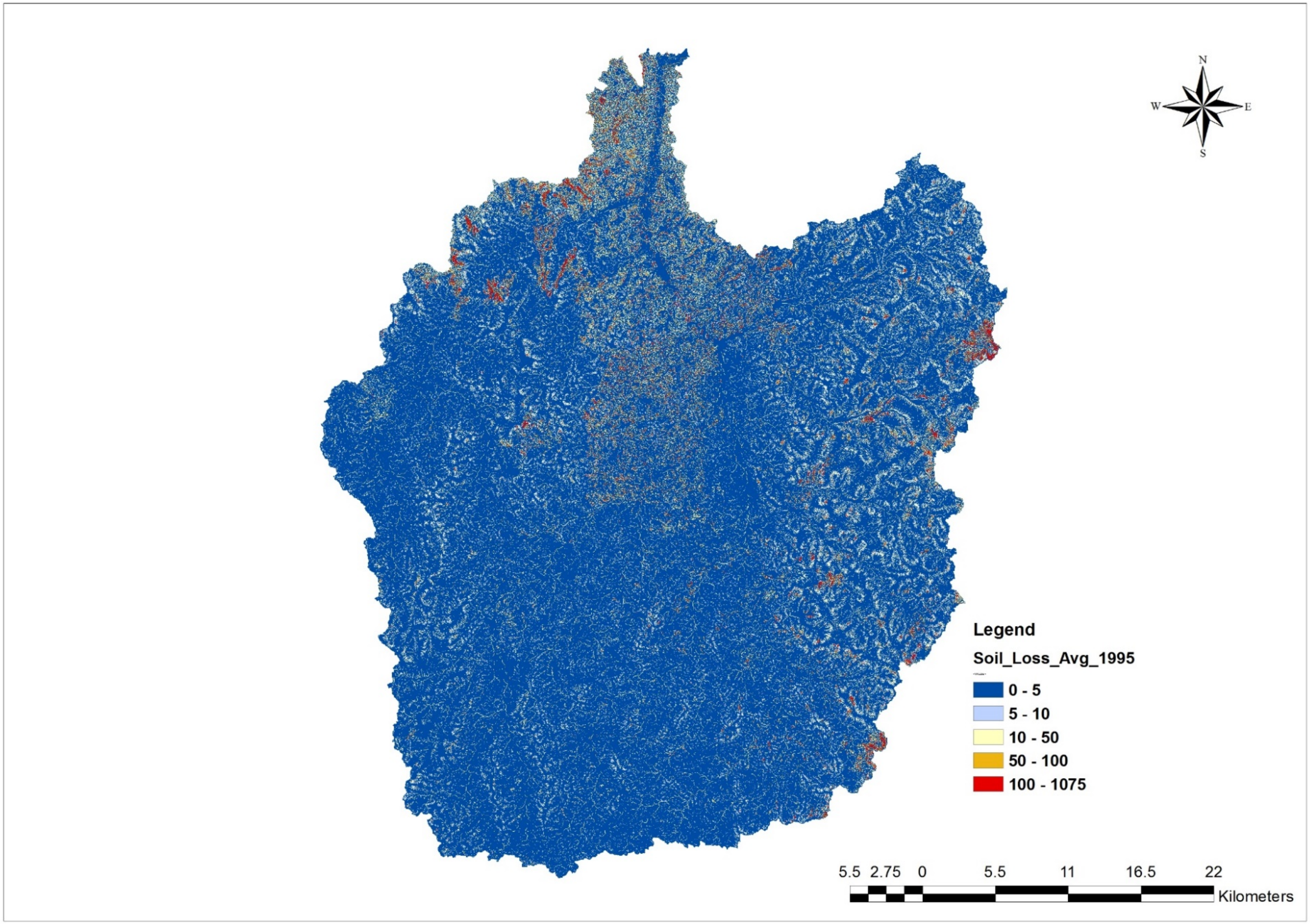

Figure 5.4 – Average annual soil loss rate map of the N'djili River Basin for conditions in 1995

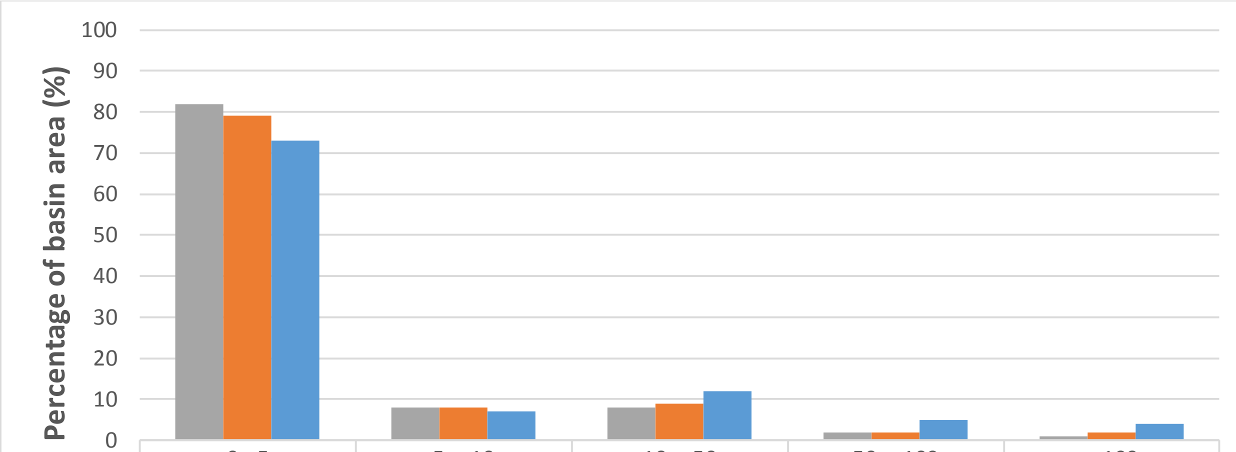

	0 - 5	5 -- 10	10 -- 50	50 -- 100	> 100
1995	82	8	8	2	1
2005	79	8	9	2	2
2013	73	7	12	5	4

Figure 5.5 - Evolution of soil loss rate tolerance in the N'djili Basin since 1995.

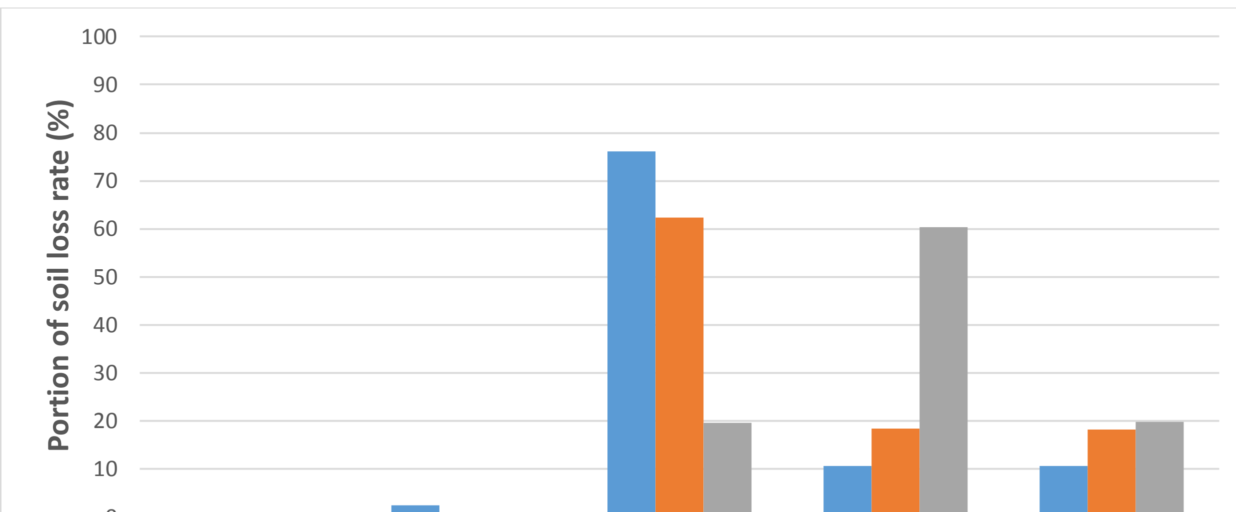

	Water	Forest (open cover)	Grass and shrubs (cover > 80%)	Bare land/burned grass/plowed land/ rainfed crops	Settlements
1995	0	2.53	76.2	10.64	10.64
2005	0	1.14	62.29	18.4	18.17
2013	0	0.11	19.65	60.3	19.93

Figure 5.6 - Annual average soil loss rate based on the land cover in the N'djili Basin since 1995.

Table 5.2 - Annual average soil loss based on the land cover in 1995

1995						
Land cover/use type	**A (km2)**	**Portion of Area (%)**	**Soil loss rate (tons/acre/year)**	**Soil loss rate (metric tons/km2/year)**	**Annual soil loss (million tons/year)**	**Portion of total annual soil loss (%)**
Water	22	1	0	0	0	0
Forest (open cover)	313	15	0.26	59	0.020	2.53
Grass and shrubs (cover > 80%)	1467	70	1.75	391	0.570	76.2
Bare land/burned grass/plowed land/ rainfed crops	122	6	2.91	653	0.080	10.64
Settlements	173	8	2.10	465	0.080	10.64
Total	2097	100			0.75	100

Table 5.3 - Annual average soil loss based on the land cover in 2001

2001						
Land cover/use type	**A (km2)**	**Portion of Area (%)**	**Soil loss rate (tons/acre/year)**	**Soil loss rate (metric tons/km2/year)**	**Annual soil loss (million tons/year)**	**Portion of total annual soil loss (%)**
Water	22	1	0	0	0	0
Forest (open cover)	213	10	0.21	47	0.010	1.1
Grass and shrubs (cover > 80%)	1437	69	1.70	379	0.545	62.3
Bare land/burned grass/plowed land/ rainfed crops	185	9	3.90	869	0.161	18.4
Settlements	240	11	3.00	662	0.159	18.2
Total	2097	100			0.875	100

Table 5.4 - Annual average soil loss based on the land cover in 2013

2013						
Land cover/use type	**A (km2)**	**Portion of Area (%)**	**Soil loss rate (tons/acre/year)**	**Soil loss rate (metric tons/km2/year)**	**Annual soil loss (million tons/year)**	**Portion of total annual soil loss (%)**
Water	22	1	0	0	0	0
Forest (open cover)	105	5	0.11	24	0.002	0.1
Grass and shrubs (cover > 80%)	1145	55	1.36	306	0.350	19.7
Bare land/burned grass/plowed land/ rainfed crops	456	22	10.51	2353	1.074	60.3
Settlements	369	17	4.30	964	0.355	20.0
Total	2097	100.0			1.781	100

5.2. Sediment yield – Sediment rating curve

For the N'djili River Basin, a short-term and a long-term sediment analysis were used to determine the daily and the annual sediment load from turbidity and sediment concentration measurements performed at the station 2 as shown in Figure 5.7.

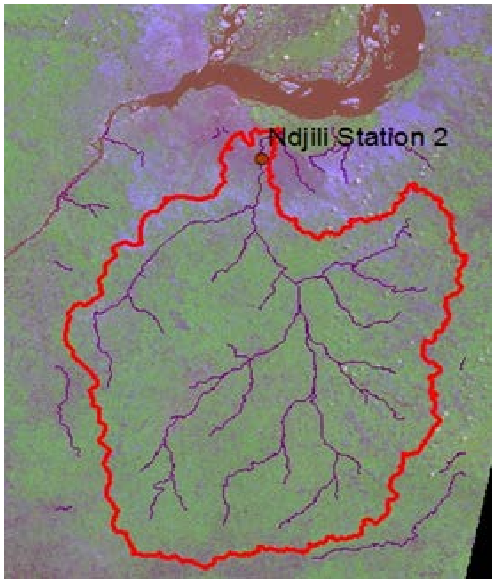

Figure 5.7 – Location of N'djili Station 2

5.2.1. Daily sediment load or sediment rating curve of the N'djili River

For the N'djili River Basin, Equation 2.1 was used to compute the daily sediment load of the N'djili River at station 2 from the sediment concentration, turbidity and daily flow measurements performed at the station 2 (section 3.2.5 of Chapter 3).

The plots of Figures 5.8 and 5.9 present the daily sediment load vs the daily mean water discharge for years 2005 and 2013, while Figures 5.10 and 5.11 illustrate the sediment concentration relationship as function of discharge. Equations 5.1, 5.2, 5.3 and 5.4 give the regression equations derived from the plots of Figure 5.8 to 5.11. The detailed results obtained from the equation 5.1 are presented in appendix E.

$$Q_s = 0.0409\ Q^{2.902}, \text{for } 2005 \qquad \text{(Eq. 5.1)}$$

$$Q_s = 0.0418\ Q^{2.887}, \text{for } 2013 \qquad \text{(Eq. 5.2)}$$

$$C = 0.473\ Q^{1.902}, \text{for } 2005 \qquad \text{(Eq. 5.3)}$$

$$C = 0.4838\ Q^{1.887}, \text{for } 2013 \qquad \text{(Eq. 5.4)}$$

Where:

Q_s = the total sediment discharge in tons per day;

Q = the daily mean water discharge in m^3/s.

C = the daily sediment concentration in mg/L.

It can be noted that the Equations 5.3 and 5.4 giving the daily sediment concentration are very similar.

5.2.2. Annual sediment load of the N'djili River

In the case of the N'djili River Basin, the flow duration curve approach was employed to determine the annual sediment loads in 2005 and 2013. This approach combines the sediment-rating curve and the flow-duration curve.

To determine the flow-duration curves of the N'djili River at station 2 for years 2005 and 2013, the following operations have been performed using an Excel spreadsheet:

- Sort the daily discharge by magnitude from largest to smallest using the "sort" command in Excel;

- Determine the rank of each discharge in the period of record (one year) using the “rank” function in Excel;
- Calculate the exceedance probability (P) as follows:

$$p = 100 \frac{M}{n+1} \qquad \text{(Eq. 5.5)}$$

p = the probability that a given flow will be equaled or exceeded (% of time)

M = the ranked position on the listing (dimensionless)

n = the number of events for period of record (dimensionless)

- Graph the exceedance probability versus the discharge.

Figure 5.12 presents the flow duration curves of the N’djili River, at station 2 for years 2005 and 2013 respectively.

The general procedure followed to determine the annual sediment load of the N’djili River at the station 2, using a spreadsheet, is as follows:

- Build the first column with the time interval in %;
- Create column (2) with the interval midpoint in %;
- Create the column (3) representing the duration of each time period in %;
- Derive column (4) from the flow-duration curve, considering abscissa of the column (2);
- Create the column (5) for sediment concentration following Equations 5.4 and 5.5 developed in section 5.2.1
- Create column (6) by multiplying columns (3) and (4);
- Create column (7) by multiplying columns (5) and (6).

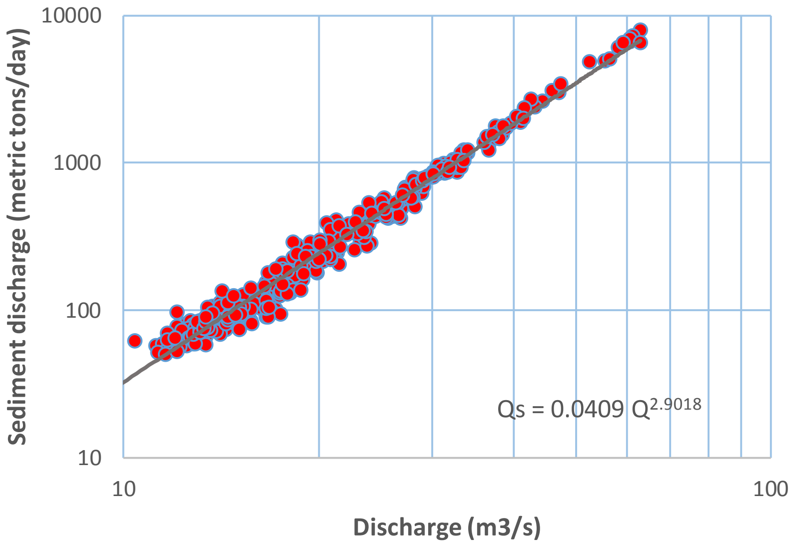

Figure 5.8 - Sediment rating curve of the N'djili River (2005)

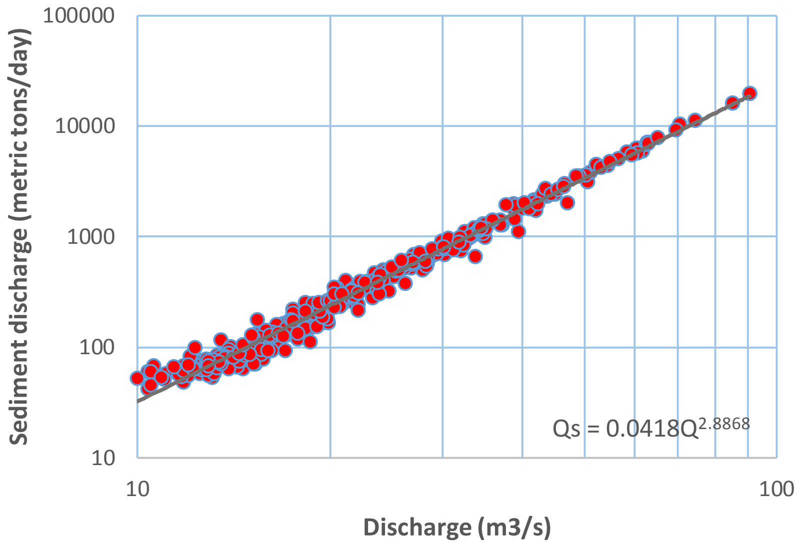

Figure 5.9 - Sediment rating curve of the N'djili River (2013)

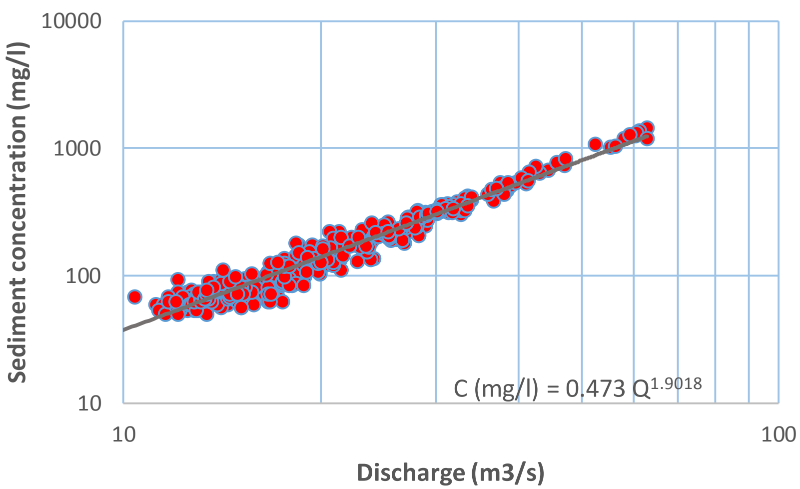

Figure 5.10 - Sediment concentration of the N'djili River (2005)

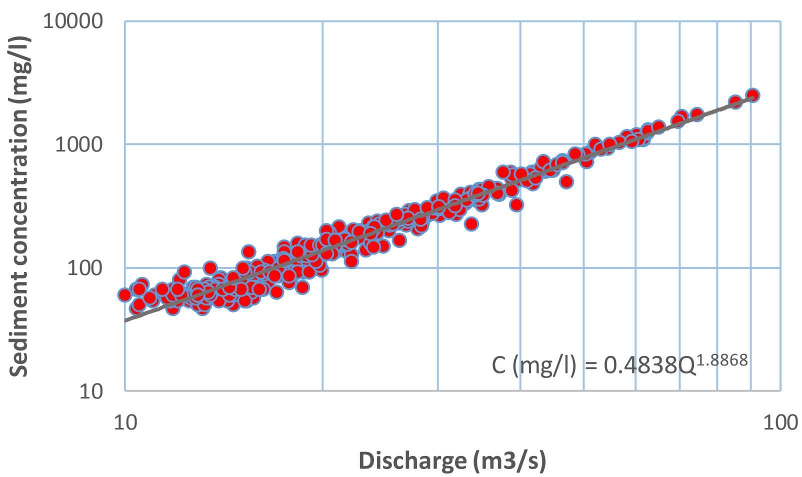

Figure 5.11 - Sediment concentration of the N'djili River (2013)

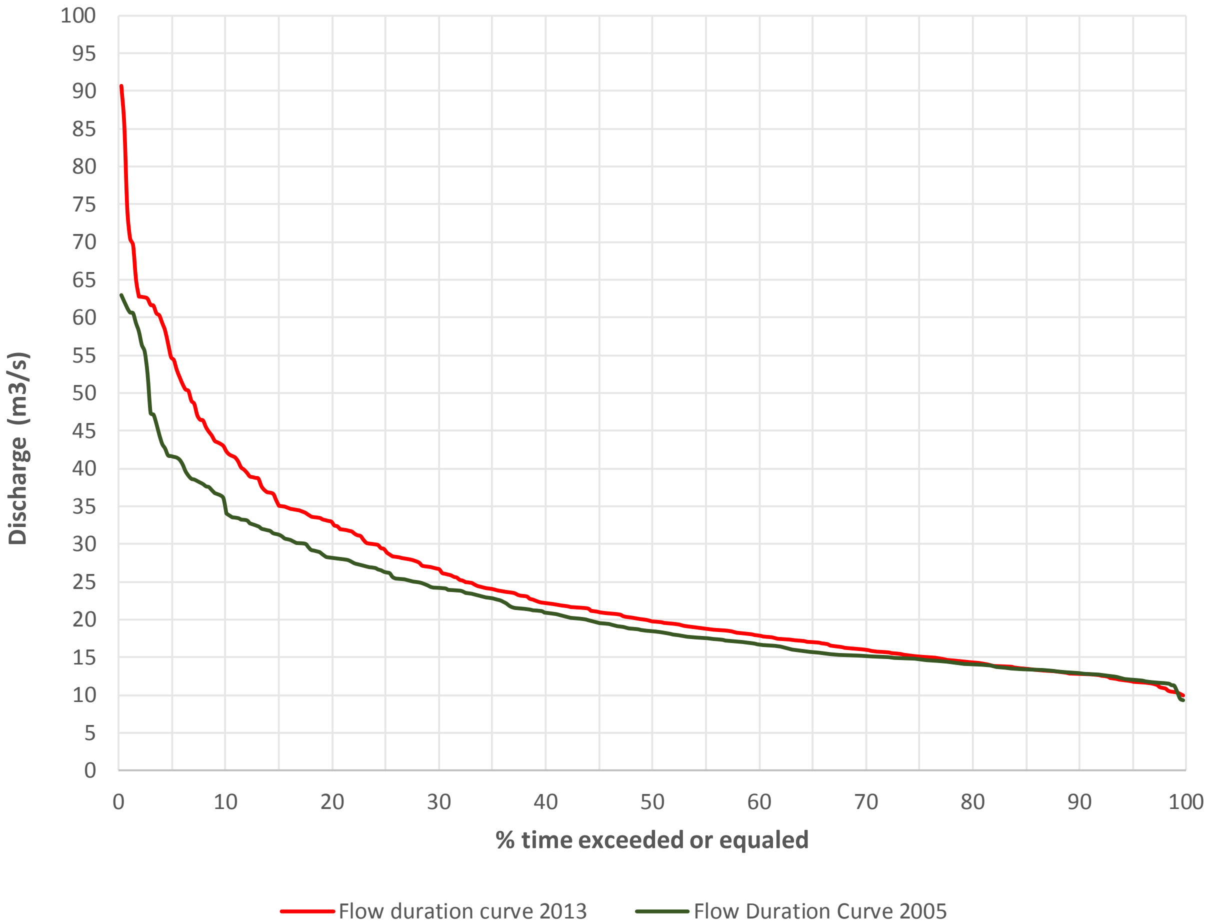

Figure 5.12 - Flow duration curves of the N'djili River for years 2005 and 2013

The results obtained using this procedure are illustrated in Tables presented in Appendix E. From those results, the estimated annual sediment load for 2005 is 189,030 metric tons/year while it is about 315,000 metric tons/year for 2013. So from 2005 to 2013, the annual sediment load increased by about 67%.

5.3. Specific Degradation of the N'djili River Basin

Specific degradation values of the N'djili River basin for years 2005 and 2013 are presented in Table 5.5.

Table 5.5 - Specific degradation values of the N'djili River Basin in 2005 and 2013.

Year	**2005**	**2013**
Sediment Yield (metric tons/year)	189,030	315,000
Drainage area (km2)	2,097	2,097
Average Annual rainfall (mm)	1470	1470
Specific Degradation SD (metric tons/km2.year)	90.1	150.2

Kane and Julien (2007) compiled several field measurements of sedimentation in US reservoirs to determine relationship between SD and drainage area A of watershed in one hand, and relationship between SD and mean annual rainfall R in the other hand. Those results served to compare and validate the sediment yield data derived from the sediment rating curves computed in the previous paragraph. Hence, the values of SD presented in Table 5.8 have been plotted with respect to the average annual rainfall and the drainage area on the log normal specific degradation plots (Figure 5.13) derived by Kane and Julien (2007).

From Figure 5.13, it can be noticed that the specific degradation values of the N'djili River Basin computed from 2005 and 2013 sediment data are within 95% confidence intervals specified by Kane and Julien (2007).

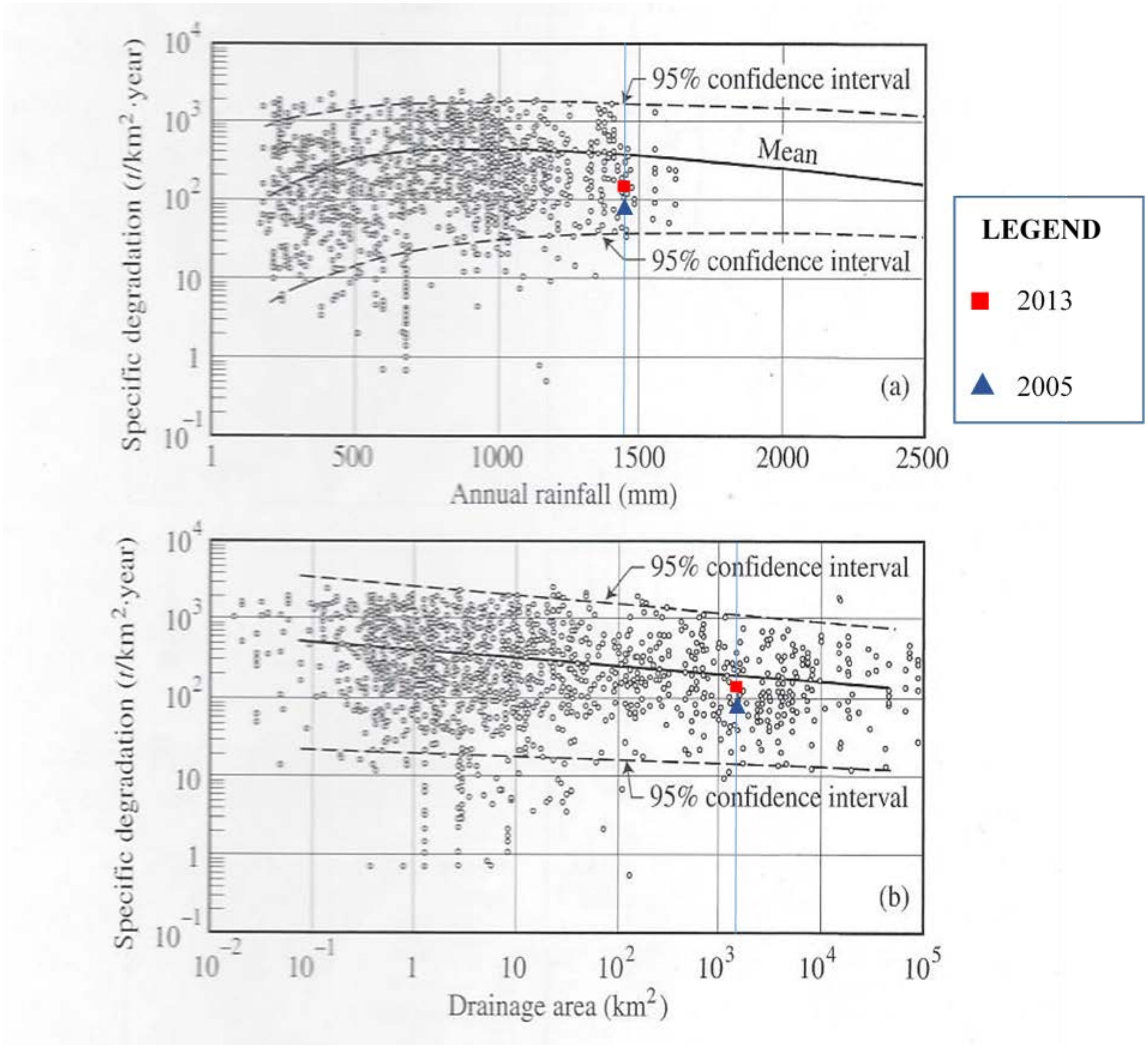

Figure 5.13 - Specific Degradation (after Kane and Julien, 2007) versus a) Annual Rainfall; and b) Drainage Area (Julien, 2010)

5.4. Sediment Delivery Ratio

As defined in paragraph 2.8, the sediment delivery ratio (S_{DR}) is the ratio of the sediment yield Y at a given stream cross-section to the gross erosion A_T from the watershed upstream of the measuring point (Julien 2010). At this point, for the N'djili River Basin, the annual sediment yields for years 2005 and 2013 are available, as well as the soil gross erosion for conditions in 1995, 2001 and 2013. Therefore, the sediment delivery ratio for 2005 was computed for gross soil loss conditions in 2001 and using the sediment data of 2005. For 2013, the sediment delivery ratio was estimated using the gross soil erosion of 2013 and the annual sediment yield calculated for the same year. Table 5.6 presents values of sediment delivery ratio observed at the station N'djili 2, and the ratios calculated using the relationships after Renfro (1975) and Boyce (1975).

Table 5.6 - Sediment Delivery Ratios

Year	N'djili Basin Area	Sediment Yield	Soil Loss rate by RUSLE		Sediment Delivery Ratio (%)		
	(km2)	(metric tons/year)	(tons/acre/year)	(metric tons/km2/year)	Renfro	Boyce	Observed
2005	2,097	189,030	8.7	1,957	21	4.1	4.6
2013	2,097	315,000	16	3,650	21	4.1	4.1

The results from Table 5.6 are plotted in the Boyce (1975) graph presented in Figure 5.14. The results show that the sediment delivery ratio observed at the N'djili Station 2, is almost equal to the mean S_{DR} derived by Boyce (1975). Moreover, the sediment delivery ratio estimates in 2005 (4.6 %) and 2013 (4.1 %) are almost equal. These low values of sediment delivery ratio can be due to the following reasons:

a. Soil eroded from upland areas is trapped on flood plains covered by grass, shrubs and trees and in small ponds made for the artisanal sandpit along of the N'djili river and its tributaries;

b. Soil types encountered in the N'djili basin have high percentage of sand in their texture. Since sand is coarser than clay and loam, it can be inferred that a relatively high proportion of sand is deposited over flood plains and stream bed, and sediment yield is mainly constituted by clay, loam and fine sand particles. This hypothesis shall be verified by laboratory experiments such as sieving test and hydrometer analysis to be performed on sediment yield samples.

T

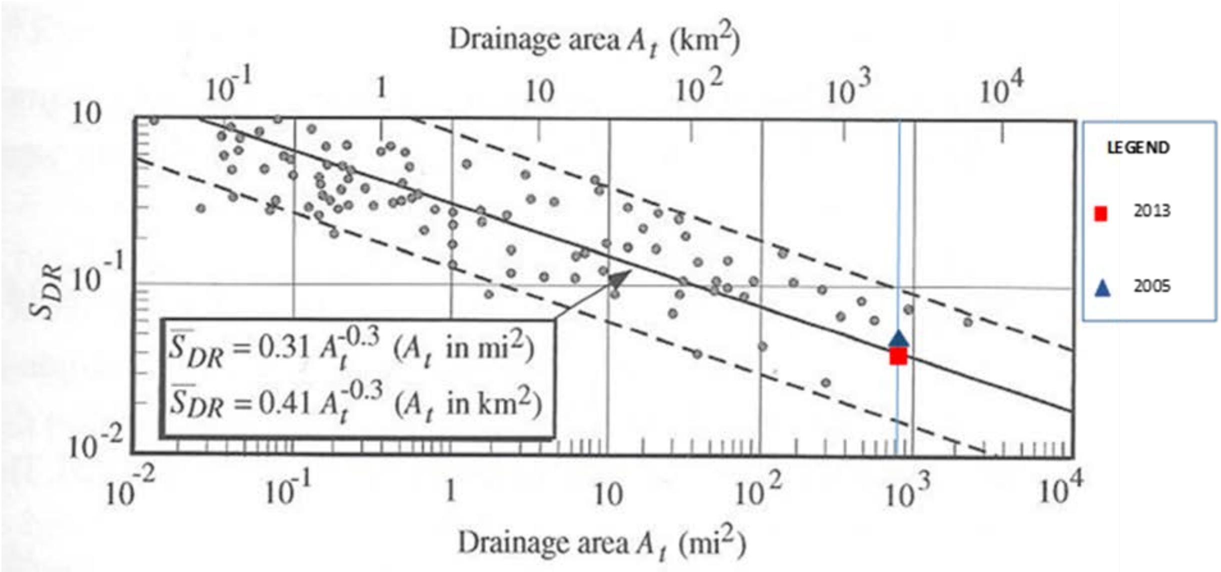

Figure 5.14 - Sediment Delivery Ratio of the N'djili River Basin

5.5. Discussion of results and Limitations

RUSLE method is known to be dependent on the accuracy of its parameter estimation. The accurate estimation of the RUSLE parameters depends on availability and quality of data. For the N'djili River Basin, there are some limitations due to the availability and quality of data.

1. Rainfall-runoff erosivity factor (R):

The rainfall-runoff erosivity factor in the RUSLE should be calculated using the maximum rainfall 30-min intensity (I_{30}). Since only average daily precipitation data are available for the N'djili Basin, the Renard and Freimund equation (1993) based on average annual precipitation was used, despite that this equation was derived from US precipitation data. The second limitation for computing the R-factor is the spatial distribution of the climatic stations over the N'djili Basin. Most of the precipitation stations are located in the north-western part of the basin, so this data exhibit a spatial clustering which wasn't impossible to correct before performing the spatial interpolation. Nevertheless, a spatial interpolation has been performed giving that the range of the average annual precipitation from these climatic stations is relatively low to lead to great discrepancies between interpolated and measured values, as shown by the prediction standard error incorporated with precipitation uncertainty map of the N'djili River Basin in Appendix B. Lastly, for the computation of the R-factor, the spatial interpolation performed on precipitation data didn't take into account the topography of the basin.

2. Soil Erodibility Factor (K):

The 1:2,000,000 soil map developed by Soil and Terrain database of Central Africa (SOTERCAF, version 1.0) and on which the K-factor is based, doesn't accommodate local variability of soil type in the basin. Therefore, K-factor is limited based on the current data availability and may change when more detailed soil map will be available.

3. Slope Length and Slope Steepness Factor (LS):

The slope length factor (L) and the steepness factor (S) account for the effects of topography on upland soil erosion. Terrain attributes are readily estimated from DEMs, but the estimated values are sensitive to DEM accuracy (Sasowsky et al., 1992; Bolstad and Stowe, 1994; Giles and Franklin, 1996; Hunter and Goodchild, 1997; Holmes et al., 2000) and grid size (Thieken et al., 1999; Thompson et al., 2001). For the N'djili River basin, the ASTER GDEM V2 was selected for this study at the expense of ASTER GDEM V1 and SRTM DEMs because it is more accurate and has the smallest cell size of the DEMs actually available for the N'djili basin. According to Erskine et al. (2007), estimates of slope is more sensitive to DEM accuracy due to the data source than to grid size. So, it can be inferred that when more accurate DEMs will be available for the N'djili Basin River, factor L and particularly factor S won't remain equal to those computed in this study. Indeed, Ouyang and Bartholic (2001) demonstrated in Table 5.7 that the soil erosion is more sensitive to the slope steepness than to slope length, while other RUSLE factors remain the same.

Table 5.7 - Sensitivity analysis of soil erosion and slope (a); slope length (b) (Ouyang and Bartholic 2001)

Slope (%)	1	3	6	8	10	14	16	20
Soil erosion (tons/acre/yr.)	1.14	2.38	4.09	5.04	6.37	9.50	10.93	13.8

Slope length (ft.)	25	50	100	150	200	250	300	400
Soil erosion (tons/acre/ yr.)	1.14	1.24	1.33	1.43	1.52	1.62	1.62	1.71

It might be useful to study the effect of DEM accuracy and grid size on the soil erosion in the N'djili Basin.

The second limitation is about the maximum slope allowed in RUSLE (60%). Fortunately, only 0.5% of the basin area has a slope greater than 60%. These locations with very steep slopes may produce large amount of soil erosion so caution should be used while interpreting these results.

4. Cover Management Factor (C):

The C factor is designed to reflect the effect of cropping and management practices on erosion rates, and is the factor used most often to compare the relative impacts of management options on conservation plans. The N'djili Basin River does not have a locally-developed C-factor table to be used in RUSLE. Also, available land cover maps covering the N'djili Basin have coarse resolution that doesn't fit the RUSLE modeling of a mid-size basin like the N'djili Basin. Therefore, the option of creating land cover maps from Landsat image classification was adopted. Due to technical issues experienced by the Landsat 7 mission since May 2003, images from 2003 to 2011 are almost useless , unless to perform a time consuming mosaicking operation which doesn't often reflect the real land cover in place. So, to predict the average annual soil erosion in 2005, the most appropriate image scene close to this date, with a less cloud cover percentage was the one taken on 2001/04/30. Hence, the erosion prediction for 2005 has been based on image classification of 2001 scene, introducing a bias in the gross soil erosion analysis.

With a scene of 2005, the average annual soil erosion predicted in this study for 2005 might change. Another bias in the gross soil erosion estimation was introduced when the satellite images to use for this study were selected. Indeed, to be consistent in the trend analysis of the soil gross erosion, images taken at relatively the same period of the year should have been used during the study. Unfortunately, due to Landsat 7 issue as explained in Chapter 3 and to the cloud coverage over the N'djili Basin, images from different periods of the year were selected for years 1995, 2001 and 2013.Another limitation regarding the C-factor is about the classification method used to derive the land cover/use maps for the N'djili River from satellite images. Indeed, a simple classification method was used in this study: the isoclust method from an unsupervised classification. The accuracy of classification performed in this study is presented in Appendix C. If sophisticated classification methods are used to derive these land cover/use maps, the annual average soil losses predicted in this study might be different from the ones predicted using sophisticated classification methods to derive the land cover/use of the N'djili River Basin.

Moreover, the estimate of the C factor of burned areas in Chapter 4 was performed using the equations giving the percent of bare soil after the Bobcat fire in Colorado (USA). Since the vegetation regrowth rate is much faster in the N'djili River Basin than in the Bobcat watershed, the real percent of bare soil for the burned areas should be lower than the one estimated in paragraph 4.1.4, reducing therefore the amount of the eroded soil.

5. Sediment delivery ratio (C):

The sediment delivery ratio for year 2005 was estimated using the gross soil erosion for conditions in 2001 and the annual sediment yield of 2005. Following the trend of gross soil erosion in the N'djili Basin, the amount of eroded soil in 2005 would be greater than the one estimated in 2001. Thus, the sediment delivery ratio estimated for year 2005 would be much closer to the one calculated for year 2013, confirming that all the assumptions made for this modeling are appropriate. Nevertheless, the sediment delivery ratios found for years 2005 (4.6%) and 2013 (4.1%) validate the soil erosion modeling done for the N'djili River Basin using the RUSLE.

5.6. Summary:

Annual average soil loss rate of the N'djili River Basin is estimated to be 7 tons/acre/year (1,570 metric tons/km^2/year) in 1995, 8.7 tons/acre/year (1,950 metric tons/km^2/year) in 2001, and 16 tons/acre/year (3,650 metric tons/km^2/year) in 2013.

The estimation of sediment yield at the intake of the N'djili water treatment plant (N'djili Station 2), which is close to the basin outlet, is based on turbidity, sediment concentration and flow discharge measurements performed in 2005 and 2013 by different agencies. Using the sediment rating curve method, the sediment yield at the N'djili station 2 is almost equal to 189,030 metric tons/year for year 2005, while it is about 315,000 metric tons/year for 2013. So from 2005 to 2013, the annual sediment load increased by about 67%.

The specific degradation values of the N'djili River Basin computed from 2005 (SD = 90.1 metric tons/km^2/year) and 2013 (SD = 150.2 metric tons/km^2/year) sediment data are within 95% confidence intervals specified by Kane and Julien (2007).

The estimated values of the sediment delivery ratio in 2005 (4.6 %) and 2013 (4.1 %) are almost equal. They are in the range of sediment delivery ratio models established by Renfro (1975) and Boyce (1975).

CHAPTER 6 : SUMMARY AND CONCLUSIONS

Accelerated soil erosion by water is a worldwide problem because of its economic and environmental consequences. Especially in the N'djili River Basin, deforestation and indiscriminate land clearing for agricultural, urbanization and informal settlements have resulted in widespread soil erosion over the land surface, and subsequently in high level of turbidity in the N'djili River. To understand the link between deforestation – land clearing and increasing of turbidity in N'djili River during last decades, a comprehensive modeling combining ArcGIS with RUSLE was used to estimate the gross erosion rates and to predict the spatial distribution of soil rates for land use observed in 1995, 2005 and 2013 over the basin. Then, using the turbidity measurements, sediment concentration and flow discharges observed in 2005 and 2013, the sediment delivery ratio of the basin was evaluated and compared with delivery ratio models from Boyce and Renfro. Finally, the effect of ash concentration on turbidity was assessed in a laboratory experiment to understand the role played by the wildfire in the turbidity at the beginning of the rain season.

Specifically, this study came to the following conclusions:

1. From image classification performed on satellite images captured in 1995, 2005 and 2013, the bare land/burned grass/agricultural land cover represented almost 22% of the N'djili basin area in 2013 whereas it was covering only 6% of the basin area in 1995. Also, settlements, which covered about 8% of the basin area in 1995, represented about 18% of the N'djili Basin area. The expansion of settlements, bare land, burned areas and agricultural lands was realized at the expense of the forest and grass and shrubs covers. Thereby, the forest cover was reduced from 15% of the basin

area in 1995 to 5% in 2013, while the grass and shrubs lost about 22% of their cover during the same period.

2. The annual average soil loss rate of the N'djili River Basin was estimated to be 7 tons/acre/year for 1995, 8.7 tons/acre/year for 2005 and 16.3 tons/acre/year for 2013. In 1995, most of the annual soil loss (about 76%) was produced by grass and shrubs, while bare land/burned areas/rainfed crops were producing about 10 % of the total annual soil loss, for a cover of 5.8 % of the basin area. In 2013, with a percent cover of 21.8% of the basin area, bare land/burned areas/rainfed crops became the first contributor to the annual soil loss, producing about 60% of the soil loss. Also, in 1995, settlements was covering about 8% of the basin area and producing 0.08 million tons/year of sediment (10.6% of the annual soil loss in 1995). In 2013, the settlement covering surface was about 17.6% of the basin area and the annual soil loss due to settlement reached 0.36 million tons/year (19.93% of the annual soil loss in 2013). So, the tremendous increasing of sediment production by bare land/burned areas/rainfed crops and settlements are certainly one of the reasons of the increase of turbidity in the N'djili River between 2005 and 2013. The role played by the precipitations in the increase of turbidity might be analyzed in another study. Regarding the spatial distribution of the soil erosion rates in the N'djili River Basin, the analysis of the relationship between probability and annual average soil loss rates indicated that up to 82, 79, and 73% of the mean annual soil loss rates are in the range of tolerable soil (0 – 5 tons/acre /year) in 1995, 2005 and 2013 respectively.

3. Using the turbidity measurements, sediment concentration and flow discharges observed in 2005 and 2013, this study predicted a sediment delivery ratio of 4.6% in

2005 and 4.1% in 2013. So, the sediment delivery ratio for the N'djili River Basin is close to the values predicted by Boyce and in the similar range of the ones predicted by Renfro. These relatively low values of sediment delivery ratio suggest that important amount of sediment from upland areas of the basin is trapped on flood plains covered by grass, shrubs and trees and in small ponds made for the artisanal sandpit along of the N'djili river and its tributaries. The particle size distribution of the eroded soil could give indication about the reasons that lower the sediment delivery ratio in the N'djili River Basin.

4. The laboratory experiment carried out to assess the effect of ash concentration on the turbidity reveals that turbidity increases as a power function of ash concentration. So at the beginning of the rain season when ash concentration is relatively high, elevated turbidity values can be observed in the N'djili River.

The results presented and discussed in this thesis can be a big asset for understanding the link between deforestation – land clearing and increasing of turbidity in N'djili River during last decades. Understanding of contribution of dominant factors including land cover, land use, precipitation and topography to the soil erosion in the N'djili River Basin as brought by this thesis could be valuable for Kinshasa municipal and Water Utility authorities to set up plan for mitigating soil erosion in the basin in order to reduce turbidity of the N'djili River and sustain economically and technically the water production from the N'djili River and its tributaries. Several other recommendations including for further studies and soil erosion mitigation can be found in Chapter 6.

CHAPTER 7 : RECOMMENDATIONS AND PERSPECTIVES

The accuracy of the soil erosion rates estimation for the N'djili River Basin can be improved by additional research based on upgraded data acquisition techniques and other scientific methods developed by several other authors. Specifically:

1. The national meteorological agency (METTELSAT) and/or the national water utility (REGIDESO) are required to rehabilitate the existing climatic and stream gauging stations and create several other ones through the N'djili River Basin and at the water treatment plant intakes. Those new and upgraded climatic and stream gauging stations would provide continuous and long-term records of hydrological parameters like 15-minute rainfall data from which 30-minute rainfall intensity can be derived. So, since the rainfall-runoff erosivity factor R is a key input of the RUSLE method, improvements in data measurement would certainly increase the accuracy of the soil erosion loss.
2. In the computation of C-value maps, methods that derive C-factor from the NDVI (Normalized Difference Vegetation Index) or using the k-NN (k-nearest neighbors) classification can improve the accuracy of C-factor estimate based on satellite images. Also, supervised classification methods relying on an integrated field survey including land use types and soil erosion status across the N'djili Basin can be used to increase the accuracy of soil erosion prediction. Furthermore, surveys should be done to produce detailed soil map of the N'djili Basin.
3. A short-term soil erosion model can be developed in order to predict daily turbidity in the N'djili River after a rainstorm event, using the sediment delivery ratio computed for different sub-watersheds, the half-month climate variables, and soil loss ratio

(SLR) calculated for each time period of 15 days. This model could be calibrated with observed turbidity values.

REFERENCES

Abbott, M. B., Bathurst, J. C., Cunge, J. A., O'Connell, P. E., and Rasmussen, J. (1986a). "An introduction to the European Hydrological System—Système Hydrologique Européen, 'SHE.' 1: History and philosophy of a physically based distributed modeling system." *Journal of Hydrology* 87(1–2): 45–59.

Abbott, M. B., Bathurst, J. C., Cunge, J. A., O'Connell, P. E., and Rasmussen, J. (1986b). "An introduction to the European Hydrological System—Système Hydrologique Européen, 'SHE.' 2: Structure of a physically based distributed modeling system." *Journal of Hydrology* 87(1–2): 61–77.

Ambrose, R.B., Martin, J.L. and Wool, T.A. (1993). *WASP5, A hydrodynamic and water quality model - Model theory, user's manual, and programmer's guide.* U.S. Environmental Protection Agency, Office of Research and Development, Environmental Research Laboratory, Athens, Georgia.

Arnoldus, H.M.J., (1977). *Methodology used to determine the maximum potential average annual soil loss due to sheet and rill erosion in Morocc*o. FAO Soils Bull., 34:39 51.

Bakker, M.M., Govers, G., Doorn, A.V., Quetier,F., Chouvardas, D., Rounsevell, M., *The response of soil erosion and sediment export to land use change in four areas of Europe: The importance of landscape pattern, Geomorphology*. Volume 98, Issues 3–4, 15 June 2008, Pages 213-226.

BCEOM-société Française d'ingénierie. (2006). *Plan directeur de l'alimentation en eau potable de la ville de Kinshasa: Rapport programmation – plan directeur*. Technical report, Kinshasa, DRC.

Beasley, D.B., Huggins, L.F., and Monke, E.J. (1980). *ANSWERS: a model for watershed planning*. Transactions of the American Society of Agricultural Engineers 23: pp. 938–44.

Bertoni, J., Lombardi Neto, F., (1990). *Conservação do solo Ícone Editora*. São Paulo, Brazil 355 pp. Brazilian Institute for Geography and Statistic (IBGE)

Boko, M., Niang, I., Nyong, A., Vogel, C., Githeko, A., Medany, M., Osman-Elasha, B., Tabo, R., and Yanda, P. (2007). Africa. *Climate Change 2007: Impacts, Adaptation and Vulnerability. Contribution of Working Group II to the Fourth Assessment Report of the Intergovernmental Panel on Climate Change*, M.L. Parry, O.F. Canziani, J.P. Palutikof, P.J. van der Linden and C.E. Hanson, Eds., Cambridge University Press, Cambridge UK, 433-467.

Bollinne, A., Laurant, A., Rosseau, P., Pauwels, J.M., Gabriels, D. and Aelterman, J., (1980). *Provisional rain erosivity map of Belgium*. In: M. DeBoodt and D. Gabriels (Editors), Assessment of Erosion. John Wiley & Sons, Chichester, pp. I 11-120.

Bols, P. (1978). The Iso-erodent Map of Java and Madura. *Belgian Technical Assistance Project ATA105, Soil Research Institute, Bogor*.

Bolstad, P.V., and Stowe, T. (1994). *An evaluation of DEM accuracy: Elevation, slope, and aspect*. Photogramm. Eng. Remote Sens. 60:1327–1332.

Borah, D. K., Krug, E. C., Yoder, D. (2008). “Watershed Sediment Yield”. *Sedimentation Engineering: Processes: Measurements, Modeling, and Practice*, Manuals and Reports on Engineering Practice No. 110, M. H. Garcia, ed., ASCE, Reston, Virginia.

Boyce, R. C. (1975). *Sediment routing with sediment delivery ratios. In: Present and Prospective Technology for Predicting Sediment Yields and Sources*. US Dept. Agric. Publ. ARS-S-40, 61-65.

CIA (2014). *Democratic Republic of the Congo* in The World Factbook. Langley, Virginia: Central Intelligence Agency. https://www.cia.gov/library/publications/the-world-factbook/geos/cg.html. Accessed on 30th Jun 2014.

Chen, J., Zhu, X., Vogelmann, J.E., Gao, F., Jin, S. (2011): “A simple and effective method for filling gaps in Landsat ETM+ SLC-off images.” Remote Sens. Environ., 115(2011), 1053-1064.

England, J., Velleux, M., and Julien, P.Y. (2007). *Two-dimensional simulations of extreme floods on a large watershed*. Journal of Hydrology, 347(1):229-241.

Erskine, R. H., Green, T. R., Ramirez, J. A., and MacDonald, L. H. (2007). “Digital Elevation Accuracy and Grid Cell Size: Effects on Estimated Terrain Attributes.” Soil Sci. Soc. Am. J. 71:1371-1380.

FAO (2002). *Soil and Terrain Database for Central Africa*. [CD-ROM or Data File]. FAO Land and Water Digital Media Series #32.

Flanagan, D.C., Nearing, M. A., and Laflen, J. M., eds. (1995). *USDA-Water Erosion Prediction Project: Hillslope Profile and Watershed Model Documentation*. NSERL Report No. 10. West Lafayette, Ind.: USDA-ARS National Soil Erosion Research Lab.

Fortuin, R. (2006). *Soil Erosion in Cameron Highlands, an Erosion Rate Study of Highland Area*. Saxion University Deventer.

Foster, G.R., Lane, L.J. (1987). *User Requirements: USDA-Water Erosion Prediction Project (WEPP).* NSERL Report No.1. West Lafayette, Ind.: USDA-ARS National Soil Erosion Research Lab.

Giles, P.T., and Franklin, S.E. (1996). *Comparison of derivative topographic surfaces of a DEM generated from stereoscopic SPOT images with field measurements*. Photogramm. Eng. Remote Sens. 62:1165–1171.

Goldman S.J, Jackson K, Bursztynsky T.A (1986) ‘Erosion and sediment control handbook.’ McGraw-Hill Book Company, New York.

Guosong, Z., Huaiping, X., Feng, L. (2010). *Assessment of ASTER GDEM Performance by Comparing with SRTM and ICESat/GLAS Data in Central China*. Chinese Academic of Sciences.

Haan, C.T., Barfield, B.J., and Hayes, J.C. (1994). *Design Hydrology and Sedimentology for Small Catchments*, Academic Press, San Diego, California.

Hatheway, A. (2005). "George A. Kiersch: Engineering geology applied to anthropogenic problems." *Reviews in Engineering Geology*, 16, 1-6.

Holmes, K.W., Chadwick, O.A., and Kyriakidis, P.C. (2000). *Error in a USGS 30-meter digital elevation model and its impact on terrain modeling*. J. Hydrol. 233:154–173.

Hooke, R. L. (1994). "On the efficacy of humans as geomorphic agents." *GSA Today*, 4(9), 217, 224-225.

Hunter, G.J., and Goodchild, M.F. (1997). *Modeling the uncertainty of slope and aspect estimates derived from spatial databases*. Geogr. Anal. 29:35–49.

Jones, D.S., Kowalski, D.G., Shaw, R.B. (1996). *Calculating Revised Universal Soil Loss Equation (RUSLE) Estimates on Department of Defense Lands: A Review of RUSLE Factors and U.S. Army Land Condition-Trend Analysis (LCTA) Data Gaps*. Center for Ecological Management of Military Lands, Colorado State University.

Julien, P. Y. (2002). *River Mechanics*, Cambridge University Press, Cambridge, 454 p.

Julien, P. Y. (2010). *Erosion and Sedimentation*, 2nd ed. Cambridge University Press, Cambridge, 371 p.

Julien, P. Y., and Saghafian, B. (1991). CASC2D user's manual. Civil Engineering Report, Department of Civil Engineering, Colorado State University, Fort Collins, Colo.

Julien, P. Y., Saghafian, B. and Ogden, F. L. (1995). *Raster-Based Hydrologic Modeling of Spatially-Varied Surface Runoff*. JAWRA Journal of the American Water Resources Association, 31: 523–536.

Kabuya, M. (2005). *Etude du Régime Hydrologique de la Rivière N'djili*. Mémoire de Fin d'études, Faculté des Sciences Agronomiques, Université de Kinshasa.

Kane, B., and Julien, P.Y. (2007). *Specific degradation of watersheds*. International Journal of Sediment Research, 22(2), 114-119.

Kim, H. (2006). *Soil Erosion Modeling using RUSLE and GIS on the IMHA Watershed*, Master's Science Thesis, Colorado State University.South Korea.

Knisel, W. G., ed. (1980). "CREAMS: A field-scale model for chemicals, runoff, and erosion from agricultural management system." *Conservation Research Rep. 26*, USDA-SEA, Washington, D.C.

Krivoruchko, K. (2011). *Spatial Statistical Data Analysis for GIS Users*, Esri Press, Redlands, California, 928 p.

Kuenstler, W. (1998). "A guidelines for the use of the Revised Universal Soil Loss Equation (RUSLE). Chapter 5.

Laflen, J. M., Foster, G. R., and Onstad, C. A. (1985). "Simulation of individual-storm soil loss for modeling the impact of soil erosion on crop productivity." Soil Erosion and

Conservation, S.A. El-Swaify, W.C. Moldenhauer, and A. Lo, eds., Soil & Water Conservation Society of America, Ankeny, Iowa, pp. 285–295.

Lillesand, T. M., Kiefer, R.W., Chipman, J.W. (2008). *Remote Sensing and Image Interpretation*, 6th ed. John Wiley & Sons, 756 p.

Lo, A., El-Swaify, S.A., Dangler, E.W. and Shinshiro, L., (1985). *Effectiveness of El30 as an erosivity index in Hawaii*. In: S.A. E1-Swaify, W.C. Moldenhauer and A. Lo (Editors), Soil Erosion and Conservation. Soil Conservation Society of America, Ankeny, pp. 384 392.

LP DAAC (2009). ASTER GDEM V2. USGS/Earth Resources Observation and Science (EROS) Center, Sioux Falls, South Dakota.

Luboya, J. K. (2002). *Etude Systémique du Bassin Versant de la Rivière N'djili à Kinshasa*. Mémoire d'études supérieures spécialisées, Ecole Régionale Postuniversitaire d'Aménagement et Gestion Intégrés de Forêts et Territoires Tropicaux, Université de Kinshasa.

MacArthur, R. C., Neill, C. R., Hall, B. R., Galay, V. J., and Shvidchenko, A. B. (2008). "Overview of Sedimentation Engineering". *Sedimentation Engineering: Processes: Measurements, Modeling, and Practice,* Manuals and Reports on Engineering Practice No. 110, M. H. Garcia, ed., ASCE, Reston, Virginia.

MacDonald, L. H. (2012). *Post-fire Recovery and Restoration: Soils, Runoff and Erosion*. Watershed Science Program, Dpt of Ecosystem Science and Sustainability, Colorado State University.

Maner, S. B. (1962). *Factors influencing sediment delivery ratios in the Blackland Prairie land resource area*.US Dept. of Agriculture, Soil Conservation Service, Fort Worth, Texas, USA.

McCool, D.K., Brown, L.C. and Foster, G.R., (1987). *Revised slope steepness factor for the Universal Soil Loss Equation*. Transactions of the American Society of Agricultural Engineers, 30: 1387-1396.

McCool, D.K., Foster, G.R., and Weesies, G.A. (1997). *Slope length and steepness factors (LS)*, Chapter 4, pp. 101-141 in Renard et al. (1997).

Mikhailova, E.A., Bryant, R.B., Schwager, S.J., Smith, S.D. (1997). Predicting Rainfall Erosivity in Honduras. *Soil Science Society of America journal 61:* pp 273-279.

Mitasova, H., Hofierka, J., Zlocha, M., and Iverson, R. (1996). *Modeling Topographic Potential for Erosion and Deposition using GIS*. In. Journal of Geographical Information Science 10 (5), 629-641.

Moore, LD., and Burch, G.J. (1985). *Physical Basis of the Length-slope Factor in the Universal Soil Loss Equation*. Soil Sci. Soc. Am. J. 50: 1294-1298.

Morgan, R. P. C. (2011). *Handbook of erosion modelling*. Chichester, West Sussex, UK: Wiley.

Murphy, S.F., McCleskey, R.B., and Writer, J.W. (2012). *Effects of flow regimes on stream turbidity and suspended solids after wildfire, Colorado Front Range,* in Wildfire and water quality—Processes, impacts, and challenges, Conference in Banff, Canada, June 2012, Proceedings: Wallingford, Oxfordshire, U.K., International Association of Hydrological Sciences publication 354, p. 51–58.

NASA (2000). *Landsat 7 Science Data Users Handbook*. Landsat Project Science Office, Goddard Space Flight Center, Greenbelt, Maryland.

Ntale, J. P. (2010). *Evaluation de la Pression Anthropique sur les Forêts Périurbaines de la Ville de Kinshasa*. Mémoire de fin d'études, Faculté des Sciences Agronomiques, Université de Kinshasa.

O'Callaghan, J. F., and Mark, D. M., (1984). The extraction of drainage networks from digital elevation data: *Computer Vision, Graphics and Image Processing*, Vol. 28, pp. 323-344.

Omar, C. (2010). *Geographic Information System Manual.* Tenaga National Berhad.

Opti-Plus (2013). *Etudes Hydrologiques pour la réhabilitation du Pont sur la rivière N'djili*. Kinshasa, DRC.

Ouyang, D., and Bartholic, J. (2001). *Web-Based GIS Application for Soil Erosion Prediction*. Proceedings of an International Symposium, Soil Erosion Research for the 21st Century, 01, 185-189.

Refsgaard, J. C., and Storm, B. (1995). "Chapter 23: MIKE SHE." *Computer Models of Watershed Hydrology,* V. P. Singh, ed., Water Resources Publications, Highlands Ranch, Colo., 809–846.

Renard, K. G., and Freimund, J. R. (1994). *Using monthly precipitation data to estimate the R factor in the revised USLE*. Journal of Hydrology, 157(1), 287-306.

Renard, K., Foster, G., Weesies, G., McDool, D., and Yoder, D. (1997). *Predicting Soil Erosion by Water: A Guide to Conservation Planning with the Revised Universal Soil Loss Equation (RUSLE)*. Agricultural Handbook 703, USDA-ARS.

Renard, K.G., and Foster, G.R. (1983). *Soil conservation: Principles of erosion by water. Dryland Agriculture,* pp. 155-176. Agronomy Monogr. 23, Am. Soc. Agron., Crop Sci. Soc. Am., and Soil Sci. Soc. Am., Madison, Wisconsin.

Renfro, G.W. (1975). *Use of Erosion Equations and Sediment-Delivery Ratios for Predicting Sediment.* Sediment Yield. ARS-S-40.

Renschler, C.S., and Harbor, J. (2002). *Soil Erosion Assessment Tools from Point to Regional Scales-the Role of Geomorphologists in Land Management Research and Implementation*. Geomorphology 47: 189-209.

Rose, E., (1977). *Erosion et Ruissellement en Afrique de l'ouest--vingt années de mesures en petites parcelles expérimentales*. Travaux et Documents de I'ORSTOM No. 78, ORSTOM, Paris

Rudra, R.P., Dickinson, W.T., and Wall, G.J. (1986). *GAMES – a screening model of soil erosion and fluvial sedimentation on agricultural watersheds*. Canadian Water Research Journal 11: 58–71.

SAFRICAS (2005). *Projet de Réhabilitation du Captage d'Eau Brute à N'Djili et Renforcement du Système de Transfert d'Eau au Sud de Kinshasa, RDC*. Kinshasa, DRC.

Schwab, G.O., Frevert, R.K., Edminster, T.W., and Barnes, K.K. (1981). "Soil Water

Conservation Engineering", 3rd ed., Wiley, New York.

Semeki, J. N. (2003). *Impacts de l'Agriculture Itinérante sur Brulis dans la station Phytotechnique de N'djili Brasserie à Kinshasa*. Rapport technique, Faculté des Sciences Agronomiques, Université de Kinshasa.

Shen and Julien, P.Y. (1993). *Erosion and sediment transport*, in Handbook of Hydrology.

Smith, D., and Whitt, D. (1947). *Estimating Soil Losses from Field Areas of Claypan Soil*. Soil Science Society of America Proceedings, 12, 485-490.

Smithen A.A. and Schulze, R.E., (1982). *The spatial distribution in Southern Africa of rainfall erosivity for use in the universal soil loss equation*. Water S. Afr., 8(2): 74-78.

Stocking, M,A. and Elwell, H.A., (1976a). Erosivity determinations for seven rainfall stations in Rhodesia. Research Bull. No. 21, Department of Conservation and Extension, Salisbury.

Stocking, M.A. and Elwell, H.A., (1976b). Rainfall erosivity over Rhodesia. Trans. Inst. Br. Geogr., New Ser., 1: 231--245.

Summerfield, M. A., and Hutton, N. J. (1994). "Natural controls of fluvial denudation rates in major world drainage basins." *J. Geophys. Res.*, 99(B7), 13,871-13,883.

Teh, Soo Huey (2011). Soil Erosion Modeling Using RUSLE and GIS on Cameron Highlands, Malaysia For Hydropower Development.

Thieken, A.H., Lucke, A., Diekkruger, B., and Richter. O. (1999). *Scaling input data by GIS for hydrological modelling*. Hydrol. Processes 13:611–630.

Thompson, J.A., Bell, J.C., and Butler, C.A. (2001). *Digital elevation model resolution: Effects on terrain attribute calculation and quantitative soil-landscape modeling*. Geoderma 100:67–89.

Torri, D., Borselli, L., Guzzetti, F., Calzolari, C., Bazzoffi, P., Ungaro, F., Bartolini D, Sanchis MP. (2006). Soil erosion in Italy: an overview. In *Soil Erosion in Europe*, Boardman J, Poesen J. eds .Wiley: New York; pp 245-261.

Tshibangu, D. (2014): *Concentration des matières en suspension des eaux de la rivière N'djili en 2013*. Rapport de Laboratoire, Laboratoire de Chimie, Faculté des Sciences, Kinshasa, DRC.

UNEP (2010). *Water issues in the Democratic Republic of Congo, Challenges and Opportunities*. Technical report. Nairobi. KENYA.

USGS (1995). Landsat Archive, 1995, Landsat TM+, 30m scene p 1820631995032XXX01, USGS, Sioux Falls, South Dakota.

USGS (2001). Landsat Archive, 2001, Landsat ETM + SLC –on, 30m scene p 1820632001120EDC00, USGS, Sioux Falls, South Dakota.

USGS (2013). Landsat Archive, 2013, Landsat OLI_TIRS, 30m scene p 1820632013225LGN00, USGS, Sioux Falls, South Dakota.

United States Soil Conservation Service (USSCS). (1971). "Section 3, Chapter 6: Sediment sources, yields and delivery ratios." *SCS national engineering handbook*, USDA Soil Conservation Service, Washington, D.C.

Valdiya, K. S. (1998). *Dynamic Himalaya*, Universities Press, Hyderabad, India.

Van Caillie, X. (1983). Hydrologie et érosion dans la région de Kinshasa: Analyse des interactions entre les conditions du milieu, les érosions et le bilan hydrologique (Thèse de doctorat) Dpt de Geografie Geologie, KUL (554p).

Vanoni, V. A., ed. (1975). *Sedimentation engineering*. Manual 54, American Society of Civil Engineers, New York, 745 p.

Velleux, M., England, J., and Julien P. (2008). *TREX: Spatially Distributed Model to Assess Watershed Contaminant Transport and Fate*. Science of the Total Environment, 404(1):113-128.

Velleux, M., Westenbroek, S., Ruppel, J., Settles, M., Endicott, D. (2001). *A User's Guide to IPX, the In-Place Pollutant Export Water Quality Modeling Framework, Version 2.7.4*" USEPA ORD, National Health and Environmental Effects Research Laboratory, Large Lakes Research Station, Grosse Ile, Michigan. 179 p. EPA/600/R-01/079.

Warner, T. A., Campagna, D.J. (2013). *Remote Sensing with IDRISI: A Beginner's Guide*, Clark Labs, Clark University, 308 p.

Williams, J. (1975). *Sediment Yield Prediction with Universal Equation using Runoff Energy Factor*. Agricultural Research Service Report ARS-S-40, U.S. Department of Agriculture.

Wischmeier, W. H., and Smith, D.D., (1965). *Predicting rainfall-erosion losses from cropland east of the Rocky Mountains: Guide for selection of practices for soil and water conservation (Vol. 282)*. Agricultural Research Service, U.S. Department of Agriculture.

Wischmeier, W. H., and Smith, D.D., (1978). *Predicting Rainfall Erosion Losses – A Guide to Conservation Planning*. U.S. Department of Agriculture Handbook No. 537.

Wischmeier, W. H. (1960). *Cropping management factor evaluations for a Universal Soil Loss Equation*. Proceedings of Soil Science Society of America, 24, pp. 322-326.

Wischmeier, W.H. (1975). Estimating the soil loss equation's cover and management factor for undisturbed area. In: Present and Prospective Technology for Predicting Sediment Yield and Sources: Proceedings, Sediment Yield Workshop, USDA Sedimentation Laboratory, Oxford, Mississippi, and November 28-30, 1972. ARS-S-40. U.S. Department of Agriculture, Washington, D.C., pp. 118-124.

Wischmeier, W.H., Johnson, C.B., and Cross, B.V. (1971). *A soil erodibility nomograph for farmland and construction sites.* J. Soil and Water Conserv. 26:189-193.

Writer, J.H., McCleskey, R.B., and Murphy, S.F. (2012), *Effects of wildfire on source-water quality and aquatic ecosystems, Colorado Front Range,* in Wildfire and water quality—Processes, impacts, and challenges, Conference in Banff, Canada, June 2012, Proceedings: Wallingford, Oxfordshire, U.K., International Association of Hydrological Sciences publication 354, p. 117–122.

Yu, B., Rosewell, C.J., (1996). Technical Notes: A Robust Estimator of the R-Factor for the Universal Soil Loss Equation. *Transactions of the ASAE: 1996 American Society of Agricultural Engineers, Vol.39:* pp 559-561.

APPENDIX A: RAINFALL, TURBIDITY AND DISCHARGE DATASET

Monthly Rainfall Records by Climatic Stations

Station	Precipitation
Binza	mm/Month
Jan	170
Feb	140
Mar	195
Apr	209
May	142
Jun	6
Jul	3
Aug	7
Sep	39
Oct	142
Nov	248
Dec	167
Mean Annual (mm/year)	1468

Station	Precipitation
Ndolo	mm/Month
Jan	157
Feb	157
Mar	194
Apr	177
May	136
Jun	5
Jul	6
Aug	4
Sep	55
Oct	96
Nov	186
Dec	175
Mean Annual (mm/year)	1348

Station	Precipitation
N'djili	mm/Month
Jan	173
Feb	158
Mar	192
Apr	218
May	142
Jun	8
Jul	5
Aug	7
Sep	38
Oct	145
Nov	246
Dec	165
Mean Annual (mm/year)	1497

Station	Precipitation
Rifflart	mm/Month
Jan	189
Feb	152
Mar	171
Apr	173
May	95
Jun	4
Jul	4
Aug	2
Sep	115
Oct	143
Nov	217
Dec	207
Mean Annual (mm/year)	1472

Station	Precipitation
Kimwenza	**mm/Month**
Jan	194
Feb	126
Mar	196
Apr	180
May	137
Jun	4
Jul	3
Aug	24
Sep	42
Oct	125
Nov	252
Dec	208
Mean Annual (mm/year)	1491

Station	Precipitation
Kasangulu	**mm/Month**
Jan	147
Feb	92
Mar	133
Apr	170
May	130
Jun	78
Jul	43
Aug	65
Sep	88
Oct	130
Nov	245
Dec	141
Mean Annual (mm/year)	1462

Station	Precipitation
Luzumu	**mm/Month**
Jan	196
Feb	126
Mar	172
Apr	195
May	121
Jun	6
Jul	3
Aug	2
Sep	86
Oct	186
Nov	191
Dec	202
Mean Annual (mm/year)	1486

Station	Precipitation
Luila (Wolter)	**mm/Month**
Jan	130
Feb	114
Mar	179
Apr	206
May	130
Jun	10
Jul	3
Aug	2
Sep	35
Oct	130
Nov	231
Dec	192
Mean Annual (mm/year)	1362

Station	Precipitation
Kisembo	**mm/Month**
Jan	195
Feb	126
Mar	172
Apr	198
May	121
Jun	6
Jul	3
Aug	2
Sep	86
Oct	186
Nov	191
Dec	205
Mean Annual (mm/year)	1491

Station	Precipitation
Kindamba	**mm/Month**
Jan	148
Feb	139
Mar	200
Apr	191
May	117
Jun	14
Jul	3
Aug	3
Sep	38
Oct	112
Nov	247
Dec	177
Mean Annual (mm/year)	1389

Observed Values of Turbidity

Day	NTU - 2000	NTU - 2001	NTU - 2002
1	52	31	45
2	130	53	40
3	87	82	72
4	36	52	190
5	27	64	160
6	32	34	58
7	38	26	40
8	190	28	35
9	152	27	35
10	78	25	58
11	44	23	35
12	48	26	38
13	194	25	156
14	205	24	150
15	312	23	160
16	127	38	85
17	66	26	70
18	32	25	79
19	26	79	130
20	23	41	56
21	25	62	32
22	34	40	39
23	38	75	34
24	172	56	28
25	61	41	25
26	36	32	125
27	25	217	72
28	31	61	64
29	84	35	350
30	72	25	200
31	78	24	76
32	82	700	55
33	80	275	52
34	427	73	28
35	132	42	4400
36	128	150	215
37	110	120	62
38	81	83	48
39	58	86	34
40	42	58	6600
41	30	32	85
42	28	27	610
43	556	35	155
44	102	28	60
45	84	24	42
46	412	24	232
47	218	25	50
48	114	580	39
49	624	31	310
50	514	225	168
51	389	280	79
52	612	140	55
53	510	48	78
54	413	40	49
55	632	30	172
56	312	32	85
57	189	33	219
58	167	299	255
59	97	300	450
60	62	51	98
61	41	26	77
62	35	30	60
63	28	240	30
64	24	151	272
65	29	164	94
66	304	180	100
67	214	180	90
68	97	60	30
69	73	63	29
70	55	30	28
71	41	26	24
72	32	28	22
73	28	129	2200
74	31	450	50
75	34	380	28
76	28	138	26
77	25	140	28
78	31	155	93

Day	NTU - 2000	NTU - 2001	NTU - 2002
79	24	524	58
80	18	407	26
81	25	389	28
82	27	712	32
83	22	523	268
84	29	405	350
85	31	395	56
86	49	895	44
87	184	344	82
88	121	123	150
89	132	95	58
90	67	68	69
91	18	52	85
92	29	37	45
93	140	127	114
94	230	215	200
95	63	532	1000
96	154	610	8076
97	142	103	63
98	83	230	377
99	110	430	90
100	66	487	60
101	85	598	60
102	83	214	344
103	52	42	32
104	48	78	108
105	40	88	655
106	63	59	55
107	300	77	122
108	52	53	54
109	47	63	78
110	98	90	82
111	220	130	640
112	116	83	550
113	120	336	152
114	60	478	95
115	78	284	90
116	85	510	65
117	88	179	270
118	81	197	312

Day	NTU - 2000	NTU - 2001	NTU - 2002
119	55	522	2122
120	54	71	87
121	48	294	540
122	35	164	292
123	28	76	124
124	46	201	355
125	45	54	62
126	31	57	83
127	28	92	156
128	68	94	120
129	50	55	60
130	230	135	40
131	84	58	31
132	132	83	34
133	132	630	31
134	69	255	33
135	99	82	32
136	126	69	30
137	44	191	33
138	30	508	30
139	28	306	28
140	95	132	29
141	35	59	30
142	58	52	34
143	51	45	140
144	57	57	82
145	25	42	77
146	23	68	214
147	31	36	289
148	27	37	123
149	19	35	78
150	22	28	61
151	18	100	48
152	30	182	39
153	28	120	49
154	25	48	57
155	27	37	49
156	29	68	38
157	30	34	364
158	31	29	105

Day	NTU - 2000	NTU - 2001	NTU - 2002
159	26	29	213
160	27	26	89
161	23	26	67
162	26	25	36
163	23	25	32
164	22	29	27
165	24	25	27
166	29	24	28
167	34	24	29
168	30	25	25
169	29	27	27
170	22	24	26
171	22	24	23
172	21	23	28
173	21	23	27
174	21	23	25
175	21	22	26
176	21	22	23
177	20	23	28
178	23	22	26
179	23	24	27
180	23	23	25
181	23	26	26
182	21	22	26
183	21	26	25
184	23	24	26
185	22	23	28
186	21	22	28
187	21	22	25
188	22	23	27
189	21	22	26
190	26	27	28
191	22	23	24
192	21	22	26
193	22	22	26
194	20	20	30
195	22	21	24
196	23	20	27
197	23	20	27
198	21	23	30

Day	NTU - 2000	NTU - 2001	NTU - 2002
199	21	23	25
200	20	21	24
201	20	21	27
202	21	22	30
203	19	20	29
204	21	21	29
205	23	24	29
206	20	21	24
207	21	21	23
208	18	20	25
209	20	21	0
210	20	20	24
211	18	19	22
212	25	69	22
213	29	68	22
214	25	70	21
215	27	19	25
216	26	67	22
217	23	21	26
218	29	20	23
219	19	23	25
220	18	19	26
221	17	21	26
222	16	24	26
223	18	22	24
224	16	19	23
225	16	20	24
226	18	21	27
227	20	22	24
228	21	20	26
229	20	24	23
230	18	20	22
231	18	20	22
232	18	19	23
233	18	22	26
234	20	22	23
235	25	20	23
236	22	24	22
237	25	25	27
238	25	24	27

Day	NTU - 2000	NTU - 2001	NTU - 2002
239	27	21	23
240	23	27	25
241	27	26	25
242	29	67	22
243	32	22	25
244	30	22	25
245	31	22	27
246	28	22	23
247	26	24	25
248	32	24	24
249	33	23	25
250	34	22	24
251	38	23	23
252	32	25	35
253	28	25	27
254	29	24	25
255	168	23	99
256	71	23	24
257	42	23	288
258	54	23	42
259	39	23	43
260	31	25	35
261	28	29	248
262	28	25	156
263	27	23	60
264	29	25	54
265	38	24	42
266	36	24	31
267	44	22	40
268	33	22	30
269	46	23	64
270	32	22	49
271	25	22	38
272	28	96	124
273	25	63	102
274	27	62	84
275	23	34	61
276	29	30	44
277	32	28	32
278	34	22	30

Day	NTU - 2000	NTU - 2001	NTU - 2002
279	64	22	24
280	51	150	22
281	43	285	24
282	32	72	28
283	30	38	32
284	32	29	36
285	39	32	32
286	42	32	34
287	49	31	41
288	56	25	39
289	264	25	32
290	139	26	118
291	77	35	165
292	56	265	105
293	44	245	86
294	33	150	227
295	28	45	386
296	30	35	222
297	218	35	238
298	182	410	286
299	163	171	225
300	171	150	182
301	98	44	107
302	204	30	87
303	198	29	51
304	213	144	40
305	207	47	184
306	321	27	65
307	168	29	48
308	407	23	36
309	235	24	75
310	162	23	55
311	88	64	70
312	56	235	222
313	49	162	210
314	85	60	40
315	389	46	27
316	365	44	28
317	602	31	34
318	523	28	33

Day	NTU - 2000	NTU - 2001	NTU - 2002
319	489	26	400
320	435	24	120
321	365	42	85
322	312	100	110
323	129	200	120
324	88	190	400
325	63	40	171
326	87	35	210
327	134	172	312
328	287	64	340
329	379	28	130
330	422	180	80
331	588	102	55
332	637	90	400
333	620	350	140
334	370	150	146
335	128	57	146
336	52	35	80
337	150	38	52
338	125	90	120
339	65	80	120
340	63	35	355
341	67	45	246
342	180	176	120
343	0	85	243
344	1160	95	140
345	160	47	252
346	62	60	325
347	320	470	148
348	216	225	148
349	122	85	120
350	95	50	53
351	195	85	141
352	130	132	115
353	65	190	102
354	980	190	188
355	485	62	204
356	142	160	164
357	55	140	310
358	200	48	289

Day	NTU - 2000	NTU - 2001	NTU - 2002
359	190	65	184
360	40	66	107
361	31	35	62
362	31	27	53
363	35	31	14
364	49	39	10
365	51	255	155
366	40		

Day	NTU - 2003	NTU - 2004	NTU - 2005
1	44	42	77
2	35	30	32
3	50	28	269
4	122	54	57
5	160	160	190
6	99	140	140
7	114	187	40
8	138	240	165
9	92	148	99
10	59	60	49
11	83	130	82
12	121	204	120
13	112	67	51
14	113	75	218
15	108	55	92
16	85	84	66
17	60	50	75
18	58	37	159
19	85	40	60
20	103	150	108
21	49	65	55
22	57	74	59
23	46	58	49
24	31	34	32
25	27	29	30
26	76	26	57
27	112	152	115
28	60	56	82
29	188	25	51
30	112	23	35
31	50	24	51
32	41	27	30
33	38	23	24
34	26	24	25
35	2245	90	56
36	177	138	121
37	47	32	65
38	40	32	43
39	31	27	33

Day	NTU - 2003	NTU - 2004	NTU - 2005
40	3313	25	31
41	123	160	97
42	39	140	245
43	34	320	315
44	33	260	184
45	32	80	67
46	35	55	46
47	95	220	310
48	68	85	245
49	41	50	80
50	91	62	118
51	352	54	199
52	250	54	107
53	210	33	54
54	72	26	80
55	1900	27	38
56	500	185	113
57	156	260	225
58	84	70	92
59	86	53	59
60	0	35	18
61	300	27	30
62	160	24	31
63	52	76	55
64	47	55	42
65	40	70	50
66	52	114	73
67	130	126	77
68	52	33	32
69	35	800	415
70	276	150	115
71	34	144	205
72	33	50	84
73	32	55	53
74	29	255	147
75	89	42	49
76	170	27	134
77	126	30	110
78	50	31	53
79	392	37	42

Day	NTU - 2003	NTU - 2004	NTU - 2005
80	240	35	37
81	110	27	100
82	46	31	51
83	36	25	45
84	150	23	28
85	40	28	173
86	36	55	158
87	66	50	200
88	88	25	183
89	104	150	193
90	121	172	390
91	76	66	149
92	42	38	176
93	75	35	392
94	270	340	96
95	519	38	176
96	4065	54	139
97	47	31	64
98	205	32	49
99	62	33	303
100	44	28	330
101	43	25	880
102	185	25	97
103	29	25	50
104	67	25	40
105	350	45	90
106	71	86	172
107	95	68	50
108	62	69	38
109	84	89	192
110	76	70	50
111	337	33	38
112	348	146	192
113	89	26	140
114	190	285	1074
115	108	126	815
116	65	64	282
117	158	45	82
118	294	276	50
119	1144	166	48

Day	NTU - 2003	NTU - 2004	NTU - 2005
120	74	60	304
121	289	38	717
122	163	33	80
123	82	40	43
124	193	30	39
125	45	28	30
126	54	25	28
127	94	32	25
128	75	29	32
129	43	25	29
130	35	30	25
131	28	24	30
132	30	25	24
133	28	25	25
134	28	22	25
135	31	29	22
136	30	29	29
137	29	25	29
138	27	23	25
139	26	23	23
140	29	28	23
141	27	24	28
142	34	34	24
143	82	23	34
144	52	22	23
145	52	27	22
146	119	24	27
147	156	23	24
148	73	23	23
149	51	24	23
150	42	22	24
151	35	22	22
152	31	23	22
153	59	23	23
154	45	22	23
155	37	20	22
156	31	20	20
157	28	20	20
158	20	21	20
159	30	23	21

Day	NTU - 2003	NTU - 2004	NTU - 2005
160	26	25	23
161	27	19	25
162	21	23	19
163	26	21	23
164	32	20	21
165	30	20	20
166	29	20	20
167	41	20	20
168	28	20	20
169	28	21	108
170	23	20	102
171	35	20	35
172	32	19	32
173	31	19	29
174	22	119	28
175	27	20	27
176	34	18	32
177	27	19	35
178	22	19	28
179	30	18	29
180	32	20	29
181	24	20	30
182	28	20	30
183	26	20	32
184	30	20	32
185	27	19	30
186	20	19	33
187	27	21	32
188	26	24	32
189	24	19	30
190	24	20	32
191	26	18	34
192	30	19	25
193	25	20	30
194	24	19	29
195	25	19	28
196	27	19	27
197	25	19	28
198	20	19	26
199	25	18	35

Day	NTU - 2003	NTU - 2004	NTU - 2005
200	26	18	18
201	26	18	18
202	20	17	17
203	26	18	18
204	27	17	17
205	26	20	20
206	22	20	20
207	23	19	19
208	30	115	115
209	30	116	116
210	24	19	19
211	24	19	19
212	28	20	20
213	24	21	21
214	20	20	20
215	21	18	18
216	25	18	18
217	23	18	18
218	19	18	18
219	23	20	20
220	28	20	20
221	25	19	19
222	22	20	20
223	23	18	18
224	27	19	19
225	30	30	30
226	24	118	118
227	29	22	22
228	30	20	20
229	30	19	19
230	27	18	18
231	28	17	17
232	33	16	16
233	33	18	18
234	23	16	16
235	26	16	16
236	31	18	18
237	26	22	22
238	24	20	20
239	30	23	23

Day	NTU - 2003	NTU - 2004	NTU - 2005
240	30	28	28
241	23	26	26
242	26	21	21
243	29	22	22
244	26	22	22
245	24	22	22
246	23	22	22
247	24	24	24
248	30	24	24
249	25	21	21
250	22	24	24
251	28	23	23
252	35	28	28
253	35	32	32
254	22	24	24
255	24	21	21
256	24	25	25
257	23	25	25
258	19	25	25
259	24	45	45
260	22	50	50
261	19	55	55
262	35	35	35
263	35	25	23
264	35	23	160
265	35	21	150
266	25	150	36
267	20	118	29
268	25	41	79
269	25	24	30
270	0	24	30
271	28	25	24
272	35	24	23
273	27	28	24
274	51	27	63
275	73	26	254
276	65	24	68
277	40	27	22
278	25	25	25
279	24	26	21

Day	NTU - 2003	NTU - 2004	NTU - 2005
280	23	24	24
281	23	260	107
282	25	130	32
283	22	288	24
284	35	134	27
285	30	51	46
286	26	33	431
287	21	36	420
288	22	31	89
289	53	32	36
290	65	56	230
291	60	37	517
292	32	120	105
293	62	200	1000
294	28	368	486
295	24	240	310
296	22	69	70
297	50	45	45
298	24	47	33
299	75	41	150
300	50	30	148
301	30	71	150
302	145	188	135
303	164	142	50
304	67	83	608
305	32	82	132
306	37	65	92
307	22	43	985
308	425	56	820
309	200	70	166
310	118	38	230
311	89	46	94
312	100	65	49
313	73	35	230
314	160	35	143
315	85	120	90
316	320	280	130
317	232	224	57
318	96	156	109
319	63	87	90

Day	NTU - 2003	NTU - 2004	NTU - 2005
320	75	46	85
321	120	37	28
322	128	797	598
323	44	496	380
324	97	196	250
325	165	97	156
326	255	260	70
327	162	216	172
328	105	53	110
329	270	76	70
330	170	50	43
331	70	53	39
332	69	36	130
333	240	67	110
334	120	158	166
335	56	84	75
336	37	312	278
337	35	247	840
338	27	87	304
339	30	280	72
340	35	135	180
341	37	88	150
342	94	69	170
343	80	39	88
344	91	47	63
345	93	130	80
346	75	56	730
347	75	48	152
348	268	65	49
349	70	29	45
350	58	134	190
351	50	71	94
352	88	192	55
353	47	250	36
354	164	126	51
355	54	67	118
356	126	53	280
357	120	57	86
358	85	121	156
359	53	197	340

Day	NTU - 2003	NTU - 2004	NTU - 2005
360	28	90	152
361	25	46	66
362	0	26	51
363	0	62	123
364	33	43	53
365	80	220	360
366		124	

Day	NTU - 2006	NTU - 2007	NTU - 2008
1	112	40	27
2	34	47	32
3	510	34	32
4	60	36	30
5	220	50	26
6	140	46	27
7	80	38	160
8	89	218	105
9	50	103	106
10	38	180	45
11	33	333	60
12	36	195	45
13	34	106	96
14	360	40	98
15	128	35	95
16	47	35	84
17	100	36	35
18	280	138	36
19	80	366	105
20	65	152	74
21	44	80	275
22	44	270	476
23	40	81	205
24	30	44	98
25	31	520	130
26	88	211	56
27	77	330	48
28	108	265	78
29	77	94	69
30	47	44	44
31	78	38	41
32	33	340	54
33	24	152	36
34	25	92	35
35	22	325	35
36	104	215	34
37	97	64	48
38	53	45	37
39	38	43	33

Day	NTU - 2006	NTU - 2007	NTU - 2008
40	36	131	35
41	33	43	34
42	350	33	250
43	310	810	54
44	108	104	38
45	54	82	36
46	37	45	51
47	400	38	47
48	405	565	31
49	110	72	212
50	173	38	279
51	343	45	140
52	160	257	51
53	74	340	66
54	133	79	35
55	48	58	35
56	40	41	1000
57	190	37	175
58	114	35	275
59	64	64	109
60	48	66	318
61	32	33	55
62	37	178	57
63	34	142	50
64	28	33	33
65	30	25	160
66	31	25	148
67	28	61	84
68	30	174	3200
69	30	170	6980
70	80	83	95
71	265	193	68
72	117	74	464
73	50	52	211
74	39	71	73
75	55	55	56
76	241	150	288
77	190	109	352
78	75	61	152
79	47	36	82

Day	NTU - 2006	NTU - 2007	NTU - 2008
80	39	40	55
81	173	134	150
82	71	68	77
83	64	133	149
84	33	59	66
85	317	41	47
86	260	130	146
87	349	81	91
88	340	53	59
89	235	51	58
90	140	55	62
91	231	90	101
92	176	113	127
93	392	119	134
94	96	118	133
95	390	132	149
96	139	87	98
97	64	193	217
98	49	232	261
99	303	71	80
100	330	126	142
101	880	134	150
102	97	58	65
103	50	603	679
104	40	100	113
105	90	272	306
106	172	200	225
107	50	119	134
108	38	76	86
109	192	92	104
110	140	89	101
111	1074	42	214
112	815	43	155
113	282	99	220
114	82	130	281
115	50	350	165
116	48	348	131
117	304	170	322
118	717	53	85
119	80	41	293

Day	NTU - 2006	NTU - 2007	NTU - 2008
120	43	58	183
121	39	49	295
122	69	47	51
123	520	35	104
124	374	36	147
125	43	51	89
126	805	40	118
127	575	36	85
128	265	55	106
129	147	124	110
130	60	50	68
131	49	138	200
132	46	105	118
133	45	40	152
134	36	42	153
135	40	156	157
136	41	218	64
137	39	230	58
138	42	65	62
139	40	37	33
140	40	54	185
141	36	43	43
142	33	42	227
143	34	32	315
144	36	35	136
145	46	147	75
146	33	171	38
147	38	55	49
148	35	390	33
149	33	100	37
150	32	33	34
151	35	32	27
152	34	30	26
153	36	28	135
154	30	25	31
155	30	35	29
156	31	32	27
157	30	30	26
158	29	35	27
159	35	30	24

Day	NTU - 2006	NTU - 2007	NTU - 2008
160	38	63	23
161	29	33	24
162	31	31	23
163	30	31	26
164	29	29	24
165	33	26	40
166	32	28	28
167	36	24	24
168	80	26	23
169	108	27	38
170	102	30	24
171	35	27	22
172	32	55	22
173	29	30	50
174	28	26	24
175	27	26	23
176	32	25	23
177	35	28	42
178	28	27	23
179	29	24	21
180	29	31	22
181	30	23	22
182	30	21	23
183	32	24	21
184	32	22	26
185	30	22	22
186	33	20	20
187	32	22	21
188	32	23	19
189	30	20	21
190	32	20	21
191	34	24	63
192	25	23	35
193	30	22	20
194	29	22	18
195	28	24	17
196	27	23	21
197	28	23	51
198	26	21	19
199	35	21	19

Day	NTU - 2006	NTU - 2007	NTU - 2008
200	29	21	18
201	24	19	18
202	20	23	18
203	23	27	19
204	20	23	28
205	23	26	18
206	100	180	14
207	21	23	19
208	72	29	17
209	72	27	16
210	25	30	22
211	24	28	19
212	23	26	20
213	23	25	17
214	22	23	21
215	17	15	17
216	17	15	17
217	16	14	16
218	17	15	17
219	17	14	16
220	17	14	16
221	17	15	17
222	18	15	17
223	18	17	19
224	19	18	20
225	23	16	18
226	68	18	20
227	20	18	20
228	24	28	32
229	17	15	17
230	29	39	44
231	27	36	41
232	21	25	29
233	19	19	21
234	17	17	19
235	17	18	20
236	18	18	20
237	19	16	18
238	20	19	35
239	20	17	27

Day	NTU - 2006	NTU - 2007	NTU - 2008
240	22	16	24
241	21	16	26
242	19	16	29
243	19	16	27
244	26	29	26
245	23	24	29
246	24	25	26
247	23	22	33
248	25	26	23
249	32	42	26
250	42	59	24
251	31	38	24
252	35	42	22
253	29	26	24
254	24	24	27
255	22	22	33
256	25	25	24
257	26	27	42
258	25	25	29
259	40	34	32
260	40	29	26
261	40	24	125
262	18	0	49
263	27	30	27
264	92	23	31
265	155	160	26
266	93	150	28
267	33	36	24
268	54	29	25
269	55	79	26
270	30	30	30
271	25	26	24
272	22	21	23
273	25	26	24
274	44	25	63
275	141	28	254
276	45	21	68
277	23	23	22
278	26	27	25
279	23	24	21

Day	NTU - 2006	NTU - 2007	NTU - 2008
280	27	30	24
281	68	28	107
282	29	25	32
283	26	27	24
284	25	22	27
285	33	20	46
286	227	23	431
287	224	28	420
288	59	29	89
289	30	23	36
290	126	22	262
291	271	25	517
292	70	35	105
293	513	26	1000
294	256	26	486
295	173	35	310
296	50	29	70
297	37	29	45
298	28	23	33
299	89	28	150
300	110	72	148
301	89	27	150
302	143	151	135
303	47	44	50
304	327	45	608
305	285	438	132
306	89	86	92
307	813	640	985
308	487	153	820
309	118	70	166
310	196	162	230
311	391	687	94
312	325	600	62
313	230	230	420
314	143	143	237
315	90	90	190
316	130	130	206
317	57	57	78
318	109	109	72
319	90	90	67

Day	NTU - 2006	NTU - 2007	NTU - 2008
320	85	85	53
321	419	810	51
322	818	1037	93
323	240	100	105
324	555	859	75
325	416	675	800
326	94	118	146
327	344	515	53
328	513	915	489
329	700	1330	752
330	70	96	204
331	61	82	249
332	127	123	245
333	246	382	860
334	458	750	185
335	83	90	190
336	255	232	133
337	456	71	102
338	207	110	92
339	59	45	181
340	430	680	97
341	276	402	178
342	148	126	409
343	294	500	394
344	110	156	179
345	73	65	49
346	448	165	160
347	132	112	200
348	53	57	107
349	123	200	45
350	188	185	90
351	80	65	75
352	49	43	48
353	36	36	38
354	43	34	370
355	76	34	85
356	157	34	51
357	60	33	300
358	93	29	400
359	187	33	52

Day	NTU - 2006	NTU - 2007	NTU - 2008
360	91	30	43
361	58	50	222
362	42	32	130
363	78	33	59
364	42	30	42
365	195	29	38
366			35

Day	NTU - 2009	NTU - 2010	NTU - 2011
1	192	43	361
2	122	920	0
3	67	130	117
4	38	60	158
5	54	420	122
6	300	90	71
7	77	54	94
8	40	75	45
9	553	71	33
10	155	252	216
11	600	81	267
12	170	910	742
13	41	145	750
14	37	80	265
15	37	35	742
16	175	125	37
17	48	115	29
18	460	52	133
19	870	170	42
20	85	775	208
21	40	217	450
22	282	525	425
23	191	450	3230
24	145	100	371
25	225	89	96
26	38	566	179
27	38	178	174
28	528	96	55
29	303	51	38
30	69	310	34
31	44	40	218
32	37	35	54
33	214	210	34
34	67	76	27
35	56	35	216
36	43	28	45
37	35	32	663
38	284	35	107
39	243	40	42

Day	NTU - 2009	NTU - 2010	NTU - 2011
40	73	43	39
41	153	1020	75
42	46	95	134
43	31	43	65
44	285	30	107
45	91	27	235
46	38	32	250
47	100	22	235
48	41	27	53
49	33	32	38
50	22	30	28
51	33	29	27
52	33	23	26
53	32	27	31
54	33	35	444
55	615	28	415
56	138	28	199
57	111	30	68
58	345	30	36
59	104	38	98
60	77	31	141
61	54	24	46
62	37	39	590
63	42	300	190
64	34	39	52
65	28	33	34
66	36	31	27
67	175	28	27
68	600	30	23
69	70	500	68
70	38	218	54
71	51	635	36
72	55	158	64
73	44	73	78
74	110	54	101
75	110	55	40
76	52	72	440
77	29	191	190
78	29	70	130
79	30	66	38

Day	NTU - 2009	NTU - 2010	NTU - 2011
80	29	93	28
81	28	443	30
82	27	190	38
83	27	446	25
84	37	140	43
85	31	99	25
86	65	397	25
87	70	204	28
88	34	140	23
89	64	92	37
90	105	40	62
91	44	162	132
92	85	267	70
93	33	65	348
94	33	110	300
95	150	169	177
96	158	103	65
97	130	506	88
98	42	682	146
99	30	126	109
100	340	50	83
101	380	41	80
102	131	34	51
103	50	32	2180
104	76	40	260
105	760	153	106
106	380	306	65
107	252	115	78
108	43	196	46
109	131	112	102
110	123	114	98
111	396	164	154
112	190	110	215
113	62	620	52
114	152	732	52
115	235	276	39
116	62	120	254
117	306	118	650
118	98	27	157
119	51	99	828

Day	NTU - 2009	NTU - 2010	NTU - 2011
120	196	118	296
121	616	227	141
122	43	25	103
123	29	20	296
124	30	290	170
125	32	160	105
126	250	47	95
127	127	46	110
128	42	240	70
129	224	111	33
130	99	71	55
131	466	67	135
132	190	53	150
133	420	33	54
134	116	33	360
135	133	32	358
136	57	30	126
137	100	31	63
138	137	33	38
139	46	30	33
140	70	27	520
141	54	34	55
142	684	34	40
143	297	29	725
144	57	27	370
145	151	26	73
146	63	28	37
147	46	88	28
148	30	29	52
149	31	27	65
150	38	29	45
151	34	27	30
152	29	31	27
153	390	38	23
154	53	24	26
155	36	23	39
156	33	28	29
157	30	26	32
158	31	28	32
159	27	29	24

Day	NTU - 2009	NTU - 2010	NTU - 2011
160	24	29	23
161	27	26	26
162	28	23	25
163	28	28	31
164	24	26	31
165	28	71	35
166	28	27	38
167	24	25	30
168	24	23	30
169	24	71	33
170	24	24	32
171	21	24	29
172	20	23	30
173	20	116	29
174	23	28	30
175	26	23	28
176	23	26	28
177	90	21	28
178	23	25	28
179	23	21	27
180	25	20	28
181	25	20	29
182	27	21	29
183	19	23	29
184	23	21	42
185	26	20	26
186	21	20	26
187	21	22	27
188	18	19	27
189	24	19	28
190	23	19	28
191	163	20	27
192	73	17	25
193	23	18	24
194	18	20	21
195	19	18	21
196	26	18	27
197	135	17	19
198	26	17	20
199	22	18	23

Day	NTU - 2009	NTU - 2010	NTU - 2011
200	23	15	21
201	23	15	21
202	25	16	20
203	26	18	19
204	22	54	17
205	24	15	21
206	24	0	21
207	22	22	19
208	24	17	16
209	18	19	17
210	35	19	18
211	26	18	18
212	29	20	17
213	21	18	17
214	36	17	17
215	19	20	19
216	21	18	16
217	21	17	16
218	25	15	17
219	20	16	16
220	23	16	14
221	21	16	18
222	24	16	17
223	26	16	21
224	33	17	16
225	28	15	16
226	27	22	18
227	30	19	17
228	68	19	18
229	23	15	19
230	28	25	92
231	25	20	90
232	30	16	49
233	22	25	24
234	23	19	22
235	27	17	22
236	23	17	27
237	20	16	23
238	30	14	26
239	25	17	21

Day	NTU - 2009	NTU - 2010	NTU - 2011
240	23	17	21
241	25	13	22
242	23	16	21
243	21	18	22
244	27	14	17
245	29	23	28
246	22	20	25
247	20	22	23
248	23	20	20
249	21	25	22
250	23	22	21
251	24	25	21
252	25	24	62
253	25	22	25
254	27	22	20
255	27	22	19
256	26	22	19
257	35	22	19
258	93	24	19
259	33	22	18
260	29	29	21
261	26	22	24
262	29	28	20
263	28	23	27
264	23	24	20
265	22	22	23
266	24	29	18
267	80	22	21
268	137	20	260
269	92	22	60
270	41	24	36
271	29	27	28
272	41	23	17
273	26	46	17
274	28	48	19
275	23	21	22
276	21	25	17
277	20	17	17
278	19	19	18
279	19	19	17

Day	NTU - 2009	NTU - 2010	NTU - 2011
280	18	19	25
281	21	18	28
282	18	19	34
283	20	19	24
284	24	19	19
285	163	129	18
286	27	104	160
287	34	43	142
288	29	240	22
289	30	83	29
290	182	40	55
291	79	120	125
292	51	222	190
293	41	248	45
294	47	49	36
295	44	32	49
296	133	34	71
297	284	190	47
298	216	45	64
299	2100	830	30
300	650	165	125
301	88	637	250
302	85	159	136
303	78	72	867
304	238	45	115
305	55	406	200
306	36	205	130
307	230	221	176
308	390	135	873
309	490	1050	880
310	70	880	537
311	149	867	1078
312	440	143	374
313	62	55	1664
314	37	33	1000
315	33	81	79
316	32	822	530
317	42	1018	211
318	29	148	3755
319	340	155	175

Day	NTU - 2009	NTU - 2010	NTU - 2011
320	380	490	640
321	445	980	599
322	171	120	405
323	460	60	387
324	600	346	200
325	392	510	112
326	40	389	346
327	35	258	546
328	63	523	530
329	174	124	110
330	311	79	55
331	415	383	46
332	366	275	340
333	271	150	1666
334	99	95	256
335	52	45	63
336	115	38	45
337	476	54	610
338	79	37	740
339	1118	286	480
340	540	109	152
341	118	58	660
342	42	112	842
343	540	130	114
344	310	42	70
345	213	29	480
346	143	115	381
347	84	508	105
348	544	216	51
349	412	122	38
350	82	77	207
351	71	48	81
352	52	49	38
353	760	48	93
354	560	31	52
355	580	172	37
356	220	219	35
357	74	284	38
358	104	346	33
359	395	330	34

Day	NTU - 2009	NTU - 2010	NTU - 2011
360	280	122	35
361	82	131	48
362	54	835	41
363	51	214	70
364	47	55	42
365	48	37	38
366			

Day	NTU - 2012	NTU - 2013
1	30	43
2	29	182
3	30	55
4	36	75
5	32	257
6	170	169
7	35	47
8	37	33
9	30	30
10	30	32
11	281	31
12	35	40
13	26	143
14	38	422
15	38	231
16	34	195
17	27	95
18	28	70
19	29	64
20	27	40
21	193	35
22	53	30
23	36	144
24	29	204
25	28	55
26	25	123
27	27	46
28	31	42
29	24	92
30	29	154
31	36	75
32	32	154
33	28	267
34	26	197
35	79	51
36	53	115
37	30	335
38	31	431
39	29	163

Day	NTU - 2012	NTU - 2013
40	28	200
41	22	464
42	33	479
43	25	90
44	130	49
45	61	52
46	27	35
47	24	30
48	54	116
49	44	365
50	27	146
51	56	53
52	62	55
53	40	26
54	368	32
55	203	390
56	54	243
57	34	126
58	34	102
59	621	35
60	127	35
61	51	58
62	34	82
63	30	32
64	29	740
65	26	195
66	68	63
67	31	340
68	37	87
69	33	66
70	31	60
71	27	98
72	252	46
73	803	39
74	96	98
75	46	78
76	38	67
77	28	196
78	80	202
79	46	118

Day	NTU - 2012	NTU - 2013
80	41	586
81	79	1564
82	68	610
83	54	338
84	55	92
85	84	54
86	131	48
87	366	41
88	44	57
89	366	35
90	159	207
91	256	28
92	116	106
93	80	48
94	48	870
95	111	790
96	158	750
97	58	106
98	113	60
99	34	43
100	116	37
101	235	35
102	520	39
103	128	43
104	76	124
105	128	666
106	115	216
107	50	110
108	33	88
109	67	305
110	756	177
111	246	449
112	78	57
113	231	425
114	467	469
115	107	315
116	283	87
117	135	106
118	81	104
119	514	133

Day	NTU - 2012	NTU - 2013
120	640	144
121	189	48
122	137	46
123	108	63
124	94	700
125	78	188
126	50	129
127	125	744
128	160	83
129	118	65
130	280	153
131	254	40
132	153	36
133	84	82
134	68	106
135	48	165
136	166	70
137	95	88
138	60	127
139	42	152
140	50	57
141	40	48
142	73	33
143	36	32
144	36	36
145	29	35
146	27	36
147	25	33
148	26	40
149	31	48
150	36	30
151	78	31
152	37	34
153	34	32
154	23	33
155	28	30
156	24	29
157	25	29
158	25	27
159	21	30

Day	NTU - 2012	NTU - 2013
160	22	28
161	21	25
162	23	27
163	25	25
164	21	29
165	20	25
166	21	26
167	21	33
168	21	87
169	19	79
170	20	37
171	20	26
172	21	14
173	21	18
174	24	24
175	20	27
176	19	23
177	17	21
178	22	23
179	19	20
180	18	23
181	21	21
182	24	24
183	19	20
184	20	20
185	19	19
186	19	22
187	21	30
188	19	21
189	24	23
190	38	23
191	25	26
192	30	22
193	15	23
194	17	23
195	16	23
196	19	22
197	17	25
198	16	23
199	16	20

Day	NTU - 2012	NTU - 2013
200	19	23
201	21	23
202	18	21
203	16	21
204	14	21
205	20	23
206	20	23
207	20	23
208	17	22
209	18	20
210	19	22
211	20	17
212	16	15
213	16	15
214	17	19
215	18	17
216	18	16
217	16	15
218	16	19
219	18	16
220	21	17
221	18	16
222	16	18
223	17	17
224	18	16
225	15	20
226	17	18
227	18	17
228	18	17
229	17	18
230	19	17
231	16	23
232	15	20
233	19	20
234	20	20
235	17	25
236	79	22
237	25	18
238	20	21
239	16	22

Day	NTU - 2012	NTU - 2013
240	20	19
241	17	22
242	18	20
243	18	22
244	15	19
245	19	24
246	78	21
247	40	25
248	32	22
249	34	22
250	17	17
251	19	20
252	20	17
253	18	20
254	23	19
255	81	19
256	24	23
257	21	22
258	23	36
259	14	22
260	34	18
261	19	21
262	33	22
263	34	22
264	40	22
265	58	22
266	122	22
267	55	21
268	29	19
269	25	32
270	19	31
271	20	33
272	25	31
273	86	31
274	74	65
275	264	63
276	30	51
277	68	50
278	27	36
279	107	28

Day	NTU - 2012	NTU - 2013
280	36	39
281	71	42
282	128	30
283	56	288
284	34	74
285	111	120
286	33	97
287	29	134
288	29	596
289	58	116
290	61	196
291	24	244
292	22	86
293	150	71
294	21	90
295	80	33
296	205	29
297	517	85
298	212	366
299	63	214
300	37	1017
301	45	181
302	32	61
303	52	63
304	58	45
305	31	69
306	29	166
307	26	111
308	24	60
309	35	58
310	109	90
311	63	280
312	36	56
313	366	145
314	216	70
315	52	33
316	40	71
317	126	850
318	625	300
319	830	200

Day	NTU - 2012	NTU - 2013
320	167	67
321	2555	39
322	418	40
323	73	126
324	131	520
325	625	112
326	157	200
327	285	275
328	227	82
329	344	323
330	888	139
331	338	55
332	161	357
333	115	165
334	140	58
335	107	434
336	130	560
337	162	191
338	115	118
339	230	43
340	71	172
341	60	816
342	100	103
343	350	96
344	144	76
345	30	96
346	110	136
347	317	426
348	715	1000
349	827	810
350	202	1724
351	82	128
352	988	68
353	1040	58
354	108	260
355	235	125
356	147	63
357	170	55
358	102	1228
359	42	202

Day	NTU - 2012	NTU - 2013
360	38	205
361	898	62
362	197	46
363	124	657
364	63	180
365	75	75
366	76	

Turbidity Exceedance Probability Curves (2000 to 2013)

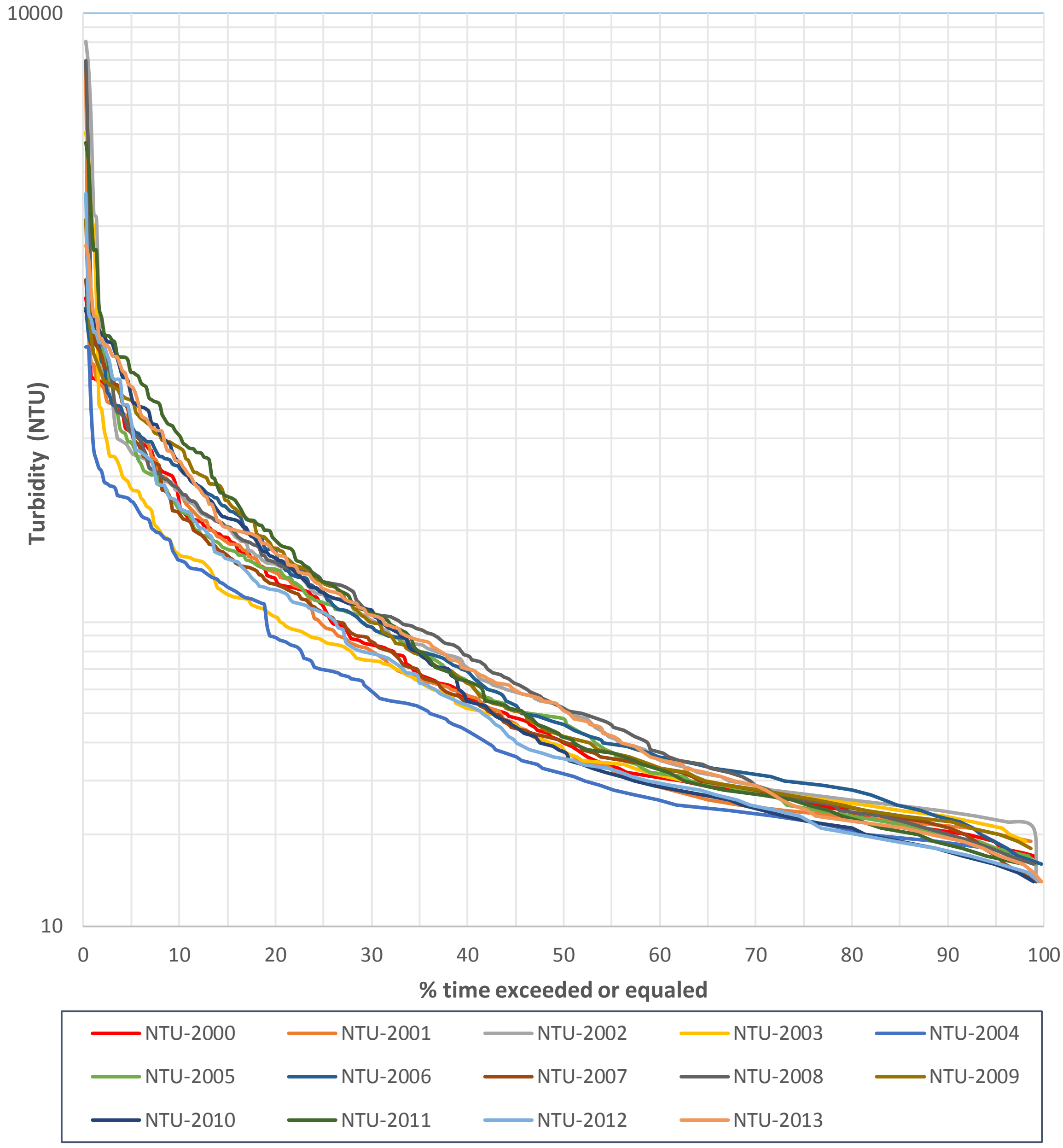

TSS vs Turbidity (2005)

NTU	TSS (mg/l)
28	93.2
35	114.2
27	88.4
60	171.1
149	422
195	588.9
126	311.1
68	223.5
47	144.3
25	78.5
101	313.5
43	129.4
169	494.4
189	526.4
486	1317.6
22	71.2
21	71.1
18	63
66	194.9
17	54
24	77.2
19	59.2
23	78.9
20	71.4
41	133.4
143	406.2
33	101.2
235	604.5
270	763.5
63	165.1
34	104.8
129	399
288	808.9
92	259.5
98	305.1
110	288.2
94	287.2
40	127.2
394	1012.4

TSS vs Turbidity (2013)

NTU	TSS (mg/l)
294	852.9
112	295.2
31	112.4
117	327
27	104.4
461	1342.4
418	1122.4
87	254.8
49	168.3
115	308.2
252	694.5
46	151.2
13	64
59	188.3
357	920.2
82	241.5
141	334
63	178.1
605	1934
459	1329.6
208	598.9
317	955
548	1745
493	1482.3
922	3221.2
99	311.2
148	451

Discharge vs Water Level

W (cm)	Q (m3/s)
121.8	10.8
126.6	11.2
129.0	11.4
130.0	11.9
134.0	12.3
134.3	12.5
143.2	13.3
145.0	14.1
150.0	14.5
159.4	15.4
166.7	16.0
185.0	17.4
195.0	17.8
195.0	18.4
214.0	21.0
226.0	21.4
254.0	28.4
259.0	29.0
260.0	31.3
269.8	32.4
297.0	40.9

APPENDIX B: RAINFALL-RUNOFF EROSIVITY FACTORS & CROSS VALIDATION OF INTERPOLATION METHODS

Rainfall-Runoff Erosivity Factor Relationships

- From Bols (1978). [Relationship based on empirical study in Indonesia]

$$R = \frac{2.5\ P^2}{100\ (0.073P + 0.73)}$$

Where:

R = the annual rainfall erosivity, expressed in Mj · mm · ha^{-1} · h^{-1}· $year^{-1}$;
P = the annual precipitation (mm).

- From Yu and Rosewell (1996). [Relationship used in southeastern Australia in 1996]

$$R = 0.0438\ P^{1.61}$$

Where:

R = the annual rainfall erosivity, expressed in Mj · mm · ha^{-1} · h^{-1}· $year^{-1}$;
P = the annual precipitation (mm).

- From Mikhailova et al. (1997). [Relationship based on annual rainfall and elevation in Honduras]

$$R = -3172 + 7.562\ P$$

Where:

R = the annual rainfall erosivity, expressed in Mj · mm · ha^{-1} · h^{-1}· $year^{-1}$;
P = the annual precipitation (mm).

- From Torri et al. (2006). [Relationship based on annual rainfall in Italy]

$$R = -944 + 3.08\ P$$

Where:

R = the annual rainfall erosivity, expressed in Mj · mm · ha^{-1} · h^{-1}· $year^{-1}$;
P = the annual precipitation (mm).

Tables of Rainfall-Runoff Erosivity Factor Used from 8 Us States

ALABAMA		
County	**Annual Precipitation (in)**	**R_Factor**
Autauga County	55.0	417
Barbour County	52.5	429
Bibb County	58.3	424
Blount County	56.5	365
Bullock County	54.1	422
Butler County	57.6	475
Calhoun County	54.8	338
Chambers County	55.8	393
Cherokee County	56.5	338
Chilton County	56.4	412
Choctaw County	59.7	504
Clarke County	59.8	539
Clay County	58.3	394
Cleburne County	56.1	355
Coffee County	56.9	531
Colbert County	55.8	374
Coosa County	56.8	408
Covington County	59.7	547
Crenshaw County	56.6	497
Cullman County	57.6	372
Dale County	55.5	500
Dallas County	54.7	435
De Kalb County	58.2	343
Elmore County	55.5	410
Etowah County	55.5	338
Fayette County	58.9	434
Franklin County	57.7	392
Geneva County	57.7	543
Greene County	54.3	412
Hale County	55.3	420
Henry County	54.9	463
Houston County	55.4	520
Jackson County	57.8	332
Jefferson County	56.9	381
Lamar County	59.0	420

ALABAMA		
County	Annual Precipitation (in)	R_Factor
Lauderdale County	55.7	363
Lawrence County	56.8	369
Lee County	55.6	403
Limestone County	56.5	348
Lowndes County	54.4	442
Macon County	55.2	417
Madison County	56.2	340
Marengo County	56.0	454
Marion County	59.2	418
Marshall County	55.4	338
Monroe County	58.5	539
Montgomery County	54.4	436
Morgan County	56.6	362
Perry County	55.6	430
Pickens County	56.6	419
Pike County	54.1	454
Randolph County	55.9	362
Russell County	51.6	388
Shelby County	57.1	391
St. Clair County	56.0	370
Sumter County	55.9	445
Talladega County	56.2	380
Tallapoosa County	57.1	411
Tuscaloosa County	57.0	412
Walker County	57.6	393
Wilcox County	56.1	481
Winston County	58.4	392

ARKANSAS		
County	**Annual Precipitation (in)**	**R_Factor**
Arkansas County	51.0	357
Ashley County	54.7	425
Bradley County	54.0	413
Calhoun County	52.4	394
Chicot County	53.4	405
Clark County	53.7	390
Cleburne County	51.2	325
Cleveland County	52.9	388
Columbia County	51.1	400
Crittenden County	50.9	338
Dallas County	52.1	384
Desha County	52.1	382
Drew County	53.8	399
Faulkner County	50.1	332
Garland County	55.8	393
Grant County	52.4	371
Hempstead County	52.6	397
Hot Spring County	54.8	393
Howard County	54.1	397
Jefferson County	51.4	362
Lafayette County	50.2	391
Lee County	51.9	351
Lincoln County	52.4	381
Monroe County	50.4	348
Montgomery County	55.8	394
Nevada County	53.0	398
Ouachita County	52.0	391
Perry County	50.7	350
Phillips County	52.5	370
Pike County	55.7	410
Polk County	56.3	407
Prairie County	50.2	339
Pulaski County	50.2	343
Saline County	53.5	375
Scott County	50.2	339
Sevier County	52.5	385
St. Francis County	51.0	340

ARKANSAS		
County	Annual Precipitation (in)	R_Factor
Union County	52.6	410
Van Buren County	51.6	325
White County	51.0	334
Woodruff County	50.1	333

GEORGIA		
County	Annual Precipitation (in)	R_Factor
Atkinson County	50.1	424
Baker County	52.2	445
Banks County	54.9	309
Barrow County	51.3	296
Bartow County	52.8	304
Brantley County	51.6	451
Brooks County	52.2	464
Calhoun County	51.8	425
Camden County	51.2	452
Carroll County	54.5	342
Catoosa County	54.3	299
Charlton County	52.1	467
Chattahoochee County	50.2	377
Chattooga County	55.8	319
Cherokee County	56.2	319
Clay County	52.9	440
Clayton County	50.8	309
Clinch County	52.3	464
Cobb County	54.4	323
Colquitt County	50.6	437
Cook County	50.4	432
Coweta County	52.7	336
Dade County	59.9	340
De Kalb County	53.0	313
Decatur County	54.4	502
Dougherty County	51.2	418
Douglas County	53.8	334
Early County	53.7	465
Echols County	53.3	483
Fayette County	51.5	325

GEORGIA		
County	Annual Precipitation (in)	R_Factor
Floyd County	54.6	310
Forsyth County	57.3	329
Franklin County	52.6	299
Fulton County	53.5	318
Glynn County	50.7	443
Gordon County	54.3	299
Grady County	54.0	486
Gwinnett County	54.3	320
Hall County	57.7	325
Haralson County	55.5	335
Harris County	52.2	377
Hart County	51.1	292
Heard County	54.4	349
Henry County	50.5	320
Jackson County	52.9	298
Lamar County	50.2	327
Lanier County	51.6	444
Lowndes County	52.5	463
Madison County	50.2	292
McIntosh County	50.8	433
Meriwether County	52.2	343
Miller County	53.2	472
Mitchell County	52.1	454
Murray County	58.3	318
Muscogee County	51.1	371
Paulding County	54.5	327
Pickens County	59.8	340
Pike County	51.3	337
Polk County	53.9	315
Quitman County	51.5	417
Randolph County	51.2	413
Rockdale County	50.7	310
Seminole County	54.2	504
Spalding County	51.2	325
Stephens County	57.3	317
Talbot County	51.7	370
Terrell County	50.1	395
Thomas County	52.8	471
Troup County	53.7	359

GEORGIA		
County	**Annual Precipitation (in)**	**R_Factor**
Upson County	50.6	340
Walker County	57.6	322
Walton County	50.5	292
Ware County	50.8	445
Wayne County	50.0	424
Whitfield County	55.7	306

LOUISIANA		
County	**Annual Precipitation (in)**	**R_Factor**
Acadia County	59.3	594
Beauregard County	57.7	552
Bienville County	53.8	443
Calcasieu County	57.2	564
Caldwell County	56.3	483
Cameron County	58.0	588
Catahoula County	58.6	532
Claiborne County	52.7	419
Concordia County	60.0	561
East Carroll County	55.7	455
Franklin County	55.2	470
Grant County	58.2	522
Jackson County	55.3	458
Jefferson Davis County	59.5	590
La Salle County	59.3	537
Lafayette County	59.2	618
Lincoln County	53.5	432
Madison County	56.1	468
Morehouse County	54.2	428
Natchitoches County	54.1	485
Orleans County	58.9	625
Ouachita County	52.7	436
Rapides County	59.8	562
Red River County	51.1	425
Richland County	54.0	448
Sabine County	52.6	460
Tensas County	56.0	480
Union County	53.2	422

LOUISIANA		
County	**Annual Precipitation (in)**	**R_Factor**
Vernon County	56.7	531
Webster County	50.8	405
West Carroll County	54.9	436
Winn County	57.9	514

MISSISSIPI		
County	**Annual Precipitation (in)**	**R_Factor**
Alcorn County	55.0	374
Attala County	57.5	441
Benton County	56.8	388
Bolivar County	53.6	391
Calhoun County	55.9	416
Carroll County	56.7	435
Chickasaw County	56.0	401
Choctaw County	56.7	432
Claiborne County	56.9	505
Clarke County	58.7	498
Clay County	56.8	422
Coahoma County	53.3	383
Copiah County	58.1	527
Covington County	59.5	544
De Soto County	52.4	351
Grenada County	56.4	418
Hinds County	55.8	466
Holmes County	56.2	447
Humphreys County	56.1	438
Issaquena County	55.7	452
Itawamba County	57.8	402
Jasper County	58.1	488
Jefferson County	58.0	528
Jones County	58.7	531
Kemper County	55.8	438
Lafayette County	56.6	402
Lauderdale County	57.1	471
Lawrence County	59.9	541
Leake County	56.2	449
Lee County	56.4	399

MISSISSIPI		
County	**Annual Precipitation (in)**	**R_Factor**
Leflore County	55.6	419
Lowndes County	57.2	426
Madison County	55.6	447
Marshall County	54.7	374
Monroe County	57.1	408
Montgomery County	56.6	433
Neshoba County	56.9	452
Newton County	57.0	471
Noxubee County	54.8	427
Oktibbeha County	56.2	425
Panola County	55.2	398
Pontotoc County	57.1	417
Prentiss County	56.1	399
Quitman County	54.4	385
Rankin County	56.4	470
Scott County	57.7	479
Sharkey County	55.0	447
Simpson County	58.6	515
Smith County	58.6	511
Sunflower County	54.9	410
Tallahatchie County	55.3	408
Tate County	53.4	374
Tippah County	56.6	383
Tishomingo County	56.1	378
Tunica County	52.8	367
Union County	57.0	411
Warren County	56.0	464
Washington County	53.5	402
Wayne County	59.3	538
Webster County	56.2	421
Winston County	56.9	449
Yalobusha County	56.4	410
Yazoo County	56.5	461

PUERTO RICO		
County	**Annual Precipitation (in)**	**R_Factor**
Aguada	54.0	468
Aguada	58.9	512
Aguadilla	51.0	431
Aguadilla	55.1	466
Aguadilla	59.0	499
Aguas Buenas	58.0	355
Aibonito	50.0	323
Aibonito	55.5	364
Aibonito	59.2	398
Arecibo	54.8	417
Arecibo	59.1	453
Arroyo	51.2	308
Arroyo	55.1	333
Arroyo	59.2	367
Barceloneta	54.9	401
Barceloneta	59.1	432
Barranquitas	55.2	351
Barranquitas	59.3	367
Cabo Rojo	51.1	429
Cabo Rojo	54.5	464
Cabo Rojo	57.4	498
Caguas	58.0	361
Camuy	51.2	415
Camuy	55.1	450
Camuy	58.9	483
Carolina	54.8	332
Carolina	58.8	349
Catano	58.0	379
Cayey	56.3	407
Cayey	59.1	431
Ceiba	51.5	269
Ceiba	55.4	287
Ceiba	59.5	307
Ciales	58.0	414
Cidra	54.0	377
Cidra	59.2	407
Coamo	51.1	358
Coamo	55.0	382

PUERTO RICO		
County	**Annual Precipitation (in)**	**R_Factor**
Coamo	58.8	401
Comerio	50.0	312
Comerio	55.4	343
Comerio	58.8	364
Corozal	58.0	392
Fajardo	55.4	281
Fajardo	59.6	300
Florida	58.0	430
Guayama	51.3	345
Guayama	55.2	374
Guayama	59.1	399
Guayanilla	50.8	372
Guayanilla	54.7	399
Guayanilla	58.7	434
Hatillo	51.7	416
Hatillo	54.4	439
Hatillo	59.0	481
Hormigueros	54.0	472
Hormigueros	59.2	518
Isabela	51.0	430
Isabela	54.8	461
Isabela	58.8	495
Juana Diaz	51.0	331
Juana Diaz	55.2	354
Juana Diaz	58.7	365
Lajas	50.3	415
Lajas	53.5	429
Lajas	56.4	452
Loiza	50.0	303
Loiza	54.5	326
Loiza	59.2	350
Luquillo	58.0	308
Manati	55.6	398
Manati	59.0	424
Mayaguez	59.9	522
Naguabo	55.8	293
Naguabo	58.9	309
Patillas	52.7	309
Patillas	55.1	323

PUERTO RICO		
County	**Annual Precipitation (in)**	**R_Factor**
Patillas	59.1	346
Penuelas	51.6	364
Penuelas	55.1	390
Penuelas	58.5	413
Ponce	50.9	350
Ponce	55.0	376
Ponce	58.8	397
Quebradillas	51.0	423
Quebradillas	55.1	459
Quebradillas	59.1	496
Rincon	54.0	468
Rincon	58.7	508
Sabana Grande	50.7	416
Sabana Grande	54.8	461
Sabana Grande	59.0	503
Salinas	51.1	364
Salinas	54.8	393
Salinas	58.4	418
San German	51.3	438
San German	54.6	472
San German	59.1	517
San Juan	54.0	335
San Juan	59.8	376
Toa Baja	58.0	382
Vega Alta	58.0	396
Vega Baja	54.0	383
Vega Baja	59.5	430
Villalba	51.8	317
Villalba	55.9	345
Villalba	58.9	365
Yauco	51.6	401
Yauco	55.1	429
Yauco	59.2	461

SOUTH CAROLINA		
County	**Annual Precipitation (in)**	**R_Factor**
Anderson County	50.3	279
Beaufort County	51.1	411
Berkeley County	50.5	386
Charleston County	50.9	400
Colleton County	50.5	387
Dorchester County	50.3	374
Georgetown County	51.4	396
Greenville County	56.6	317
Jasper County	50.4	397
Pickens County	60.0	332
Spartanburg County	51.2	284

TENNESSEE		
County	**Annual Precipitation (in)**	**R_Factor**
Anderson County	55.9	271
Bedford County	55.1	316
Benton County	54.0	320
Bledsoe County	57.7	304
Blount County	53.4	272
Bradley County	55.2	301
Campbell County	53.6	258
Cannon County	56.3	316
Carroll County	53.5	329
Cheatham County	51.0	286
Chester County	53.7	347
Claiborne County	51.0	235
Clay County	53.0	271
Coffee County	56.7	325
Crockett County	52.3	327
Cumberland County	58.2	297
De Kalb County	55.2	304
Decatur County	54.4	340
Dickson County	52.5	303
Dyer County	51.1	310
Fayette County	53.2	354
Fentress County	54.6	273
Franklin County	57.8	333

TENNESSEE		
County	Annual Precipitation (in)	R_Factor
Gibson County	53.3	324
Giles County	55.4	344
Hamilton County	55.7	303
Hardeman County	53.9	355
Hardin County	56.1	362
Haywood County	52.4	329
Henderson County	52.3	334
Henry County	53.2	308
Hickman County	53.6	320
Houston County	53.0	300
Humphreys County	54.3	319
Jackson County	54.0	282
Knox County	50.4	247
Lauderdale County	51.4	316
Lawrence County	55.8	352
Lewis County	55.0	335
Lincoln County	54.9	328
Loudon County	53.2	272
Macon County	54.3	285
Madison County	52.8	336
Marion County	58.6	329
Marshall County	54.6	334
Maury County	54.3	324
McMinn County	56.4	294
McNairy County	55.5	365
Meigs County	54.9	285
Monroe County	57.5	298
Montgomery County	50.9	275
Moore County	56.0	325
Morgan County	56.7	283
Obion County	51.8	317
Overton County	54.4	282
Perry County	55.4	342
Pickett County	52.8	264
Polk County	58.3	316
Putnam County	56.4	296
Rhea County	57.4	297
Roane County	54.4	273
Robertson County	50.2	269

TENNESSEE		
County	**Annual Precipitation (in)**	**R_Factor**
Rutherford County	53.7	311
Scott County	54.3	265
Sequatchie County	59.1	323
Sevier County	52.2	261
Shelby County	52.0	345
Smith County	53.6	282
Stewart County	52.4	287
Sumner County	51.3	276
Tipton County	51.7	326
Trousdale County	53.1	283
Unicoi County	50.6	231
Union County	51.9	243
Van Buren County	57.2	309
Warren County	54.9	307
Wayne County	56.8	366
Weakley County	53.5	313
White County	56.1	299
Williamson County	52.7	303
Wilson County	53.1	294

Cross Validation of Deterministic Interpolation Methods

Inverse Distance Weighting Method

Regression function: -0.142518319159947 * x + 500.984518950821

Cross Validation

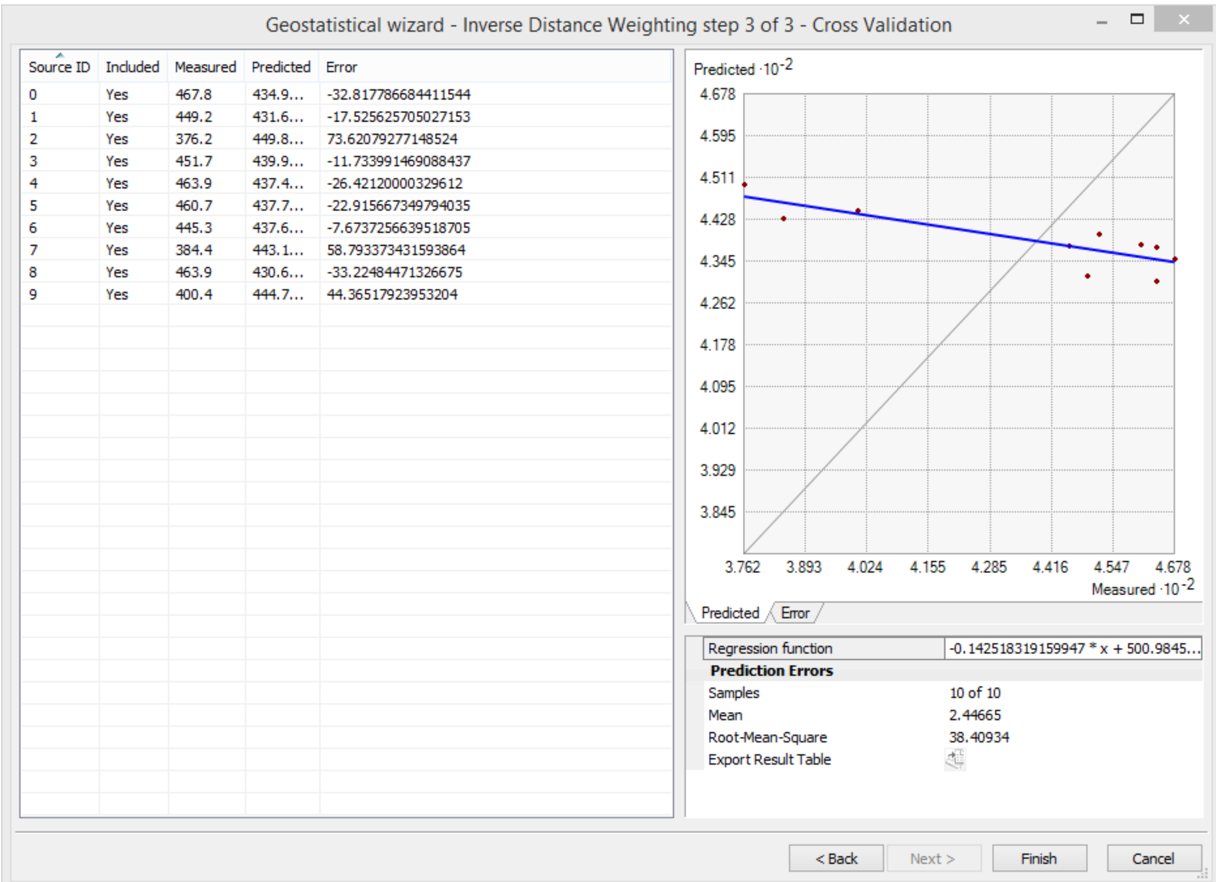

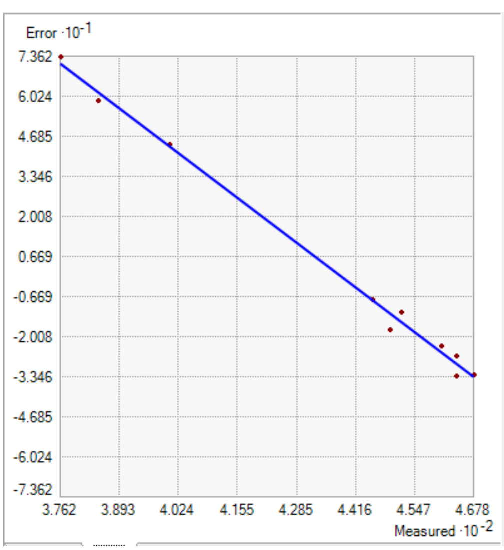

Global Polynomial Interpolation

Regression function: 0.0332408590870944 * x + 425.567191002319

Cross Validation

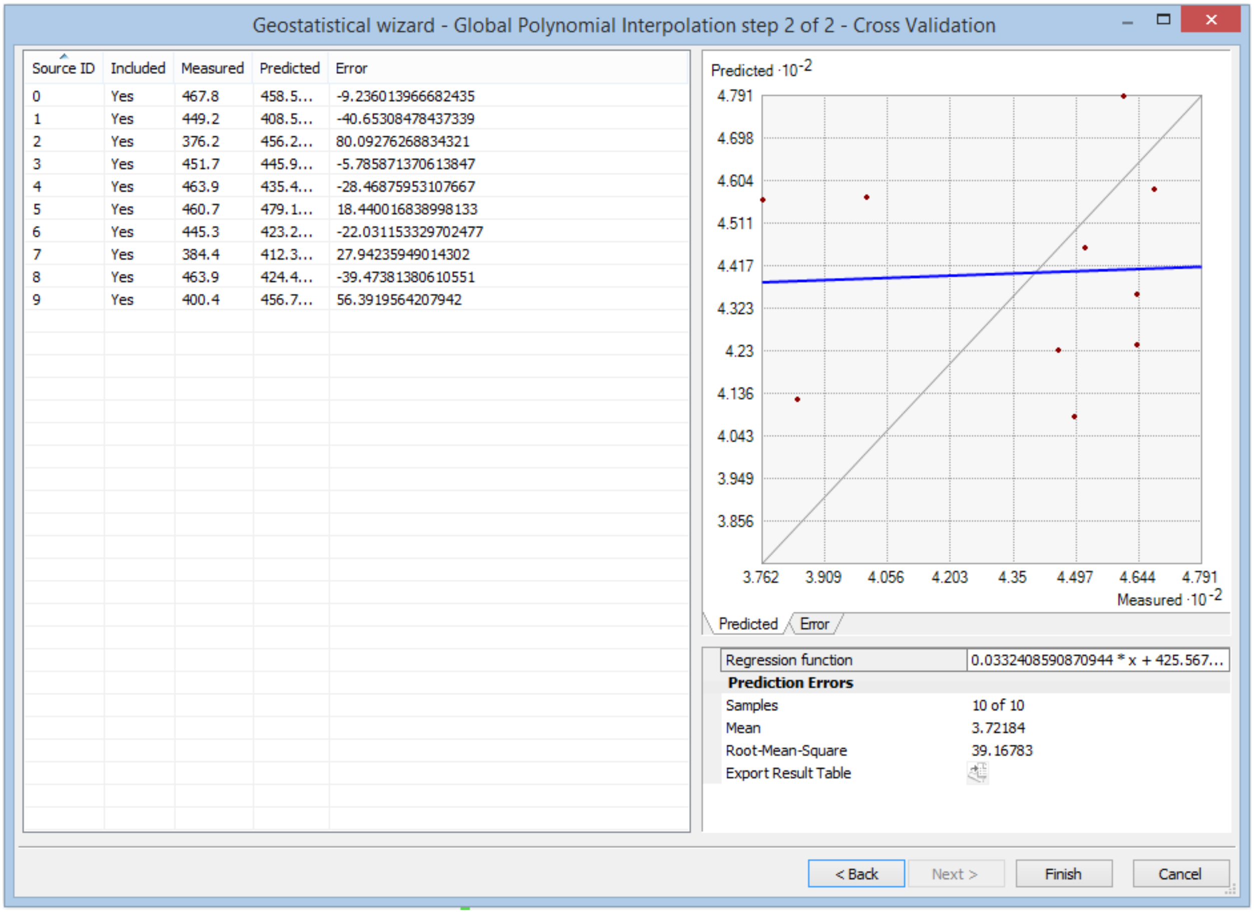

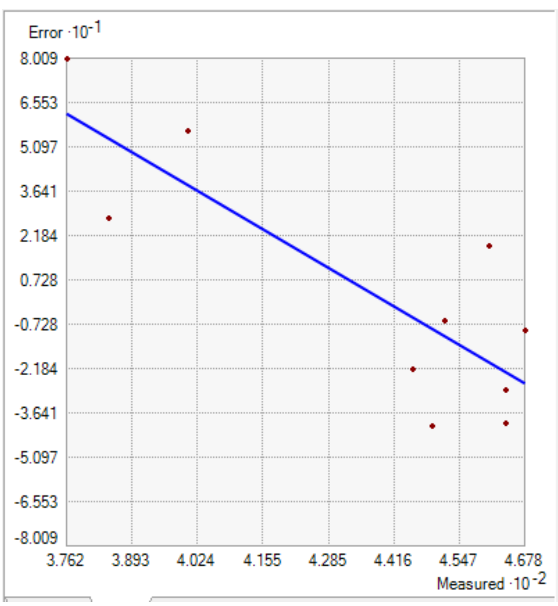

Local Polynomial Interpolation

Regression function: -0.104076952679077 * x + 483.56594277478

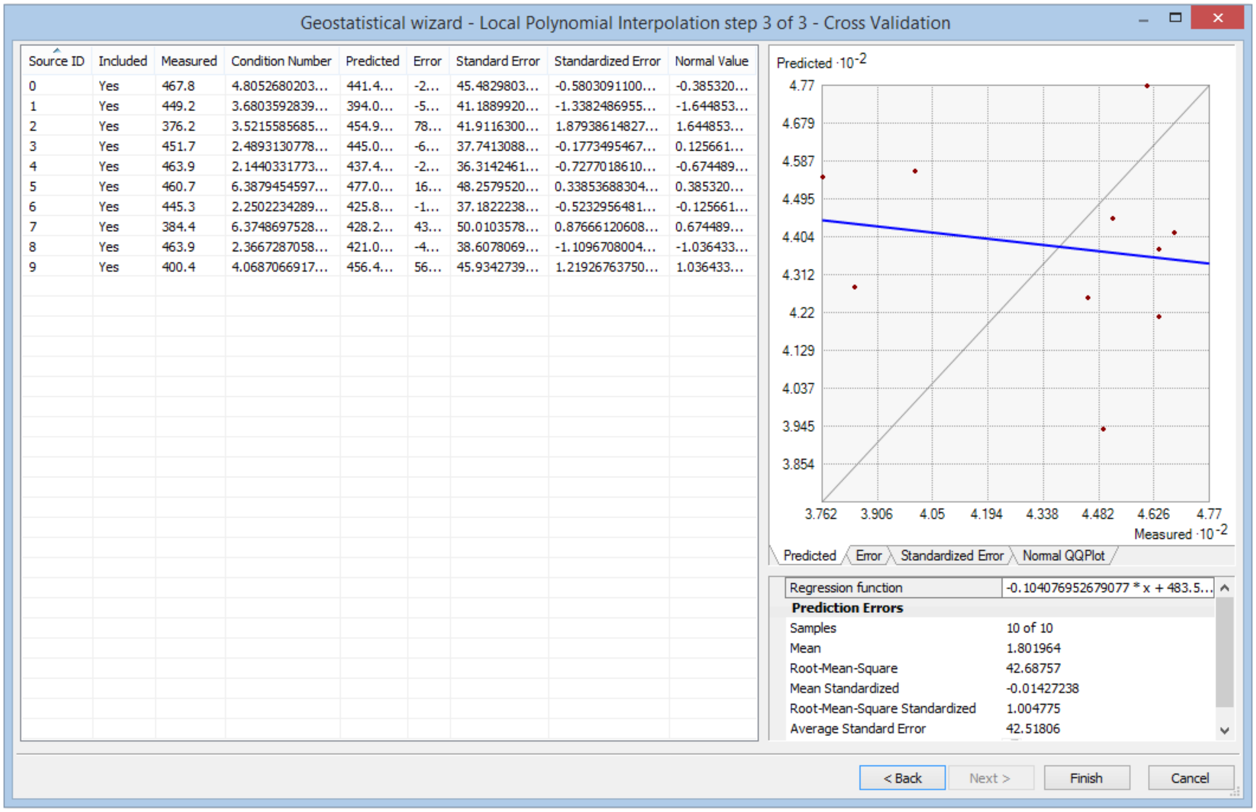

Source ID	Included	Measured	Condition Number	Predicted	Error	Standard Error	Standardized Error	Normal Value
0	Yes	467.8	4.8052680203...	441.4...	-2...	45.4829803...	-0.5803091100...	-0.385320...
1	Yes	449.2	3.6803592839...	394.0...	-5...	41.1889920...	-1.3382486955...	-1.644853...
2	Yes	376.2	3.5215585685...	454.9...	78...	41.9116300...	1.87938614827...	1.644853...
3	Yes	451.7	2.4893130778...	445.0...	-6...	37.7413088...	-0.1773495467...	0.125661...
4	Yes	463.9	2.1440331773...	437.4...	-2...	36.3142461...	-0.7277018610...	-0.674489...
5	Yes	460.7	6.3879454597...	477.0...	16...	48.2579520...	0.33853688304...	0.385320...
6	Yes	445.3	2.2502234289...	425.8...	-1...	37.1822238...	-0.5232956481...	-0.125661...
7	Yes	384.4	6.3748697528...	428.2...	43...	50.0103578...	0.87666120608...	0.674489...
8	Yes	463.9	2.3667287058...	421.0...	-4...	38.6078069...	-1.1096708004...	-1.036433...
9	Yes	400.4	4.0687066917...	456.4...	56...	45.9342739...	1.21926763750...	1.036433...

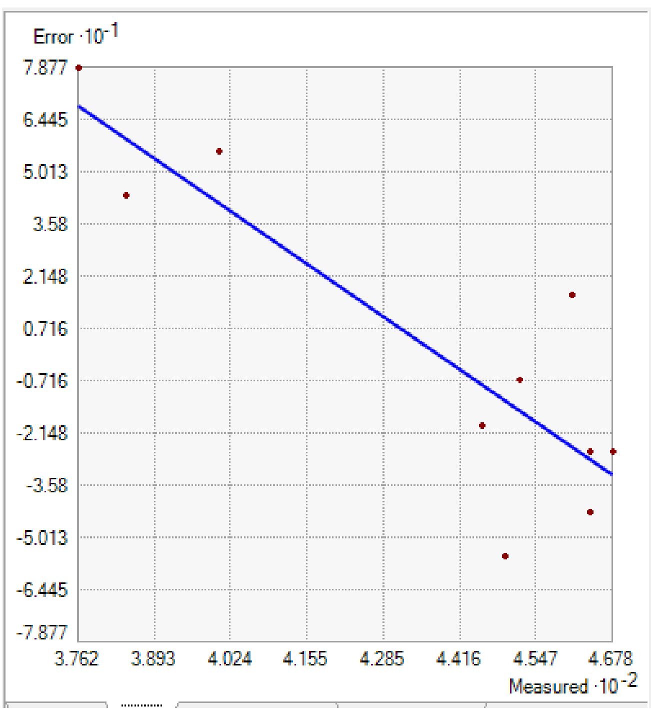

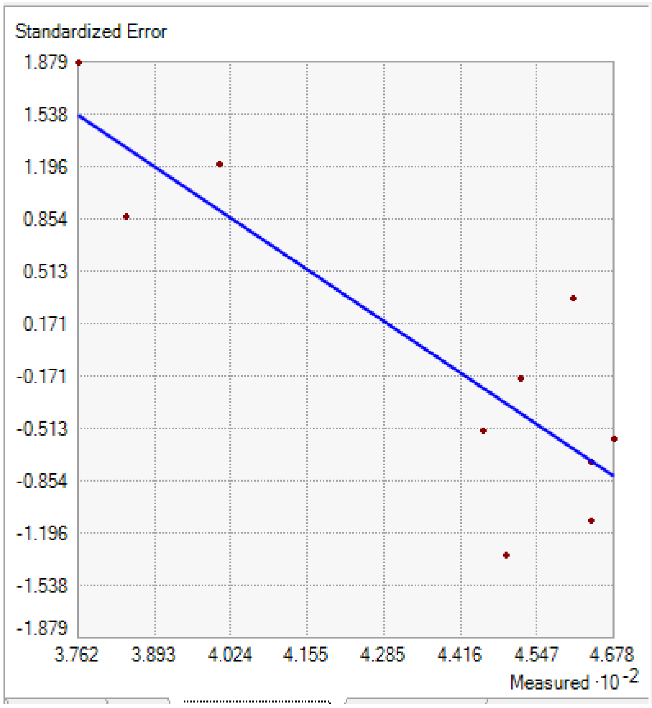

Standardized Error
1.879
1.538
1.196
0.854
0.513
0.171
-0.171
-0.513
-0.854
-1.196
-1.538
-1.879
3.762
3.893
4.024
4.155
4.285
4.416
4.547
4.678
Measured ·10^-2

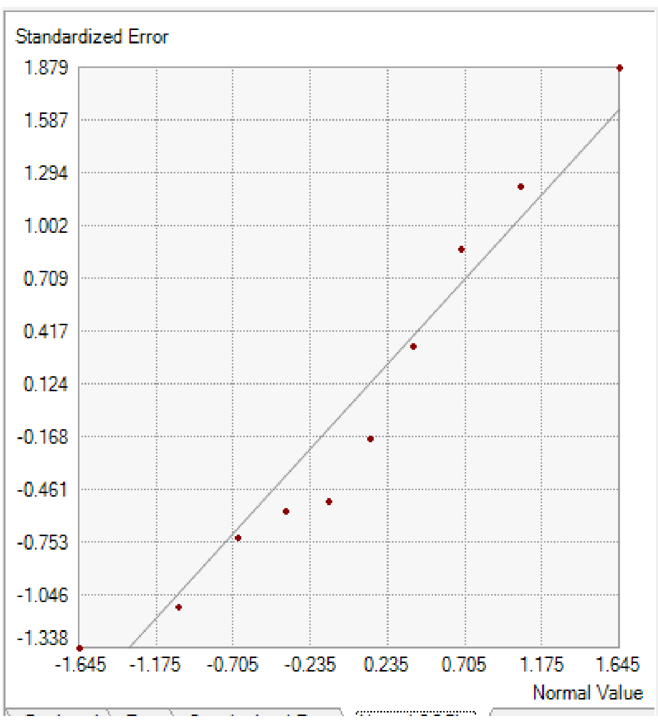

Standardized Error
1.879
1.587
1.294
1.002
0.709
0.417
0.124
-0.168
-0.461
-0.753
-1.046
-1.338
-1.645
-1.175
-0.705
-0.235
0.235
0.705
1.175
1.645
Normal Value

APPENDIX C: SHORT TERM C-FACTOR & CLASSIFICATION ERROR ANALYSIS

Short-term C-factor estimate for land cover "Bare land/burned grass/plowed land/rainfed crops"

June				
	Area (km^2)	Minimum (%) Bare soil	C_i	C
Bare land	45.6		0.5	0.31
Rainfed Crop Land	177.9		0.35	
Burn areas	232.7	76	0.24	
Total	456.2			
July				
	Area (km^2)	Minimum (%) Bare soil	C_i	C
Bare land	45.6		0.5	0.42
Rainfed Crop Land	177.9		0.35	
Burn areas	232.7	85	0.45	
Total	456.2			
August				
	Area (km^2)	Minimum (%) Bare soil	C_i	C
Bare land	45.6		0.5	0.42
Rainfed Crop Land	177.9		0.35	
Burn areas	232.7	90	0.45	
Total	456.2			
September				
	Area (km^2)	Minimum (%) Bare soil	C_i	C
Bare land	45.6		0.5	0.29
Rainfed Crop Land	177.9		0.35	
Burn areas	232.7	70	0.2	
Total	456.2			
October				
	Area (km^2)	Minimum (%) Bare soil	C_i	C
Bare land	45.6		0.5	0.27
Rainfed Crop Land	177.9		0.35	
Burn areas	232.7	65	0.17	
Total	456.2			
November				
	Area (km^2)	Minimum (%) Bare soil	C_i	C
Bare land	45.6		0.5	0.27
Rainfed Crop Land	177.9		0.35	
Burn areas	232.7	61	0.16	
Total	456.2			

Short-term C-factor estimate for land cover "Bare land/burned grass/plowed land/rainfed crops"

December				
	Area (km2)	Minimum (%) Bare soil	C_i	C
Bare land	45.6		0.5	0.26
Rainfed Crop Land	177.9		0.35	
Burn areas	232.7	57	0.15	
Total	456.2			
January				
	Area (km2)	Minimum (%) Bare soil	C_i	C
Bare land	45.6		0.5	0.26
Rainfed Crop Land	177.9		0.35	
Burn areas	232.7	55	0.14	
Total	456.2			
February				
	Area (km2)	Minimum (%) Bare soil	C_i	C
Bare land	45.6		0.5	0.25
Rainfed Crop Land	177.9		0.35	
Burn areas	232.7	52	0.13	
Total	456.2			
March				
	Area (km2)	Minimum (%) Bare soil	C_i	C
Bare land	45.6		0.5	0.25
Rainfed Crop Land	177.9		0.35	
Burn areas	232.7	50	0.12	
Total	456.2			
April				
	Area (km2)	Minimum (%) Bare soil	C_i	C
Bare land	45.6		0.5	0.24
Rainfed Crop Land	177.9		0.35	
Burn areas	232.7	48	0.11	
Total	456.2			
May				
	Area (km2)	Minimum (%) Bare soil	C_i	C
Bare land	45.6		0.5	0.24
Rainfed Crop Land	177.9		0.35	
Burn areas	232.7	45	0.1	
Total	456.2			

APPENDIX D: PICTURES OF LABORATORY EXPERIMENT

Brush fire in the N'djili Basin (July 2014)

Ash sampling site in the N'djili Basin (July 2014)

Raw ashes from Field

Crushed ashes

Precision scale

Mixing water and ashes

Mixing water and ashes **Turbiditymeter**

Water-ashes mixture after 0 hour of settling **Water-ashes mixture after 24 hours of settling**

(Photos by: Patrick Ndolo Goy, July 2014)

APPENDIX E: ANNUAL AVERAGE SOIL LOSS MAPS, SEDIMENT RATING CURVES, ANNUAL SEDIMENT LOAD.

Annual Average Soil loss rate map of the N'djili River Basin for year 2001

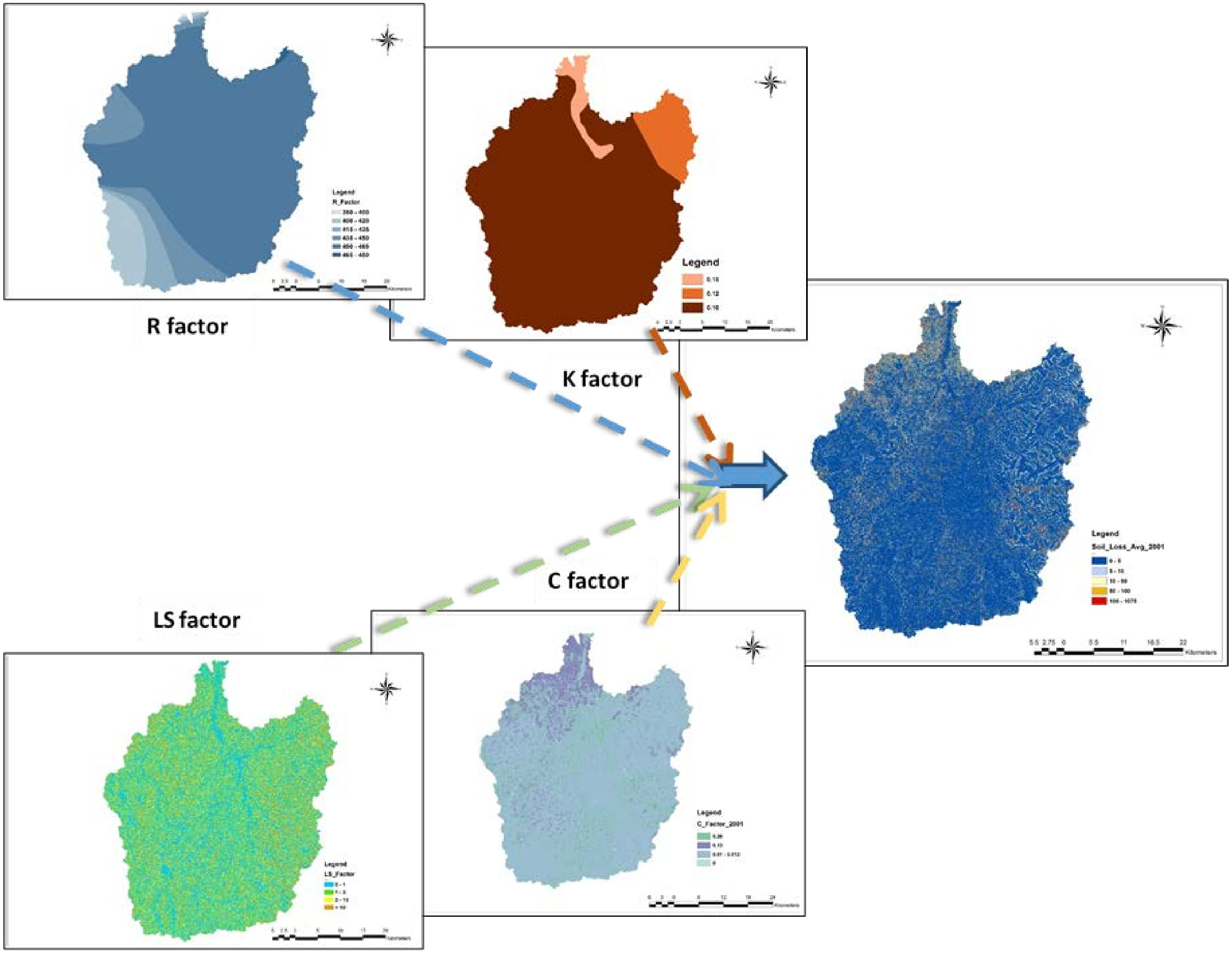

Annual Average Soil loss rate map of the N'djili River Basin for year 1995

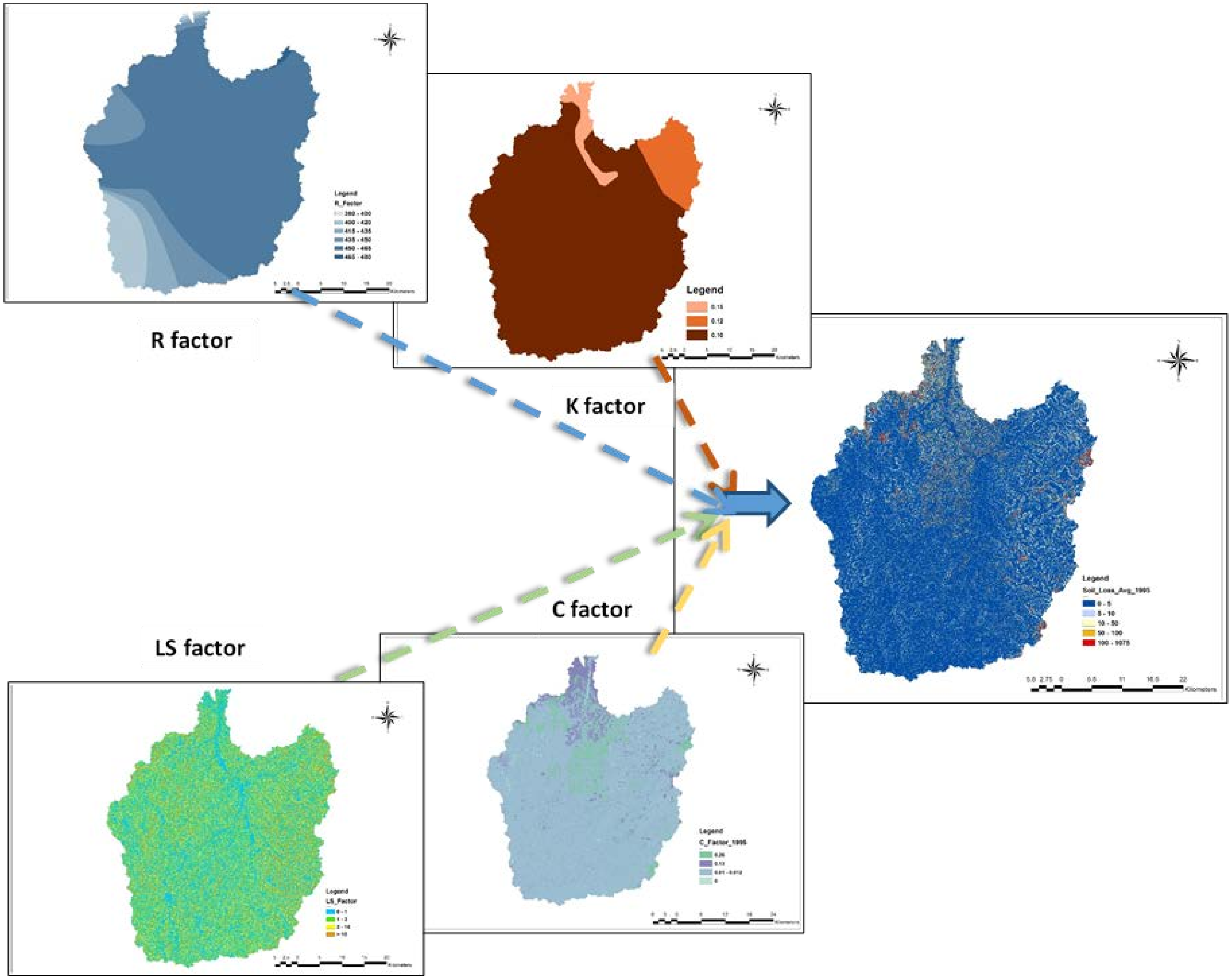

Average annual soil loss rate histogram (2013)

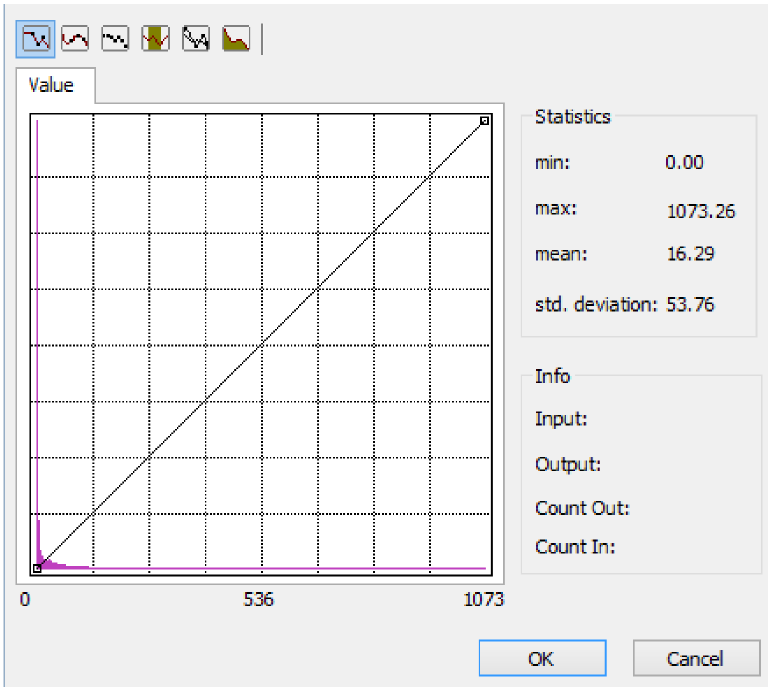

Average annual soil loss rate histogram (2001)

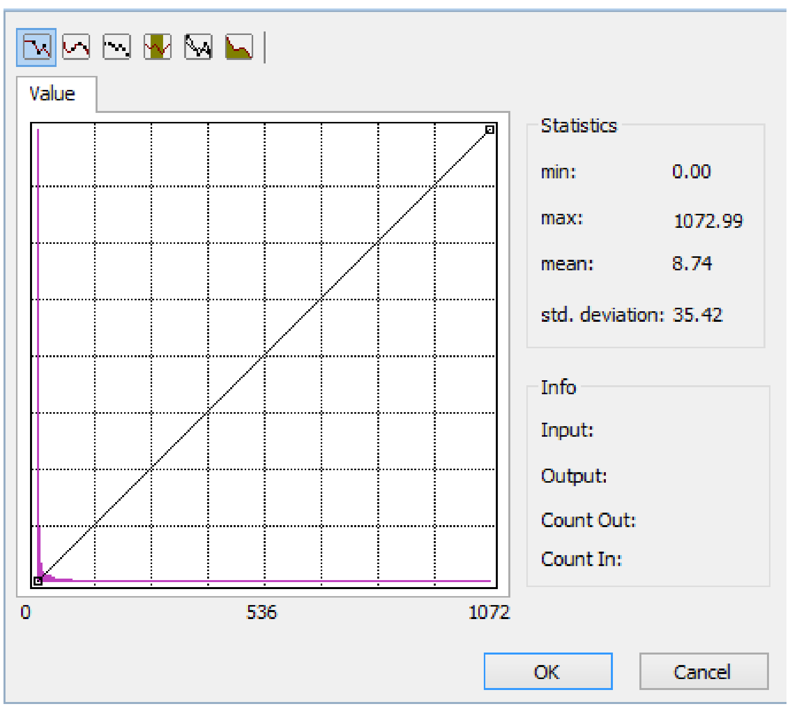

Average annual soil loss rate histogram (1995)

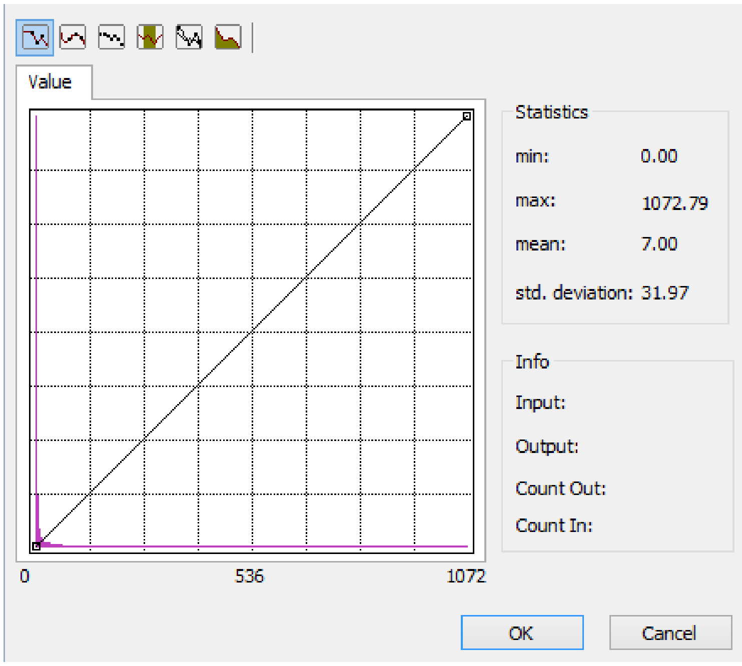

Daily sediment load vs Discharge (2005)

Day	TSS (mg/l) - 2005	Qobs [2005] (m3/s)	Qs (metric tons/day) - [2005]
1-Jan-05	173.9	22.6	339.6
2-Jan-05	93.0	17.2	138.1
3-Jan-05	421.1	36.7	1335.3
4-Jan-05	133.9	21.4	247.6
5-Jan-05	311.8	30	808.1
6-Jan-05	279.2	27.4	661.0
7-Jan-05	95.9	15.4	127.6
8-Jan-05	368.1	31.2	992.3
9-Jan-05	224.3	21.3	412.7
10-Jan-05	139.7	19.5	235.3
11-Jan-05	176.7	22.5	343.6
12-Jan-05	249.1	28.9	622.0
13-Jan-05	133.9	21.4	247.6
14-Jan-05	386.7	36.7	1226.2
15-Jan-05	190.8	21.8	359.4
16-Jan-05	159.7	18.8	259.4
17-Jan-05	148.3	18.6	238.3
18-Jan-05	314.5	28.9	785.2
19-Jan-05	125.2	19.1	206.7
20-Jan-05	215.9	24.3	453.4
21-Jan-05	142.6	19.8	243.9
22-Jan-05	145.4	23.4	294.0
23-Jan-05	122.3	21.2	224.1
24-Jan-05	95.9	15.4	127.6
25-Jan-05	90.0	15.4	119.7
26-Jan-05	128.1	18.4	203.7
27-Jan-05	218.7	24.2	457.3
28-Jan-05	193.6	22.9	383.1
29-Jan-05	125.2	20.2	218.6
30-Jan-05	98.9	18.9	161.5
31-Jan-05	122.3	20.9	220.9
1-Feb-05	84.0	17	123.4
2-Feb-05	72.0	13	80.8
3-Feb-05	75.0	12.5	81.0
4-Feb-05	119.4	17.4	179.5
5-Feb-05	221.5	20.6	394.2
6-Feb-05	156.9	21.2	287.3
7-Feb-05	110.7	17.7	169.2
8-Feb-05	93.0	17.2	138.1
9-Feb-05	87.0	18	135.3
10-Feb-05	182.4	26.8	422.3
11-Feb-05	423.8	33.5	1226.5
12-Feb-05	543.8	37.6	1766.5
13-Feb-05	362.8	30.7	962.2
14-Feb-05	173.9	18.5	278.0
15-Feb-05	131.0	19.5	220.8
16-Feb-05	486.7	38.3	1610.4
17-Feb-05	468.4	38.5	1558.0
18-Feb-05	210.4	26.9	489.0
19-Feb-05	235.3	25.4	516.5
20-Feb-05	360.1	30.5	948.9
21-Feb-05	246.4	24.8	527.9
22-Feb-05	139.7	18.7	225.7
23-Feb-05	173.9	19.4	291.5
24-Feb-05	110.7	17.2	164.4
25-Feb-05	210.4	24.8	450.8
26-Feb-05	397.3	34	1167.2
27-Feb-05	204.8	23.5	415.8
28-Feb-05	145.4	23.2	291.5
1-Mar-05	53.6	12.8	59.2
2-Mar-05	87.0	15.3	115.0
3-Mar-05	87.0	17.7	133.0
4-Mar-05	125.2	21.1	228.3
5-Mar-05	110.7	21.5	205.6
6-Mar-05	116.5	16.9	170.1
7-Mar-05	154.0	19.2	255.5
8-Mar-05	165.4	20.5	293.0
9-Mar-05	93.0	12.1	97.2
10-Mar-05	608.1	41.4	2175.2
11-Mar-05	224.3	26.2	507.7
12-Mar-05	362.8	33.4	1046.8
13-Mar-05	193.6	26.1	436.6
14-Mar-05	122.3	20.3	214.6
15-Mar-05	249.1	25	538.1
16-Mar-05	122.3	18.6	196.6

Day	TSS (mg/l) - 2005	Qobs [2005] (m3/s)	Qs (metric tons/day) - [2005]
17-Mar-05	232.6	25.3	508.4
18-Mar-05	240.9	26.9	559.8
19-Mar-05	136.8	19.5	230.5
20-Mar-05	116.5	18	181.2
21-Mar-05	104.8	17.7	160.2
22-Mar-05	190.8	23.9	394.0
23-Mar-05	136.8	24.1	284.9
24-Mar-05	113.6	17.3	169.8
25-Mar-05	81.0	14.3	100.1
26-Mar-05	290.1	27.2	681.7
27-Mar-05	295.5	28.1	717.5
28-Mar-05	354.7	31.9	977.7
29-Mar-05	378.7	32.3	1057.0
30-Mar-05	376.1	33.1	1075.5
31-Mar-05	623.5	41.7	2246.2
1-Apr-05	314.5	31.3	850.4
2-Apr-05	362.8	30.6	959.1
3-Apr-05	679.5	44.4	2606.7
4-Apr-05	229.8	26.5	526.2
5-Apr-05	362.8	32	1003.0
6-Apr-05	306.4	32.7	865.5
7-Apr-05	165.4	21.5	307.2
8-Apr-05	133.9	20.2	233.7
9-Apr-05	476.2	37.5	1543.0
10-Apr-05	528.2	41.1	1875.8
11-Apr-05	1267.7	60.5	6626.7
12-Apr-05	227.0	23.9	468.8
13-Apr-05	136.8	17.6	208.0
14-Apr-05	113.6	17.2	168.8
15-Apr-05	182.4	18.3	288.3
16-Apr-05	330.6	30.1	859.8
17-Apr-05	131.0	20.2	228.7
18-Apr-05	107.7	18.4	171.3
19-Apr-05	327.9	32.7	926.5
20-Apr-05	131.0	22.7	257.0
21-Apr-05	107.7	16.6	154.5
22-Apr-05	327.9	28.1	796.2
23-Apr-05	265.6	25.3	580.5

Day	TSS (mg/l) - 2005	Qobs [2005] (m3/s)	Qs (metric tons/day) - [2005]
24-Apr-05	1460.1	62.9	7934.8
25-Apr-05	1199.9	58.1	6023.2
26-Apr-05	515.3	39	1736.3
27-Apr-05	202.0	24.2	422.4
28-Apr-05	142.6	21.2	261.1
29-Apr-05	133.9	23.8	275.4
30-Apr-05	494.5	37.9	1619.2
1-May-05	1021.5	55.4	4889.6
2-May-05	188.0	23.9	388.2
3-May-05	122.3	20.9	220.9
4-May-05	113.6	19.3	189.4
5-May-05	87.0	15.1	113.5
6-May-05	78.0	12.7	85.6
7-May-05	75.0	12.1	78.4
8-May-05	84.0	13.7	99.4
9-May-05	84.0	15.5	112.5
10-May-05	75.0	14.6	94.6
11-May-05	84.0	16.4	119.0
12-May-05	72.0	15.3	95.1
13-May-05	75.0	14.7	95.2
14-May-05	75.0	13.6	88.1
15-May-05	68.9	11.7	69.7
16-May-05	81.0	15.2	106.4
17-May-05	81.0	16.5	115.5
18-May-05	75.0	16.2	105.0
19-May-05	72.0	14.9	92.6
20-May-05	72.0	14	87.0
21-May-05	81.0	15.3	107.1
22-May-05	72.0	15.6	97.0
23-May-05	87.0	15.6	117.3
24-May-05	72.0	16.4	102.0
25-May-05	68.9	12.8	76.2
26-May-05	75.0	13.1	84.9
27-May-05	72.0	12.8	79.6
28-May-05	68.9	12.6	75.0
29-May-05	68.9	14.1	84.0
30-May-05	68.9	13.5	80.4
31-May-05	68.9	14.6	86.9

Day	TSS (mg/l) - 2005	Qobs [2005] (m3/s)	Qs (metric tons/day) - [2005]
1-Jun-05	68.9	17.2	102.4
2-Jun-05	68.9	16.9	100.6
3-Jun-05	68.9	12.9	76.8
4-Jun-05	65.9	13.9	79.1
5-Jun-05	62.8	13.2	71.6
6-Jun-05	62.8	14.2	77.1
7-Jun-05	62.8	16.6	90.1
8-Jun-05	62.8	17.5	95.0
9-Jun-05	65.9	12.4	70.6
10-Jun-05	68.9	12.3	73.2
11-Jun-05	59.7	13	67.1
12-Jun-05	68.9	15	89.3
13-Jun-05	65.9	14.6	83.1
14-Jun-05	62.8	14.3	77.6
15-Jun-05	62.8	14.9	80.9
16-Jun-05	59.7	11.6	59.9
17-Jun-05	59.7	11.2	57.8
18-Jun-05	251.9	25	544.0
19-Jun-05	210.4	24.2	439.9
20-Jun-05	101.8	17	149.6
21-Jun-05	95.9	17.9	148.4
22-Jun-05	84.0	18.1	131.4
23-Jun-05	87.0	18.3	137.6
24-Jun-05	81.0	14.1	98.7
25-Jun-05	90.0	14.9	115.8
26-Jun-05	95.9	16	132.6
27-Jun-05	87.0	15.2	114.3
28-Jun-05	84.0	17.4	126.3
29-Jun-05	84.0	16.1	116.9
30-Jun-05	84.0	18.8	136.5
1-Jul-05	84.0	14.8	107.4
2-Jul-05	90.0	15.1	117.4
3-Jul-05	90.0	15.5	120.5
4-Jul-05	87.0	15.8	118.8
5-Jul-05	90.0	16	124.4
6-Jul-05	87.0	17.4	130.8
7-Jul-05	90.0	17.5	136.1
8-Jul-05	90.0	15.2	118.2

Day	TSS (mg/l) - 2005	Qobs [2005] (m3/s)	Qs (metric tons/day) - [2005]
9-Jul-05	90.0	13.7	106.5
10-Jul-05	90.0	13.5	105.0
11-Jul-05	75.0	13.2	85.5
12-Jul-05	84.0	15.3	111.1
13-Jul-05	81.0	15.9	111.3
14-Jul-05	81.0	15.9	111.3
15-Jul-05	84.0	17.9	129.9
16-Jul-05	81.0	15.1	105.7
17-Jul-05	75.0	13.4	86.8
18-Jul-05	93.0	14.1	113.2
19-Jul-05	56.7	9.3	45.5
20-Jul-05	56.7	12	58.7
21-Jul-05	53.6	12.5	57.9
22-Jul-05	56.7	13.4	65.6
23-Jul-05	53.6	13	60.2
24-Jul-05	59.7	14.4	74.3
25-Jul-05	62.8	15.7	85.2
26-Jul-05	59.7	11.8	60.9
27-Jul-05	199.2	22.3	383.8
28-Jul-05	196.4	20.9	354.7
29-Jul-05	59.7	11.9	61.4
30-Jul-05	59.7	12.8	66.1
31-Jul-05	59.7	14.1	72.8
1-Aug-05	62.8	13.4	72.7
2-Aug-05	62.8	14.9	80.9
3-Aug-05	56.7	15.1	73.9
4-Aug-05	56.7	11.6	56.8
5-Aug-05	56.7	12	58.7
6-Aug-05	53.6	12.2	56.5
7-Aug-05	59.7	14	72.3
8-Aug-05	59.7	14	72.3
9-Aug-05	59.7	15.8	81.6
10-Aug-05	59.7	12.6	65.0
11-Aug-05	56.7	11.8	57.8
12-Aug-05	59.7	11.5	59.4
13-Aug-05	78.0	15.3	103.1
14-Aug-05	204.8	24.5	433.5
15-Aug-05	65.9	13.3	75.7

Day	TSS (mg/l) - 2005	Qobs [2005] (m3/s)	Qs (metric tons/day) - [2005]
16-Aug-05	59.7	12.7	65.6
17-Aug-05	56.7	15.1	73.9
18-Aug-05	53.6	11.7	54.1
19-Aug-05	53.6	11.3	52.3
20-Aug-05	50.5	11.6	50.6
21-Aug-05	56.7	14.1	69.0
22-Aug-05	50.5	13.4	58.4
23-Aug-05	50.5	12.1	52.7
24-Aug-05	53.6	12.9	59.7
25-Aug-05	62.8	12.8	69.5
26-Aug-05	59.7	13.9	71.8
27-Aug-05	65.9	13.4	76.3
28-Aug-05	81.0	16.6	116.2
29-Aug-05	75.0	15	97.2
30-Aug-05	62.8	13.6	73.8
31-Aug-05	62.8	16.7	90.6
1-Sep-05	65.9	13.1	74.6
2-Sep-05	62.8	11.7	63.5
3-Sep-05	62.8	13.1	71.1
4-Sep-05	68.9	13.5	80.4
5-Sep-05	72.0	14.9	92.6
6-Sep-05	65.9	14.4	82.0
7-Sep-05	68.9	14.5	86.3
8-Sep-05	62.8	12	65.1
9-Sep-05	75.0	13	84.2
10-Sep-05	87.0	14.1	106.0
11-Sep-05	68.9	10.4	61.9
12-Sep-05	65.9	13.3	75.7
13-Sep-05	75.0	14.6	94.6
14-Sep-05	75.0	15.7	101.7
15-Sep-05	75.0	14.7	95.2
16-Sep-05	104.8	19.9	180.2
17-Sep-05	125.2	17.6	190.4
18-Sep-05	148.3	18.5	237.0
19-Sep-05	95.9	15.3	126.8
20-Sep-05	68.9	9.5	56.6
21-Sep-05	268.3	27.6	639.8
22-Sep-05	276.5	29.1	695.2

Day	TSS (mg/l) - 2005	Qobs [2005] (m3/s)	Qs (metric tons/day) - [2005]
23-Sep-05	101.8	16.5	145.2
24-Sep-05	81.0	15.3	107.1
25-Sep-05	154.0	23.5	312.7
26-Sep-05	87.0	14.9	112.0
27-Sep-05	81.0	15.1	105.7
28-Sep-05	72.0	14.5	90.1
29-Sep-05	72.0	16.6	103.2
30-Sep-05	72.0	16.8	104.4
1-Oct-05	128.1	20.9	231.4
2-Oct-05	407.9	33.2	1170.1
3-Oct-05	145.4	18.3	229.9
4-Oct-05	65.9	13.5	76.8
5-Oct-05	72.0	15.2	94.5
6-Oct-05	65.9	13.3	75.7
7-Oct-05	72.0	14.9	92.6
8-Oct-05	190.8	25.6	422.0
9-Oct-05	90.0	14.5	112.7
10-Oct-05	72.0	13.4	83.3
11-Oct-05	81.0	13.7	95.9
12-Oct-05	104.8	15.7	142.1
13-Oct-05	646.4	43.2	2412.8
14-Oct-05	735.2	47.1	2991.9
15-Oct-05	190.8	22.9	377.5
16-Oct-05	107.7	19.8	184.3
17-Oct-05	370.8	32.7	1047.5
18-Oct-05	780.5	45.9	3095.4
19-Oct-05	229.8	23.1	458.7
20-Oct-05	1366.6	61.2	7226.0
21-Oct-05	730.2	42.6	2687.5
22-Oct-05	543.8	39.6	1860.5
23-Oct-05	168.2	23	334.3
24-Oct-05	122.3	18.8	198.7
25-Oct-05	98.9	17.6	150.4
26-Oct-05	271.0	27.9	653.3
27-Oct-05	287.4	27.3	677.8
28-Oct-05	319.9	28	773.8
29-Oct-05	276.5	28.2	673.7
30-Oct-05	125.2	19.8	214.2

Day	TSS (mg/l) - 2005	Qobs [2005] (m3/s)	Qs (metric tons/day) - [2005]
31-Oct-05	1043.6	56.3	5076.6
1-Nov-05	319.9	30.5	842.9
2-Nov-05	207.6	28.2	505.8
3-Nov-05	1332.9	60.6	6978.8
4-Nov-05	1275.0	59.2	6521.4
5-Nov-05	349.4	31.4	947.9
6-Nov-05	442.2	36	1375.3
7-Nov-05	243.6	28	589.3
8-Nov-05	107.7	19	176.8
9-Nov-05	413.2	34	1213.8
10-Nov-05	281.9	27.1	660.1
11-Nov-05	202.0	21.5	375.3
12-Nov-05	290.1	28.3	709.3
13-Nov-05	145.4	21.6	271.4
14-Nov-05	215.9	24.9	464.6
15-Nov-05	240.9	27.8	578.5
16-Nov-05	190.8	26.6	438.5
17-Nov-05	78.0	13.4	90.3
18-Nov-05	835.7	47.3	3415.1
19-Nov-05	659.2	41.6	2369.2
20-Nov-05	478.8	36.4	1505.9
21-Nov-05	330.6	31.8	908.4
22-Nov-05	168.2	23.7	344.5
23-Nov-05	309.1	30.1	803.7
24-Nov-05	235.3	26.3	534.8
25-Nov-05	165.4	20.7	295.8
26-Nov-05	119.4	17.6	181.6
27-Nov-05	110.7	14.2	135.8
28-Nov-05	260.1	23.9	537.1
29-Nov-05	260.1	27	606.7
30-Nov-05	338.7	31	907.1
1-Dec-05	171.1	23.4	345.9
2-Dec-05	442.2	38.1	1455.6
3-Dec-05	1207.2	62.9	6560.4
4-Dec-05	536.0	38.6	1787.6
5-Dec-05	171.1	22.1	326.7
6-Dec-05	317.2	31.7	868.7
7-Dec-05	325.2	33.2	932.9

Day	TSS (mg/l) - 2005	Qobs [2005] (m3/s)	Qs (metric tons/day) - [2005]
8-Dec-05	357.4	33.5	1034.5
9-Dec-05	202.0	22.8	397.9
10-Dec-05	151.2	18.5	241.6
11-Dec-05	171.1	20.1	297.1
12-Dec-05	1075.5	52.4	4869.2
13-Dec-05	300.9	29	754.0
14-Dec-05	133.9	20.5	237.2
15-Dec-05	119.4	17.9	184.7
16-Dec-05	319.9	29.6	818.0
17-Dec-05	196.4	25.4	431.0
18-Dec-05	139.7	19.1	230.5
19-Dec-05	98.9	14.8	126.4
20-Dec-05	125.2	16.7	180.7
21-Dec-05	218.7	24.2	457.3
22-Dec-05	486.7	37.1	1560.0
23-Dec-05	204.8	25.4	449.5
24-Dec-05	311.8	29.2	786.5
25-Dec-05	587.6	40.5	2056.0
26-Dec-05	322.5	30.1	838.8
27-Dec-05	162.6	20.1	282.3
28-Dec-05	128.1	17.2	190.4
29-Dec-05	224.3	25.3	490.2
30-Dec-05	128.1	20	221.4
31-Dec-05	556.7	41.5	1996.0

Daily sediment load vs Discharge (2013)

Day	TSS (mg/l) - 2013	Qobs corr [2013] (m3/s)	Qs (metric tons/day) - [2013]
1-Jan-13	124.9	18.7	201.8
2-Jan-13	330.6	32	913.9
3-Jan-13	137.5	21.7	257.7
4-Jan-13	171.6	22.2	329.1
5-Jan-13	481.1	41.9	1741.7
6-Jan-13	327.6	39.5	1118.1
7-Jan-13	134.3	18.3	212.4
8-Jan-13	99.5	13.5	116.1
9-Jan-13	96.3	15.4	128.1
10-Jan-13	102.7	17.5	155.3
11-Jan-13	96.3	17.8	148.1
12-Jan-13	112.3	18.9	183.3
13-Jan-13	280.3	31.7	767.8
14-Jan-13	725.9	50.5	3167.4
15-Jan-13	501.1	47.1	2039.2
16-Jan-13	397.6	37.2	1278.1
17-Jan-13	232.5	23.5	472.0
18-Jan-13	180.8	20.8	324.9
19-Jan-13	159.2	21.2	291.7
20-Jan-13	115.4	18.6	185.5
21-Jan-13	102.7	18	159.7
22-Jan-13	89.9	16.2	125.8
23-Jan-13	271.4	32	750.4
24-Jan-13	391.8	33.1	1120.6
25-Jan-13	143.7	19.2	238.4
26-Jan-13	241.5	25.7	536.2
27-Jan-13	124.9	18.4	198.6
28-Jan-13	115.4	18	179.5
29-Jan-13	199.2	24.3	418.1
30-Jan-13	327.6	31.4	888.8
31-Jan-13	208.3	27.9	502.1
1-Feb-13	312.9	31.1	840.8
2-Feb-13	532.4	38.8	1784.7
3-Feb-13	394.7	32.5	1108.4
4-Feb-13	146.8	17.5	222.0
5-Feb-13	238.5	24.9	513.1
6-Feb-13	594.6	41.7	2142.2
7-Feb-13	863.8	51.2	3821.4
8-Feb-13	351.1	34.5	1046.5
9-Feb-13	388.9	33.5	1125.8
10-Feb-13	836.4	50.3	3634.9
11-Feb-13	830.9	49	3517.7
12-Feb-13	226.4	33.7	659.3
13-Feb-13	140.6	23.3	283.0
14-Feb-13	134.3	15.4	178.7
15-Feb-13	105.9	17.1	156.5
16-Feb-13	93.1	16.3	131.1
17-Feb-13	223.4	26.8	517.3
18-Feb-13	611.5	43.7	2308.6
19-Feb-13	327.6	35	990.7
20-Feb-13	156.1	20.1	271.2
21-Feb-13	131.2	18.8	213.1
22-Feb-13	80.2	12.1	83.8
23-Feb-13	93.1	12.3	98.9
24-Feb-13	622.7	43.3	2329.5
25-Feb-13	441.0	36.7	1398.2
26-Feb-13	265.4	30.2	692.6
27-Feb-13	235.5	28.4	577.8
28-Feb-13	102.7	19	168.6
1-Mar-13	99.5	16.8	144.4
2-Mar-13	134.3	20.9	242.6
3-Mar-13	177.7	23.2	356.3
4-Mar-13	96.3	18.7	155.6
5-Mar-13	1108.3	61.6	5898.5
6-Mar-13	412.1	33.6	1196.4
7-Mar-13	171.6	21	311.3
8-Mar-13	594.6	38.7	1988.1
9-Mar-13	217.4	21.2	398.1
10-Mar-13	177.7	23.1	354.7
11-Mar-13	180.8	24.1	376.5
12-Mar-13	232.5	26.1	524.2
13-Mar-13	128.1	22.1	244.5
14-Mar-13	112.3	22.1	214.4
15-Mar-13	229.5	25	495.6

Day	TSS (mg/l) - 2013	Qobs corr [2013] (m3/s)	Qs (metric tons/day) - [2013]
16-Mar-13	211.3	24.5	447.3
17-Mar-13	168.5	22.2	323.2
18-Mar-13	351.1	33.3	1010.1
19-Mar-13	420.8	34.7	1261.5
20-Mar-13	268.4	28.9	670.2
21-Mar-13	929.5	54.4	4368.6
22-Mar-13	2203.2	85.4	16256.8
23-Mar-13	1111.0	61.7	5922.5
24-Mar-13	647.9	43	2407.1
25-Mar-13	238.5	24.2	498.6
26-Mar-13	159.2	18.3	251.8
27-Mar-13	146.8	19.7	249.9
28-Mar-13	124.9	19.1	206.1
29-Mar-13	146.8	21	266.4
30-Mar-13	105.9	19.8	181.2
31-Mar-13	365.7	33.6	1061.5
1-Apr-13	93.1	15.9	127.9
2-Apr-13	214.3	23.9	442.6
3-Apr-13	124.9	18.7	201.8
4-Apr-13	1314.3	62.8	7131.4
5-Apr-13	1199.6	60.3	6249.7
6-Apr-13	1255.7	62.5	6780.8
7-Apr-13	277.4	28.2	675.8
8-Apr-13	162.3	21.7	304.4
9-Apr-13	131.2	19.6	222.2
10-Apr-13	112.3	17.7	171.7
11-Apr-13	112.3	18.3	177.5
12-Apr-13	112.3	16.9	163.9
13-Apr-13	115.4	17.2	171.5
14-Apr-13	244.5	26	549.2
15-Apr-13	1002.9	52.1	4514.5
16-Apr-13	426.6	35.1	1293.6
17-Apr-13	277.4	29.4	704.5
18-Apr-13	199.2	25.2	433.6
19-Apr-13	518.2	39.9	1786.3
20-Apr-13	359.8	34.7	1078.8
21-Apr-13	748.1	46.5	3005.7
22-Apr-13	153.0	18.8	248.6
23-Apr-13	725.9	43.5	2728.4
24-Apr-13	841.9	48.6	3535.2
25-Apr-13	574.8	41.5	2061.1
26-Apr-13	223.4	25.3	488.4
27-Apr-13	241.5	27	563.3
28-Apr-13	235.5	28.2	573.7
29-Apr-13	339.4	33	967.6
30-Apr-13	301.1	30.1	783.0
1-May-13	131.2	19.6	222.2
2-May-13	124.9	18.5	199.7
3-May-13	153.0	21.5	284.3
4-May-13	1092.1	60.6	5718.1
5-May-13	435.2	34.7	1304.8
6-May-13	292.2	27.1	684.2
7-May-13	1154.0	58.3	5812.8
8-May-13	199.2	22.8	392.3
9-May-13	165.4	21.9	313.0
10-May-13	307.0	29.5	782.5
11-May-13	118.6	19.4	198.8
12-May-13	105.9	19	173.9
13-May-13	180.8	23.2	362.4
14-May-13	226.4	24.4	477.4
15-May-13	351.1	29.9	906.9
16-May-13	177.7	22.4	344.0
17-May-13	193.1	24.2	403.6
18-May-13	244.5	27.9	589.4
19-May-13	298.1	32.4	834.6
20-May-13	153.0	20.8	275.0
21-May-13	137.5	20.1	238.7
22-May-13	96.3	17.3	144.0
23-May-13	93.1	18.1	145.6
24-May-13	99.5	19.5	167.7
25-May-13	99.5	15.8	135.8
26-May-13	102.7	16.6	147.3
27-May-13	99.5	15.3	131.6
28-May-13	112.3	16.5	160.0
29-May-13	124.9	18.9	204.0
30-May-13	89.9	17.3	134.3

Day	TSS (mg/l) - 2013	Qobs corr [2013] (m3/s)	Qs (metric tons/day) - [2013]
31-May-13	96.3	16.3	135.6
1-Jun-13	105.9	19.6	179.3
2-Jun-13	96.3	19.9	165.6
3-Jun-13	102.7	15.9	141.1
4-Jun-13	89.9	16.2	125.8
5-Jun-13	89.9	17.1	132.8
6-Jun-13	86.6	16.4	122.8
7-Jun-13	83.4	17.9	129.0
8-Jun-13	93.1	18.7	150.4
9-Jun-13	83.4	14	100.9
10-Jun-13	80.2	13.9	96.3
11-Jun-13	83.4	15.1	108.8
12-Jun-13	76.9	16.1	107.0
13-Jun-13	86.6	17.7	132.5
14-Jun-13	80.2	15.6	108.0
15-Jun-13	86.6	17.1	128.0
16-Jun-13	93.1	15.5	124.7
17-Jun-13	180.8	22.3	348.4
18-Jun-13	183.9	21.9	347.9
19-Jun-13	102.7	17.3	153.5
20-Jun-13	63.8	13.3	73.3
21-Jun-13	47.1	13.1	53.3
22-Jun-13	57.1	13	64.2
23-Jun-13	76.9	17.8	118.3
24-Jun-13	73.6	13.9	88.4
25-Jun-13	70.4	12.7	77.2
26-Jun-13	67.1	13.6	78.8
27-Jun-13	70.4	13.8	83.9
28-Jun-13	67.1	13.9	80.6
29-Jun-13	70.4	14.7	89.4
30-Jun-13	67.1	14.6	84.6
1-Jul-13	73.6	13.3	84.6
2-Jul-13	63.8	11.6	63.9
3-Jul-13	63.8	13.1	72.2
4-Jul-13	60.5	12.9	67.4
5-Jul-13	67.1	15	86.9
6-Jul-13	76.9	16.5	109.6
7-Jul-13	67.1	14.6	84.6

Day	TSS (mg/l) - 2013	Qobs corr [2013] (m3/s)	Qs (metric tons/day) - [2013]
8-Jul-13	73.6	13.9	88.4
9-Jul-13	63.8	12.9	71.1
10-Jul-13	67.1	10.4	60.3
11-Jul-13	60.5	11.8	61.6
12-Jul-13	70.4	13.7	83.3
13-Jul-13	67.1	13.6	78.8
14-Jul-13	70.4	15.8	96.1
15-Jul-13	67.1	14.7	85.2
16-Jul-13	70.4	18.6	113.1
17-Jul-13	63.8	12.6	69.4
18-Jul-13	60.5	11.1	58.0
19-Jul-13	67.1	11.8	68.4
20-Jul-13	73.6	10.6	67.4
21-Jul-13	57.1	12.8	63.2
22-Jul-13	60.5	14.3	74.7
23-Jul-13	63.8	13.9	76.6
24-Jul-13	70.4	15.8	96.1
25-Jul-13	70.4	15	91.2
26-Jul-13	70.4	12.8	77.8
27-Jul-13	70.4	13.4	81.5
28-Jul-13	67.1	10.5	60.8
29-Jul-13	60.5	11.9	62.2
30-Jul-13	53.8	12.5	58.1
31-Jul-13	47.1	11.8	48.0
1-Aug-13	50.4	12.9	56.2
2-Aug-13	53.8	15.2	70.7
3-Aug-13	53.8	14.3	66.5
4-Aug-13	53.8	11.7	54.4
5-Aug-13	47.1	10.4	42.3
6-Aug-13	57.1	12.6	62.2
7-Aug-13	50.4	13.2	57.5
8-Aug-13	53.8	12	55.8
9-Aug-13	50.4	14.6	63.6
10-Aug-13	57.1	12.8	63.2
11-Aug-13	53.8	11.7	54.4
12-Aug-13	50.4	10.5	45.8
13-Aug-13	60.5	13.3	69.5
14-Aug-13	57.1	13.4	66.2

Day	TSS (mg/l) - 2013	Qobs corr [2013] (m3/s)	Qs (metric tons/day) - [2013]
15-Aug-13	53.8	14.3	66.5
16-Aug-13	53.8	15.3	71.1
17-Aug-13	57.1	15.7	77.5
18-Aug-13	57.1	11.6	57.3
19-Aug-13	63.8	12.1	66.7
20-Aug-13	60.5	12.9	67.4
21-Aug-13	60.5	13.6	71.0
22-Aug-13	57.1	13.3	65.7
23-Aug-13	70.4	14.4	87.5
24-Aug-13	67.1	15.1	87.5
25-Aug-13	53.8	13.9	64.6
26-Aug-13	60.5	14.6	76.3
27-Aug-13	67.1	13.7	79.4
28-Aug-13	60.5	14.4	75.2
29-Aug-13	67.1	15.8	91.6
30-Aug-13	63.8	15.6	86.0
31-Aug-13	70.4	14.8	90.0
1-Sep-13	60.5	12.3	64.3
2-Sep-13	67.1	13.2	76.5
3-Sep-13	60.5	13.5	70.5
4-Sep-13	73.6	15.1	96.1
5-Sep-13	67.1	16.2	93.9
6-Sep-13	63.8	13.4	73.8
7-Sep-13	53.8	15.2	70.7
8-Sep-13	60.5	11.8	61.6
9-Sep-13	53.8	11	51.1
10-Sep-13	60.5	10	52.2
11-Sep-13	57.1	10.9	53.8
12-Sep-13	60.5	12.9	67.4
13-Sep-13	70.4	15.6	94.8
14-Sep-13	67.1	14.7	85.2
15-Sep-13	89.9	16.3	126.6
16-Sep-13	67.1	15	86.9
17-Sep-13	60.5	12.2	63.7
18-Sep-13	67.1	12	69.5
19-Sep-13	67.1	11.4	66.1
20-Sep-13	67.1	12.9	74.8
21-Sep-13	67.1	14.1	81.7

Day	TSS (mg/l) - 2013	Qobs corr [2013] (m3/s)	Qs (metric tons/day) - [2013]
22-Sep-13	70.4	14.4	87.5
23-Sep-13	67.1	16	92.7
24-Sep-13	63.8	17	93.7
25-Sep-13	60.5	12.9	67.4
26-Sep-13	83.4	14.6	105.2
27-Sep-13	93.1	16.1	129.5
28-Sep-13	93.1	17.4	140.0
29-Sep-13	93.1	18.3	147.2
30-Sep-13	93.1	19.1	153.6
1-Oct-13	149.9	24.7	320.0
2-Oct-13	153.0	20.4	269.8
3-Oct-13	134.3	17.5	203.1
4-Oct-13	140.6	20.4	247.8
5-Oct-13	99.5	17.1	147.0
6-Oct-13	86.6	17.8	133.3
7-Oct-13	105.9	19.8	181.2
8-Oct-13	112.3	19.5	189.1
9-Oct-13	93.1	15.2	122.3
10-Oct-13	569.2	39	1917.9
11-Oct-13	193.1	20.5	341.9
12-Oct-13	271.4	27.1	635.5
13-Oct-13	226.4	25.6	500.8
14-Oct-13	268.4	28	649.4
15-Oct-13	1035.4	56.6	5063.4
16-Oct-13	262.5	28.4	644.0
17-Oct-13	356.9	33.2	1023.8
18-Oct-13	435.2	35	1316.0
19-Oct-13	205.2	22.3	395.4
20-Oct-13	174.7	21.6	326.0
21-Oct-13	199.2	20.3	349.3
22-Oct-13	93.1	16.6	133.5
23-Oct-13	86.6	16.9	126.5
24-Oct-13	177.7	22.7	348.6
25-Oct-13	625.5	44.9	2426.5
26-Oct-13	426.6	38.9	1433.6
27-Oct-13	1693.7	70.5	10316.9
28-Oct-13	365.7	30.6	966.8
29-Oct-13	165.4	21.7	310.2

Day	TSS (mg/l) - 2013	Qobs corr [2013] (m3/s)	Qs (metric tons/day) - [2013]
30-Oct-13	156.1	21.7	292.8
31-Oct-13	128.1	19.3	213.5
1-Nov-13	159.2	23.7	326.1
2-Nov-13	309.9	30	803.4
3-Nov-13	271.4	26.7	626.1
4-Nov-13	153.0	19.2	253.9
5-Nov-13	156.1	21.1	284.7
6-Nov-13	199.2	23.6	406.1
7-Nov-13	506.8	41	1795.3
8-Nov-13	146.8	23.9	303.2
9-Nov-13	280.3	31.2	755.7
10-Nov-13	153.0	19.8	261.8
11-Nov-13	99.5	15.1	129.8
12-Nov-13	153.0	20.9	276.4
13-Nov-13	1309.0	62.7	7091.2
14-Nov-13	625.5	44.4	2399.5
15-Nov-13	441.0	36.9	1405.8
16-Nov-13	168.5	26.2	381.5
17-Nov-13	118.6	17.4	178.3
18-Nov-13	115.4	17.5	174.5
19-Nov-13	244.5	25	528.1
20-Nov-13	926.7	53.1	4251.7
21-Nov-13	259.5	27.2	609.8
22-Nov-13	386.0	34.2	1140.7
23-Nov-13	538.1	42.3	1966.4
24-Nov-13	220.4	28.3	538.9
25-Nov-13	577.7	40.2	2006.4
26-Nov-13	298.1	27.6	710.9
27-Nov-13	153.0	20	264.5
28-Nov-13	597.4	37.7	1945.9
29-Nov-13	356.9	31.9	983.7
30-Nov-13	156.1	21.8	294.1
1-Dec-13	687.0	45.5	2700.8
2-Dec-13	1067.8	59.3	5471.1
3-Dec-13	403.4	36.9	1286.2
4-Dec-13	253.5	27	591.3
5-Dec-13	131.2	20.7	234.6
6-Dec-13	321.7	31.8	884.0

Day	TSS (mg/l) - 2013	Qobs corr [2013] (m3/s)	Qs (metric tons/day) - [2013]
7-Dec-13	1290.4	62.8	7001.4
8-Dec-13	247.5	28.2	603.0
9-Dec-13	208.3	23.9	430.1
10-Dec-13	171.6	21.6	320.2
11-Dec-13	217.4	24	450.7
12-Dec-13	309.9	28.9	773.9
13-Dec-13	714.8	46.4	2865.7
14-Dec-13	1544.4	69.6	9287.0
15-Dec-13	1399.2	65.1	7870.3
16-Dec-13	2509.4	90.7	19664.5
17-Dec-13	312.9	30.1	813.7
18-Dec-13	196.1	22.7	384.6
19-Dec-13	171.6	20.3	301.0
20-Dec-13	455.3	35.9	1412.3
21-Dec-13	274.4	25.9	614.0
22-Dec-13	162.3	22.1	310.0
23-Dec-13	131.2	20.3	230.1
24-Dec-13	1751.1	74.5	11271.7
25-Dec-13	400.5	34.2	1183.6
26-Dec-13	386.0	35.1	1170.7
27-Dec-13	168.5	20.9	304.3
28-Dec-13	134.3	18.3	212.4
29-Dec-13	1005.6	54.8	4761.2
30-Dec-13	400.5	34.5	1193.9
31-Dec-13	190.0	23.7	389.1

Annual sediment load in 2005

Time intervals (%) (1)	Interval midpoint (%) (2)	Interval Δp (%) (3)	Discharge Q (m3/s) (4)	Concentration C (mg/l) (5)	Q x Δp (m3/s) (6)	Sediment Load Qs x Δp (tons/year) (7)
0.00 - 0.02	0.01	0.02	62.6	1234.8	0.01252	487
0.02 - 0.1	0.06	0.08	62.4	1227.3	0.04992	1930
0.1 - 0.5	0.3	0.4	61.5	1193.8	0.246	9251
0.5 - 1.5	1	1	60.5	1157.2	0.605	22053
1.5 - 5.0	3.25	3.5	47.5	730.5	1.6625	38255
5 - 15	10	10	34.8	404.2	3.48	44308
15 - 25	20	10	28.2	271	2.82	24073
25 - 35	30	10	24.1	201	2.41	15259
35 - 45	40	10	21.1	156.1	2.11	10375
45 - 55	50	10	18.1	116.6	1.81	6648
55 - 65	60	10	17	103.5	1.7	5542
65 - 75	70	10	15	81.6	1.5	3856
75 - 85	80	10	14.8	79.5	1.48	3706
85 - 95	90	10	12.6	58.6	1.26	2326
95 - 100	97.5	5	11.8	51.7	0.59	961
Total		100			21.735	**189,030**

Annual sediment load in 2013

Time intervals (%) (1)	Interval midpoint (%) (2)	Interval Δp (%) (3)	Discharge Q (m3/s) (4)	Concentration C (mg/l) (5)	Q x Δp (m3/s) (6)	Sediment Load Qs x Δp (tons/year) (7)
0.00 - 0.02	0.01	0.02	91.2	2414.3	0.01824	1387
0.02 - 0.1	0.06	0.08	91	2404.3	0.0728	5514
0.1 - 0.5	0.3	0.4	90.7	2389.3	0.3628	27305
0.5 - 1.5	1	1	70.5	1485.4	0.705	32987
1.5 - 5.0	3.25	3.5	61.8	1158.5	2.163	78934
5 - 15	10	10	42.5	571.6	4.25	76523
15 - 25	20	10	33.1	356.7	3.31	37191
25 - 35	30	10	26.5	234.4	2.65	19567
35 - 45	40	10	21.8	162.2	2.18	11138
45 - 55	50	10	19.5	131.4	1.95	8071
55 - 65	60	10	17.1	102.6	1.71	5527
65 - 75	70	10	15.9	89.4	1.59	4478
75 - 85	80	10	14.1	71.3	1.41	3167
85 - 95	90	10	12.8	59.4	1.28	2395
95 - 100	97.5	5	11.2	46.2	0.56	815
Total		100			24.21184	**315,000**